



Viki Joergens *Editor*

5,800 K

3,600 K

2,600 K

950 K

300 K

125 K

# 50 Years of Brown Dwarfs

From Prediction to Discovery  
to Forefront of Research

ASSL

 Springer

# 50 Years of Brown Dwarfs

For further volumes:  
<http://www.springer.com/series/5664>

# Astrophysics and Space Science Library

---

## EDITORIAL BOARD

### *Chairman*

W. B. BURTON, *National Radio Astronomy Observatory, Charlottesville, Virginia, U.S.A. (bburton@nrao.edu); University of Leiden, The Netherlands (burton@strw.leidenuniv.nl)*

F. BERTOLA, *University of Padua, Italy*

C. J. CESARSKY, *Commission for Atomic Energy, Saclay, France*

P. EHRENFREUND, *Leiden University, The Netherlands*

O. ENGVOLD, *University of Oslo, Norway*

A. HECK, *Strasbourg Astronomical Observatory, France*

E. P. J. VAN DEN HEUVEL, *University of Amsterdam, The Netherlands*

V. M. KASPI, *McGill University, Montreal, Canada*

J. M. E. KUIJPERS, *University of Nijmegen, The Netherlands*

H. VAN DER LAAN, *University of Utrecht, The Netherlands*

P. G. MURDIN, *Institute of Astronomy, Cambridge, UK*

B. V. SOMOV, *Astronomical Institute, Moscow State University, Russia*

R. A. SUNYAEV, *Space Research Institute, Moscow, Russia*

Viki Joergens  
Editor

# 50 Years of Brown Dwarfs

## From Prediction to Discovery to Forefront of Research



Springer

*Editor*

Viki Joergens

Max-Planck-Institute for Astronomy  
Institute of Theoretical Astrophysics  
Heidelberg  
Germany

ISSN 0067-0057

ISBN 978-3-319-01161-5

e-ISBN 978-3-319-01162-2 (eBook)

DOI 10.1007/978-3-319-01162-2

Springer Cham Heidelberg New York Dordrecht London

Library of Congress Control Number: 2013954670

© Springer International Publishing Switzerland 2014

This work is subject to copyright. All rights are reserved by the Publisher, whether the whole or part of the material is concerned, specifically the rights of translation, reprinting, reuse of illustrations, recitation, broadcasting, reproduction on microfilms or in any other physical way, and transmission or information storage and retrieval, electronic adaptation, computer software, or by similar or dissimilar methodology now known or hereafter developed. Exempted from this legal reservation are brief excerpts in connection with reviews or scholarly analysis or material supplied specifically for the purpose of being entered and executed on a computer system, for exclusive use by the purchaser of the work. Duplication of this publication or parts thereof is permitted only under the provisions of the Copyright Law of the Publisher's location, in its current version, and permission for use must always be obtained from Springer. Permissions for use may be obtained through RightsLink at the Copyright Clearance Center. Violations are liable to prosecution under the respective Copyright Law.

The use of general descriptive names, registered names, trademarks, service marks, etc. in this publication does not imply, even in the absence of a specific statement, that such names are exempt from the relevant protective laws and regulations and therefore free for general use.

While the advice and information in this book are believed to be true and accurate at the date of publication, neither the authors nor the editors nor the publisher can accept any legal responsibility for any errors or omissions that may be made. The publisher makes no warranty, express or implied, with respect to the material contained herein.

*Cover illustration:* Comparison of sizes and effective temperatures of the Sun, the red dwarf star Gliese 229A, the young brown dwarf Teide 1, the old brown dwarf Gliese 229B, the coolest known brown dwarf WISE 1828+2650, and Jupiter. Graphic after American Scientist/Linda Huff using NASA satellite images (Sun, Jupiter) and NASA artist work (Gliese 229A+B, Teide 1, WISE1828+2650). Copyright MPIA/Viki Joergens.

Printed on acid-free paper

Springer is part of Springer Science+Business Media ([www.springer.com](http://www.springer.com))

# Foreword

This book tells the story that contains all the excitement involved in the process of scientific discovery. Amazingly, from that perspective, brown dwarfs are not unlike pulsars, despite their being so extremely different in nearly every way. In 1934, Walter Baade and Fritz Zwicky predicted the existence of neutron stars. Five years later, in 1939, Robert Oppenheimer and George Volkoff calculated their properties, based on the still very young science of quantum mechanics, and even more recent neutron detection. Just about 30 years after Baade and Zwicky, in 1962–1963, Shiv Kumar published a series of calculations, in which he predicted the existence of substellar objects that would not be massive enough to function like stars, slowly cooling down and contracting to a steady-state supported by the quantum mechanical electron degeneracy.

In the times of Oppenheimer and Volkoff, nobody knew how would the objects so extreme as neutron stars reveal themselves to astronomers. Luckily, almost 30 years later, in 1967, Anthony Hewish and Jocelyn Bell made a serendipitous discovery of radio pulsars, which turned out to be one of the several observational manifestations of neutron stars. In the case of brown dwarfs, it was quite clear from the very start what to look for. However, the practical searches proved to be difficult and frustrating, and lasted over 30 years to finally culminate in almost simultaneous identifications of the first three brown dwarfs by Tadashi Nakajima, Ben Oppenheimer, Rafael Rebolo, Gibor Basri, and their teams, in 1995.

These developments have revealed to us the two radically different endpoints of the evolution of baryonic matter, both supported by quantum mechanical equilibria, discovered in the amazingly similar, roughly 30-year cycles, with the two Oppenheimers involved in the process. Even more incredibly, some brown dwarfs do, in fact, behave like pulsars, emitting radio pulses of coherent radiation once every rotation period!

However, these astrophysical and historical coincidences pale in the face of the most dramatic one, which is that the discovery of the first planet orbiting a normal, Sun-like star was announced by Michel Mayor and Didier Queloz at the same 1995 Cool Stars meeting in Florence, Italy, at which the first brown dwarf was uncovered by Ben Oppenheimer. It is hard not to think about the simultaneity of these two

events as of a symbolic, almost prophetic emphasis on the special role that brown dwarfs play in astrophysics by sharing properties of stars and planets.

This collection of articles is about the past, the present, and the future of the brown dwarf research seen through the eyes of experts. It looks back at the brown dwarf history with reverence, but, perhaps even more importantly, it is full of enthusiastic anticipation and excitement about future discoveries. Reading this book, especially for a newcomer to the field like myself, feels very much like watching science fiction become reality. Enjoy!

Pennsylvania, USA

June 2013

Alex Wolszczan

# Preface

“Brown dwarfs don’t exist” expressed the culmination of frustration in 1994 after decades of unsuccessful searches for these cool and dim objects. Starting in the early 1960s, theorists like Hayashi, Kumar, and Nakano followed by many others had worked out the properties of brown dwarfs in great detail. Whether our universe is home to such objects, however, remained a completely open question for more than 30 years. Then in 1994/1995 everything seemed to be happening at the same time. Within only two months in the fall of 1994, Tadashi Nakajima and Ben Oppenheimer detected in a coronographic observation “something quite red” next to the red dwarf star Gliese 229, Rafael Rebolo and his team confirmed the object Teide 1 by high-resolution spectroscopy to be a late M-type brown dwarf in the Pleiades, and Gibor Basri and co-workers used the brand-new 10 m Keck telescope and detected the “brown dwarf test element” lithium in PPI 15. These news reached the public in 1995 after the data were carefully analyzed, the journal referees satisfied, and the Gliese 229B team pinned down their detection by finding “There’s methane in that thing!”

Brown dwarfs play a key role to understand both planets and stars as they are the link between these two populations. This position became even more pronounced with the recent discoveries of free-floating ultra-cool brown dwarfs with temperatures and masses in the canonical planetary regime. The cover of this book shows an artist’s view of some of the first discovered brown dwarfs (Teide 1, Gliese 229B) and of the coolest brown dwarf known to date (WISE 1828 + 2650; cf. also Fig. 1). They are compared in this illustration to our Sun, a very low-mass red dwarf star – the host star of Gliese 229B happens to be such an M dwarf – and Jupiter. Two of the characteristics of brown dwarfs can be seen in this graphic. Firstly, brown dwarfs have no substantial inner energy source, and therefore, after birth “they cool off inexorably like dying embers plucked from a fire” as phrased dramatically by Adam Burrows in 2001. Teide 1 and Gliese 229B have a similar mass, but Teide 1 is still in its adolescence and therefore slightly bigger and significantly hotter than Gliese 229B. The chart shows another peculiarity of brown dwarfs: after an early contraction phase, all brown dwarfs have roughly the same size of about one Jupiter radius regardless of their mass. This phenomenon has its reason in quantum

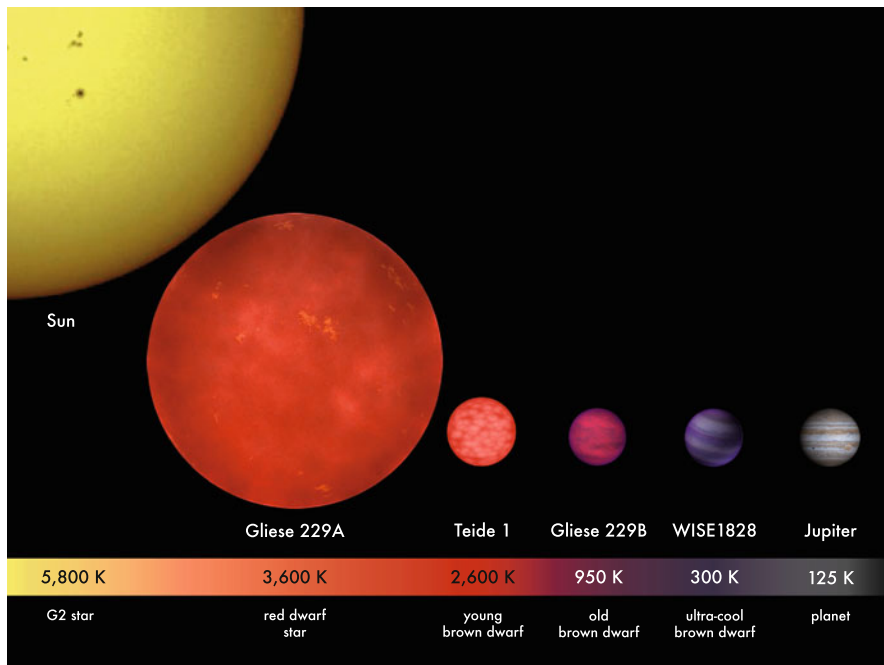


**Fig. 1** Comparison of sizes and effective temperatures of the Sun, the red dwarf star Gliese 229A, the young brown dwarf Teide 1, the old brown dwarf Gliese 229B, the coolest known brown dwarf WISE 1828 + 2650, and Jupiter. Graphic after American Scientist/Linda Huff using NASA satellite images (Sun, Jupiter) and NASA artist work (Gliese 229A + B, Teide 1, WISE1828 + 2650) (Copyright MPIA/V. Joergens)

mechanical effects. As can be seen, Gliese 229B, WISE 1828 + 2650, and Jupiter have about the same size but span a mass range of several tenth of Jupiter masses.

The idea for a book featuring the discoverers of brown dwarfs was born during the Ringberg conference on “50 Years of Brown Dwarfs: from Theoretical Prediction to Astrophysical Studies” which took place in October 2012 (<http://www.mpia.de/homes/joergens/ringberg2012.html>). It was a great pleasure and honor to welcome there Shiv Kumar, Gibor Basri, Ben Oppenheimer, Rafael Rebolo, and many of the leading experts in the field of brown dwarfs. The conference took place 50 years after the submission of Kumar’s two relevant papers to a scientific journal in 1962, and the book is published 50 years after the pioneering theoretical work by Kumar, and Hayashi and Nakano went into print in 1963.

The authors of this book tell in the articles their story of the theoretical and observational discovery and characterization of brown dwarfs. This story starts with the visionary theoretical prediction of the existence of brown dwarfs, as described in a summary of the work of S. Kumar and in an article from Takenori Nakano. Before brown dwarfs were actually discovered, they were given their today’s name. Jill Tarter describes in this book how and why she introduced the term “brown

dwarf” in 1975. Then follow the thrilling stories of the first brown dwarf discoverers Rebolo, Basri, and Oppenheimer, who share their personal memories of the wild discovery days. These first detections opened the door to almost two decades of detailed characterization of brown dwarfs. Michael Cushing, who found the coolest known brown dwarf, the planetary-like Y-dwarf WISE 1828 + 2650, reviews the development of the surveys to probe for cooler and cooler brown dwarfs and of the substellar spectral sequence. Our understanding of the physics of brown dwarfs is inextricably linked with the name of Isabelle Baraffe, who reviews in her article the current state and open questions in this field.

The creation of this book involved the commitment of many people. Foremost, I would like to thank the authors. It is through their work, expertise, and openness to share their memories and thoughts that we have been able to prepare a book on brown dwarfs in which exciting science is embedded into historical and personal background stories in a wonderful and unique way. Furthermore, I am very grateful to Thomas Henning for his support during the preparation of this book. I would also like to thank Nicola Reusch, Alex Golovin, Christian Fendt, Ramon Khanna, and Markus Pössel for their support.

Heidelberg, Germany  
June 2013

Viki Joergens



# Contents

<b>The Theoretical Prediction of the Existence of Brown Dwarfs</b>	
<b>by Shiv S. Kumar</b>	1
Viki Joergens	
<b>Pre-main Sequence Evolution and the Hydrogen-Burning Minimum Mass</b>	5
Takenori Nakano	
<b>Brown Is Not a Color: Introduction of the Term ‘Brown Dwarf’</b>	19
Jill Tarter	
<b>Teide 1 and the Discovery of Brown Dwarfs</b>	25
Rafael Rebolo	
<b>The Discovery of the First Lithium Brown Dwarf: PPI 15</b>	51
Gibor Basri	
<b>Companions of Stars: From Other Stars to Brown Dwarfs to Planets and the Discovery of the First Methane Brown Dwarf</b>	81
Ben R. Oppenheimer	
<b>Ultracool Objects: L, T, and Y Dwarfs</b>	113
Michael C. Cushing	
<b>Latest News on the Physics of Brown Dwarfs</b>	141
Isabelle Baraffe	
<b>Index</b>	165

# The Theoretical Prediction of the Existence of Brown Dwarfs by Shiv S. Kumar

Viki Joergens

**Abstract** This article summarizes the theoretical work by Shiv S. Kumar in the years 1958–1963 on very low-mass degenerate objects, which he called “black dwarfs” and which we know today as “brown dwarfs”. He found that there exists a limiting mass below which a contracting star cannot reach the hydrogen-burning main-sequence stage. He predicted that after a warm phase in their early life time objects below this mass cool down and evolve to a completely quantum mechanically degenerate configuration and never go through a normal stellar evolution. After his pioneering theoretical prediction, he had to wait more than 30 years until observations confirmed these ideas.

There are many examples in astronomy of the discovery of astronomical objects that no one has anticipated to exist. These discoveries are then often followed by long lasting attempts to explain their existence theoretically. The story of the discovery of brown dwarfs was another: After the theoretical prediction in the early 1960s of the existence of a completely new class of very low-mass degenerate objects that never reach the main-sequence stage, a long search for them started which lasted more than 30 years before they were finally discovered observationally in 1995. Shiv S. Kumar was one of the main pioneers in the theoretical prediction of brown dwarfs, which he called ‘black dwarfs’ at that time. He published a series of abstracts and papers in 1962–1963, which inspired observers to search for these cool objects and theorists to further develop their properties. The term ‘brown dwarf’ goes back to J. Tarter in 1975 (see [Tarter \(1986\)](#) and also the chapter by J. Tarter in this volume). Kumar had to wait more than 30 years to see his theoretical ideas to be confirmed by

---

V. Joergens (✉)

Max-Planck-Institute for Astronomy, Königstuhl 17, 69117 Heidelberg, Germany

Center for Astronomy Heidelberg, Institute of Theoretical Astrophysics,  
Albert-Ueberle-Str. 2, 69120 Heidelberg, Germany

e-mail: [viki@mpia.de](mailto:viki@mpia.de)

the discovery of the first unequivocal brown dwarfs (see the chapters by R. Rebolo, G. Basri, and B. Oppenheimer in this volume).

The historical review by Shiv S. Kumar himself on *The Bottom of the Main Sequence and Beyond: Speculations, Calculations, Observations, and Discoveries* (1958–2002), which he wrote at the occasion of the IAU Symposium on Brown Dwarfs in 2002 (Kumar 2003), forms along with his papers the basis of the following summary of his experience. In his review article from 2003, Shiv S. Kumar describes amongst others his theoretical work on very low-mass degenerate objects during the time period 1958 and 1963. During this time he theoretically inferred the existence of brown dwarfs, as he realized that “there exists a limiting mass below which a contracting star cannot reach the main-sequence stage because the temperature and density at the center are too low for hydrogen-burning to start” (Kumar 1963a). After a warm phase during the early evolution “the star begins to cool slowly and evolves towards a completely degenerate configuration. Thus it becomes a “black” dwarf without ever going through normal stellar evolution.” (Kumar 1962a).

Kumar (2003) reports how he started to work “on the effects of electron degeneracy on the structure and evolution of the contracting stars of very low mass in the Fall of 1958 at the University of Michigan” at Ann Arbor. While the theoretical calculations on the pre-main sequence contraction phase at that time were carried out under the assumption that the material in the interior obeyed the ideal gas statistics, it became clear to him that “for a sufficiently low mass, the slow rise in the central temperature coupled with the rapid rise in the central density will cause the gaseous material to become partially [quantum mechanically] degenerate before the central temperature could get high enough for the onset of the hydrogen burning thermonuclear reactions” (Kumar 2003).

During his stay at the Smithsonian Astrophysical Observatory at Cambridge in 1960–1961 and as young postdoc at the NASA’s Goddard Institute for Space Studies at New York in 1962 when he was only 23 years old, Shiv S. Kumar further developed his ideas on the existence of gaseous objects with a mass below the hydrogen-burning limit. For example, he included interior models in convective equilibrium (Hayashi 1961) in his calculations in addition to those in radiative equilibrium. He describes how he wrote and submitted two papers to the PASP journal (*Publications of the Astronomical Society of the Pacific*) in July 1961 and April 1962 in which he concluded that “stars with mass below a certain critical mass (the minimum H-burning mass) would keep on contracting until they become completely degenerate objects”. Both papers were rejected by the journal because the referee did not agree with his conclusions (Kumar 2003).

He continued by calculating convective interior models for stars with masses between 0.09 and 0.04 solar masses ( $M_{\odot}$ ) by applying an equation of state which takes into account effects of non-relativistic electron degeneracy. He estimated the hydrogen-burning mass limit to be  $0.07 M_{\odot}$  for objects with population I composition and to be  $0.09 M_{\odot}$  for those with population II composition, respectively (Kumar 1963a,b). This is in agreement with early and later self-consistent calculations of this value (e.g., Hayashi and Nakano (1963), Burrows et al. (1997)

and Chabrier and Baraffe (2000), cf. also the chapters by T. Nakano and I. Baraffe in this volume).

Shiv S. Kumar presented a paper on his results at the *111th American Astronomical Society meeting* at Yale University on August 29, 1962 (Kumar 2003). The abstract of this paper appeared in the Astronomical Journal in November 1962 (Kumar 1962a) and a similar report in Kumar (1962b). He proceeded to write two papers with the titles *The Structure of Stars of Very Low Mass* and *The Helmholtz-Kelvin Time Scale for Stars of Very Low Mass* and submitted them on October 20, 1962 to the Astrophysical Journal. They were both accepted for publication in November 1962 and went into print in May 1963 (Kumar 1963a,b).

Almost exactly 50 years after the submission of these two papers to the Astrophysical Journal on October 20, 1963, a Ringberg conference on brown dwarfs took place (“50 Years of Brown Dwarfs: from Theoretical Prediction to Astrophysical Studies”, Oct. 21–24, 2012, Ringberg castle, Germany, <http://www.mpia.de/homes/joergens/ringberg2012.html>). It was a pleasure and honor to welcome Shiv S. Kumar, his wife, and other family members as well as the first brown dwarf discoverers at this conference and celebrate “50 Years of Brown Dwarfs”.

## References

- Burrows, A., Marley, M., Hubbard, W.B., et al.: A nongray theory of extrasolar giant planets and Brown dwarfs. *ApJ* **491**, 856 (1997)
- Chabrier, G., Baraffe, I.: Theory of low-mass stars and substellar objects. *ARA&A* **38**, 337 (2000)
- Hayashi, C.: Stellar evolution in early phases of gravitational contraction. *PASJ* **13**, 450–452 (1961)
- Hayashi, C., Nakano, T.: Evolution of stars of small masses in the pre-main-sequence stages. *Prog. Theor. Phys.* **30**, 460 (1963)
- Kumar, S.S.: Study of degeneracy in very light stars. *AJ* **67**, 579 (1962a)
- Kumar, S.S.: Models for stars of very low mass. Institute for Space Studies Report, No. X-644-62-78, 1 (1962b)
- Kumar, S.S.: The structure of stars of very low mass. *ApJ* **137**, 1121 (1963a)
- Kumar, S.S.: The Helmholtz-Kelvin time scale for stars of very low mass. *ApJ* **137**, 1126 (1963b)
- Kumar, S.S.: The bottom of the main sequence and beyond: speculations, calculations, observations, and discoveries (1958–2002). In: Martín, E.L. (ed.) *IAU Symposium*, Hawaii, vol. 211 (2003)
- Tarter, J.C.: An historical perspective: Brown is not a color. In: Kafatos, M.C., Harrington, R.S., Maran, S.P. (eds.) *Astrophysics of Brown Dwarfs*, pp. 121–138. Cambridge University Press, Cambridge/New York (1986)

# Pre-main Sequence Evolution and the Hydrogen-Burning Minimum Mass

Takenori Nakano

**Abstract** There is a lower limit to the mass of the main-sequence stars (the hydrogen-burning minimum mass) below which the stars cannot replenish the energy lost from their surfaces with the energy released by the hydrogen burning in their cores. This is caused by the electron degeneracy in the stars which suppresses the increase of the central temperature with contraction. To find out the lower limit we need the accurate knowledge of the pre-main sequence evolution of very low-mass stars in which the effect of electron degeneracy is important. We review how Hayashi and Nakano (1963) carried out the first determination of this limit.

## 1 Introduction

The stars on the main sequence replenish the energy lost outward from their surfaces with the energy released by the hydrogen burning in their cores. Because the nuclear energy is huge, the stars can maintain this steady state for a long time. There is a lower limit to the mass of such main-sequence stars, which we call *the hydrogen-burning minimum mass* hereafter.

The self-consistent determination of the hydrogen-burning minimum mass was first carried out by [Hayashi and Nakano \(1963\)](#). In this article I will review how they performed this determination.

The failure of attaining the steady state due to hydrogen burning is caused by the electron degeneracy in the star. The electron degeneracy is a quantum mechanical phenomenon. Electrons are fermions and obey the Pauli exclusion principle which allows only one particle per quantum state. For the gas of free electrons only two electrons (because of the two spin states) can take the state of the momentum

---

T. Nakano (✉)

National Astronomical Observatory of Japan, 2-21-1, Ohsawa, Mitaka, Tokyo, 181-8588, Japan  
e-mail: [nakanoft@zeus.eonet.ne.jp](mailto:nakanoft@zeus.eonet.ne.jp)

$p = 0$ , and the other electrons are forced to have non-zero momentum even at the temperature of  $T = 0$  K. Therefore, the electron gas has non-zero pressure even at  $T = 0$  K. The deviation from the ideal gas induced by the electron degeneracy is large at very high densities or very low temperatures. Protons (or neutrons) may also degenerate but only at much higher densities than electrons, e.g., in neutron stars, because of their large masses.

The pressure of the gas with degenerate electrons is much higher than the pressure of the gas with the electrons assumed to be in the Boltzmann distribution when compared at the same temperature and density. Therefore, the star with degenerate electrons can be in hydrostatic equilibrium even at the temperature of 0 K as long as the stellar mass is smaller than the Chandrasekhar limit given by Eq. (8) below. Therefore, the nuclear burning may not occur in stars with degenerate electrons.

To determine the stellar mass below which the steady state with the hydrogen burning cannot be attained, we need the accurate knowledge of the evolution of the stars in the pre-main sequence stage.

## 2 Stars with Degenerate Electrons

Stellar structure with degenerate electrons was investigated in the early twentieth century as the model of the white dwarfs ([Chandrasekhar 1939](#)). We give in the following a brief summary on the stellar structure with degenerate electrons and the start of electron degeneracy in the stars.

### 2.1 Stellar Structure

In hydrostatic equilibrium the central pressure  $P_c$  and the central density  $\rho_c$  of the star are given by (see e.g., [Hayashi et al.1962](#))

$$P_c = aGM^2/R^4, \quad (1)$$

$$\rho_c = bM/R^3, \quad (2)$$

where  $G$  is the gravitational constant,  $M$  and  $R$  are the stellar mass and radius, respectively, and  $a$  and  $b$  are constants of order 1 whose values are determined by the structure, e.g. by the polytropic index for the polytropic stars. See Eq. (5) below for the polytropic index. We are not concerned about the stars with some special structure such as red giants which have very dense cores and extended envelopes with nuclear burning shells in between. By eliminating  $R$  from Eqs. (1) and (2) we obtain

$$P_c \propto M^{2/3} \rho_c^{4/3}. \quad (3)$$

This relation holds for the stars in hydrostatic equilibrium irrespective of the equation of state. The equation of state is an equation which gives the relation among the density  $\rho$ , the temperature  $T$ , and the pressure  $P$  of the gas, and is indispensable in solving the stellar structure.

Let  $p_F$  be the Fermi momentum of the electron, i.e., the momentum corresponding to the maximum energy of the free electron when all the lower energy levels are occupied. The number of the quantum states per unit volume for the free electrons with the momentum between  $p$  and  $p + dp$  is equal to  $8\pi p^2 dp / h^3$ , where  $h$  is the Planck constant. Therefore, we find that  $p_F$  is proportional to  $(\rho/\mu_e)^{1/3}$ , where  $\rho$  is the density of the gas by mass and  $\mu_e$  is the mean molecular weight for electrons, or the number of nucleons per electron. Let  $X$ ,  $Y$ , and  $Z$  be the fractions by mass of hydrogen, helium, and the heavier elements, respectively. Then we have  $\mu_e^{-1} = X + (Y + Z)/2 = (1 + X)/2$  because the heavier elements are dominated by C, N, and O whose atomic numbers are half their mass numbers.

The pressure  $P$  of the gas is the momentum flux of the gas particles, and is on the order of  $n\bar{v}\bar{p}$ , where  $n$  is the number density of the gas particles and  $\bar{v}$  and  $\bar{p}$  are the mean values of the velocity and the momentum of the particles, respectively.

When electrons are completely degenerate and non-relativistic,  $\bar{p}$  is some fixed fraction of  $p_F$ , and then the pressure  $P$  is proportional to  $p_F^2(\rho/\mu_e)$ , and we obtain the equation of state omitting the coefficient

$$P \propto (\rho/\mu_e)^{5/3}. \quad (4)$$

Thus, the structure of the star in this situation is represented by a polytrope of index  $N = 1.5$ .

The polytropic index  $N$  characterizes the relation between the distribution of  $P$  and the distribution of  $\rho$  in the star, and is defined by

$$1 + \frac{1}{N} = \frac{d \log P / dr}{d \log \rho / dr}, \quad (5)$$

where  $r$  is the distance from the center. Thus  $N$  is in general a function of the position  $r$  in the star. But with the equation of state (4),  $N$  takes a constant value 1.5 throughout the star.

By eliminating  $P_c$  and  $\rho_c$  from Eqs. (2) and (3) using the equation of state (4) and bringing back the coefficient we find

$$R = 0.0400\mu_e^{-5/3}(M/1M_\odot)^{-1/3}R_\odot. \quad (6)$$

For the stars supported by the gas of non-relativistic completely degenerate electrons, the radius  $R$  is a decreasing function of the mass  $M$ .

Even when electrons are only partially degenerate and non-relativistic, the stellar structure is also represented by a polytrope of  $N = 1.5$  as long as the distribution of the specific entropy  $s$  in the star is uniform, or the star is fully convective (Hayashi et al. 1962). See Sect. 3.2 below for the relation between the distribution of  $s$  and the convection.

Eliminating  $P_c$  from Eqs. (3) and (4) we find  $\rho_c \propto M^2$  for the stars with non-relativistic degenerate electrons. As  $M$  increases,  $\rho_c$ , and then  $p_F$ , increase, and at some stellar mass electrons become relativistic.

When electrons are extremely relativistic and completely degenerate, the pressure  $P$  is proportional to  $p_F(\rho/\mu_e)$  because most of the electrons have a velocity, or  $\bar{v}$ , close to the light velocity, and we obtain the equation of state

$$P \propto (\rho/\mu_e)^{4/3}. \quad (7)$$

Thus, the star in this situation has a polytropic structure with  $N = 3$ . However, because this pressure in the equation of state and the pressure for hydrostatic equilibrium given by Eq. (3) have the same dependence on the density, the equilibrium with this equation of state is realized only at a special value of  $M$ , which is called the Chandrasekhar mass and is given numerically by (e.g., [Hayashi et al. 1962](#))

$$M_{\text{Ch}} = 5.75\mu_e^{-2}M_\odot. \quad (8)$$

For the white dwarfs composed of pure helium or pure carbon, we find  $\mu_e = 2$ , and then we obtain the well-known value  $M_{\text{Ch}} = 1.44M_\odot$ . For  $M$  slightly smaller than  $M_{\text{Ch}}$ , electrons are not extremely relativistic, and the dependence of the pressure on the density is slightly steeper than in Eq. (7). Therefore, hydrostatic equilibrium can be realized.

For the population I chemical composition, e.g., with 72 and 26 % by mass of hydrogen and helium, respectively, we have  $\mu_e = 1.16$  and then  $M_{\text{Ch}} = 4.27M_\odot$ . This does not mean that a star of mass close to this value can attain the equilibrium state with degenerate electrons without burning hydrogen. In order to find out the mass of the stars which can attain this state, we have to follow the stellar evolution prior to the hydrogen burning.

## 2.2 Start of Electron Degeneracy

When the temperature is so high and/or the density is so low that  $kT \gg p_F^2/(2m_e)$  holds, where  $k$  is the Boltzmann constant and  $m_e$  is the mass of the electron, only a very small fraction of the quantum levels with the energy less than  $kT$  are occupied by electrons, hence the electrons are not degenerate, and the gas follows the ideal gas law.

For the stars with negligible electron degeneracy and negligible radiation pressure the central temperature is given by (see e.g., [Hayashi et al. 1962](#))

$$T_c = f \frac{\mu m_H}{k} \frac{GM}{R}, \quad (9)$$

where  $\mu$  is the mean molecular weight of the gas,  $m_{\text{H}}$  is the mass of the hydrogen atom, and  $f$  is a constant of order 1 whose value is determined by the structure, e.g. by the polytropic index  $N$  for the polytropic stars. Eliminating  $R$  from Eqs. (2) and (9) we obtain

$$\rho_c \propto \mu^{-3} M^{-2} T_c^3. \quad (10)$$

The Fermi energy of the non-relativistic electron is given by  $p_{\text{F}}^2/(2m_e)$ . The Fermi energy at the center is proportional to  $(\rho_c/\mu_e)^{2/3}$ , which is proportional to  $R^{-2}$  for a fixed  $M$  as seen from Eq. (2), while the thermal energy at the center  $kT_c$  is proportional to  $R^{-1}$  as Eq. (9) shows. As  $R$  decreases by contraction, the Fermi energy increases faster than the thermal energy. Therefore, the degree of electron degeneracy increases as the star contracts. Electron degeneracy becomes nonnegligible when  $p_{\text{F}}^2/(2m_e) \approx kT$  holds because a significant fraction of the quantum levels with the energy less than  $kT$  are occupied by electrons. At the center this relation can be written as

$$(\rho_c/\mu_e)^{2/3} \propto T_c. \quad (11)$$

Eliminating  $\rho_c$  from Eqs. (10) and (11) we obtain

$$T_c \propto \mu_e^{2/3} \mu^2 M^{4/3}. \quad (12)$$

This means that in a star of smaller mass  $M$  the electron degeneracy becomes efficient at lower central temperature.

As the degree of degeneracy rises with contraction, the rise in the central temperature  $T_c$  slows down. Some time later  $T_c$  takes a maximum value at some radius  $R$ , and then decreases. Because the electron degeneracy becomes efficient at lower  $T_c$  for smaller  $M$ , the maximum attainable value of  $T_c$  is lower for the star of smaller mass  $M$ , suggesting the existence of the hydrogen-burning minimum mass.

### 3 Discovery of the Hayashi Phase

Determination of the hydrogen-burning minimum mass is crucially related to the pre-main sequence evolution. First we review how the Hayashi phase was discovered and what the Hayashi phase is.

#### 3.1 Prior to Hayashi's Theory

The Hertzsprung-Russell diagram (HR diagram) is a useful tool in the study of the stars, in which the stellar luminosity is plotted against the effective temperature.

In the HR diagram of star clusters there is a region in which no stars exist with the effective temperature  $T_{\text{eff}}$  less than several thousand Kelvin (e.g., [Sandage 1957](#)). The reason for this was not known until 1961. For instance, [Sandage and Schwarzschild \(1952\)](#) investigated the stellar evolution after the exhaustion of hydrogen in the core, and were confronted with the unlimited decrease of the effective temperature. They presumed that the set-in of the shell hydrogen burning would increase the luminosity and stop the decrease of the effective temperature. It seems to have been considered in those days that the non-existence of stars in this low effective temperature region was peculiar to the advanced stage of stellar evolution and did not apply to the pre-main sequence stage. Stars in the pre-main sequence stage were considered to be in radiative equilibrium and the evolution calculation was started at fairly low effective temperature (e.g., [Henyey et al. 1955](#)).

### 3.2 Boundary Conditions at the Stellar Surface

The problem in these previous evolution calculations was in the boundary conditions at the stellar surface. In the late-type stars the hydrogen ionization zone lies inside the photosphere and has an effect of making the stellar envelope convectively unstable and suppresses the decrease of the effective temperature. The previous papers cited above neglected the convection induced by the H-ionization zone. [Hayashi and Hoshi \(1961\)](#) solved the structure of the stellar atmosphere taking into account the effect of the H-ionization zone and used this as the boundary condition for the internal structure. We describe this in more detail in the following.

In the stars the energy is transported by radiation and convection. Here we do not consider the thermal conduction by gas particles because it is efficient only in some restricted situations. Strictly speaking, convection occurs in the regions where the specific entropy  $s$  decreases outward,  $ds/dr < 0$ . However,  $s$  can effectively be regarded constant in the convection zone except at a very thin layer near the stellar surface because the energy transport by convection is so efficient that the negligibly small outward decrease of  $s$  is enough to maintain the necessary energy flux. In the radiative zone the local luminosity  $L_r$ , the amount of the energy crossing a sphere of radius  $r$  in a unit time, is proportional to the temperature gradient defined by  $\nabla_{\text{rad}} \equiv (d \log T / d \log P)_{\text{rad}}$ , the exact expression of which is given by Eq. (13) below. In the convection zone the temperature gradient is given by  $\nabla_s \equiv (d \log T / d \log P)_s$ , the derivative under the constant  $s$ . Convection occurs only where  $\nabla_s < \nabla_{\text{rad}}$ . Usually  $\nabla_{\text{rad}}$  takes a value  $\sim 1$ , while  $\nabla_s = 0.4$  for the fully ionized ideal gas with negligible radiation pressure. Therefore, in order to find out where the convection occurs, we have to solve the stellar structure accurately.

In the H-ionization zone in the stellar atmosphere,  $\nabla_s$  is much smaller than 1 because the ionization potential of the hydrogen atom is much larger than the thermal energy  $kT$ . Therefore, convection easily occurs. Because  $\nabla_s \ll 1$ , the decrease of  $\log T$  outward in the H-ionization zone is much smaller than the decrease of  $\log P$  and  $\log \rho$ . Because  $\log P$  and  $\log \rho$  decrease by orders of

magnitude in the H-ionization zone, the outer boundary of the H-ionization zone has very low density, and hence is usually not very far from the photosphere. Thus, the effective temperature  $T_{\text{eff}}$  is not very low compared with the temperature at the outer boundary of the H-ionization zone.

[Hayashi and Hoshi \(1961\)](#) determined by numerical calculation the critical effective temperature  $T_{\text{eff}}^{(\text{cr})}$  as a function of the stellar mass and radius, which is several times  $10^3$  K and has the following characteristics. For  $T_{\text{eff}} = T_{\text{eff}}^{(\text{cr})}$  the stellar structure is represented by the Emden solution for a polytrope of index  $N = 1.5$  throughout the star, and the star is fully convective. For  $T_{\text{eff}} > T_{\text{eff}}^{(\text{cr})}$  the solution of the Lane-Emden equation for  $N = 1.5$  is of the centrally condensed type singular at the center  $r = 0$  with  $\rho = \infty$  and  $M_r > 0$ , where  $M_r$  is the mass included inside a sphere of radius  $r$ , indicating that there is a point mass at the center. This solution can be fitted at a finite radius  $r > 0$  with a regular core solution with the effective polytropic index, the mean value of  $N$  defined by Eq.(5) in the core,  $\bar{N} > 1.5$ . Thus, the star with  $T_{\text{eff}} > T_{\text{eff}}^{(\text{cr})}$  is composed of a convective envelope and a radiative core. For  $T_{\text{eff}} < T_{\text{eff}}^{(\text{cr})}$  the solution of the Lane-Emden equation for  $N = 1.5$  is of the collapsed type in which  $M_r$  decreases to 0 before reaching the center  $r = 0$ . This solution can be fitted at a position with  $M_r > 0$  only with a regular core solution with the effective polytropic index  $\bar{N} < 1.5$ . However, in such a core solution the entropy  $s$  decreases outward and violent convection occurs changing the distribution of  $s$  in a dynamical time scale. Therefore, stars cannot be in hydrostatic equilibrium with such  $T_{\text{eff}}$ . [Hayashi and Hoshi \(1961\)](#) found that the red giant branches of the star clusters in the HR diagram are close to the lines of  $T_{\text{eff}} = T_{\text{eff}}^{(\text{cr})}$  for appropriate values of the stellar mass.

### 3.3 Hayashi's Theory

Because there is no equilibrium state at  $T_{\text{eff}} < T_{\text{eff}}^{(\text{cr})}$  in any stage of stellar evolution, [Hayashi \(1961\)](#) considered that at least the final phase of star formation is dynamical and the star appears on the line of  $T_{\text{eff}} = T_{\text{eff}}^{(\text{cr})}$  in the HR diagram. The line of  $T_{\text{eff}} = T_{\text{eff}}^{(\text{cr})}$  is now called the Hayashi line and the region of  $T_{\text{eff}} < T_{\text{eff}}^{(\text{cr})}$  is called Hayashi's forbidden region.

[Hayashi \(1961\)](#) considered that the star, which appeared on the Hayashi line, contracts along the Hayashi line decreasing its luminosity, and changes the path to the higher temperature part of the radiative path ([Heney et al. 1955](#)) near the cross point of these lines. The path along the Hayashi line is called the Hayashi track and the radiative path the Heney track. The phase on the Hayashi track is called the Hayashi phase. The stellar luminosity on the Hayashi track is higher than that on the lower temperature part of the radiative path in the old theory when compared at the same stellar radius, and the contraction time of the star along the Hayashi track is shorter than along the lower temperature part of the radiative path in the old theory.

A possibility of the high luminosity phase for the primitive sun greatly stimulated the research on the origin of the solar system.

The reason why the star changes from the Hayashi track to the Henyey track may be explained in the following way. The temperature gradient  $\nabla_{\text{rad}}$  is given by [Hayashi et al. \(1962\)](#)

$$\nabla_{\text{rad}} = g \frac{P}{T^4} \frac{\kappa L_r}{M_r}, \quad (13)$$

where  $\kappa$  is the Rosseland mean opacity and  $g$  is a constant. This gives the temperature gradient necessary to transport the energy flow  $L_r$  by the radiation alone. In the stars of intermediate and small mass the opacity is mainly contributed by the bound-free and free-free transitions and can be approximated by the Kramers' law  $\kappa \propto \rho T^{-3.5}$ . The star on the Hayashi track is fully convective and its structure is represented by the Emden solution for  $N = 1.5$ . Introducing  $\theta \equiv T/T_c$ , which is called the Emden function, we have  $\rho/\rho_c = \theta^{1.5}$  and  $P/P_c = \theta^{2.5}$ . Substituting these relations into Eq. (13) and eliminating  $P_c$ ,  $\rho_c$  and  $T_c$  by using Eqs. (1), (2) and (9) we obtain

$$\nabla_{\text{rad}} \propto \theta^{-3.5} \frac{R^{0.5} L}{M^{5.5}} \left( \frac{L_r/L}{M_r/M} \right), \quad (14)$$

where  $L$  is the stellar luminosity. The energy release rate per unit mass,  $dL_r/dM_r$ , is proportional to  $T ds/dt$  according to the first law of thermodynamics. Therefore, we have  $L_r = \int_0^{M_r} (dL_r/dM_r) dM_r \propto (ds/dt) \int_0^{M_r} T dM_r$  because  $s$  is uniform in the star. Thus,  $L_r/M_r$  is proportional to the mean temperature inside  $M_r$ , which we write  $T_c \bar{\theta}$ . Because  $L$  is proportional to  $T_c ds/dt$ , Eq. (14) can be rewritten as

$$\nabla_{\text{rad}} \propto \theta^{-2.5} \left( \frac{\bar{\theta}}{\theta} \right) \frac{R^{0.5} L}{M^{5.5}}. \quad (15)$$

The Emden function  $\theta$  is a decreasing function of  $r/R$ . The mean interior temperature  $\bar{\theta}$  also decreases outward, but more slowly than  $\theta$ . Therefore,  $\nabla_{\text{rad}}$  takes a minimum value at the center  $r = 0$ . Because  $L$  is nearly proportional to  $R^2$  on the Hayashi track,  $\nabla_{\text{rad}}$  decreases as the star contracts, and finally becomes smaller than  $\nabla_s = 0.4$  at the center. In this way the convection stops at the center and a radiative core appears. With a radiative core the effective temperature  $T_{\text{eff}}$  becomes higher than the critical value  $T_{\text{eff}}^{(\text{cr})}$  which corresponds to the Hayashi line. As the star contracts, the radiative core grows and the star gradually moves away from the Hayashi line.

[Hayashi et al. \(1962\)](#) investigated numerically the evolution from the Hayashi phase to the main sequence via the Henyey track for some values of the stellar mass and showed the evolutionary paths on the HR diagram in their Fig. 10-2.

## 4 Pre-main Sequence Evolution of Low-mass Stars

In the case of low-mass stars we have to take into account some effects which are not important for the stars of  $M \gtrsim 1 M_{\odot}$ . One is the effect of H<sub>2</sub> molecules on the structure of the atmosphere and another is the electron degeneracy.

### 4.1 The Effect of H<sub>2</sub>-Dissociation Zone

As shown by [Hayashi and Hoshi \(1961\)](#),  $T_{\text{eff}}^{(\text{cr})}$  decreases as the stellar mass decreases when compared at a fixed stellar radius. Therefore, for stars of sufficiently small mass the H<sub>2</sub>-dissociation zone must lie inside the photosphere. The H<sub>2</sub>-dissociation zone has the effect of making the stellar envelope convectively unstable and suppressing the decrease of the effective temperature as the H-ionization zone does. [Hayashi and Nakano \(1963\)](#) investigated the pre-main sequence evolution of low-mass stars taking into account the effect of the H<sub>2</sub>-dissociation zone.

The H<sub>2</sub>-dissociation zone has been found to have a great effect. If the formation of H<sub>2</sub> molecules is neglected, the effective temperature on the Hayashi line decreases rapidly as the stellar radius decreases while with H<sub>2</sub> formation the decrease of the effective temperature is very slow as long as the stellar radius is somewhat larger than the limiting value of the degenerate star given by Eq. (6), as shown in figure 3 of [Hayashi and Nakano \(1963\)](#).

### 4.2 The Zero-Age Main Sequence and Its Minimum Mass

In the pre-main sequence stage of the stars with mass  $M \gtrsim 0.4 M_{\odot}$  the effect of electron degeneracy is negligible, and the central temperature  $T_c$  increases in proportion to  $R^{-1}$  as shown in Eq. (9). Finally at  $T_c \approx 10^7$  K the hydrogen burning sets in and soon the stars settle down on the main sequence (the zero-age main sequence: ZAMS).

ZAMS is the stage at which  $L_H = L$  holds for the first time in the pre-main sequence contraction phase, where  $L_H$  is the energy released by hydrogen burning in the star per unit time and  $L$  is the stellar luminosity or the energy emitted from the stellar surface per unit time.

$L_H$  is determined by the structure of the central part of the star though it is not completely independent of the structure of the outer part. If the star is in the Hayashi phase, the structure is represented by the polytrope of  $N = 1.5$ , and  $L_H$  can be determined easily for given  $M$  and  $R$  by using the Emden solution. To obtain  $L_H$  for a star on the Henyey track we have to begin by solving the stellar structure.

To determine  $L$  we have to solve in general the whole structure of the star from the center to the surface. The structure of the outer part is sometimes very important

in determining  $L$ . However, for the stars in the Hayashi phase,  $L$  for a given  $R$  can be determined easily if the Hayashi line is known. The cross point of the Hayashi line and the line of constant  $R$  in the HR diagram gives  $L$ .

Thus, to determine ZAMS for a given stellar mass  $M$  we need both  $L_H$  and  $L$  as functions of  $R$ . Schematically speaking, the cross point of the two curves  $L_H(R)$  and  $L(R)$  on the  $(\log R - \log L_X [L_H \text{ or } L])$  plane gives ZAMS.

For a star of not very small mass in which the effect of electron degeneracy is very small, the central temperature  $T_c$  increases in proportion to  $R^{-1}$  with contraction. The increase of  $L_H$  therewith is much steeper because the rate of the nuclear burning is very sensitive to the temperature.

As the star contracts along the Hayashi track,  $L$  decreases. If the star moves to the Henyey track,  $L$  turns to increase though very slowly. Because this increase is much slower than the increase of  $L_H$ , the two curves  $L_H(R)$  and  $L(R)$  on the  $(\log R - \log L_X)$  plane cross each other at some  $R$ , and the state of  $L_H = L$  is attained. In this way the ZAMS state is realized. When  $L_H$  has increased to a significant fraction of  $L$  on the Henyey track, the structure is affected by the increase of  $L_r$ , or by the increase of  $\nabla_{\text{rad}}$ , in the central region. As a result,  $L$  decreases just before the star settles down on the main sequence as shown in the figures of [Henyey et al. \(1955\)](#). Thus, to obtain the exact ZAMS state we have to solve the stellar structure accurately even by taking into account the effect of hydrogen burning.

For the stars which settle down to ZAMS on the Hayashi track, the start of hydrogen burning does not affect the stellar structure. By the increase of  $L_r$  in the core  $\nabla_{\text{rad}}$  increases. But  $\nabla_{\text{rad}}$  was larger than  $\nabla_s$  even before the hydrogen burning sets in. The start of the hydrogen burning just makes the star more convectively unstable, and the star keeps the polytropic structure with  $N = 1.5$ . Determination of ZAMS on the Hayashi track is much easier than that on the Henyey track.

As discussed in Sect. 2.2, the electron degeneracy becomes efficient at lower  $T_c$  for a star of smaller mass. The electron degeneracy has an effect of slowing down the increase of  $T_c$  with contraction, and in course of time  $T_c$  takes a maximum value at some  $R$ , and then decreases. Consequently,  $L_H$  takes a maximum value at some  $R$ , and then decreases. Such effect of electron degeneracy is important in determining ZAMS for low-mass stars with  $M \lesssim 0.2M_\odot$ . The maximum value of  $L_H$  decreases so fast as the stellar mass  $M$  decreases that the two curves  $L_H(R)$  and  $L(R)$  on the  $(\log R - \log L_X)$  plane do not cross or touch each other, and the state of  $L_H = L$ , or ZAMS, cannot be realized at the stellar mass  $M$  smaller than some critical value. This critical value is the lower-mass limit to the main sequence, or the hydrogen-burning minimum mass.

There is a paper which claims to have determined the hydrogen-burning minimum mass by assuming the value of  $L$  ([Kumar 1963](#)). However, the hydrogen-burning minimum mass is not known beforehand, nor is the luminosity of the star of this mass when it settles down on the main sequence as discussed by [Nakano \(2012\)](#).

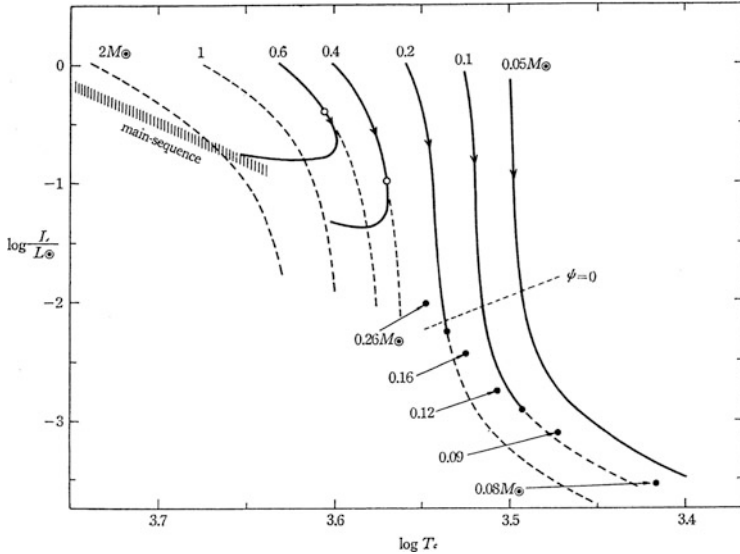


**Fig. 1** The evolutionary paths (solid lines) and the positions of ZAMS (filled dots) of low-mass stars on the HR diagram. The open circles on the evolutionary paths indicate the stage at which the fully convective phase ends. The evolutionary path of a star of mass  $M = 0.05 M_{\odot}$  is also shown. This star cannot settle down on ZAMS, and contracts to the limiting radius given by Eq. (6) cooling down indefinitely. The solid lines except below the open circles and the thick dashed lines are the Hayashi lines. The thin dashed line represents the state of  $\psi = 0$  where the effect of the electron degeneracy becomes nonnegligible for the fully convective stars. This is a copy of figure 2 of [Hayashi and Nakano \(1963\)](#)

### 4.3 Numerical Results

[Hayashi and Nakano \(1963\)](#) investigated the pre-main sequence evolution for the stars of mass  $M \leq 0.6 M_{\odot}$ . Their results are shown in Fig. 1, which is a copy of their figure 2.

The open circles on the evolutionary paths in Fig. 1 (solid lines) indicate the stage at which the fully convective phase ends. Afterwards the radiative core grows and the star moves to the Heney track. The length of the Heney track until the star arrives at the main sequence is shorter for stars of smaller mass. The stars with  $M \leq 0.26 M_{\odot}$  do not experience the phase on the Heney track. When these stars settle down on the main sequence, they have the fully convective structure. The filled dots in Fig. 1 show the positions of ZAMS for some values of the stellar mass down to  $0.08 M_{\odot}$ .

[Hayashi and Nakano \(1963\)](#) also investigated the evolution of a star of mass  $M = 0.07 M_{\odot}$ . The evolutionary sequence of this star is shown in Table 1, which is a reproduction of their table III. In this table,  $\psi$  in the first column represents the degree of electron degeneracy, or the chemical potential of the

**Table 1** The evolutionary sequence of a star of  $M = 0.07 M_{\odot}$  with the population I chemical composition. This is a reproduction of table III of [Hayashi and Nakano \(1963\)](#)

$\psi^a$	$\log L/L_{\odot}$	$\log T_{\text{eff}}$	$\log R/R_{\odot}$	$\log T_c$	$\log \rho_c(\text{g cm}^{-3})$	$L_{\text{H}}/L$	Age ( $10^8$ year)
3.0	-2.90	3.48	-0.89	6.52	2.43	0.015	0.8
5.0	-3.23	3.45	-0.99	6.54	2.74	0.090	1.5
7.0	-3.45	3.42	-1.05	6.52	2.82	0.17	3.1
9.0	-3.63	3.40	-1.09	6.49	3.05	0.23	4.6
11.0	-3.74	3.38	-1.12	6.45	3.26	0.19	6.2

<sup>a</sup>  $\psi$  is the degree of electron degeneracy, or the chemical potential of the electron divided by  $kT$

electron divided by  $kT$ . The effect of electron degeneracy becomes nonnegligible around the state of  $\psi = 0$ , which is shown by the dashed line in Fig. 1 for the fully convective stars. In the stars with uniform  $s$ ,  $\psi$  is also uniform. Around the stage  $\psi = 5.0$  the central temperature takes the maximum value  $\log T_c \approx 6.54$ , and thereafter the core gradually cools down. At  $\psi \approx 9.0$ ,  $L_{\text{H}}/L$  takes the maximum value  $\approx 0.23$  and then decreases. This maximum value is far below the value for the steady state hydrogen burning,  $L_{\text{H}}/L = 1$ . Therefore, this star cannot attain the ZAMS state. In this way [Hayashi and Nakano \(1963\)](#) concluded that the hydrogen burning minimum mass is between 0.08 and  $0.07 M_{\odot}$ .

This is for the population I chemical composition. The abundance of heavy elements might have some effect on the Hayashi line, and then on the hydrogen-burning minimum mass, through the opacity. [Hayashi and Nakano \(1963\)](#) confirmed that the minimum mass is hardly affected by the change of the heavy element abundance even by a factor of 5, although it is significantly affected by the change of the helium content through the change of the mean molecular weight of electrons  $\mu_e$ . Because it is known now that the helium content is almost the same for population I and II, the hydrogen-burning minimum mass for the population II stars is almost the same as the one for the population I stars.

The stars of mass smaller than this critical value cool down indefinitely, and are now called brown dwarfs. [Hayashi and Nakano \(1963\)](#) investigated the evolution of a star of mass  $M = 0.05 M_{\odot}$  as an example of such stars although the term “brown dwarf” was not yet used in those days (see the chapter by J. Tarter in this volume). The evolutionary path of this star on the HR diagram is shown in Fig. 1. This must be the first evolutionary path of brown dwarfs drawn on the HR diagram.

The lithium burning becomes efficient around  $T \approx 3 \times 10^6$  K, significantly lower than the temperature of hydrogen burning. Lithium in the stellar envelope is depleted by the burning near the bottom of the convective envelope in the pre-main sequence stage. For the star of larger mass the radiative core appears at a lower central temperature. Therefore, the amount of lithium depletion in the atmosphere depends on the stellar mass. [Hayashi and Nakano \(1963\)](#) investigated this dependence at  $M \geq 0.4 M_{\odot}$ . At the smaller stellar masses where the electron degeneracy can be efficient, the maximum central temperature attained during the contraction is lower for the smaller stellar mass. As seen from Table 1, the maximum  $T_c$  for the star of  $M = 0.07 M_{\odot}$  is  $3.5 \times 10^6$  K. At slightly smaller  $M$ , lithium hardly burns. Later on

it was pointed out that the abundance of lithium in the stellar atmosphere can be used to test whether the candidate stars for brown dwarfs are really brown dwarfs or not (e.g., [Rebolo et al. \(1992\)](#), see also the chapters by R. Rebolo and G. Basri in this volume).

Finally, I would like to point out that the newest results I know give the hydrogen-burning minimum mass between 0.08 and  $0.075 M_{\odot}$  ([Burrows et al. 1997](#)), which is almost the same as the results of [Hayashi and Nakano \(1963\)](#).

## References

- Burrows, A., Marley, M., Hubbard, W.B., Lunine, J.I., Guillot, T., Saumon, D., Freedman, R., Sudarsky, D., Sharp, C.: A nongray theory of extrasolar giant planets and brown dwarfs. *ApJ* **491**, 856–875 (1997)
- Chandrasekhar, S.: An Introduction to the Study of Stellar Structure. Dover, New York (1939)
- Hayashi, C.: Stellar evolution in early phases of gravitational contraction. *PASJ* **13**, 450–452 (1961)
- Hayashi, C., Hoshi, R.: The outer envelope of giant stars with surface convection zone. *PASJ* **13**, 442–449 (1961)
- Hayashi, C., Nakano, T.: Evolution of stars of small masses in the pre-main-sequence stages. *Prog. Theor. Phys.* **30**, 460–474 (1963)
- Hayashi, C., Hoshi, R., Sugimoto, D.: Evolution of the stars. *Prog. Theor. Phys. Suppl.* **22**, 1–183 (1962)
- Henyey, L.G., LeLevier, R., Levée, R.D.: The early phases of stellar evolution. *PASP* **67**, 154–160 (1955)
- Kumar, S.S.: The structure of stars of very low mass. *ApJ* **137**, 1121–1125 (1963)
- Nakano, T.: In: Umemura, M., Omukai, K. (eds.) First Stars IV—From Hayashi to the Future, pp. 15–21. American Institute of Physics, New York (2012)
- Rebolo, R., Martín, E.L., Magazzù, A.: Spectroscopy of a brown dwarf candidate in the Alpha Persei open cluster. *ApJ* **389**, L83–L86 (1992)
- Sandage, A.: Observational approach to evolution. II. A computed luminosity function for K0-K2 stars from  $M_v = +5$  to  $M_v = -4.5$ . *ApJ* **125**, 435–444 (1957)
- Sandage, A.R., Schwarzschild, M.: Inhomogeneous stellar models. II. Models with exhausted cores in gravitational contraction. *ApJ* **116**, 463–476 (1952)

# Brown Is Not a Color: Introduction of the Term ‘Brown Dwarf’

Jill Tarter

**Abstract** This contribution provides a very brief, personal comment on the remarkable past five decades of progress in our understanding of small-mass objects that try, but do not succeed in stably fusing hydrogen. This article describes the origin of the term ‘brown dwarf’ as introduced by me in 1975.

## 1 Introduction

Four decades ago I was working on a Ph.D. thesis with Prof. Joseph Silk trying to understand the composition of the matter that the community was then calling the ‘missing mass’ in the Coma Cluster and within the Milky Way Galaxy – the ‘bricks in the interstellar medium’ that Prof. George Field used to quip could remain hidden from all our astronomical instruments. I was interested in finding out whether something between small stars and big planets might do the job. Prof. P.J.E. Peebles was an external member of my thesis committee, so I was familiar with his work on models for Jupiter and Saturn (Peebles 1964), and my literature searches had revealed the early work of Prof. Shiv Kumar on low mass, degenerate ‘black dwarfs’, and ‘red’ dwarfs (Kumar 1963); objects he sometimes called infrared (IR) dwarfs. From the start, it was obvious that we needed another name for them because all suggested names had some difficulties with them. ‘Failed star’ might equally refer to a mass too small to fragment within a molecular cloud; black dwarf was already used as the end-point of classical white dwarf cooling; red dwarfs were successful stars making their living by fusing hydrogen; and since early in their lives these objects might be detectable in the visible, the IR label wasn’t right either. I casually suggested ‘brown’ dwarf as somewhere between red and black on

---

J. Tarter (✉)  
SETI Institute, 189 Bernardo Avenue, Mountain View, CA 94043, USA  
e-mail: [tarter@seti.org](mailto:tarter@seti.org)

**Table 1** Earlier suggested names for brown dwarfs (from Tarter 1986)

Suggested name	By	Problem with the suggested name
Lilliputian Star	Shapley (1958)	Not stars: no equilibrium H burning
Black Dwarf	Kumar (1963)	Already means the end product of a chemically evolved White Dwarf
Infrared Dwarf	Davidson (1975)	Too predictive: implies they are observable only in the IR whereas they may be young and hot or old and very cold
“Jupiters” or Super-Jupiters	Many authors	They do not necessarily require a star about which to orbit and may have formed in a fashion very different from the formation of the gas giant planets in a planetary system
Extreme Red Dwarf	Few authors	Admits a confusion about the end of the hydrogen-burning main sequence rather than defining a difference
Sub-stellar Objects	Reynolds et al. (1980)	Can apply to planets as well

a color palette – later I would have better reasons for this choice. Table 1 lists some other names that were suggested early-on and reasons why they weren’t particularly appropriate. Joe Silk at first demurred and then accepted my terminology ‘brown dwarf’ and we pushed ahead.

## 2 My 1975 Ph.D. Thesis

The fourth chapter of my 1975 Ph.D. thesis from UC Berkeley is entitled “Brown Dwarf Stars and How They Grew Old”. This marks the first written use of the term brown dwarfs. To investigate whether these objects could constitute the missing mass, it was necessary to determine their cooling curves (how long they would remain visible, at what frequencies) for an assumed initial mass function and birthrate. My thesis was all about observable consequences and not about getting the equation of state for these exotic objects exactly correct. I needed to know how bright they would be for how long. Given the ties between UC Berkeley and the Lawrence Livermore Laboratory, it seemed natural to make use of the extensive work by Harold Grabske, Allan Grossman and their co-authors. These physicists were using modified bomb codes to compute the interior structures of low-mass stars or deuterium-burning stellar-wannabes as correctly as possible (Grossman and Grabske (1973) and previous papers in series). A complicated process of extrapolation eventually gave me what I needed. If only David Stevenson had finished his excellent work on just this topic (Stevenson 1978) a bit sooner, I could have saved myself huge effort and ended up with simpler cooling curves.

Based on the extrapolated cooling curves, and a set of models for stellar initial mass and birthrate functions for galaxies in the Coma Cluster and the Milky Way, I tried to predict the observable parameters of these objects as a guide to searching for them with the *Space Infrared Telescope Facility* (SIRTF). All those decades ago, SIRTF was still the shuttle IR telescope facility being developed at NASA Ames which was later named *Spitzer Space Telescope*. At the time, the opacity tables for the low temperatures, densities, and pressures relevant for these objects were not very good. The idea of fitting an atmosphere onto an interior model in order to calculate a color temperature was not justified. In my thesis these objects were treated as black body radiators at the effective temperatures given by their cooling curves. This is the real reason that brown dwarf was an appropriate name. It was not feasible to compute a color temperature, therefore the name should not imply a color. No less than Edmond Land, of Polaroid fame, had remarked to a friend of mine working in his lab that brown was not a color; Joe Silk didn’t think that brown was a color. Therefore, astronomical objects with unpredictable color temperatures could reasonably be called brown dwarfs. In the modern era, we know that their atmospheric molecular composition makes them bluer than one might have expected from their effective temperatures.

### 3 Post-thesis Interactions with Brown Dwarfs

After finishing my thesis, I was able to work as a postdoc with the SIRTF team at NASA Ames to better understand how to search for these objects. The cooling curves from my thesis and from Stevenson’s paper were extrapolated by the SIRTF group and others preparing for *Hubble Space Telescope* to predict how many brown dwarfs would be found by these future instruments. In the end, neither of these instruments was responsible for the first discovery. For me, the proximity to John Billingham’s newly-formed “Interstellar Communications Committee” at Ames was too tempting, and I began to consider how one might search for extraterrestrial technological civilizations; something that turns out to be far harder than searching for brown dwarfs (e.g., [Tarter et al. \(2010\)](#) for a recent review on the Search for Extra Terrestrial Intelligence (SETI)).

I did not reconnect with brown dwarfs until a decade later, when a false positive claim led to the organization of a topical conference at George Mason University. At that first Brown Dwarf Symposium, I presented a paper with a title similar to this contribution and provided a summary of the rationale for the term ([Tarter 1986](#)), as well as a summary of the thesis results that I had never managed to get past a referee and into publication. Clearly that explanation of the name didn’t satisfy everyone either then or now. As recently as 2009 Ken Brecher gave an amusing talk at a meeting of the *American Astronomical Society* entitled “How, Now, Brown Dwarf?” in which he criticized the name (he prefers the term infrared dwarf). He also showed off a flashlight that he said emitted the color of a brown dwarf; that particular red-orange color can be rendered on the RGB scale as: R-235, G-75,



*"Face it—in this town, either you're a star or you're just another brown dwarf."*

**Fig. 1** Cartoon from Mick Stevens published in the New Yorker magazine issue 01/08/1996 (Reprinted with permission by The Cartoon Bank)

B-3 ([Brecher 2009](#)). But the entire point of choosing a non-color for the name was to avoid being too prescriptive before we knew whether these objects actually existed. Furthermore, no one color can describe the full range of brown dwarfs whose temperatures and atmospheric compositions vary widely over the spectral classes M to Y. I'm not inclined to take criticism of the name very seriously. As a profession, we've managed to work around lots of historic misnomers, whose designations purported to refer to one thing, when they actually measured another. The question 'What is' is far more important than 'what should be'. I think we ought leave the last word to Francesca D'Antona, who titled her [1998](#) conference summary paper 'Brown Is Now A Color' ([D'Antona 1998](#)).

The first discoveries and confirmations of brown dwarfs did not come until 1994–1995 ([Rebolo et al. 1995](#); [Nakajima et al. 1995](#); [Oppenheimer et al. 1995](#); [Basri et al. 1995, 1996](#)) two decades after my thesis work. While I was extraordinarily excited by these discoveries, it was something far more mundane that made me feel that my choice of a name had actually made an impact; a 1996 cartoon in the New Yorker magazine! I actually purloined that magazine from my doctor's office, cut out this cartoon and hung it on my office door where it survived for many years. The cartoon image is of two cool Hollywood types sitting at a restaurant table (Fig. 1). The male is telling the female, "Face it - in this town either you're a star or you're just another

brown dwarf”. I figured that if the term brown dwarf had made it into our comedic lexicon, then the name was certainly here to stay.

I was also delighted years later, when a group of summer students at the *Very Large Array*, a famous radio observatory, ignored the wisdom of their advisors and used their precious allotment of antenna time to look at LP 944-20, a brown dwarf that had been previously reported as flaring in X-Rays. Score one for the students; this brown dwarf was, in fact, an unexpectedly strong radio source – they got lucky (Berger et. al. 2001). Right now we are using the *Allen Telescope Array* to explore confirmed and candidate exoplanets seeking evidence of radio technologies from distant civilizations. Since it now looks like every star has a planet, we are planning to augment the current exoplanet target list with our nearest 100 neighboring systems. In March of 2013 the WISE mission informed us that the previously-unknown third closest system to the Sun, at just over 2 pc away, in fact consists of a binary pair of brown dwarfs (Luhman 2013). Therefore, I will once again be getting up close and personal with brown dwarfs, combining those now successful searches for elusive substellar objects with our not-yet-successful search for Extra Terrestrials (ET). Conventional wisdom suggests that there are many reasons why brown dwarfs and ET should not be co-located, but for the sake of thoroughness, we will conduct the volume-complete observations. That is the appropriate, systematic way to move forward; like those students at the VLA, we too might get lucky. To quote the last sentence of the first SETI paper “The probability of success is difficult to estimate; but if we never search, the chance of success is zero” (Cocconi and Morrison 1959).

The 22 March 2013 issue of Science magazine contains a report of a very high-resolution spectrum obtained by directly imaging HR 8799c – a young giant exoplanet with an atmospheric temperature of 1,100 K (Konopacky et al. 2013). The spectrum shows the presence of water and carbon monoxide, but no methane. The perspective discussing this paper (Marley 2013) contains a remarkable rendered image that attempts to compare the cloud layers, composition, and vertical mixing in HR 8799c, a modeled 1,100 K brown dwarf (spectral class T), and a giant planet with atmospheric temperature of 125 K. Over the past 50 years, brown dwarfs have taken us on a remarkably interesting journey from a lack of evidence, and dubious credibility, to the brown dwarf database BDNYC (<http://www.bdnyc.org>) listing 875 objects and discussions of atmospheric dynamics involving clouds of sulfides, Mg-silicates, iron metal liquid, perovskite, and corundum. I wonder where they will take us next.

**Acknowledgements** I want to acknowledge the assistance that Viki Joergens has provided in preparing this text. Without her persistent prodding and editorial skills, my words would never have found their way into this anniversary volume. It is a privilege to have my thoughts associated (by proximity) with the fascinating research that now accompanies what was, within my lifetime, previously undetectable.

## References

- Basri, G., Marcy, G.W., Graham, J.R.: The first lithium brown dwarf: PPL 15. In: American Astronomical Society Meeting Abstracts #186, Pittsburgh. Bulletin of the American Astronomical Society, vol. 27, p. 1214 (1995)
- Basri, G., Marcy, G., Graham, J.: Lithium in brown dwarf candidates: the mass and age of the faintest Pleiades stars. *ApJ* **458**, 600 (1996)
- Berger, E., 13 co-authors: Discovery of radio emission from the brown dwarf LP944-20. *Nature* **410**, 338–340 (2001)
- Brecher, K.: How, now, brown dwarfs? *BAAS* **41**, 273 (2009)
- Cocconi, G., Morrison, P.: Searching for interstellar communications. *Nature* **184**, 844–849 (1959)
- D'Antona, F.: Conference summary: brown is now a color. In: Rebolo, R., Martín, E.L., Zapatero Osorio, M.R. (eds.) *Brown Dwarfs and Extrasolar Planets*, Proceedings of a Workshop held in Puerto de la Cruz, 17–21 Mar 1997. ASP Conference Series, vol. 134, p. 545
- Davidson, K.: Does the solar system include distant but discoverable infrared dwarfs? *Icarus* **26**, 99–101 (1975)
- Grossman, A.S., Graboske, H.C.: Evolution of low-mass stars. V. Minimum mass for the deuterium main sequence. *ApJ* **180**, 195–198 (1973)
- Konopacky, Q.M., Barman, T.S., Macintosh, B.A., Marois, C.: Detection of carbon monoxide and water absorption lines in an exoplanet atmosphere. *Science* **339**, 1398–1401 (2013)
- Kumar, S.S.: The structure of stars of very low mass. *ApJ* **137**, 1121–1125 (1963)
- Luhman, K.L.: Discovery of a binary brown dwarf at 2 pc from the sun. *ApJ Lett.* **767**, 6–12 (2013)
- Marley, M.S.: Probing an extrasolar planet. *Science* **339**, 1393–1394 (2013)
- Nakajima, T., Oppenheimer, B.R., Kulkarni, S.R., Golimowski, D.A., Matthews, K., Durrance, S.T.: Discovery of a cool brown dwarf. *Nature* **378**, 463 (1995)
- Oppenheimer, B., Kulkarni, S.R., Matthews, K., Nakajima, T.: Infrared spectrum of the cool brown dwarf Gl 229B. *Science* **270**, 1478 (1995)
- Peebles, P.J.E.: The structure and composition of Jupiter and Saturn. *ApJ* **140**, 328–347 (1964)
- Rebolo, R., Zapatero Osorio, M., Martín, E.: Discovery of a brown dwarf in the Pleiades star cluster. *Nature* **377**, 129 (1995)
- Reynolds, R.T., Tarter, J.C., Walker, R.G.: A proposed search on the solar neighborhood for substellar objects. *Icarus* **44**, 772–779 (1980)
- Shapley, H.: *Of Stars and Men: The Human Response to an Expanding Universe*, p. 60. Beacon Press, Boston (1958)
- Stevenson, D.J.: Brown and black dwarfs - their structure, evolution and contribution to the missing mass *Proc. Astron. Soc. Aust.* **3**, 227–229 (1978)
- Tarter, J.C.: An historical perspective: Brown is not a color. In: Kafatos, M.C., Harrington, R.S., Maran, S.P. (eds.) *Astrophysics of Brown Dwarfs*, pp. 121–138. Cambridge University Press, Cambridge/New York (1986)
- Tarter, J.C., Agrawala, A., Ackermann, R., et al.: SETI turns 50: five decades of progress in the search for extraterrestrial intelligence. *Proc. SPIE* **7819**, 1 (2010)

# Teide 1 and the Discovery of Brown Dwarfs

Rafael Rebolo

**Abstract** In 1995, after many years of intense observational efforts, brown dwarfs were finally discovered in a star cluster and also orbiting a star. The work that led to the discovery and characterization of the brown dwarf Teide 1 is described here. This very red object was detected in optical images of the central region of the Pleiades cluster obtained by our group with the IAC80 telescope (Teide Observatory, Tenerife) in January 1994. Follow-up spectroscopy in December 1994 with the 4.2 m William Herschel Telescope (Roque de los Muchachos Observatory, La Palma) confirmed its cool nature. Teide 1 was one of the coolest objects known at that time and the coolest found in a star cluster. The location, photometric and spectroscopic properties, the measured proper motion and kinematics fully supported membership in the young Pleiades cluster and set strong constraints on its age. According to evolutionary models the low luminosity and cool atmospheric temperature of such a young object implied a mass significantly below the minimum required for stable hydrogen burning. On 22 May 1995, we submitted to *Nature* a manuscript reporting the discovery of Teide 1. By the time of the publication, on 14 September 1995, we had already extended the survey and found other similar objects in the Pleiades cluster, among them, Calar 3. Evidence for full preservation of lithium in the atmospheres of these two brown dwarfs was obtained with the Keck telescope on 20–21 November 2005. These early findings suggested the existence of a large number of brown dwarfs in the Pleiades and indicated by extrapolation that billions of these objects could populate our Galaxy. Subsequent surveys have confirmed such a numerous population of brown dwarfs. Remarkably, the nearest brown dwarf to the Sun may still remain undetected.

---

R. Rebolo (✉)

Instituto de Astrofísica de Canarias, C/Via Láctea s/n 38200, La Laguna, Tenerife, Spain

e-mail: [rjl@iac.es](mailto:rjl@iac.es)

## 1 Introduction

On 14 September 1995, our group at Instituto de Astrofísica de Canarias published in vol. 377 of the journal *Nature* the article entitled “Discovery of a brown dwarf in the Pleiades star cluster” by Rebolo, Zapatero Osorio and Martín. We reported the discovery of Teide Pleiades 1 (hereafter Teide 1) and claimed its brown dwarf nature on the basis of the photometric, spectroscopic and astrometric/radial velocity information that we had obtained using several telescopes in the Canary Islands (Spain). The result was highlighted in the front page of the journal issue with a remarkable editorial statement “Brown dwarfs exist – official”. As time went on and additional data was obtained, our claim of the substellar nature of Teide 1 was not disproved; on the contrary, the substellar condition of the object was reinforced, and Teide 1 remains classified today as a brown dwarf.

The paper announcing the discovery of Teide 1 was the culmination of research initiated by our group in the early 1990s. I will describe in the following sections details on how, when, why and who carried out the work that led to this discovery and immediate follow-up work. In those years, there was a large interest to know if nature could produce brown dwarfs and, if so, to establish the main properties of these objects. Many research groups were very active in the field: some were searching for brown dwarfs in star clusters and star-forming regions, and others were searching for low-luminosity objects around nearby stars and free floating in the general field. Other surveys aimed to detect microlensing events which could reveal a population of these very faint objects in the halo or in the bulge of our Galaxy.

In spite of decade-long efforts to find brown dwarfs, all proposed candidates were controversial in the early 1990s. In 1994, at the ESO Workshop “The Bottom of the Main Sequence – and Beyond” organised by C. Tinney, the existence of brown dwarfs was still under debate, partly because we did not reliably know the atmospheric properties (photometric and spectroscopic characteristics) of objects unable to burn hydrogen. After briefly describing the context and some aspects of early searches for brown dwarfs in clusters and in the field, I will then focus on our own studies that led to the discovery of Teide 1 and the first brown dwarfs in the Pleiades.

## 2 Brown Dwarf Searches in the Early 1990s

Since the original proposal by S. Kumar about the formation and evolution of brown dwarfs, young stellar clusters and star-forming regions were the focus of many of the searches for these elusive objects. Several candidates were reported in young stellar clusters like the Pleiades (Jameson and Skillen 1989; Stauffer et al. 1989, 1994) and star-forming regions like  $\rho$  Ophiuchi (Rieke and Rieke 1990) or Taurus (Stauffer et al. 1991), but their luminosities and effective temperatures were consistent with

those predicted for stars just above the hydrogen-burning limit; hence, the substellar nature for these candidates could not be reliably established at that time. The same was true for low-luminosity objects detected in the general field. The uncertainty in the ages prevented any firm conclusion on their nature. These objects could be either very low-mass stars or young brown dwarfs.

The luminosity and atmospheric temperatures of low-mass stars remain stable during the long duration of the hydrogen-burning phase, the so-called main-sequence phase. On the contrary, the atmospheres of brown dwarfs are expected to cool down continuously as time progresses, reaching temperatures, at sufficiently old ages, far below the minimum temperatures reached by the stars. At very early stages of evolution, a brown dwarf may display atmospheric temperatures similar to those of much older low-mass stars, making it difficult to distinguish among them. In particular, this difficulty applied to the very interesting object GD 165B (Becklin and Zuckerman 1988; Zuckerman and Becklin 1992) whose spectral energy distribution was rather unusual at that time and suggestive of a rather low atmospheric temperature. The age of this system was not well known, and therefore, the mass was not well constrained. At the end of the 1990s, other objects with similar spectral energy distribution were identified (e.g. Kirkpatrick et al. 1999), and it became clear that GD 165B was the first identified object of the new spectral class designated with “L”. While the classification as L type is indicative of a rather low atmospheric temperature (below approx. 2,000 K), it is not a guarantee, however, for the absence of hydrogen-burning in the interior. As we will see below, the detection of the fragile element lithium in the atmosphere of L-type dwarfs is a proof of a mass below the minimum required for stable hydrogen-burning. Lithium has been detected in many L-type dwarfs, thus confirming their brown dwarf nature, but not yet in GD 165B, for which neither a dynamical mass has been determined, and therefore, its substellar nature is not established yet.

## 2.1 Our First Approach to the Brown Dwarf Problem

In March 1990, while conducting observations at the 2.5 m Isaac Newton Telescope (INT, Observatory Roque de los Muchachos, La Palma) for a spectroscopic programme on pre-main-sequence lithium depletion in low-mass young stars (with E. Martín, Ph.D. student at that time, and A. Magazzù, staff of the Catania Observatory), I used to check the presence of faint companions by increasing the contrast of the display of the acquisition camera (Fig. 1). Unexpectedly, we noticed the presence of a faint object close (2–3 arcsec) to UX Tau A, a member of a known young pre-main-sequence binary in the Taurus star-forming region. This faint third component of the binary system, which would be named UX Tau C, prompted many interesting questions to us. The object had been noticed first by G. Herbig (see Jones and Herbig 1979), but very little was known about it.

We obtained spectroscopy for the three components of the system in order to carry out a spectral characterization and to investigate the presence of lithium (Fig. 2). We found prominent Li 670.8 nm resonance lines in the three

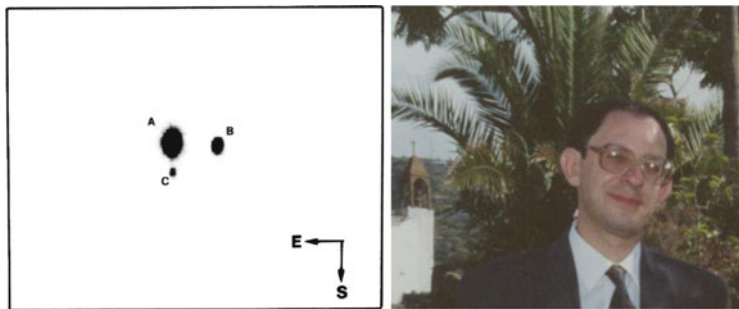


**Fig. 1** *Left:* Image of the young, pre-main-sequence triple system UX Tau in the Taurus star-forming region obtained with the acquisition camera at the 2.5 m INT (Magazzù et al. 1991). *Right:* A. Magazzù in the early 1990s

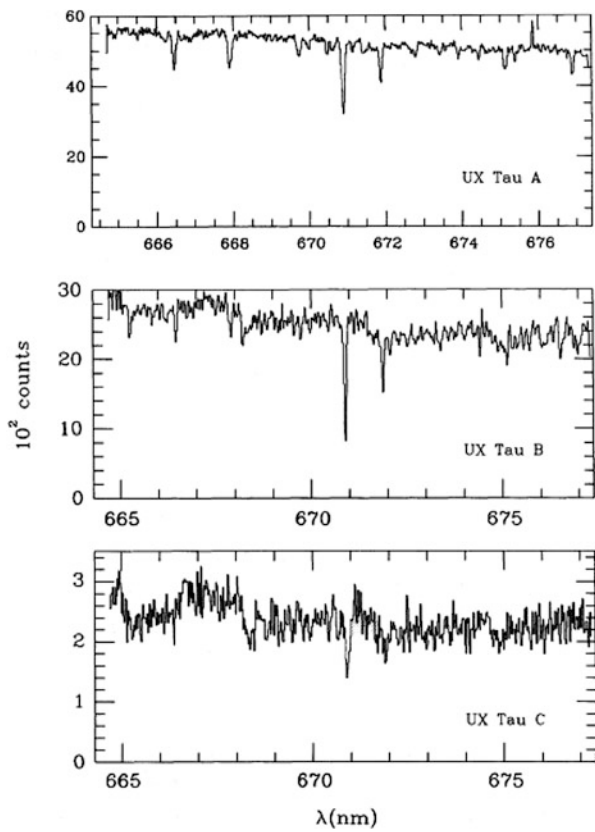


**Fig. 2** Spectroscopy of the three components in the UX Tau system. The lithium resonance line at 670.8 nm is detected in all the components (after Magazzù et al. 1991)

components. According to evolutionary models (D'Antona and Mazzitelli 1985), we determined that UX Tau C, with spectral type M6, was close to the hydrogen-burning limit (Magazzù et al. 1991), but a dynamical mass determination was not feasible given the large physical separation (hundreds of AUs) from the object to the primary star. Such large separation implies very long orbital periods and will require observations of the system extended over many decades.

Was UX Tau C a brown dwarf? We still do not know with confidence the mass of this very young and low-luminosity object. At the typical age of the Taurus star-forming region (1–2 Myr), its mass must be very close to the substellar limit, but evolutionary models are rather uncertain at these very young ages (see I. Baraffe, this volume), preventing a reliable mass estimate from the luminosity and effective temperature. The set of observations that we acquired for UX Tau C prompted our interest on brown dwarfs and led us to further important considerations on the role that lithium could play to establish the substellar nature of a brown dwarf candidate.

### 3 The Lithium Test

How can we distinguish objects above and below the hydrogen-burning mass limit? In the late 1980s and early 1990s, we were conducting observational programmes to investigate the rate of lithium destruction in the early evolution of low-mass stars. This research was carried out mainly in collaboration with R. J. García López (a former student of mine), E. Martín and visiting senior collaborators Y. Pavlenko and A. Magazzù. Our work led to a series of papers on lithium in T Tauri stars (Magazzù and Rebolo 1989; Magazzù et al. 1992), in the low-mass stars of the Pleiades cluster (García López et al. 1991, 1994) and in post T Tauri stars (Martín et al. 1992). It was obvious that fully convective very low-mass stars are very efficiently depleting lithium, as these are fully convective objects, and the minimum core temperature for hydrogen-burning is significantly higher than the minimum temperature for lithium burning. It was also expected that a brown dwarf of sufficiently low mass would never reach in its core the temperature to burn lithium and would therefore preserve the initial lithium content (Rebolo 1991; Magazzù et al. 1991; Pozio 1991).

At that time I was also working with other colleagues on a search for super Li-rich carbon stars (Abia et al. 1991, 1993). These very cool stars display extremely prominent Li resonance lines in their spectra. It was natural to establish the link between the two programmes and realise that sufficiently low-mass brown dwarfs with insufficient mass to reach the lithium-burning temperature in their cores would preserve lithium and this lithium could be observed in their spectra via the resonance line at 670.8 nm as the atmospheric temperatures would be similar to those of the coolest carbon stars (Rebolo 1991). The use of lithium spectroscopy as a criterion for substellarity was published as the “lithium test for brown dwarfs” (Rebolo et al. 1992). Later, this test has been used widely to identify brown dwarfs and continues to be used today. For example, it was applied to establish the substellar nature of

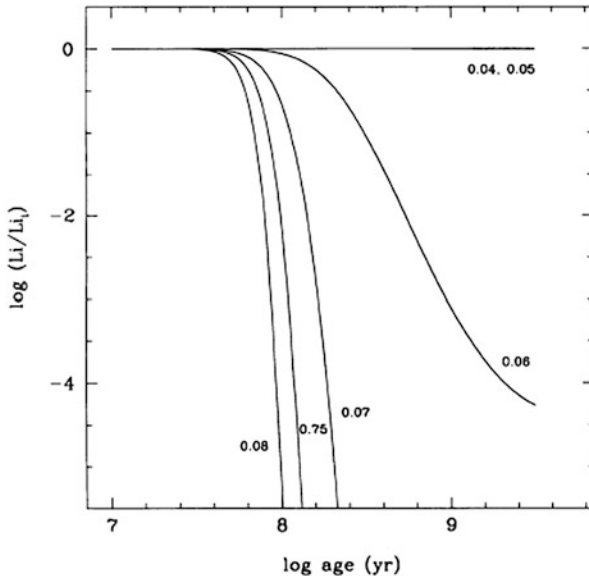


**Fig. 3** Lithium depletion curves for objects with masses above and below the hydrogen-burning limit (original figure from Magazzù et al. 1993). Li abundance is given in logarithmic scale with respect to the initial lithium content,  $\text{Li}_i$ . Note the typo in the label 0.75 which should read 0.075. Mass labels are in units of the solar mass. It can be seen that objects with 0.07–0.08 solar masses deplete lithium to levels of the order 0.01% in less than 200 Myr, while objects of 0.04–0.05 solar masses do not deplete any lithium

the nearest ( $d \sim 2$  pc) L-dwarf to the Sun, recently reported by Luhman (2013). At the time of our test proposal, it was not so easy to find lithium in brown dwarf candidates, mainly because the available candidates were in fact not so low-mass objects.

Between 1992 and 1993, we started an extensive programme to search for lithium in brown dwarf candidates; we used telescopes at La Palma and at La Silla Observatories with disappointing results. No single candidate was confirmed (Magazzù et al. 1993; Martín et al. 1994). We observed a large fraction of the coolest objects reported in the literature with little success. Among them were some remarkable objects, such as Gl 569 B (Forrest et al. 1988), which at that time was not known to be a binary itself. The dynamical mass estimates for the two components of this binary have been later measured at 0.068 and 0.057 solar masses (Zapatero Osorio et al. 2005). Likely, the lower-mass component in this system has preserved a fraction of its original lithium content. Another interesting object, HHJ 10 (PPI 10) with spectral type M5.5, was among the faintest objects discovered in the Pleiades at that time (Stauffer et al. 1994), but our spectrum did not show any evidence for lithium. At the age of the Pleiades cluster ( $\sim 120$  Myr), we find a sharp lithium destruction precisely at the hydrogen-burning mass limit, as we see in Fig. 3. Objects close to the hydrogen-burning frontier (0.075 solar masses) may retain some of its

initial lithium. The preserved amount depends on the age of the cluster. Clearly, low-luminosity Pleiades members showing a full preservation of lithium would be brown dwarfs.

## 4 A Search for Brown Dwarfs in the Pleiades: Chronology of the Discovery of Teide 1

By mid-1993, we decided to carry out our own search for brown dwarfs in the Pleiades star cluster, and I submitted a project to the IAC Research Board requesting the award of a Ph.D. student grant to help in this research. Maria Rosa Zapatero Osorio, who at that time just graduated at University Complutense de Madrid, was awarded one of these 1993 IAC Ph.D. grants. In October 1993, she joined our small group (see Fig. 4) and started to work on this project as Ph.D. student under my supervision. She took major responsibility for the imaging and photometry work in the Pleiades. Eduardo Martín was then a postdoctoral researcher at IAC.

### 4.1 *First Photometry of Teide 1*

We did take advantage of the recently built IAC80 telescope to conduct an imaging search in the Pleiades at red optical wavelengths (R band and I band). The set of observations that led to the discovery and characterization of Teide 1 started with a photometric campaign at the IAC80 on 5–7 January 1994. The IAC80 had started scientific operation very recently. It was equipped with a camera which offered a modest field of view, adequate for a systematic search for brown dwarfs in a few degrees of the cluster area. Our goal was to find cluster members with colours of dwarfs of spectral type later than M7 (Fig. 5).

Previous searches in the cluster had frequently made use of V and I filters (centred in the blue and red part of the optical spectrum, respectively). Such ultracool dwarfs have very red colours of V-I more than 4.5 magnitudes (implying that the difference between the fluxes emitted in the V and I bands is close to a factor 100). For this reason, the observations in V band were very demanding in terms of exposure time, so we decided to use the reddest optical filters R (600 nm) and I (850 nm) for our search. Cluster ultracool dwarfs were expected to show a colour of R-I more than 2 (i.e. approx. a factor 5 in flux between these two bands). The observing programme was designed with exposure times for each filter that would facilitate detection of such cool dwarfs in the Pleiades, if they were brighter than magnitude I = 19. The regions to be observed were mainly selected in areas previously surveyed by R. Jameson and I. Skillen who had used the 2.5 m Isaac Newton Telescope in 1986 to conduct a search for brown dwarfs in the cluster. The time baseline between their survey and ours was almost 8 years, sufficient



**Fig. 4** In the *left* image, María Rosa Zapatero Osorio at her office in the Instituto de Astrofísica de Canarias (IAC). *Right*: Eduardo Martín and Rafael Rebolo at Museo del Cosmos, next to IAC Headquarters in La Laguna (Tenerife)

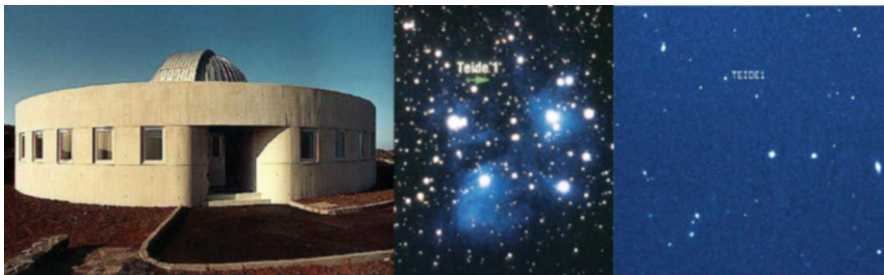


**Fig. 5** The IAC80 telescope at Teide Observatory (*left* image). The location of Teide 1 in the Pleiades cluster (*middle panel*) and image of this brown dwarf obtained at the Nordic Optical Telescope (*right*)

to measure the proper motion of any interesting candidate we could find in both surveys and establish its membership in the cluster.

After reduction of the data of the first useful campaign at the IAC80 (Fig. 6), a red object ( $R-I > 2$ ) with magnitude  $I = 18.8$  was particularly interesting. This object was not previously reported by any other surveys (including Jameson and Skillen) so we decided to obtain additional more precise photometry with a larger telescope. This was possible on 1 May 1994 at the Nordic Optical Telescope (Roque de los Muchachos Observatory, La Palma). The red colour of the object was confirmed as  $R-I = 2.74 \pm 0.10$ , and the brown dwarf candidate became a truly interesting object which deserved full spectroscopic characterization. We designated this object as Teide Pleiades 1 following the same kind of convention that J. Stauffer had recently adopted for his search from Palomar Observatory which led to the series of Palomar Pleiades objects (PPI objects; Stauffer et al. 1994; Fig. 6).

CAMPANAS DE OBSERVACIÓN			
1:	9-11 Nov 1993 → NOT CAT	Imagen directa → Pleíades CCD IAC	Mal tiempo
2:	20-22 Nov 1993 → JKT CAT	Imagen directa → Pleíades CCD Tek	Mal tiempo
3:	8-15 Dic 1993 → TCS CAT	CVF fotometría IR	Estrellas A → Pistas. técnicas
4:	30-31 MAYO 1994 → TCS 1-3 JUN 1994 CAT	CVF fotometría IR	Estrellas A
5:	5-7 ENERO 1994 → IAC80 Comisioning	Imagen directa → Pleíades (fotom. mov. propio) CCD	
6:	13-14 ENERO 1994 → NOT Intercambio	Imagen directa → Pleíades CCD IAC	Mal tiempo
7:	1-3 FEB 1994 → IAC80 Comisioning	Imagen directa → Pleíades CCD	fotometría Halo
8:	30 ABRIL 1994 → NOT 1 MAYO 1994 Servicio	Imagen directa → Halo CCD IAC	mov. propio
9:	29-30 Mayo 1994 → IAC80 Comisioning	CM Dra Halo	
10:	28-31 Julio 1994 → IAC80 1-3 Agosto 1994 Comisioning	CM Dra Halo	
11:	5-9 OCT 1994 → IAC80 Comisioning	Pleíades	2 noches buenas (fotometría)
12:	22-28 OCT 1994 → IAC80 Comisioning	Pleíades m's M (rotación)	5 noches buenas

**Fig. 6** Maria Rosa's original manuscript notes (in Spanish) of the first observing campaigns she carried out for her Ph.D. thesis work. After four nights of bad weather (marked in the list with “mal tiempo”) which affected the first two Pleiades campaigns with labels number 1 and 2, campaign number 5 at the IAC80 on 5–7 January 1994 led to the detection of Teide 1. This campaign was shortly followed by campaign number 6 at the Nordic Optical Telescope (NOT) with unfortunate non-photometric conditions. The campaign listed with number 8 at NOT provided precise photometry of Teide 1 on 1st May 1994 which was reported at the discovery paper. Campaigns 11 and 12 in October 1994 and other subsequent campaigns extended the Pleiades survey to detect additional brown dwarfs

## 4.2 First Spectroscopy of Teide 1

A first spectrum of Teide 1 was obtained on 14 October 1994 at the 2.5 m INT using observing time awarded to E. Martín and me (see log in Fig. 7). This 1,800 s

## INT observing log for night: Fri 14 Oct 1994

Observers: Eduardo Martín, Rafael Rebolo, Emilio Harlaftis

Telescope operator: Jose Norberto Glez

Support astronomer: Emilio Harlaftis

Tape: INTD

Focus: CASS

Instrument: IDS

Collimator: AgRed

Pixels: 1124x1124

Pixel size (microns): 24.0 Window: X1= -49, Xs=1124, Y1= 1, Ys=1123; Binning: in X=1, in Y=1

Run No.	Object name	RA	DEC	Eqnx	Eqny	UT start	ZD start	HA start	Time sec	Air mass	GDX	GDY	Slit H	PA o	PA l	Grat o	Grat l	Cen.
65	PLEIAID BD	03:47:16.6	24:12:08	05:34	29.4	02:10	1800.0	1.148	503815	584029	2.16	270.0	74	105.81	766			
66	CU NE	03:47:17.7	24:12:06	06:08	36.9	02:44	0.0	1.249	503273	584029	2.16	270.0	74	105.81	766			
67	JET	03:46:06.2	34:06:29	06:13	14.0	01:00	300.0	1.030	503273	584029	2.16	270.0	108	105.81	766			
68	CUNE	03:46:06.1	34:06:29	06:21	15.6	01:08	1.0	1.038	503273	584029	2.16	270.0	105	105.81	766			
69	HD 19445 FLUX	03:45:28.6	26:09:04	06:29	49.3	03:44	30.0	1.530	503273	584029	2.16	270.0	73	105.81	766			
70	JET	03:46:05.5	34:06:15	06:32	17.8	01:19	400.0	1.050	503273	584029	2.16	270.0	102	105.81	766			
71	CUNE	03:46:05.6	34:06:14	06:41	19.7	01:28	1.0	1.062	503273	584029	1.73	270.0	99	105.81	766			
72	HR1664 FAST ROT	05:33:54.7	14:18:25	06:56	28.4	01:45	10.0	1.137	503273	584029	2.16	270.0	55	105.81	766			
73	CUNE	05:33:54.7	14:18:25	06:59	29.1	01:48	1.0	1.144	503273	584029	2.16	270.0	55	105.81	766			
74	HR1664	05:33:54.6	14:18:26	07:02	29.6	01:51	5.0	1.149	503273	584029	2.16	270.0	56	105.81	766			
75	FLAT LAMP + ND	07:32:40.3	97:51:33	07:09	68.7	-00:00	5.0	2.735	503273	584029	2.16	269.9	180	105.82	769			
76	FLAT LAMP + ND	07:34:25.3	28:34:10	07:10	0.2	-00:00	5.0	1.000	503273	584029	2.16	270.0	33.5	105.82	769			
77	FLAT LAMP + ND	07:36:10.0	28:34:10	07:12	0.2	-00:00	5.0	1.000	503273	584029	2.16	270.0	33.5	105.81	766			
78	FLAT LAMP + ND	07:37:54.6	28:34:09	07:14	0.2	-00:00	5.0	1.000	503273	584029	2.16	270.0	33.5	105.81	766			
79	FLAT LAMP + ND	07:39:39.1	28:34:09	07:16	0.2	-00:00	5.0	1.000	503273	584029	2.16	270.0	33.5	105.81	766			
80	Bias frame	07:43:25.9	28:34:10	07:19	0.2	-00:00	5.0	1.000	503273	584029	2.16	270.0	33.5	105.81	766			

Fig. 7 Log of the first spectroscopic observations of Teide 1 at the 2.5 m Isaac Newton Telescope on 14 October 1994. The object designated as PLEIAD BD is Teide 1



**Fig. 8** The 4.2 m William Herschel Telescope at Roque de los Muchachos Observatory (La Palma) was used for the final spectroscopic characterization of Teide 1

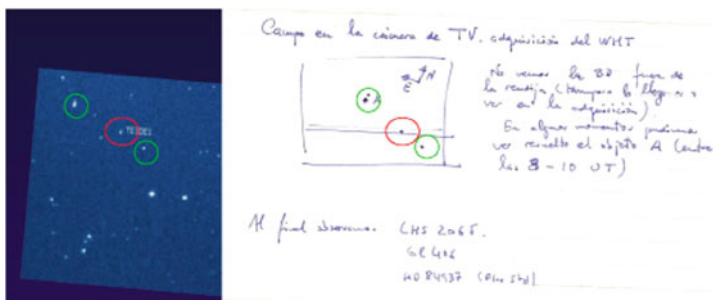


**Fig. 9** Diagrams and manuscript notes produced by R. Rebolo during the spectroscopic observations of Teide 1 with the 4.2 m WHT on 29 December 1994. *Left:* Image obtained at the NOT showing Teide 1 (red circle) and other nearby objects. *Right:* The manuscript diagram depicts the objects seen in the acquisition camera of the 4.2 m telescope during the spectroscopic run. The horizontal line in the diagram represents the slit of the spectrograph. Encircled in red, the object identified as Teide 1 sits on the slit. Some reference objects are encircled in green

exposure spectrum was never published, as the quality was just sufficient to confirm that the object was indeed a very red dwarf. This encouraged us to obtain a much better spectrum as soon as possible. On 29–30 December 1994, E. Martín and I obtained a much better quality spectrum of our brown dwarf candidate using the spectrograph ISIS of the 4.2 m William Herschel Telescope (Figs. 8, 9 and 10). This spectrum was later published in the discovery paper. Two exposures of 3,600 and 2,200 s were taken around midnight followed by the corresponding CuNe lamp for wavelength calibration (this lamp provided a good set of spectral lines with known


**WHT observing log for night: 1994 Dec 29/30**

Observers: R. Rebolo, E. Martínez; M. Breage, N. Walton  
 Support astronomer: M. Breage  
 Telescope operator: J. Rey  
 PATT/CAT ref.: C14; V39  
 Weather: GOOD, few high clouds  
 Seeing (first half, arcsec): 1.0  
 Temp. (first half, °C): 4.4  
 Humidity (first half, %): 76  
 Telescope focus: 97.10  
 Focal station: CASS  
 Instrument: ISIS  
 Dichroic: 6100  
 Programme: El objeto menos luminoso de las  
 Phase of moon: D

Arm	RED	BLUE	POS	AUX	UES
Detector:	TEK2	TEK1	FOS	TEK5	
Pixel-size(microns):	1124X1124	1124X1124	400X590	1124X1124	-
Collimator focus:	24	24	24	24	
	10403	6001			

window red changed from run 132286 onwards: start 0,295 size 1124,400

Windows (bottom-corner, size): 1,250 1123,500 (R) 1,285 1123,400 (B) 0,0 0,0 (F) 0,0 0,0 (A) 0,0 0,0 (U) 0,0 0,0 ( )

Number	Object name	RA hh:mm:ss.ss	Dec. dd:mm:ss.s	Eqnx. UT yyyy:hh:mm	Airm. sec	I Exp. PA	Sky PA	Sli wid"	Slit len"	Grat A	Cew /r	AutogX /theta	AutogY filt f	Aux P
132280	PLBD	03:44:18.45	24:13:15.9	B1950 23:28 1.033	3600	295.0		0.925		R158R	7492	25002	169998 B	
132281	PLBD	03:44:18.45	24:13:15.8	B1950 00:29 1.131	R	2200	285.0	0.925		R158R	7492	25002	169998 B	
132282	CUNE	03:44:18.44	24:13:15.8	B1950 01:08 1.242	R	4	285.0	0.925		R158R	7492	25002	169998 R	
132283	LHS2065	09:51:05.61	-03:18:07.1	B1950 01:13 1.445	R	600	317.0	0.925		R158R	7492	25002	169998 R	
132284	FLUXST	09:46:12.56	13:58:41.6	B1950 01:25 1.401	R	30	300.0	0.925		R158R	7492	20975	160000 R	4U
132285	CUNE	09:46:12.59	13:58:42.1	B1950 01:28 1.389	R	4	300.0	0.925		R158R	7492	20975	160000 R	
132286	CUAR 30 SEC	10:47:01.40	17:16:30.6	J2000 01:37 1.662	B	30	293.0	1.097		R158B	4896	20975	160000 R	
132287	CUAR 2 SEC	10:47:01.39	17:16:30.6	J2000 01:38 1.659	R	2	293.0	1.097		R158R	7541	20975	160000 R	
132288	CUNE 2 SEC	10:47:01.39	17:16:30.6	J2000 01:41 1.631	R	2	293.0	1.097		R158R	7541	16988	109002 R	
132289	CUNE 7 SEC	10:47:01.39	17:16:30.6	J2000 01:41 1.628	B	7	293.0	1.097		R158B	4896	16988	109002 R	
132290	SW1994AE R FIL	10:47:01.39	17:16:30.6	J2000 01:46 1.592	A	10	293.0					16988	109002 R	
132291	SW1994AE VFILT 1	10:47:01.39	17:16:40.6	J2000 01:50 1.561	A	10	293.0					16988	109002 V	
132292	SW1994AE BFILT 3	10:47:02.09	17:16:40.6	J2000 01:55 1.529	A	30	293.0					16988	109002 B	
132293	SW1994AE IFILT 3	10:47:02.79	17:16:40.6	J2000 01:57 1.512	A	30	293.0					16988	109002 I	
132294	SW1994AE UFFILT 1	10:47:02.79	17:16:40.6	J2000 02:00 1.496	A	120	293.0					16988	109002 U	
132295	SW1994AE UFFILT 3	10:47:02.79	17:16:40.6	J2000 02:03 1.477	A	300	293.0					16988	109002 U	
132296	SW1994AE 200S	10:47:01.39	17:16:30.3	J2000 02:14 1.412	R	200	293.0	1.097		R158R	7450	16988	109002 U	
132297	SW1994AE 200S	10:47:01.39	17:16:30.4	J2000 02:14 1.410	B	200	293.0	1.097		R158B	4927	16988	109002 U	
132298	SW1994AE 300S	10:47:01.38	17:16:30.4	J2000 02:19 1.385	B	300	293.0	1.097		R158B	4927	16988	109002 U	

**Fig. 10** Log of observations (page 2) of the spectroscopic campaign carried out at WHT on 29–30 December 1994. Teide 1 was designated in the log as PLBD (coordinates of the telescope R.A 03:44:18.45 Dec +24:13:15.8, B1950)

wavelengths which covered well the spectral range of our observations). We also observed the field ultracool dwarf LHS 2065 and a flux standard star, both with the same instrument configuration than Teide 1. These objects were taken to control the instrumental response and check for any systematic effect introduced by the spectrograph. Interestingly, as it can be seen in the official log of the telescope, that same night we observed supernova SN 1994AE, as part of a completely different research programme aimed to obtain spectroscopy of recent supernova explosions.

The comparison of the spectra obtained for Teide 1 and LHS 2065 was straightforward and very exciting. We already realised at the telescope control room that both objects had very similar spectral energy distributions. Teide 1 was then classified as a M9 dwarf (we would revise this later to M8). Only half a dozen objects of this spectral type were known in the whole sky at that time (in fact we had searched for lithium in many of them). Given the small space density of such ultracool dwarfs, it was very unlikely that our new object was a contaminant nearby field dwarf in the line of sight of the cluster. Already in the course of the observations we became aware of the high probability that Teide 1 was indeed a very cool member of the Pleiades cluster. A demonstration of membership in the cluster was of exceptional importance since this would set strong constraints on the age of the object which would then constrain its mass using state-of-the-art evolutionary models. It was therefore very important to investigate the kinematics of Teide 1 and

confirm that it was consistent with the well-known kinematic properties of Pleiades stars. We therefore concentrated our efforts to measure (a) the radial velocity using the Doppler effect caused by the relative speed of the object with respect to the observer and (b) the motion in the plane of the sky of the object with respect to very distant stars.

After reduction of the spectra, back at the IAC headquarters, we worked with Maria Rosa to determine a radial velocity via cross-correlation with other M-dwarf spectra which we had observed the same night at the end of December. We found the radial velocity of Teide 1 was consistent with that of brighter Pleiades cluster stars (average value of 5.9 km/s, Rosvick et al. 1992).

In the following months, using the images recorded in 1986 by Jameson and Skillen, we measured the proper motion of Teide 1, which also resulted consistent with membership in the Pleiades. Teide 1 was recorded in the 1986 images, although the object was not previously noticed/reported, possibly because it was located at the edge of the detector in a region where the photometry was considered uncertain. However, we found these images extremely useful for astrometry.

Based on the photometric, spectroscopic and astrometric data, we arrived to the conclusion that the new object was the coolest- and lowest-luminosity dwarf ever found in the Pleiades. According to all the evolutionary models available to us (Burrows and Liebert 1993; D'Antona and Mazzitelli 1995; Nelson et al. 1993; Baraffe et al. 1995), its mass had to be significantly below the hydrogen-burning mass limit; therefore, we concluded that Teide 1 was a brown dwarf.

### **4.3 Writing, Submission and Publication of the Discovery Paper**

We wrote our manuscript in the first months of 1995 and submitted the article to *Nature* on 22 May 1995. At that time it was also known to us that the M6 dwarf PPI 15 (discovered by Stauffer et al. 1994) had a little amount of lithium left in the atmosphere (detected by G. Basri et al. 1996). PPI 15 was sitting precisely at the border between stars and brown dwarfs in the Pleiades. It was impossible to say at that time whether it was a star or a brown dwarf. However, the small lithium abundance in the atmosphere of PPI 15 was a very good indication that the brown dwarf frontier was at reach. Teide 1, at least one magnitude fainter in the I band than PPI 15 and with a much lower luminosity, was well located in the brown dwarf domain.

In the spring of 1995, we had a fluent exchange of information with Gibor Basri who made us participants of his discovery of lithium in PPI 15, and we informed him about the discovery of Teide 1 prior to submission of our paper. We established a collaboration aimed at further characterization of these and other objects and in particular at searching for lithium in Teide 1 using the Keck telescope.

## LETTERS TO NATURE

## Discovery of a brown dwarf in the Pleiades star cluster

R. Rebolo, M. R. Zapatero Osorio & E. L. Martín

Instituto de Astrofísica de Canarias, 38200 La Laguna, Tenerife, Spain

BROWN dwarfs are cool star-like objects that have insufficient mass to maintain stable nuclear fusion in their interiors. Although brown dwarfs are not stars, they are expected to form in the same way, and their frequency of occurrence should reflect the trends seen in the birthrates of low-mass stars. But finding brown dwarfs has proved to be difficult, because of their low intrinsic luminosity. The nearby Pleiades star cluster is widely recognized as a likely host for detectable brown dwarfs because of its young age—the still-contracting brown dwarfs should radiate a large fraction of their gravitational energy at near-infrared wavelengths. Here we report the discovery of a brown dwarf near the centre of the Pleiades. The luminosity and temperature of this object are so low that its mass must be less than 0.08 solar masses, the accepted lower limit on the mass of a true star<sup>1–3</sup>. The detection of only one brown dwarf within our survey area is consistent with a smooth extrapolation of the stellar mass function of the Pleiades<sup>4</sup>, suggesting that brown dwarfs, although probably quite numerous in the Galactic disk, are unlikely to comprise more than ~1% of its mass.

Only about half a dozen extremely cool dwarfs with spectral types M9 or later have been identified<sup>5</sup>. At present they are the best candidates for brown dwarfs. Their mass–luminosity and mass-spectral-type relationships<sup>6,7</sup> show that these objects are indeed very close to the substellar limit, but uncertainties in

**Fig. 11** Abstract of the Letter to *Nature* in vol. 377 reporting the discovery of Teide 1 (Rebolo et al. 1995)

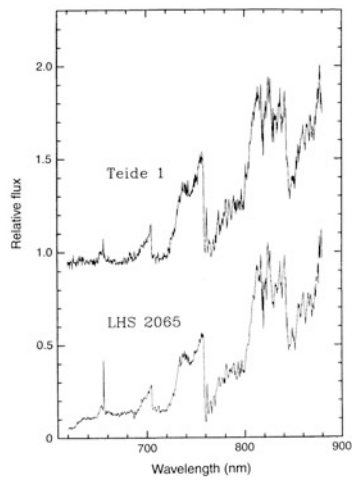


FIG. 1. The optical spectrum of Teide 1 (upper trace) and of the M9 dwarf LHS 2065 (lower trace). The flux scale of both spectra is normalized to unity at 825 nm. An offset has been added to the spectrum of Teide 1 for clarity.

In the summer, we received the report from the anonymous referees selected by *Nature* who made some comments and questions and requested some clarifications. In general they were positive about our work. We elaborated a response to these reports as quickly as possible, and fortunately, our response was well received by both referees and the editor; so on 14 August 1995, the paper was accepted and finally published on 14 September 1995 (Fig. 11).

A few sentences extracted from the last paragraph of the published article are worth considering here:

We have presented compelling evidence for membership of an M9 dwarf in a young open cluster of known age. This allowed us to estimate an upper limit for the mass that is below the substellar borderline, and conclude that the body is a brown dwarf. It is encouraging that our survey to limiting magnitude  $I = 19$  ( $R = 21.5$ ) so far covering only  $\sim 0.3\%$  of the total Pleiades cluster area has provided one object of this nature. This was, in fact, what we had expected from a smooth extrapolation of the available mass function of the cluster. This extrapolation predicts that 175 brown dwarfs in the mass range  $80\text{--}40 \text{ M}_{\text{Jup}}$  may be present in the cluster, forming one of the most populated mass intervals . . . .

Subsequent work has shown that indeed an abundant population of brown dwarfs exist in the Pleiades cluster which extends down to  $20\text{--}25 \text{ M}_{\text{Jup}}$  (see e.g. Bihain et al. 2006, 2010). Our original estimates on the number of brown dwarfs in this cluster appear basically correct, as several tens of brown dwarfs are already identified and very likely many more, particularly the least massive ones, remain to be found.

#### **4.4 Immediate Follow-up Work After the Publication of Teide 1**

Our immediate goals after the publication of Teide 1 were essentially two: (a) to extend the imaging search for other similar objects in the Pleiades and in other clusters and (b) to obtain further spectroscopic characterization of Teide 1 and any new candidates found in our search.

In September, just after the publication of Teide 1, we had deadlines for submission of proposals to the telescopes in Calar Alto and in the Canary Islands. As it is written in the proposal submitted to the WHT on 30 September 1995 (see Fig. 12), we already had identified 9 brown dwarf candidates in the Pleiades with similar colours and magnitudes than Teide 1. These candidates resulted from imaging campaigns at the Calar Alto 2.2 m telescope in November 1994, with the IAC80, the NOT and other telescopes.

Among the new brown dwarf candidates, the most remarkable one was Calar 3. We were able to confirm with spectroscopy about 7 weeks later that Calar 3 is a likely twin of Teide 1 with a brightness of  $I = 19$  and very similar photometric colours (Fig. 13).

### **5 Lithium in Teide 1 and Calar 3**

On 20–21 November 1995 and thanks to the collaboration with Gibor Basri and Geoff Marcy, our group had access to the Keck telescope to obtain spectroscopy of Teide 1 and study the presence of lithium. Before the observing campaign, Eduardo and I met Gibor and Geoff in Berkeley to prepare the details of the observations. Then the four of us travelled to Hawaii.

It was a memorable campaign. Our expectation was that two nights of spectroscopy at the largest optical telescope in the world should be sufficient to show the presence of lithium in Teide 1. We had agreed that we would invest any available time to observe Teide 1 while the target was high in the sky. We also had Calar 3 in the list of targets and some other promising field dwarfs, but observing time would be invested in them only if we had a successful detection of lithium in Teide 1. The observations were very successful as it can be seen from the log of observations (see its first page in Fig. 14) handwritten by Gibor. The observations were carried out under very good weather and atmospheric conditions, as it is written in the log with “clear skies” and sub-arcsecond seeing (Figs. 14 and 15).

The first night we took several spectra of Teide 1, the first two spectra were exposed 3,600 s each and then three spectra were taken of 4,800 s each. After Teide 1, we obtained spectroscopy of UX Tau C which we knew had lithium in the atmosphere. This would provide a good reference spectrum against which we could compare any detection of lithium in Teide 1. While Gibor and Geoff controlled the instrument, Eduardo and I reduced the spectra using IRAF. The combination of the first two spectra already gave a marginal detection of lithium in Teide 1. We



# INSTITUTO DE ASTROFÍSICA DE CANARIAS

38200-La Laguna. Tenerife. (Islas Canarias)

Teléfono: (922) 60 52 00; Telex 92640 iace e; Telefax: (922) 60 52 10

## PETICIÓN DE TIEMPO DE OBSERVACIÓN (CAT NOCTURNO)

Observatorios del Roque de Los Muchachos y del Teide

©JCN

- 1.** Título (Máx. 10 palabras): Palabras clave: 1  2  3  4  5  6   
Espectroscopía de candidatos a enana marrón en los cúmulos de las Pléyades y Praesepe.

- 2. Investigador Principal** Centro  
María Rosa ZAPATERO OSORIO Instituto de Astrofísica de Canarias, IAC

### Coinvestigadores

- Rafael REBOLO IAC  
Eduardo L. MARTÍN IAC

### Contacto Principal

Nombre: María Rosa ZAPATERO OSORIO  
Dirección: Instituto de Astrofísica de Canarias  
Vía Láctea S/N  
38200 La Laguna, Tenerife

Teléfono: (922) 605369  
FAX: (922) 605210  
E-MAIL: mosorio@iac.es (Internet)

**3. Resumen del Programa:**

Como resultado de la búsqueda fotométrica que nuestro grupo está realizando en las Pléyades, hemos encontrado 9 nuevos candidatos a enana marrón con fotometría similar a Teide 1 y, por tanto, dentro del dominio subestelar admitido para el cúmulo, sugiriéndose un aparente incremento en la función de luminosidad, hasta hoy día desconocido, para las magnitudes más débiles y los colores más rojos [ $I>18$ ,  $(R-I)>2.3$ ]. Con esta propuesta pretendemos obtener la espectroscopía de baja resolución que nos permita confirmar la pertenencia de estos nuevos objetos a las Pléyades. Un resultado afirmativo implicaría que el número de enanas marrones con  $18<I<19$  presentes el cúmulo sería  $\sim 30$  veces mayor que el número estimado a partir las funciones de luminosidad más recientes que hay para las Pléyades y, por tanto, la contribución de estos objetos a la masa total del cúmulo sería mucho mayor que la esperada. Para la segunda parte de la noche, proponemos la espectroscopía de los objetos menos luminosos y más fríos en Praesepe con el fin de seguir caracterizando la baja secuencia principal muy próxima al límite subestelar de los cúmulos abiertos en la Galaxia.

- 4. ¿Es parte de una Tesis?**  Nombre del doctorando: María Rosa ZAPATERO OSORIO

**5. Tiempo de observación solicitado:**

Telescopio	Instrumento y detector	Noches	Luna	Fechas óptimas	Fechas imposibles
WHT	FOS-II	2(1)	0	Febrero	Las restantes

Justificar las fechas imposibles: Por la posición de los objetos.

Comentarios: Es importante que el cúmulo de las Pléyades esté visible el mayor tiempo posible, y en el semestre 96A ocurre para el mes de febrero.

- 6. Fecha/Firma Investigador Principal** Fecha/Firma Director Centro

30/09/1995

R. Rebolo

**Fig. 12** First page of the proposal submitted on 30 September 1995 to the Spanish Allocation Time Panel of the Telescopes in the Canary Islands. Just 2 weeks after the publication of the discovery paper of Teide 1, we state in the first and second line of the abstract “hemos encontrado 9 nuevos candidatos a enana marrón con fotometría similar a Teide 1...” which is translated as “we have found 9 new brown dwarf candidates with similar photometry to Teide 1”. The proposal requested spectroscopic observations with the WHT to confirm these new brown dwarf candidates found by our group in the Pleiades

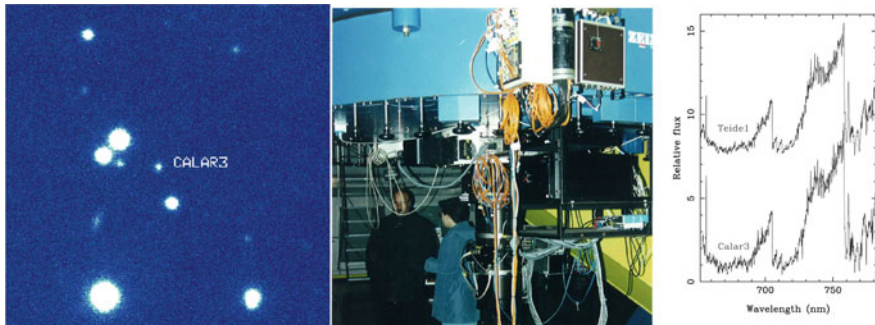


**Fig. 13** Identification chart for Calar 3 (*left*), which is the second brown dwarf discovered by our group. M. R. Zapatero Osorio and R. Rebolo at the Calar Alto 3.5 m telescope in 1995 (*centre*). At the *right*, spectra of Calar 3 and Teide 1 obtained at Keck on 20–21 November 1995 (Rebolo et al. 1996)

were very excited. The combination of the three next spectra provided a definitive detection. The strength of the 670.8 nm resonance line was consistent with full preservation of the initial content of lithium. In addition to the resonance line, we did detect the subordinate lithium line at 812.6 nm.

The observations went so well that during the second night we decided to obtain spectroscopy of Calar 3. We also detected lithium in this object with strength consistent with full preservation of this element. Overall, this was a very satisfying confirmation of our ideas about the lithium test and a demonstration of the consistency between evolutionary models and observations. On my return to Tenerife, after several long flights, I had already drafted a Letter to report these findings which would be eventually published a few months later in *The Astrophysical Journal* with the title “Brown dwarfs in the Pleiades cluster confirmed by the lithium test” (Rebolo et al. 1996). A strong destruction of lithium was quite apparent in PPI 15 and located this object in the frontier between stars and brown dwarfs. In 1996 it was impossible to establish with any confidence the nature of PPI 15, while Teide 1 and Calar 3 were fully confirmed as brown dwarfs (see Figs. 16 and 17).

## 6 Subsequent Brown Dwarf Discoveries

One year after the discovery of Teide 1, several bona fide brown dwarfs in the Pleiades cluster had been identified (Zapatero Osorio et al. 1997; Bouvier et al. 1998) and the first measurements of the Pleiades substellar mass function were published (Fig. 18).

In subsequent years, tens of brown dwarfs were discovered in the Pleiades (see e.g. Bihain et al. 2010) and in other clusters and star-forming regions (e.g.



KECK HIRES SPECTROGRAPH OBSERVING LOG					
Observer(s): Baeri, Marc J., Rebolo, Martin		Chip(s):			
U.T. Date: 21 Nov 95		Binning:	$1x1 \rightarrow 2x2$	Decker:	
Tape Number:		Windowing:	0 - 2047 col 700 - 1400 row	Slit: 0.7" and 1.0"	
G-RATING: 1200 g/mm angle					
Focus: 2620 Camera:  low gain					

Tp #	Object	Time		Comments	
		Start (U.T.)	$\Delta$ (s)		
1	Ne-Ar	05:07	2	Slit = 0.7"	FWHM = 3.5" OG 570
2	Dark	05:10	1	"	
3	Flat	05:12	4	"	3600 DN OG 570
4	Flat	05:15	30	"	OG 570
5	Ne Ar	05:17	2	Slit = 1.0" (test)	FWHM = 4.1
6	Ne Ar	05:21	2	"	no filter FWHM 3.7
7	Ne Ar	05:25	2	slit = 0.7"	FWHM = 2.5
8	vB 10	05:27	300	seeing = 0.7" 2000 raw DN/pixel no filter 300 DN/pixel + Li	Li expected 1753
9	PC0025	05:48	3600	Clear Skies 0.8" seeing	Hα at 1980
10	Flat	06:55	30	Saturated	
11	Teide 1	07:07	3600	upper spectrum start = 7:07	
12	"	08:08	3600		
13	Flat	09:20	5	slit changed to 1.0" no filter	
14	"	09:22	5		
15	Teide 1	09:25	4800	Clear Skies	
16	Ne Ar	10:51	2		
17	Flat	10:53	5	22,000 DN/pixel	
18	Flat	10:55	3	BINNING x2 in rows, no binning along slit = 1"	dispersion
19	Flat	10:57	3	no filter	
20	Ne Ar	10:58	2		

**Fig. 14** Log of the spectroscopic observations at the Keck telescope which led to the discovery of lithium in Teide 1

Luhman et al. 2000; Comerón et al. 2000; Lodieu et al. 2012). In the general field, following the discovery of Kelu 1 (Ruiz et al. 1997), hundreds of brown dwarfs were identified by large-scale surveys (DENIS and 2MASS, SDSS, UKIDDS, Pan-STARRS and WISE). Cluster and field searches have provided a unique insight

KECK HIRES SPECTROGRAPH OBSERVING LOG					
Observer(s): Basri, Marcy, Rebolo, Martin	Chip(s):	Binning: (2x2)	Decker:	Slit: 1.0"	
U.T. Date: 21 Nov 95		Windowing: col 0-2047	Focus:	2620	
Tape Number:		Ech-Ang: row 350 to 700	Camera:		
	XD-Ang:				
		Grating			

Tp #	Object	Time		Comments	
		Start (U.T.)	$\Delta$ (s)		
21	Teide 1	11:04	4800	Binning 1x2, slit=1"	no filters
				seeing ~ 0.2"	
22	Teide 1	12:35	4800	Clear Sky	
23	UX Tau C	13:58	200	guided carefully on C; excluded A	
24	HHJ339	14:04	600		
25	G-191B2B	14:19	20		
26	G-191B2B	14:20	90		
27	V410 X3	14:26	390		strong <sup>2</sup> paper
28	V410 X6	14:36	300		
29	LHS 2065	14:53	120		
30	"	14:57	300		
31	NeAr	15:04	2		
32	Flat	15:06	3		no filters
33	Flat	15:07	3		
34	Prsospe	15:27	300	2048x2048 IMAGING MODE R filter	
35	"	15:28	300	I filter	moved the field about <del>1</del> 36 pixels I field
37	LHS 2065 field	15:44	3	I filter	
38	"	15:47	3	R filter	
39	Done flat		3	R filter	
40	Done flat	16:12	6	R filter	
41	Done I flat	16:14	6	I filter	
42	"	16:17	6	I filter	

Fig. 15 Log of the spectroscopic observations at the Keck telescope which led to the discovery of lithium in Teide 1

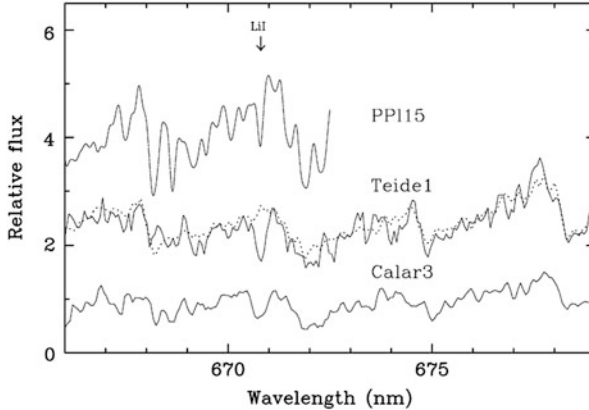


**Fig. 16** Spectra displaying the Li resonance line at 670.8 nm in Teide 1, Calar 3 and PPI 15 (After Rebolo et al. 1996). The dotted line displays for comparison the spectrum of the ultracool dwarf vb10 with no evidence for the Li line

on the substellar initial mass function down to a few times the mass of Jupiter (Béjar et al. 2011).

Gliese 229 B (Nakajima et al. 1995) and G 196-3B (Rebolo et al. 1998) were the first examples of brown dwarfs imaged as stellar companions. Many more have been detected since then, including companions to very nearby stars as epsilon Indi (McCaughrean et al. 2004). The detection of brown dwarfs in binary/multiple systems is of crucial importance since they provide dynamical mass determinations (Zapatero Osorio et al. 2005; Stassun et al. 2006; Dupuy et al. 2010) which are a key to understand the evolution of these objects (see Baraffe, this volume).

Today, a lot is known about the L and T dwarfs, but new challenges appear with the discovery of even cooler objects, the Y dwarfs (Cushing et al. 2011; Kirkpatrick et al. 2012; see also Cushing, this volume). These new spectral classes will likely describe old very low-mass brown dwarfs and (not so old) planetary mass objects with several times the mass of Jupiter (Leggett et al. 2013). The existence of free-floating planetary mass objects was already claimed in star clusters like sigma Orionis more than a decade ago. Zapatero Osorio et al. (2000) discovered very young L-type dwarfs populating the sigma Orionis cluster. The masses of these objects are still uncertain, but quite likely about a few times the mass of Jupiter. At the age of the Sun, old counterparts of these objects in the solar neighbourhood have cooled down to atmospheric temperatures as low as 400 K and beyond. Extensive research is carried out to identify objects with even lower effective temperatures free floating in the solar neighbourhood. The extrapolation of the mass function of stellar clusters to the planetary domain leads to predict a large number of these objects populating the solar neighbourhood. These objects are extremely difficult to

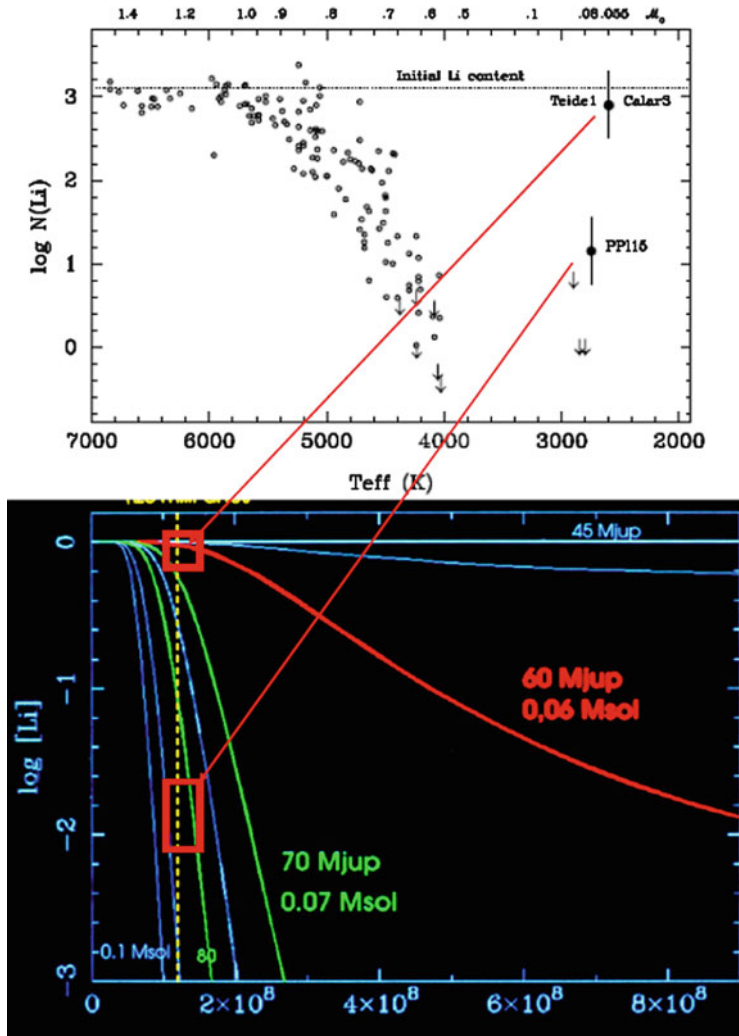
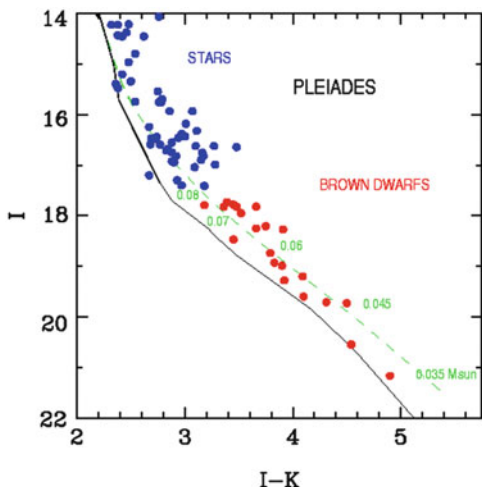


**Fig. 17** Li abundance versus effective temperature of stars and brown dwarfs in the Pleiades cluster (*top panel* from Rebolo et al. 1996). Approximate masses are indicated at the *upper* part. In the *bottom panel*, lithium destruction curves versus age (in years) for objects with 0.045–0.1 solar masses. The lines connecting the two diagrams indicate the positions of Teide 1/Calar 3 and PPI 15, respectively

detect given their very low luminosities but offer new opportunities for exceptional very exciting discoveries.

**Fig. 18** Colour-magnitude diagram showing the sequence of the first brown dwarfs identified in the Pleiades cluster



## 7 Concluding Remarks

I have described the early preparatory work, the set of photometric observations that led to the discovery of the Pleiades brown dwarf Teide 1 at the beginning of 1994, the subsequent analysis of photometric properties and spectroscopic characterization during the same year and its eventual publication in *Nature* on 14 September 1995. Teide 1 was discovered in the course of a survey originally designed to explore the existence of brown dwarfs in the Pleiades cluster. By the time of the publication, several photometric analogues were already identified in this cluster, indicating that the number of free-floating brown dwarfs could be similar to that of stars. Two months after its publication, with the Keck telescope, we could demonstrate that Teide 1 (and also Calar 3) preserved the initial lithium content and that satisfied the so-called lithium test for brown dwarfs.

At the end of November 1995, the extraordinary discovery of the methane brown dwarf Gliese 229B, the prototype T dwarf, was published (Nakajima et al. 1995; Oppenheimer et al. 1995; see contribution to this volume by [B. Oppenheimer](#)). Teide 1 and Gliese 229B are young and old examples, respectively, of brown dwarfs with masses around 50 times the mass of Jupiter. The large difference in luminosity and effective temperature between both objects shows the strong evolution with age of the physical properties of brown dwarfs. These brown dwarfs and several hundred more that have been subsequently discovered are a demonstration of the great scientific vision of S. Kumar in the early 1960s ([Kumar 1963](#)).

**Acknowledgements** During more than 20 years, I have had the great pleasure and privilege to collaborate with many colleagues sharing their interest and efforts to study low-mass stars and brown dwarfs. I wish to thank all for their dedication and invaluable contributions to these studies. My thanks go to M. R. Zapatero Osorio, E. Martín and A. Magazzù for providing photographic

material. I also want to give special thanks to the Instituto de Astrofísica de Canarias and Spanish Academic authorities that have continuously supported substellar research throughout many years and hopefully will continue doing so.

## References

- Abia, C., Boffin, H.M.J., Isern, J., Rebolo, R.: IY Hya – A new super Li-rich carbon star. *Astron. Astrophys.* **245**, L1–L4 (1991)
- Abia, C., Boffin, H.M.J., Isern, J., Rebolo, R.: Lithium abundances in a flux-limited sample of galactic carbon stars. *Astron. Astrophys.* **272**, 455 (1993)
- Baraffe, I., Chabrier, G., Allard, F., Hauschildt, P.H.: New evolutionary tracks for very low mass stars. *Astrophys. J.* **446**, L35 (1995)
- Basri, G., Marcy, G.W., Graham, J.R.: Lithium in Brown Dwarf candidates: the mass and age of the faintest Pleiades stars. *Astrophys. J.* **458**, 600 (1996)
- Becklin, E.E., Zuckerman, B.: A low-temperature companion to a white dwarf star. *Nature* **336**, 656–658 (1988)
- Béjar, V.J.S., Zapatero Osorio, M.R., Rebolo, R., Caballero, J.A., Barrado, D., Martín, E.L., Mundt, R., Bailer-Jones, C.A.L.: The substellar population of sigma Orionis: a deep wide survey. *Astrophys. J.* **743**, 64 (2011)
- Bihain, G., Rebolo, R., Béjar, V.J.S., Caballero, J.A., Bailer-Jones, C.A.L., Mundt, R., Acosta-Pulido, J.A., Manchado Torres, A.: Pleiades low-mass brown dwarfs: the cluster L dwarf sequence. *Astron. Astrophys.* **458**, 805–816 (2006)
- Bihain, G., Rebolo, R., Zapatero Osorio, M.R., Béjar, V.J.S., Caballero, J.A.: Near-infrared low-resolution spectroscopy of Pleiades L-type brown dwarfs. *Astron. Astrophys.* **519**, A93 (2010)
- Bouvier, J., Stauffer, J.R., Martín, E.L., Barrado y Navascués, D., Wallace, B., Béjar, V.J.S.: Brown dwarfs and very low-mass stars in the Pleiades cluster: a deep wide-field imaging survey. *Astron. Astrophys.* **336**, 490–502 (1998)
- Burrows, A., Liebert, J.: The science of brown dwarfs. *Rev. Mod. Phys.* **65**, 301–336 (1993)
- Comerón, F., Neuhäuser, R., Kaas, A.A.: Probing the brown dwarf population of the Chamaeleon I star forming region. *Astron. Astrophys.* **359**, 269–288 (2000)
- Cushing, M.C., et al.: The discovery of Y dwarfs using data from the wide-field infrared survey explorer (WISE). *Astrophys. J.* **743**, 50 (2011)
- D'Antona, F., Mazzitelli, I.: Evolution of very low mass stars and brown dwarfs. I – The minimum main-sequence mass and luminosity. *Astrophys. J.* **296**, 502–513 (1985)
- D'Antona, F., Mazzitelli, I.: New pre-main-sequence tracks for  $M$  less than or equal to 2.5 solar mass as tests of opacities and convection model. *Astrophys. J. Suppl. Series* **90**, 467–500 (1995)
- Dupuy, T.J., Liu, M.C., Bowler, B.P., Cushing, M.C., Helling, C., Witte, S., Hauschildt, P.: Studying the physical diversity of late-M dwarfs with dynamical masses. *Astrophys. J.* **721**, 1725–1747 (2010)
- Forrest, W.J., Shure, M., Skrutskie, M.F.: A possible brown dwarf companion to Gliese 569. *Astrophys. J.* **330**, L119–L123 (1988)
- García López, R.J., Rebolo, R., Magazzù, A., Beckman, J.E.: Chromospheric activity and Lithium abundances in Pleiades low-mass stars. *Memorie della Società Astronomica Italiana* **62**, 187 (1991)
- García López, R.J., Rebolo, R., Martín, E.L.: Pre-main sequence lithium burning. 2: Pleiades low mass stars. *Astron. Astrophys.* **282**, 518–528 (1994)
- Jameson, R.F., Skillen, I.: A search for low-mass stars and brown dwarfs in the Pleiades. *Mon. Notices Royal Astron. Soc.* **239**, 247–253 (1989)
- Jones, B.F., Herbig, G.H.: Proper motions of T Tauri variables and other stars associated with the Taurus-Auriga dark clouds. *Astron. J.* **84**, 1872–1889 (1979)

- Kirkpatrick, J.D., Reid, I.N., Liebert, J., Cutri, R.M., Nelson, B., Beichman, C.A., Dahn, C.C., Monet, D.G., Gizis, J.E., Skrutskie, M.F.: Dwarfs cooler than “M”: the definition of spectral type “L” using discoveries from the 2 micron all-sky survey (2MASS). *Astrophys. J.* **519**, 802–833 (1999)
- Kirkpatrick, J.D., et al.: Further defining spectral type “Y” and exploring the low-mass end of the field brown dwarf mass function. *Astrophys. J.* **753**, 156 (2012)
- Kumar, S.S.: The structure of stars of very low mass. *Astrophys. J.* **137**, 1121–1125 (1963)
- Leggett, S.K., Morley, C.V., Marley, M.S., Saumon, D., Fortney, J.J., Visscher, C.: A comparison of near-infrared photometry and spectra for Y dwarfs with a new generation of cool cloudy models. *Astrophys. J.* **763**, 130 (2013)
- Lodieu, N., Deacon, N.R., Hambly, N.C., Boudreault, S.: Astrometric and photometric initial mass functions from the UKIDSS Galactic Clusters Survey – II. The alpha Persei open cluster. *Mon Notices Royal Astron. Soc.* **426**, 3403–3418 (2012)
- Luhman, K.L.: Discovery of a binary brown dwarf at 2 pc from the sun. *Astrophys. J.* **767**, L1 (2013)
- Luhman, K.L., Rieke, G.H., Young, E.T., Cotera, A.S., Chen, H., Rieke, M.J., Schneider, G., Thompson, R.I.: The initial mass function of low-mass stars and brown dwarfs in young clusters. *Astrophys. J.* **540**, 1016–1040 (2000)
- McCaughrean, M.J., Close, L.M., Scholz, R.-D., Lenzen, R., Biller, B., Brandner, W., Hartung, M., Lodieu, N.: Epsilon Indi Ba, Bb: the nearest binary brown dwarf. *Astron. Astrophys.* **413**, 1029–1036 (2004)
- Magazzù, A., Rebolo, R.: Lithium in T Tauri stars. *Memorie della Societa Astronomica Italiana* **60**, 105–109 (1989)
- Magazzù, A., Rebolo, R., Pavlenko, I.V.: Lithium abundances in classical and weak T Tauri stars. *Astrophys. J.* **392**, 159–171 (1992)
- Magazzù, A., Martín, E.L., Rebolo, R.: Lithium in the pre-main sequence triple system UX Tauri. *Astron. Astrophys.* **249**, 149–155 (1991)
- Magazzù, A., Martín, E.L., Rebolo, R.: A spectroscopic test for substellar objects. *Astrophys. J.* **404**, L17–L20 (1993)
- Martín, E.L., Magazzù, A., Rebolo, R.: On the post-T-Tauri nature of late-type visual companions to B-type stars. *Astron. Astrophys.* **257**, 186–198 (1992)
- Martín, E.L., Rebolo, R., Magazzù, A.: Constraints to the masses of brown dwarf candidates form the lithium test. *Astrophys. J.* **436**, 262–269 (1994)
- Nakajima, T., Oppenheimer, B.R., Kulkarni, S.R., Golimowski, D.A., Matthews, K., Durrance, S.T.: Discovery of a cool brown dwarf. *Nature* **378**, 463–465 (1995)
- Nelson, L.A., Rappaport, S., Chiang, E.: On the Li and Be tests for brown dwarfs. *Astrophys. J.* **413**, 364–367 (1993)
- Oppenheimer, B.R., Kulkarni, S.R., Matthews, K., Nakajima, T.: Infrared spectrum of the cool brown dwarf Gl 229B. *Science* **270**, 1478–1479 (1995)
- Pozio, F.: Li in brown dwarfs and very low mass pre-MS stars. *Memorie della Societa Astronomica Italiana* **62**, 171–179 (1991)
- Rebolo, R.: Lithium and beryllium in main sequence stars. IAU Symp 145 Evolution of Stars: The Photospheric Abundance Connection **145**, 85 (1991)
- Rebolo, R., Martín, E.L., Magazzù, A.: Spectroscopy of a brown dwarf candidate in the Alpha Persei open cluster. *Astrophys. J.* **389**, L83–L86 (1992)
- Rebolo, R., Zapatero Osorio, M.R., Martín, E.L.: Discovery of a brown dwarf in the Pleiades star cluster. *Nature* **377**, 129 (1995)
- Rebolo, R., Martín, E.L., Basri, G., Marcy, G.W., Zapatero-Osorio, M.R.: Brown dwarfs in the Pleiades cluster confirmed by the lithium test. *Astrophys. J.* **469**, L53 (1996)
- Rebolo, R., Zapatero Osorio, M.R., Madruga, S., Béjar, V.J.S., Arribas, S., Licandro, J.: Discovery of a low-mass brown dwarf companion of the young nearby star G 196–3. *Science* **282**, 1309 (1998)
- Rieke, G.H., Rieke, M.J.: Possible substellar objects in the Rho Ophiuchi cloud. *Astrophys. J.* **362**, L21–L24 (1990)

- Roswick, J.M., Mermilliod, J.C., Mayor, M.: Investigation of the Pleiades cluster. I – Radial velocities of corona stars. *Astron. Astrophys.* **255**, 130–138 (1992)
- Ruiz, M.T., Leggett, S.K., Allard, F.: Kelu-1: A free-floating brown dwarf in the solar neighborhood. *Astrophys. J.* **491**, L107 (1997)
- Stassun, K.G., Mathieu, R.D., Valenti, J.A.: Discovery of two young brown dwarfs in an eclipsing binary system. *Nature* **440**, 311–314 (2006)
- Stauffer, J., Hamilton, D., Probst, R., Rieke, G., Mateo, M.: Possible Pleiades members with  $M$  of about 0.07 solar mass – identification of brown dwarf candidates of known age, distance, and metallicity. *Astrophys. J.* **344**, L21–L24 (1989)
- Stauffer, J., Herter, T., Hamilton, D., Rieke, G.H., Rieke, M.J., Probst, R., Forrest, W.: Spectroscopy of Taurus cloud brown dwarf candidates. *Astrophys. J.* **367**, L23–L26 (1991)
- Stauffer, J.R., Liebert, J., Giampapa, M., Macintosh, B., Reid, N., Hamilton, D.: Radial velocities of very low mass stars and candidate brown dwarf members of the Hyades and Pleiades. *Astron. J.* **108**, 160–174 (1994)
- Zapatero Osorio, M.R., Béjar, V.J.S., Martín, E.L., Rebolo, R., Barrado y Navascués, D., Bailer-Jones, C.A.L., Mundt, R.: Discovery of young, isolated planetary mass objects in the sigma Orionis star cluster. *Science* **290**, 103–107 (2000)
- Zapatero Osorio, M.R., Lane, B.F., Pavlenko, Y., Martín, E.L., Britton, M., Kulkarni, S.R.: Dynamical masses of the binary brown dwarf GJ 569 Bab. *Astrophys. J.* **615**, 958–971 (2005)
- Zapatero Osorio, M.R., Rebolo, R., Martín, E.L., Basri, G., Magazzù, A., Hodgkin, S.T., Jameson, R.F., Cossburn, M.R.: New brown dwarfs in the pleiades cluster. *Astrophys. J.* **491**, L81 (1997)
- Zuckerman, B., Becklin, E.E.: Companions to white dwarfs – very low-mass stars and the brown dwarf candidate GD 165B. *Astrophys. J.* **386**, 260–264 (1992)

# The Discovery of the First Lithium Brown Dwarf: PPI 15

Gibor Basri

**Abstract** The search for brown dwarfs (BDs) covered decades between the time they were first proposed theoretically and the time that a public announcement of the discovery of a BD was made which did not have to be recanted later (as was the case for a number of previous announcements). In a convergence of scientific progress, 1995 saw 3 real discoveries of BDs, as well as the first exoplanets. The substellar realm had suddenly opened up. This chapter describes the process that led to the first of these announcements: the identification of PPI 15 as a BD. It lay just below the substellar limit in the Pleiades cluster. To distinguish it from very similar-looking stars, the first successful application of the “lithium test” was applied by my group at UC Berkeley using the new Keck 10 m telescope and HIRES spectrograph. As part of the analysis, the new technique of “lithium dating” was developed. I place this discovery in the context of the broader search for BDs, and of the subsequent discoveries and progress in the field.

## 1 Introduction: Search Techniques for Brown Dwarfs

The search for BDs was a long and frustrating process, if measured from the time that they were first posited theoretically ([Kumar 1963](#)). It was known from the outset that BDs would start off rather faint and cool, and by their very substellar nature, grow continuously fainter and cooler with time. This imposes several observational constraints on search techniques. One is that the search should be conducted as redward as possible in the optical band, or even better, at near infrared wavelengths. The technology to do this efficiently did not really come into its own until the 1990s. Red sensitivities of photographic film were not high, and CCDs were only

---

G. Basri (✉)

Astronomy Department, University of California, Berkeley, CA 94720, USA

e-mail: [basri@berkeley.edu](mailto:basri@berkeley.edu)

introduced in the previous decade. Most BDs lay beyond the sensitivity of older surveys like the Palomar Sky Survey because of their faintness and extremely red colors. Even cooler M stars were very sparsely known. Infrared detectors did not have many pixels until then, meaning that angular coverage was extremely limited.

The alternate approach is to search for BDs when they are very young, which means they will be at their brightest and warmest. Indeed, very young BDs actually have the M spectral class (and it turned out later that some long known nearby M stars are actually BDs). The problem in this case is finding a way to distinguish between objects of M spectral class that are true stars from those that are substellar. The obvious thing to do is find them in binaries in which a mass determination can be made from the orbit. Unless it is an eclipsing system, however, one cannot be sure whether the inclination is small enough to cause what is actually a star to appear to have an apparently substellar mass. The other approach is to find a nuclear diagnostic that proves that the object has not undergone nuclear burning under conditions only a true star can achieve. Such a diagnostic was proposed by [Rebolo et al. \(1992\)](#), and it is the first successful use of that lithium test that is the primary subject of this chapter. The first true discoveries of single BDs were announced in 1995 in June and September utilizing the lithium test; they are the subject of this chapter and the one by Rebolo in this volume. Extensive reviews of early observational efforts (up through the first set of successful ones) can be found in [Oppenheimer et al. \(2000\)](#) and [Basri \(2000\)](#). I next provide a brief general summary of the early campaigns to find BDs.

## 1.1 *Brown Dwarfs as Companions to Stars*

If one does not know where to look for BDs, an excellent place to start is near to a star. We know that the binary fraction of stars is high, ranging from 75 % or more around high-mass stars to about 25 % around low-mass stars ([Duchêne and Kraus 2013](#)). Although it was not clear how that applies to BDs, one does not need much angular coverage to look for companions to stars. Instead the problem is one of angular resolution, which in turn drives one to study nearby systems. One unfortunate side effect of such a search is that the typical system will be rather old, and the BD keeps fading away while its stellar companion does not. This acts as another strong driver to study nearby systems. Both the angular separation and contrast ratio will produce a detection bias for systems with large separations. It is also possible to search for BDs through the radial velocity variability they would produce on their stellar companion. This has the great advantage that the faintness of the BD is irrelevant, but it is strongly biased to detect close companions.

One of the first efforts to directly image BDs as companions to nearby stars was made by [McCarthy et al. \(1985\)](#). Using an infrared speckle technique, they reported a companion to VB8, with inferred properties that would guarantee its substellar status. This was the highlight of the first conference on BDs ([Kafatos et al. 1986](#)). Unfortunately, their result was never confirmed. Later surveys did not find good

BD candidates, but several very low-mass stellar companions. In a survey of white dwarfs, Becklin and Zuckerman (1988) turned up a very red and faint companion, GD 165B, whose spectrum was quite enigmatic. This was, in retrospect, the discovery of the first L dwarf. Kirkpatrick et al. (1999) argue that it is also probably a BD, but that is hard to confirm (cf. the chapter by Cushing in this volume).

The next good candidate BD came from a radial velocity survey. Latham et al. (1989) were conducting a survey of about 1,000 stars with 0.5 km/s precision. Among their roughly 20 radial velocity standards, HD 114762 exhibited periodic variability just at their limit of detectability. Its orbit has been confirmed by the precision radial velocity groups, and implies a lower-mass limit for the companion of about  $11 M_{\text{Jup}}$ . The difficulty is that its orbital inclination is not known, and it is one of very few objects in the “brown dwarf desert” (Grether and Lineweaver 2006). This term refers to the dearth of BDs as close companions to solar-type stars, confirmed by the results of many radial-velocity extrasolar planetary searches. With so few real objects in a large sample, it is possible that any given one is a stellar mass companion seen nearly pole-on.

Oppenheimer describes in another chapter the discovery of the companion to a low-mass star that has come to be accepted as the “first incontrovertible brown dwarf”. Gliese 229B was first detected in 1994, but the group showed commendable forbearance in waiting for proper motion confirmation that it was physically associated with the primary (allowing the known parallax of the primary to be applied to find its luminosity). They also obtained a spectrum that confirmed the remarkably low temperature implied by its luminosity (Oppenheimer et al. 1995). In particular, the spectrum contains methane bands at  $2 \mu\text{m}$ ; features that had previously been detected only in planetary atmospheres (and which are not expected in any main-sequence star). This has now become the defining characteristic of T dwarfs. The announcement of Gliese 229B came at the same Cool Stars conference in Florence in October 1995 as the discovery of the first extrasolar planet. Thus 1995 was the year when the substellar domain was fully opened to observations.

## 1.2 *Brown Dwarfs in the Field*

The most straightforward and unbiased sort of search is to simply look for BDs “in the field”, meaning at random locations in the sky. Once all-sky surveys at appropriate wavelengths (DENIS and 2MASS) became possible in the mid-1990s, the discovery of field BDs became much easier (none were identified before that time). The DENIS survey began in 1996 but conducted a pilot survey in 1995. It has one optical color (I) and two infrared colors (J, K), and operated primarily in the southern hemisphere. The 2MASS survey began regular operations in 1997 but was obtaining excellent data in a prototype survey by 1995. It uses the three near-infrared colors (J,H,K), and operated primarily in the northern hemisphere. Both surveys had published discoveries of field L dwarfs by 1997 (Kirkpatrick et al. 1997; Delfosse et al. 1997).

Because BDs are particularly faint, it is very difficult to see them unless they are nearby. This makes proper motion surveys a promising search tactic (if they are deep and red enough). One important early discovery was the culmination of a long search for faint red objects with high proper motion (the Calan-ESO survey). A red spectrum of a candidate was obtained (Ruiz et al. 1997) that shows the features now associated with the L dwarfs. The team dubbed the object “Kelu-1” (a Chilean native word for “red”). It also showed lithium, making it a certified BD. This discovery was closely followed by one of the DENIS objects (Martín et al. 1997).

One generally has the problem that any BDs which are in the temperature range also inhabited by main-sequence stars will be hard to distinguish as substellar. This includes all objects in the late-M spectral class, and the early half of the L dwarfs (although we still are not certain which L spectral subclass corresponds to the first guaranteed BDs). The best way to distinguish stellar from substellar objects above the minimum main-sequence temperature in the field is through the lithium test. Even for companion objects, it is very difficult to find systems in which substellar certification can quickly be accomplished dynamically. To conduct the lithium test, however, requires a medium dispersion spectrum with sufficient signal-to-noise. This test has still not been conducted on most possible BDs. For example, one of the currently known field BDs (LP 944-20, M9) was only shown to be a BD when such a spectrum was taken by Tinney (1998), long after its discovery as a late M star in a proper motion survey. We discuss the lithium test in more detail later, but its primary utility is that any object which is M8 or later and shows lithium is guaranteed to be substellar (Basri 1998).

### **1.3 Brown Dwarfs in Young Clusters and Star-Forming Regions**

It is actually easier to see young BDs, because they are not as faint and cool as the older ones. Finding young objects in the field, however, is hard since they will constitute only a small fraction of possible targets. This means that searches are best conducted in young clusters (none of which are particularly near to us, except the relatively recently discovered TW Hya group). Of course, the closer the cluster is, the larger the total angular area that it will cover (making surveys more costly in telescope time and making the identification of cluster members from field stars harder). There is therefore a trade-off to be made between the distance, age, and richness of different clusters. The closest star-forming regions (groups less than about 10 Myr old) are at distances of 150 pc or further. They have the advantage, however, that even relatively low-mass BDs are still in the late-M or early-L temperature range (as well as larger in radius), and therefore can be seen out to distances of several hundred parsecs.

During the early 1990s, there were a number of surveys aimed at finding BDs in young clusters and star-forming regions. Forrest et al. (1989) announced a number

of candidates in Taurus-Auriga, which were later shown to be background giants ([Stauffer et al. 1991](#)). Surveys of other star-forming regions (e.g. [Williams et al. 1995](#)) also found objects which might well be substellar, but with no obvious way to confirm them. [Hambly et al. \(1993\)](#) conducted a deep proper motion survey of the Pleiades, and found a number of objects (labeled with the authors' initials: HHJ) that models suggested should be substellar. [Stauffer et al. \(1994\)](#) were also conducting a survey for BDs in this cluster, working from color-magnitude diagrams. Both surveys went substantially deeper than before, and uncovered interesting objects. This set the stage for the next, ultimately successful, effort to find cluster BDs. Nonetheless, it is well to remember that at the 1994 ESO Munich conference on “The Bottom of the Main Sequence - and Beyond” (Tinney, ed.), there was a palpable sense of frustration at the failure of many efforts to confirm a single BD.

In star-forming regions, the BDs are at their brightest, so the mass function can be sampled all the way to the bottom of the BD mass range and below. Complications include variable extinction in the star-forming region and possible age spreads of order millions of years (Myr) for the objects (which are a larger fractional problem than with older clusters). The main problem is the reliability of evolutionary models which are almost exclusively the means by which masses are assigned to the individual objects. These are known to become increasingly questionable as one moves to lower masses and younger ages. The primary star-forming regions that were first studied are Taurus-Auriga, Orion (various sub-regions),  $\sigma$  Ori, IC 348,  $\rho$  Oph, Upper Sco, and Chamaeleon (various sub-regions); see ([Basri 2000](#)) for a summary. They have the advantage that one is truly measuring the *initial* mass function, as there has been no time for dynamical ejection of a substantial number of BDs.

## 2 My Search for the First Brown Dwarf

My own research had been concentrated on star formation for the decade before 1993. I came to the topic through an initial interest in stellar magnetic fields. T Tauri stars, which everyone felt in the 1970s must be very young stars, were still quite enigmatic at the beginning of the 1980s. One thing that was suggestive is that the emission line spectra from these objects looked a lot like the active Sun or even the flaring Sun. Thus, one idea was that the source of emission was very strong magnetic activity on these stars. Another was that the emission arose from either accretion or outflow activity. It turns out that all these ideas are simultaneously correct; the T Tauri stars are very young (still forming) stars which exhibit strong magnetic activity, magnetospheric accretion from an accretion disk, and strong outflows. As they age, the accretion and outflow activity wanes, but they remain very magnetically active. The relevance is that I was driven through these investigations to become familiar with young stars and low-mass stars.

In 1993 a new opportunity arose for California astronomers. The first Keck telescope, which had been designed at UC Berkeley and UC Santa Cruz with

instrumentation from there and Caltech (and major funding from Caltech) was about to be opened to our community. I think most of us tried to think of a really impactful project, given the 10 m aperture that we soon would have access to. I naturally thought about new projects involving T Tauri stars, but I also sat down with some of my friends to discuss other possibilities. Geoff Marcy and I had been collaborating for some time on magnetic studies of stars, while he also struggled to eke enough precision out of the high-resolution echelle spectrograph at Lick Observatory to detect exoplanets using the Doppler effect. Most of my own work also involved high-resolution spectroscopy, and the HIRES spectrograph at Keck was going to be like the Hamilton echelle we were familiar with, only perhaps 50 times faster! Our colleague James Graham was also interested in high-resolution spectroscopy (among other things) and low-mass stars. It was James who suggested we might pursue the discovery of BDs via the lithium test.

Graham's suggestion that we pursue the lithium test made immediate sense to me. I had become familiar with lithium as an astrophysical diagnostic in initial work with Eduardo Martín and Claude Bertout in the context of lithium as a signpost of youth in T Tauri stars. In that instance the mass range of stars under consideration (0.5–1 solar mass) burn their lithium in a few tens of Myr, but before that they display strong lithium lines (being relatively cool). This affords a nice way to distinguish post-T Tauri stars from older stars, and to put a limit on how old they are. Our work also showed, however, that one must be relatively careful to have the right effective temperature in interpreting an observed lithium line strength. What appears to be lithium depletion can simply be an error in interpreting a temperature to be a couple hundred degrees hotter than it really is.

Martín had moved on to do his thesis work with Rafael Rebolo at the Instituto de Astrofísica de Canarias (IAC). It was Rebolo's group who first proposed the lithium test for substellar objects (Rebolo et al. 1992). Their suggestion inspired us to make this our Keck project (though of course we each had other projects as well). Naturally the group at the IAC had also embarked on an effort to apply the lithium test to the best existing BD candidates. They used 4 m class telescopes at spectral resolutions ( $\frac{\lambda}{\Delta\lambda}$ ) of 14,000 for a brighter initial sample (Magazzù et al. 1993). This sample included several of the coolest known field objects (late M dwarfs). They were easily able to detect lithium in the cool (M6) T Tauri star UX Tau C, but not in any of the test objects. That object is unfortunately too young for the lithium test to work, since stars won't have had time to deplete their lithium yet.

## 2.1 *Distinguishing Stars from Brown Dwarfs: The Lithium Test*

Stars and BDs can have identical temperatures and luminosities when they are young (though the star would have to be older than the BD). “Young” in this context extends up to a gigayear or so. We therefore require a more direct test of

the substellar status of a young BD candidate before it can be certified. Since the difference between BDs and very low-mass stars lies in the nuclear behavior of their cores, it is natural to look for a nuclear test of substellarity. There is a straightforward diagnostic that is fairly simple both theoretically and observationally: the lithium test. In addition to verifying substellar status, observations of lithium can be used to assess the age of stars in clusters, which is helpful in the application of the lithium test itself. Lithium observations of very cool objects can be useful in constraining the nature of BD candidates in clusters, in the field, and in star-forming regions.

In the simplest terms, stars will burn lithium in at most 100 Myr, while most BDs will never reach the core temperature required to do so. This stems from the fact that even before normal hydrogen burning commences, core temperatures in a star reach values that cause lithium to be destroyed. On the other hand, in most BDs the requisite core temperature is never reached because of core degeneracy. Furthermore, at masses near and below the substellar boundary the objects are all fully convective, so that surface material is efficiently mixed through the core. Finally, the surface temperatures of young candidates are favorable for observation of the neutral lithium resonance line, which is strong and occurs in the red. There are some subtleties to be considered in the application of the test, as discussed below. A more comprehensive review of this subject is provided by [Basri \(1998\)](#).

The idea behind the lithium test was implicit in calculations of the central temperature of low-mass objects by [D'Antona and Mazzitelli \(1985\)](#) and others. They found that the minimum lithium-burning temperature was never reached in the cores of objects below about  $60 M_{\text{Jup}}$ . On the other hand, all M stars on the main sequence are observed to have destroyed their lithium. The first formal proposal to use lithium to distinguish between substellar and stellar objects was made by [Rebolo et al. \(1992\)](#). This induced ([Nelson et al. 1993](#)) to provide more explicit calculations useful in the application of the lithium test.

The theory of lithium depletion in very low-mass objects is comparatively simple. Because the objects are fully convective, their central temperature is simply related to their luminosity evolution. The physical complications in very low-mass objects, including partially degenerate equations of state and very complicated surface opacities, do not obscure the basic relation between the effective temperature and lithium depletion. The complications of mixing theory, which lead to many fascinating effects in the observations of surface lithium in higher-mass stars, are simply not relevant for fully convective objects.

## 2.2 *Querying the Seven Sisters*

One would like to study stars of a known age that are sufficiently old that essentially all stars will have depleted their lithium, but not much older (so that the very low-mass objects are as bright as possible, since they fade with time). Of course one also wants a cluster that has been well surveyed for very low-mass objects and that is relatively close (so they are brighter). The Pleiades cluster (also known as the “Seven

Sisters") seemed the ideal hunting ground as there were a number of studies recently published and searches continuing. We selected the study of [Hambly et al. \(1993\)](#) as our source of targets, and simply resolved to continue searching for lithium at the faintest end of known Pleiades objects. At that time everyone understood the age of the Pleiades to be 70 Myr. One could take theoretical models (for example, those of [Nelson et al. 1993](#)) and translate them to color-magnitude diagrams for different masses and ages. These implied that the faintest known Pleiades objects should already be BDs (with masses around  $60 M_{\text{Jup}}$ ).

With HIRES at Keck, we could achieve spectral resolutions of 30,000 even for the faint Pleiades objects, although it required exposures of a few hours. This allowed us to place upper limits on the equivalent width of the lithium line in the objects HHJ 3 and HHJ 14 of under  $200 \text{ m}\AA$  ([Basri et al. 1994](#)). The strength of the resonance line means that it does not begin to desaturate until more than 90 % of the initial lithium has been depleted. The timescale over which the lithium line disappears in stars is about 10 Myr, which is roughly 10 % of the age at which it occurs in substellar objects. But the observational disappearance of the line occurs even more rapidly (after desaturation). We could make a strong argument that lithium was essentially depleted in these objects, which is incompatible with their theoretical substellar mass. We also had good empirical reasons to believe that the lithium line should be strong in a BD at the temperature of our targets since it was seen in UX Tau C ([Magazzù et al. 1993](#)). Given the (not yet known) spectral type of the lithium boundary in the Pleiades, this object is quite likely to be a BD itself in retrospect.

Our puzzling failure to find lithium had three possible explanations. One which we mentioned first but discarded because the consensus was tilting the other way, is that the Pleiades could be substantially older than thought at the time. We briefly discussed an age as high as 200 Myr. Another possibility, of course, is that the interior models are seriously wrong, leading to a wrong translation of a position in the color-magnitude or color-luminosity diagram into actual mass. The third is that the translation of color-magnitude into effective temperature (which is the actual variable in the interior models) is problematic. Because at that time this was known to be problematic and inconsistent for M dwarfs, and because of my previous experience with this sort of problem in T Tauri stars, we elected to chalk up the mystery to problems with the effective temperature scale.

[Martín et al. \(1994\)](#) pursued a similar strategy as us but only had access to spectral resolution of a few thousand with 4 m telescopes (cf. the Chapter by Rebolo in this volume). Such observations are very difficult due to the faintness of very low-mass objects. They did not detect lithium in any of their candidates. For field targets (since the ages aren't known) this implied a lower-mass limit greater than  $60 M_{\text{Jup}}$ , but did not fully resolve whether they are BDs, because of the high upper limits to detectable lithium strength. Their results were also puzzling for their Pleiades candidates (though less constraining than ours). These were drawn from the same [Hambly et al. \(1993\)](#) list of very faint proper motion objects, and those authors had already suggested BD candidacy based on the color-magnitude position of the objects compared to evolutionary tracks for the age of the Pleiades (thought to

be 70 Myr). [Martín et al. \(1994\)](#) realized too that there was an inconsistency between the inferred mass of these Pleiades members and their lack of lithium.

## 2.3 *Passing the Lithium Test*

Meanwhile my group was waiting for even fainter Pleiades candidates to be found. Our break came when John Stauffer was preparing to publish the results of a survey he had been conducting for a few years for the faintest Pleiads at Palomar Observatory ([Stauffer et al. 1994](#)). Candidates were dubbed with “Palomar Pleiades” numbers, and the object PPI 15 was first found on an exposure in 1989. John and I were friends and when I asked him if he had turned anything up, he generously provided a finding chart in advance of publication. His survey was photometric rather than a proper motion survey like HHJ had been conducting. PPI 15 was only a little fainter than HHJ 3, so in order for us to successfully detect lithium, the lithium depletion boundary would have to be fairly sharp in luminosity.

In November of 1994 we obtained the first high-resolution spectra of PPI 15 (Fig. 1 shows the first page of the observing log). As noted in our subsequent paper ([Basri et al. 1996](#)) “at no time were observing conditions ideal”. There were cirrus clouds of varying thickness, and the gibbous Moon was about 60° away, producing extra sky brightness (the star had only 5–10 % the brightness of the sky). It was clear that this object (with an I magnitude barely brighter than 18) was near the limit of what could be done with HIRES at the resolution and signal-to-noise (S/N) that is needed. Geoff Marcy and I observed it 6 times over 2 nights with individual exposures of 60–90 min. Two of these were so plagued by clouds that we didn’t end up using them in our final sum. Traces of all our original spectra are shown in Fig. 2. The order containing lithium was barely visible in the raw images, so we did not know during the run whether lithium had been detected. We did do some preliminary spectral extractions on the mountain and it seemed possible that something was there, but not enough to make a note in the log. We quickly confirmed that PPI 15 had the right radial velocity and H $\alpha$  strength to be a cluster member, in addition to fitting on the cluster color-magnitude diagram.

Once home I set about trying to get the maximum information out of the spectra. After reducing them the “normal” way I tried a couple of other techniques. The optical curvature of the orders could either be removed by a geometrical interpolation, or the spectrum could be extracted along curves that were pre-determined by brighter exposures. The sky could be treated several different ways (obviously sky subtraction is very important in such faint spectra). With some special consideration, we could also weight individual pixel rows according to their S/N. It became increasingly clear to me that there was a good chance we had detected lithium, but it was not unassailable. I had many other M6 dwarf spectra to compare PPI 15 with (including HHJ 3), and several of the PPI 15 spectra were unique in showing an absorption feature at just the right stellar wavelength. Its strength was not as great as expected from undepleted lithium, and there were

KECK HIRES SPECTROGRAPH OBSERVING LOG					
Observer(s): Basri, Marcy		Chip(s): Tek 2048(LRIS) Binning: 2x2		Decker: D1 Slit: D1 Focus: Nom. Camera: Red	
U.T. Date: 22/23 Nov 94 Tape Number:		Windowing: 1024x1024 Ech-Ang: -1.080 XD-Ang: 1.372			
Tom Belds Wayne Randy					
Tp #	Object	Time		Comments	
		Start (U.T.)	Δ (s)		
1	Wide Flat	3:50	1	OG 530, NG 3	$DN_{max} = 34000$
2	*		"		
3	Th-Ar	3:52	1	OG 530, BG 13	
4	Th Ar		1	OG 530, NG 3	
5	BIAS DARK		1	Hatch closed over slit	
6	BIAS DARK		1	BIAS = .863 $\sigma = 3 DN$	
7	DARK	3:59	600	Hatch closed	
8	Twilight	4:05	120	no filter	
9	Twilight	4:10	600	OG 530	
10	W <sub>8</sub> BRI 0021	4:46	2400	no filters	seeing = 1.0" ~400 DN
11	W <sub>8</sub> RG 0050	5:40	3000		HA = 1° 20' seeing = 0.8"
12	W <sub>8</sub> CTI 0126	6:48	3600		HA = 0° 50'
13	HHJ 339	7:53	600		
14	PPL 15	8:07	3600		moon up, clouds
15	M <sub>8</sub> LP 412-31	9:22	3600	see = 0.7"	clouds
16	Wide Flat	10:37	1	OG 530, NG 3	XDANGE Moved during night to 1.357
17	Th-Ar	10:44	1	OG 530, NG 3	
18	Th-Ar	10:47	1	OG 530, BG 13	
19	Blank	10:53	1	OG 530, BG 13	
20	Th Ar	11:00	1		

DM1

Apparent 2nd order getting in  
Don't know why

**Fig. 1** The observing log from the first night of the run where we began observing PPI 15. The handwriting is mostly Geoff Marcy's; I was on the computer doing initial IDL reductions. We were still experimenting with order sorting filters (there is a puzzle noted at the bottom) but it didn't affect the PPI 15 observations. Both clouds and the Moon were noted. We observed HHJ 339 first because it was brighter (see Sect. 3.3 for its story). The other objects were on our "bottom of the main sequence" program

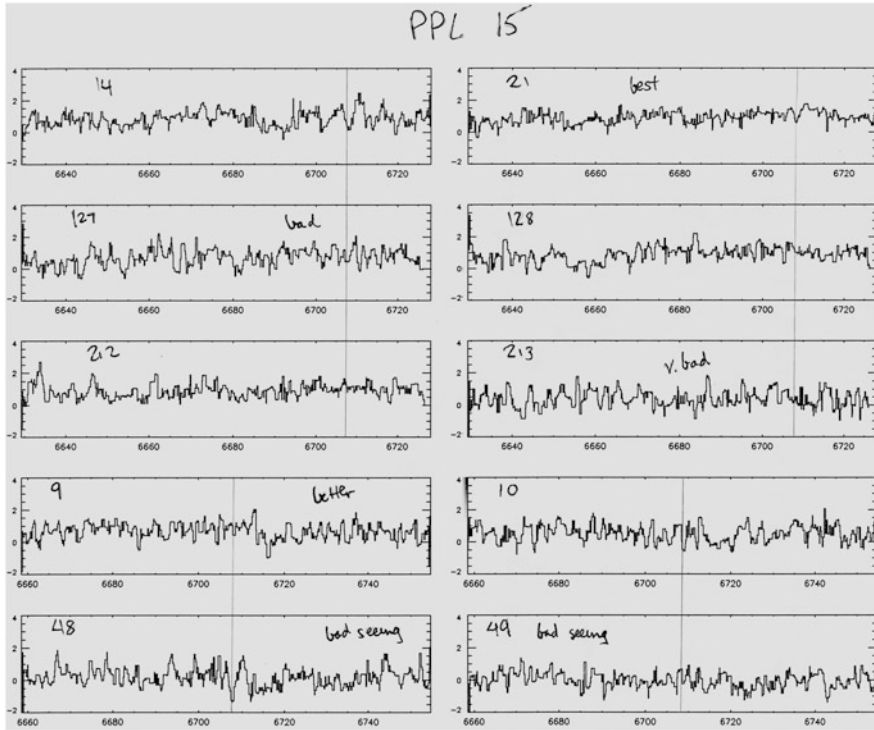


**Fig. 2** A plot I made for the group of the raw spectra obtained of PPI15 in Nov. 1994 (top 6) and Mar. 1995 (bottom 4). The numbers above each spectrum refer to the index number in our observing logs, with a few comments. The location of the lithium line is marked with a *vertical line* in each spectrum

some spectra in which one could not say that it was present with any confidence. I can remember the night I became finally convinced it was real; I savored the idea that for that brief time I was the only one who had a certified BD in my grasp. It turns out that isn't quite true, because the groups working on Teide 1 and Gliese 229B were also analyzing their data, but we didn't know about each other's discoveries.

I felt that it would really be much better if we could nail the detection down more solidly, so we returned in March 1995 to re-observed PPI 15. Unfortunately the lack of cirrus was more than compensated for by a combination of bad seeing and the fact that the Moon was now much closer to the object. The sky contribution ended up being about twice as much relative to the star as in November. The spectra really did nothing to confirm the lithium detection (actually they decreased my confidence). It turns out there was also an astrophysical reason why lithium was less visible in PPI 15 in March, but we didn't find that out until a couple of years later (see Sect. 2.6). At this point it became something of a "gut call". I consulted with my co-authors, and we finally decided that our final best reduction of all the spectra contained a clear enough signal that we could publish (Fig. 3).

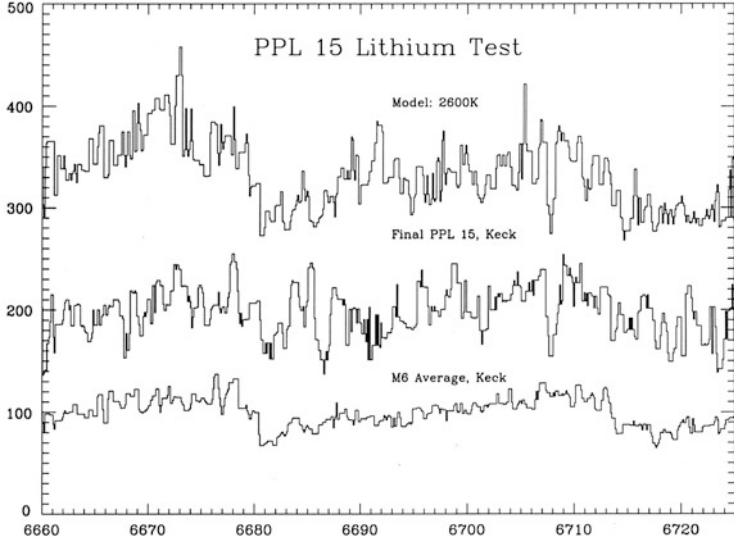


**Fig. 3** A final version of the lithium detection that we used to help us decide to publish the result. After a lot of processing of the individual spectra in Fig. 2 and weighting of spectra by their quality, it seemed clear that we really detected the line with publishable confidence. The spectrum resembled what we expected on the basis of model atmospheres, and the feature at 6,707 Å clearly did not show up in M dwarf spectra even with higher S/N. The molecular bands in this part of the spectrum have similar amplitudes

## 2.4 *The Invention of Lithium Dating*

Of course, now we had to explain how lithium could appear in PPI 15 but not in HHJ 3. We first made an empirical bolometric correction to the color-magnitude data to convert to luminosity (models compute luminosity and effective temperature). James Graham also observed the faint Pleiads in the infrared, providing a nice check on the bolometric correction. After a set of careful complementary approaches, we adopted final logarithmic bolometric luminosities for HHJ 3 and PPI 15 of  $-2.78$  and  $-2.88$  respectively (in solar units). We also had to discuss the distance modulus to the cluster (which was a bit uncertain) to convert apparent to intrinsic brightness. We then used the models of Nelson et al. (1993) to convert luminosity to mass, and also to understand the lithium depletion with age. These models were consistent with others of the time (e.g. D'Antona and Mazzitelli 1985) and these authors kindly provided us with fine grids to use. We were reasonably conservative, and also considered the range of uncertainties, but it was clear once again that for the canonical age of the Pleiades (we used 75 Myr) both these objects should be BDs and both should show lithium. HHJ 3 clearly did not, and PPI 15 appeared to have partially depleted lithium. This was not a surprising possibility given that it was barely fainter than HHJ 3 and could be just on the cusp of the depletion boundary.

At that point I revisited the possible explanations for the discrepancy. Unlike the situation in the first paper, we now had found the lithium boundary and knew what the objects that straddled the boundary were like. The proposition that the models were seriously wrong didn't look like the best bet. These objects are fully convective and at that age basically powered by gravitational contraction. The only nuclear burning that should have taken place is deuterium burning. All these things are relatively simple and should be relatively well understood. The proposition that the effective temperature scale was the problem had now effectively been dealt with by using bolometric luminosity instead. That left the age hypothesis. My insight clarified as I looked at the “waterfall diagram” shown in Fig. 4 that I constructed from our model data. This shows the abundance of lithium as a function of age and mass for very low-mass objects straddling the substellar boundary. It became clear to me that I could put HHJ 3 and PPI 15 (and later Teide 1) onto this diagram given their different lithium strengths with slightly different masses and the same age but only if the age of the Pleiades was substantially older than what everyone thought it was. This reasoning appears in [Basri et al. \(1996\)](#) in Fig. 5, with the more empirical bolometric luminosity in place of mass and reduced to a two-dimensional presentation. The observed luminosity of HHJ 3 combined with its lack of lithium force its age to be greater than 110 Myr, while the same quantities for PPI 15 force its age to be less than 125 Myr.

It didn't take me long after starting to look into this idea to find that it wasn't as radical as it first seemed. The canonical age of the Pleiades was derived in the usual fashion: by looking at the massive stars that are just turning off the main sequence. For a cluster like the Pleiades these objects have convective nuclear burning cores and radiative envelopes. Stellar evolutionists had by then been discussing for a few years what the effects of convective overshoot in the core would be. Very simply, such overshoot would reach into the unburned hydrogen of the radiative envelope and make some small fraction of it available for burning. This would allow core hydrogen burning to last longer, thus increasing the age of the star when it turned off. We cited a number of papers that discussed convective overshoot (e.g. [Meynet et al. 1993](#)) and had inferred that the Pleiades might be as old as 200 Myr, though 100 Myr seemed more reasonable. This made it clear that our proposition that the Pleiades might be 115–120 Myr old was actually in line with advanced thinking of the time. Furthermore, the technique I had now developed (which I called “lithium dating”) was itself a nuclear diagnostic of stellar age. The physics of lithium burning in a cool fully convective object is actually simpler and on firmer footing than for hydrogen core and shell burning in the presence of convective overshoot. Indeed, we suggested that lithium ages could be used to calibrate the amount of convective overshoot in massive stars.

In lithium dating the details of convection are rendered unimportant by the fully convective nature of the objects (which are forced onto adiabatic temperature gradients). The problem is so simple, in fact, that not long after developing my method I was discussing it with Lars Bildsten (at that time in the Berkeley Physics department). He decided it could be solved semi-analytically, and assigned it as a problem in his stellar structure class. It was a bit much for most of the students, but

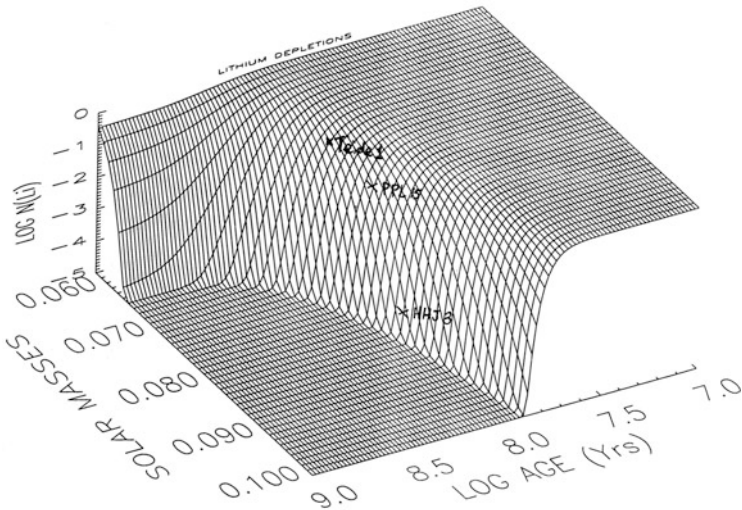


**Fig. 4** A plot I made for myself when I was trying to understand how to reconcile the lack of lithium in HHJ 3 with the presence of lithium in PPI 15. The model data was from [Nelson et al. \(1993\)](#) and the conversion from luminosity to mass for each object also relied in part on these models and in part on our method described in the text. The placement of the object with a lithium abundance also relied on model atmospheres. The placement in age I left as a free parameter, but expected that a proper solution would have all three cluster objects with similar ages. It became clear that such a solution existed, but at a substantially older age than was accepted for the cluster at that time

one came close enough that they decided to turn the exercise into a paper. [Bildsten et al. \(1997\)](#) make the point that the physics underlying lithium dating is really quite simple. As a cluster gets older, the luminosity of the lithium depletion boundary gets fainter. Thus, while the Hyades is one-third the distance of the Pleiades, its lithium boundary is at fainter apparent magnitudes because it is more than five times as old. Although  $\alpha$  Per is further away, its youth means that the apparent magnitude of the lithium boundary is similar to the Pleiades. Given a correct age, the luminosity of the substellar boundary can then be inferred from models. This will not be coincident with the depletion boundary in general (only at the age of the Pleiades). Once the boundary is established, the search for BDs can proceed to fainter objects using cluster membership as the sole criterion. The precision of lithium dating is limited by the width of the depletion boundary, errors in the conversion of magnitudes to luminosities (due to bolometric corrections and cluster distances), and possible corrections to the age scale because of opacity issues in very cool objects. But it probably has similar precision to, and greater accuracy than, classical dating methods. Lithium dating can only work up to about 200 Myr, when the lowest-mass object that can deplete lithium will have done so. Furthermore, the correction for core convective overshoot only applies for clusters younger than about 2 Gyr; stars leaving the main sequence in older clusters have radiative cores.

## The First Lithium Brown Dwarf

Gibor Basri (UC Berkeley), Geoffrey W. Marcy (SFSU), James R. Graham (UC Berkeley)

There have been many searches for brown dwarfs, and many candidates proposed, but none have been confirmed as truly substellar objects. One means of confirmation is the “lithium test”. Fully convective stars will deplete lithium from their atmospheres given a sufficiently high central temperature and enough time. In a cluster of known age, theory provides the mass–luminosity relation. For an age at which all main sequence stars have depleted their lithium, one should find it only in objects of substellar mass. Observational confirmation of both these effects is strong evidence for brown dwarfs. One caveat is the uncertainty in the age of a cluster; another is that stellar evolution theory is empirically untested for substellar objects.

We report observations with the HIRES echelle on the Keck telescope of a brown dwarf candidate in the Pleiades. PPL 15 was found by Stauffer, Hamilton, & Probst (1994). We confirm cluster membership by its radial velocity and H $\alpha$  emission. With new infrared photometry, we determine its bolometric luminosity. The spectrum of PPL 15 appears to contain the lithium resonance line with an equivalent width of 0.5Å. Regardless of its exact mass, it is the first example of an object which passes the lithium test for brown dwarfs. In order that PPL 15 show lithium while slightly brighter members (including HHJ 3) do not, the age of the Pleiades must be close to 130 Myr, given current theory. This is in contrast to its canonical age of 70 Myr. The inferred mass of PPL 15 is then  $\sim 0.075M_{\odot}$ , placing it at the upper mass limit for brown dwarfs. If the cluster is younger, the inferred mass of PPL 15 is even lower. The larger age for the Pleiades implies that many young and intermediate cluster ages have been significantly underestimated. There are several independent lines of support for this proposition.

Abstract submitted for AAS [AAS] meeting

Date submitted: May 6, 1995      Electronic form version 1.6

**Fig. 5** My copy of the abstract submitted to the June 1995 meeting of the American Astronomical Society, which formed the basis of our public announcement of the first brown dwarf. I later noticed a small grammatical error

There has been continuing controversy about the discrepancy between lithium and turnoff ages. There may be effects of stellar magnetic fields or other less simple physical effects that complicate things somewhat. [Burke et al. \(2004\)](#) discuss these issues in more detail.

## 2.5 Presenting the First Brown Dwarf

By May 1995 we were convinced we had a real lithium detection, a real BD, and a proper explanation for the enigmatic results in the Pleiades to date. We considered publishing the results in *Nature* but decided against it. The main reason for our decision was that there was a rather sophisticated and new chain of reasoning that had to be gone through to understand our claims. Unlike what happened later that year with Gliese 229B, PPI 15 didn't really appear to be any different from other M6 dwarfs except by virtue of its lithium line and age. Furthermore we were also revising the age scale for young clusters. On the other hand we recognized the importance of the result and wanted to get it out to other astronomers and the public. It was almost too late, but we submitted a late abstract to the June 6 AAS meeting in Pittsburgh (Fig. 5), and were quickly invited to do a press release as well.

Explaining the lithium test to the public was clearly a bit of a challenge, and I worked with the UC Berkeley press officer (Bob Sanders) to make the attempt. The result was the explanation shown in Fig. 6. We wanted to deal with the complication that the Sun shows depleted but visible lithium, yet is clearly not a BD. This is as hard to explain as the age error due to convective overshoot (which we did not attempt to explain to the public). It is related in a way, in that the issue is again whether convection mixes material into the burning zone. For the Sun a classical model would say that the outer convection zone does not reach sufficiently deep to mix surface lithium down to where it could be burned. Partially understood “anomalous mixing” mechanisms have to be invoked to explain the disparate lithium observations in the solar mass regime (even convective overshoot is not enough). We simplified this a great deal, and apparently reporters thought it comprehensible enough that our diagram appeared in many newspapers. The headline in the New York Times read “Big Telescope Is First to Find Brown Dwarf, Team Reports”. The San Francisco Chronicle reported “Astronomers Find Cosmic Missing Link”, and a modified color version of Fig. 6 appeared on the front page.

We submitted our paper to the *Astrophysical Journal* on July 7, 1995, and it was accepted August 24. We presented the results to the first Keck Science meeting on September 14 at Caltech (I recall that there were members of the Gliese 229B team in the audience, who kept quiet). All of this was before the other “first” announcements of the discovery of BDs. Despite that, we are often not thought of as the clear and sole discoverers of BDs for several reasons (I wonder if it would be different had we decided to submit to *Nature* in June). One of them is that [Basri et al. \(1996\)](#) did not actually appear in print until February 1996 (by which time the two *Nature* papers on Teide 1 and Gliese 229B had already been several months in print).

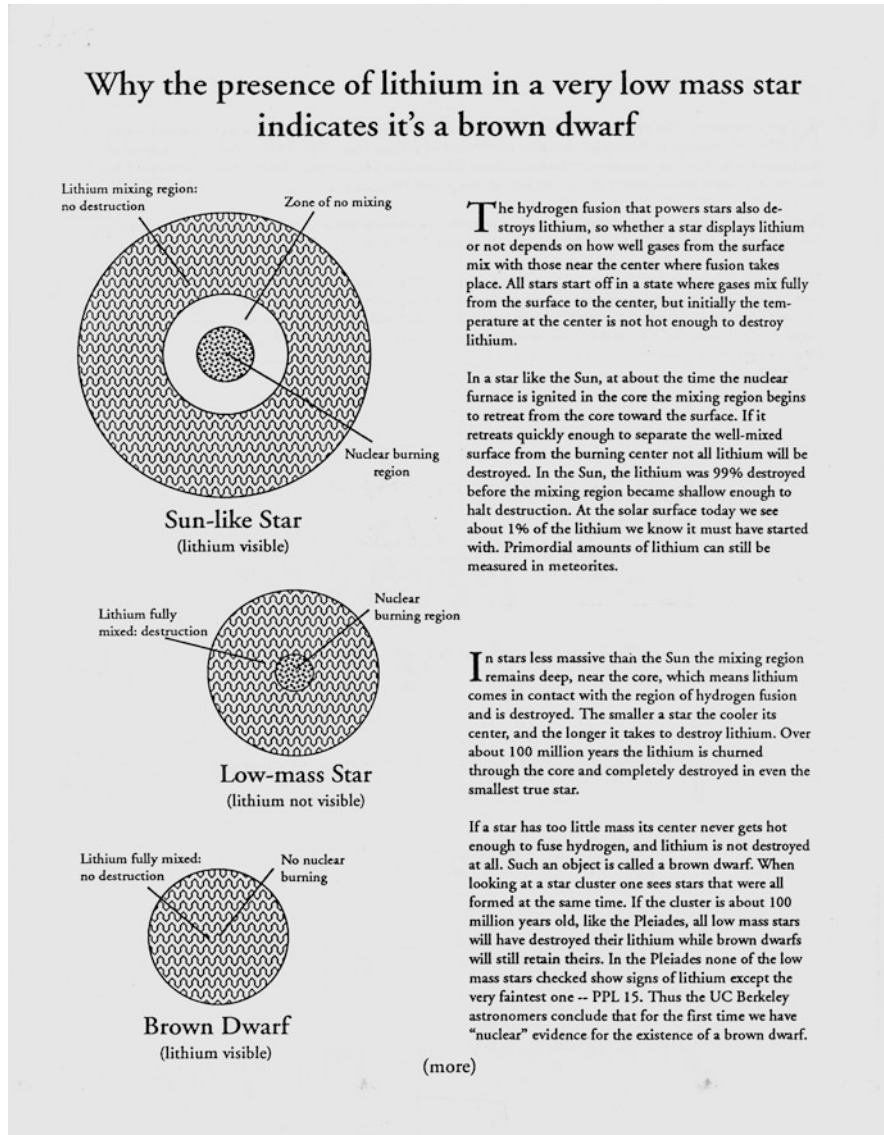


**Fig. 6** The figure in the UC Berkeley press release that discussed how the lithium test can give certification of substellar status. We included the situation for the Sun (complicated), low mass stars (simple) and BDs (also simple, but we left out the wrinkle of behavior between 60 and 75 M<sub>Jup</sub>)

At that time preprint servers were not yet in general use. Another is that both the possibly partial depletion of lithium and the most conservative (high) estimate of the mass of PPI 15 put it near the substellar boundary. It was therefore less definitive to many astronomers for whom the lithium test was new. Finally, there was the issue

of lithium dating itself; it was both a new technique and it challenged the very entrenched method of dating clusters by their upper main sequence turnoffs. Of course if one did not accept the revised age then the object moved more safely into the substellar regime. None of these issues ultimately proved to be a problem – PPI 15 is now quite definitely known to be substellar – but they delayed general acceptance of the result long enough to dilute it.

The effect of revising age significantly older is to increase the inferred masses of all the Pleiades very low-mass objects, so that HHJ 3 falls comfortably in the stellar domain, and PPI 15 moves up near (but not above) the substellar boundary. One could then quibble (and some did) about whether PPI 15 was a “true” BD or should be thought of as a transitional object. We admitted that it was transitional in some sense; in fact high-mass BDs (between 60 and 75  $M_{\text{Jup}}$ ) will eventually deplete lithium and engage in temporary hydrogen burning, but never stabilize themselves this way and so never become main-sequence stars. Only by adopting the largest plausible age correction could one push PPI 15 up near the substellar boundary; the less the age correction the less its inferred mass.

In any case, the obvious prediction was that any cluster members that are fainter than PPI 15 should show strong lithium and be further into the substellar domain. This was the situation that allowed [Rebolo et al. \(1995\)](#) a few months later to publish the fainter Pleiades member Teide 1 in *Nature* and assert (correctly) it is an obvious BD, without having actually done the lithium test. Such a claim could only be credible after we had announced our results on PPI 15. Although Teide 1 is a couple of spectral subclasses cooler than PPI 15, without the lithium detection in PPI 15 there was no guarantee that Teide 1 is below the lithium depletion boundary and therefore a true BD. There were a number of previous Pleiades objects that were expected to be BDs on the basis of their luminosity and temperature, but later failed the lithium test. A viewgraph I used sometime in 1996 to summarize the lithium results for the first Pleiades BDs is shown in Fig. 7. In early 1996 Marcy and I teamed up with Rebolo, Zapatero Osorio, and Martín to perform the lithium test at Keck on Teide 1 (and another nice object the IAC group found: Calar 3). This was done at lower resolution but good S/N given the objects’ faintness ([Rebolo et al. 1996](#)).

## 2.6 Two for One: The Final Word on PPI 15

A close look at Fig. 7 shows that the very low-mass Pleiads are somewhat spread away from the zero-age main sequence. Some authors had interpreted this as an age spread (and that was being debunked at around this time), but another good explanation for it is the presence of binaries (after acknowledging that some of it is just observational uncertainty). More careful photometry lead the IAC group to wonder whether PPI 15 sits high enough off the zero-age main sequence that it might be binary. I realized that we had looked at the radial velocity of PPI 15 in one of our best spectra to confirm cluster membership but had not repeated the determination

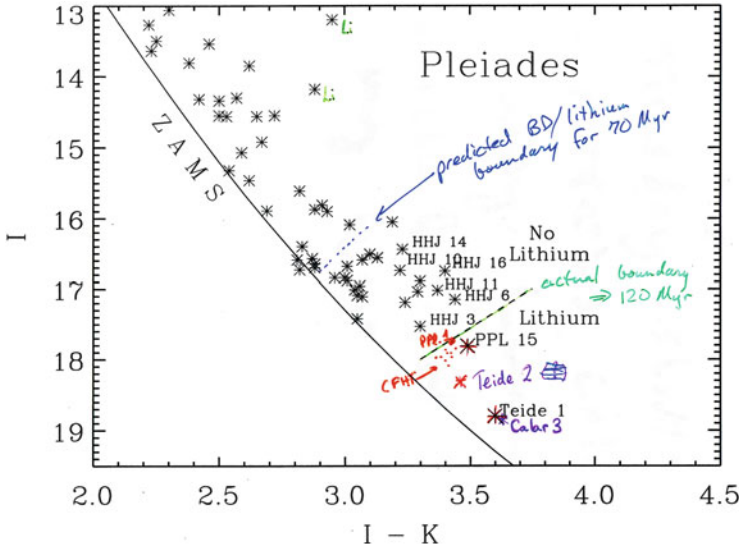


**Fig. 7** A summary of the lithium constraints and lithium boundary for the Pleiades by mid-1996. All the labeled objects had been tested for lithium. Those above the “actual boundary” did not show lithium, while all objects tested below it did. The location of the expected boundary given the previously accepted age for the Pleiades of 70 Myr is also shown (which explains why the early results of the lithium test were so perplexing). Note the two objects near the top of the diagram that are also labeled “Li”; these are explained in Sect. 3.3

for all the spectra. Of course, it seemed like it would be an incredible stroke of luck if the binary were close enough to show radial velocity variability (and even more so if it turned out to be a double-lined binary). Nonetheless, as soon as I performed the cross-correlation of PPI 15 spectra against UX Tau C, the correlation function was sometimes double-peaked! I immediately suspected that telluric lines were somehow fooling me, and spent about a week convincing myself that the effect was really stellar. There was no doubt that it was, as seen in Fig. 8.

It became rapidly apparent that the binary components were close to equal mass, and the period was very short. I could see substantial changes in the line positions from night to night. In order to get an orbit I would obviously have to return to HIRES and somehow arrange to get a whole series of nights in a row (at least for this object). I asked that my nights be scheduled within a week, and by good fortune the other observers during that time turned out to be John Stauffer and Geoff Marcy. It had taken me a couple of years to convince John of the efficacy of lithium dating, but as an ace cluster observer once he was convinced he more or less took over the field, e.g. Stauffer et al. (1998), Barrado y Navascués et al. (1999), and Stauffer et al. (1999). We were pleased with our former collaboration on PPI 15, so it took no effort to swap time during his nights with time during mine so I could get more orbital phase coverage. Geoff was happy to donate a little time from planet hunting to cooperate. The weather also cooperated just enough, and I got useable observations

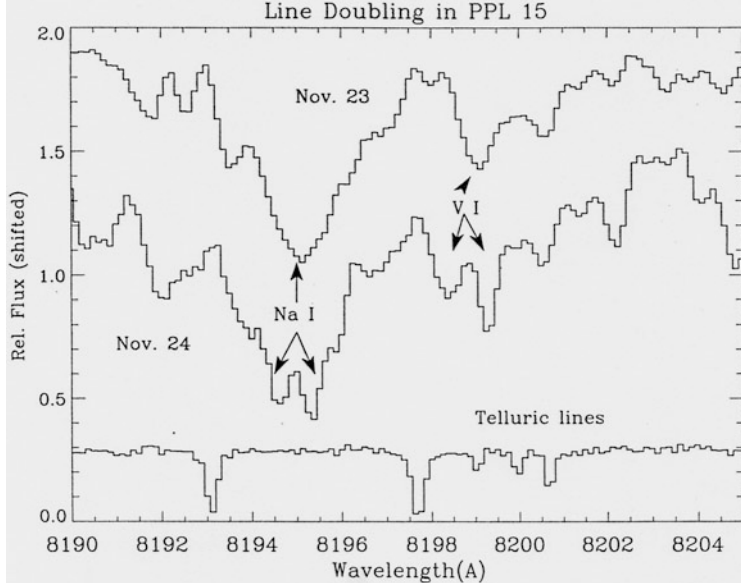


**Fig. 8** An unpublished plot showing the line doubling in the spectrum of PPI 15, as seen from our first nights of observations (which we did not notice at the time). This proves that PPI 15 is a spectroscopic binary. The fact that the sodium and vanadium lines go from single to double one night later indicates that the orbital period must be quite short. The lithium detection was more obvious on the nights where the lines were not doubled. The bottom trace shows a hot star spectrum in which only telluric lines are visible (showing they are not responsible for the double lines above)

every night from December 1 to 7, 1997. Because I was no longer searching for lithium they could be substantially shorter; doing cross-correlations near the red end of the CCD range works just fine and the object is so red that it is much brighter there. We could easily include all the previous observations of PPI 15 as well. The final phase coverage and velocity variations are shown in Fig. 9.

The orbital period we found is roughly 6 days. This is a rather rare sort of close binary; it is a remarkable bit of serendipity that the first BD should have such a striking character. Fifteen years later, the number of BD binaries that are spectroscopic binaries is still very small. There are only a handful of BD spectroscopic binaries known with solved orbits (e.g., Stassun et al. 2006; Joergens et al. 2010) and BD radial velocity surveys indicate a binary fraction of 10–20% (e.g., Joergens 2008; Blake et al. 2010). The separation of PPI 15 is only 0.03 AU. There is a bias in magnitude-limited surveys in favor of finding binaries, but no particular advantage for such close ones. The binary is also quite eccentric ( $e = 0.45$ ); that is less uncommon and does not come close to violating tidal circularization timescales. We infer an inclination of about  $50^\circ$  (this is not observed, but is compatible with the dynamical constraints on the system). We speculated that low-mass systems might also have generally lower separations, or that the system

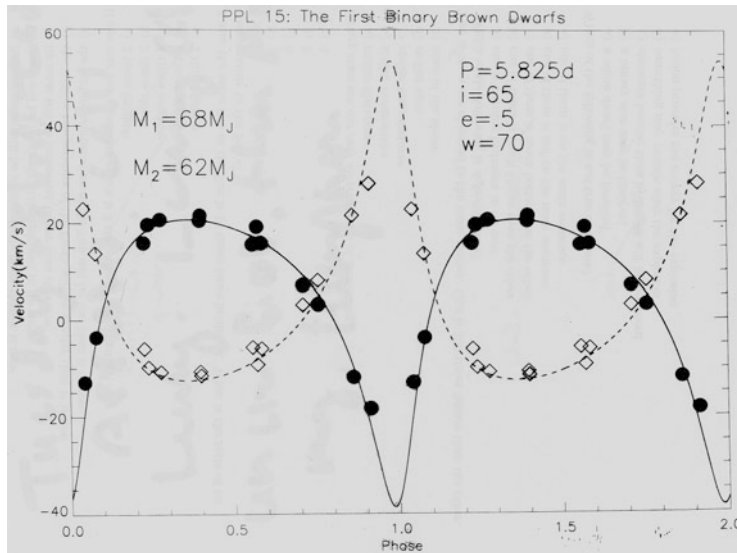


**Fig. 9** An unpublished plot of the velocity observations for both components from the PPI 15 high-resolution spectra taken with HIRES on Keck. Note that the orbit is fairly eccentric as well as very tight (short period)

is a result of an altered triple. Even now there are under five double-lined substellar systems known (Luhman 2012).

This was during the time that Eduardo came to Berkeley to work with me, so we attacked the question of the binary properties. We could see both components, and the width of the correlation function also gave us their rotational broadening. Both binary components are unusually slow rotators for very low-mass Pleiads and have similar projected rotational velocities (about 10 km/s). The lines are of nearly equal strength, but their relative strength varies with wavelength indicating that one object is redder than the other. Although we don't know the orbital inclination, the fact that both objects are contributing similar amounts of red light allows us to use models to constrain the total system mass to about 0.13 solar masses. The mass ratio comes from the total velocity separation of the components ( $\sim 0.87$ ) and the behavior of the relative line intensities (0.8–0.9). The latter also suggest spectral types for the two components of M6 and M7 (compatible with the observed M6.5). Taking a mass ratio of 0.85 with the total mass implies component masses of  $60$  and  $70 M_{\text{Jup}}$ . Thus, both components are comfortably within the substellar domain, and the lower-mass component probably will never deplete its lithium.

We could not measure the two separate components in the lithium order (S/N is too low) but we obtain an explanation of the results in our original work. The November 1994 spectra were partly taken at an orbital phase where the two components were close in velocity (which enhances the visibility of the lines), while the March 1995 observations were made at a large velocity separation (where the sky noise can attack each of the lines separately). Compounded with the extra lunar

sky light, it is no surprise that the March observations did nothing to confirm the presence of lithium. The binary nature also introduces a couple of complications. First, the equivalent width for either of the components is less clear; the hot component presumably dominates the continuum but the cooler component should have a stronger line, and what is seen depends on the phase of the observation. The second is that the expected lithium depletion is different for the two objects (which have different masses). We concluded that it is not necessarily true that lithium is partially depleted in PPI 15 (it almost certainly isn't for the cooler component). The net effect of all this is that PPI 15 is not a transitional object but a pair of true BDs ([Martín et al. 1999a](#)).

My collaborators and I were also involved in the first discoveries of resolved BD binaries. In 1998 we were involved in a survey to push ever fainter in finding Pleiades BDs in order to get some real information on the substellar mass function. One of the objects that lies significantly below the then well-established lithium boundary (CFHT-PI-18) showed up as a resolved pair with a separation of a third of an arcsec (corresponding to about 40 AU at the distance of the Pleiades). [Martín et al. \(1999a\)](#) find that both components are clearly substellar if members of the cluster, with masses of 45 and 35  $M_{\text{Jup}}$ . The separation and mass ratio would not be surprising if the system was stellar, giving an early indication that the formation processes could be similar. Our rate of success (1 out of 6 targets) was also consistent with stellar expectations. This was the first “visible” or resolved BD pair discovered, but it was still a cluster rather than a field object.

We also discovered the first field BD binary, in a two-target exploratory attempt using the NICMOS camera on the Hubble Space Telescope ([Martín et al. 1999b](#)). The targets were two of the first known field lithium BDs (discussed near the end of Sect. 3.1). It turns out that both of them are binary, although at the time the components of Kelu-1 had too low an angular separation to resolve. They were resolved a few years later as the binary orbit separated them on the sky ([Liu and Leggett 2005](#)). The other target, DENIS 1228.2-1547, did reveal both components with an angular separation of 0.275 arcsec. They are nearly equal mass, and the lithium detection implies they are both less massive than 60  $M_{\text{Jup}}$ , but the parallax was not well-known enough to convert a luminosity to a mass using evolutionary models (as we had done for CFHT-PI-18). The fact that both targets turned out to be binary is partly a selection effect due to the fact that binaries are brighter, but it conveyed the impression that BD binaries must be fairly common. We now know that BD companions occur a little less often than M dwarfs, with a frequency of roughly 20 % ([Duchêne and Kraus 2013](#)).

### 3 Further Adventures with Lithium

I refined and developed the method of lithium dating after the early successes and extended it to other clusters and field objects. This led to a summary review ([Basri 1998](#)) which advanced the adoption of the method by others. It should be clear that

I had developed a very strong working relationship with a number of astronomers at the IAC headed by Rafael Rebolo, especially Eduardo Martín who subsequently came to Berkeley as a postdoctoral researcher for several years. This collaboration was very fruitful for all of us; the IAC had a lot of surveys in progress and access to lower dispersion spectroscopy, while I had access to high-resolution spectroscopy at the Keck telescope and a long history of line profile analysis. I also had a good collaboration with the PHOENIX stellar atmospheres group ([Allard et al. 1997](#)). Our collaboration was active past the turn of the millennium.

### **3.1 The Lithium Test in the Field**

Can the lithium test be used for field objects, given that one will not generally know the age of an object? Clearly it works to distinguish main-sequence M stars from BDs less massive than 60 Jupiters (that was the original idea). [Basri \(1998\)](#) refined the discussion of how to apply the lithium test in the field. Figure 10 shows that the lithium depletion region, taken with the observed luminosity or temperature of the object, provides a lower bound to the mass and age (jointly) if lithium is not seen. Conversely, it provides an upper bound to the mass and age if lithium is seen. The temperature at which an object at the substellar limit has just depleted lithium sets a crucial boundary. It is the temperature below which, if lithium is observed, the object must automatically be substellar. More massive (stellar) objects will have destroyed lithium before they can cool to this temperature. A substellar mass limit of 75 Jupiter masses implies a temperature limit of about 2,700 K for lithium detection, which roughly corresponds to a spectral type of M6. Thus, *any object M7 or later which shows lithium must be substellar*. This form of the test is easier to apply than that employing luminosity, which requires one to know the distance and extinction to an object. Otherwise they are equivalent.

One wrinkle is that it takes stars a finite amount of time to deplete their lithium. Thus, if an object is sufficiently young, it will show lithium despite having a mass above the hydrogen-burning limit (giving the possibility of a false positive in the test). On the other hand, the minimum mass for lithium destruction is below the minimum mass for stable hydrogen burning. Thus, if we wait long enough, the high-mass BDs will deplete their lithium too (giving the possibility of a false negative in the test). For instance, the binary BDs Gl 569Ba and Bb have dynamical masses that prove they are substellar, yet lithium is not detected ([Zapatero-Osorio et al. 2005](#)). In other cases, an object could lie in the temperature range where it might be a BD and show lithium, but the age would have to be known to be sure (it might be young enough that a very low-mass star has not had time to deplete lithium). A more definitive case is provided by LP 944-20 ([Tinney 1998](#)). It is sufficiently cool (M9) that the fact that lithium is detected guarantees it is a BD even though we know little about its age; the lithium detection provides an upper limit on the age. This is an example of an object that was known for quite some

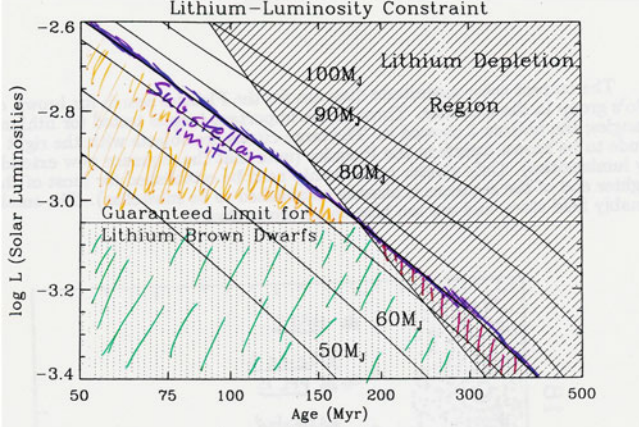


Figure 1. Figure 1. Lithium depletion in a luminosity-age diagram. Cooling curves are shown for several masses. The lithium depletion region (where lithium is reduced to 1% of its primordial value) is given by the hatched region. The region where a lithium detection guarantees a substellar object (regardless of age) is shown with stippling. If one knows the luminosity of an object, and whether lithium is detected or not, the diagram constrains its age and mass. The substellar mass limit is the dark line at  $75M_J$ .

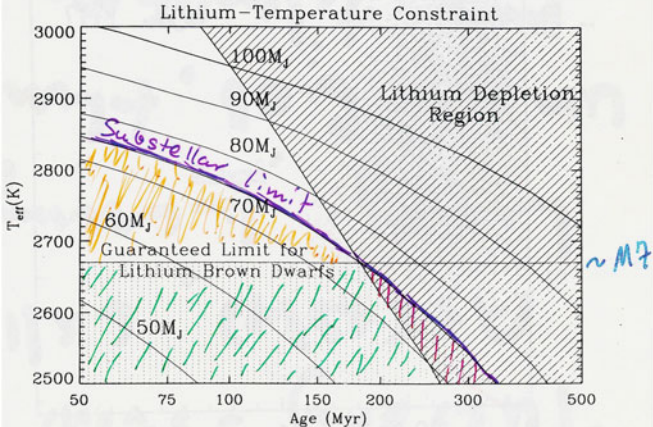


Figure 2. Lithium depletion in a temperature-age diagram, quite similar to Fig. 1. The lithium depletion region (where lithium is reduced to 1% of its primordial value) is given by the hatched region. The region where a lithium detection guarantees a substellar object (regardless of age) is shown with stippling. If one knows the spectral type of an object (and its implied effective temperature), and whether lithium is detected or not, the diagram constrains its age and mass. The substellar mass limit is the dark line at  $75 M_J$ .

**Fig. 10** Summary viewgraphs I showed in talks on the use of lithium as a substellar diagnostic. The *upper diagram* is for luminosity and the *lower diagram* is for temperature of the object being tested. These quantities are shown as a function of age for various masses (the labeled curves). The stippled region (marked with *green*) is the region in which substellar status is guaranteed through this nuclear diagnostic. The diagrams show that the situation is more complicated above that region, since BDs may not have had time to deplete their lithium. For field objects, the age is generally unknown, so only the stippled (*green*) region provides a guarantee of substellar status. Put simply, any dwarf object M7 or cooler which displays lithium must be a BD regardless of its age.

time before 1995 as a faint red object uncovered in a proper motion survey, whose substellar nature was completely unknown.

There were several large-scale field surveys underway at the time which had as one aim the discovery of field BDs. Two were major infrared surveys: 2MASS and DENIS. Another was a smaller proper motion survey. It was this latter that turned up the first field BD, dubbed Kelu-1 by Ruiz et al. (1997). That object was clearly cooler than any M dwarf (it resembled GD 165B, which was mentioned in Sect. 1.1) and it showed lithium, which guarantees that it is substellar. Shortly thereafter we applied the lithium test to a few of the most promising DENIS objects, and found lithium in DENIS 1228.2-1547 (Martín et al. 1997). This object was also cooler than the M spectral class, and it was clear that a new spectral class was needed to cover such objects (cf. the chapter by Cushing in this volume). It was in this paper that we formally proposed the L spectral class for the objects just under M dwarfs in temperature (which was adopted by the community). We showed that titanium oxide molecules had definitely disappeared, and were able to confirm the growing strength of the alkali lines, which dominate the optical spectra of cooler L dwarfs. On the other hand, our suggestion that Gliese 229B also be included in the L spectral class was not adopted; the presence of methane in the spectra came to be a hallmark of the “T” spectral class.

### 3.2 *The Lithium Test in Star-Forming Regions*

The lithium test is less obviously useful in star-forming regions. Even clear-cut stars have not had time to deplete lithium yet. Nonetheless, there have been numerous reports of BDs in star-forming regions. They are identified as BDs on the basis of their position in color-magnitude or HR diagrams, using pre-main sequence evolutionary tracks (cf. the chapter in this volume by Baraffe). One must worry whether the pre-main sequence tracks for these objects are correct, or if there are residual effects of the accretion phase. If one of these candidates doesn’t show lithium, it can be immediately eliminated as being a non-member of the star-forming regions. The lithium test as applied in the field still works: if a member of a star-forming region is cooler than about M7 (here we should be careful that the pre-main sequence temperature scale might be a little different) and the object shows lithium, then it must be substellar. Indeed, for an object to be so cool at such an early age pushes it very comfortably into the substellar domain.

Some very faint/cool objects have been found in star-forming regions whose substellar status seems relatively firm (if they are members). The lowest of these may be below the deuterium burning limit. Spectroscopic confirmation of these candidates is imperative, as has been done for a BD near the deuterium-burning boundary in  $\sigma$  Ori (Zapatero-Osorio et al. 1999). A number of objects even fainter have been found in the past decade (Béjar et al. 2011). Such observations indicate that the substellar mass function may extend right down through the lowest-mass BDs into the planetary domain. It is natural to wonder how far it goes below that,

since there is no obvious reason why it should stop just because deuterium burning ceases to function.

### 3.3 A Final Lithium Mystery in the Pleiades

Taking another look at Fig. 7 reveals one other very odd feature. There are two stars in the upper part of the diagram that appear to be pre-main sequence stars. These also arose from the search by [Hambly et al. \(1993\)](#) and so have HHJ designations as well: 339 and 430. They therefore satisfy the cluster membership criteria of the other HHJ objects which played a pivotal role in defining the lithium depletion boundary in the Pleiades. Given the age of the cluster (especially after our upward revision) one certainly does not expect pre-main sequence stars (younger than 10 Myr) to still be present. The Pleiades is known for the pictures of it which show diffuse dust surrounding the bright stars (so one might be tempted to think it is still forming stars), but that nebulosity is well-known to be dynamically unrelated to the cluster. The cluster is simply passing through a diffuse interstellar cloud at the moment. Other authors had argued for a large age spread in the cluster, but those arguments did not stand the test of time.

Of course, if the stars really were pre-main sequence stars they would be comfortably above the substellar limit but should still show lithium given their youth. Shri Kulkarni had heard about the lithium test and my plans for the Pleiades from a colloquium I gave earlier in 1994 at Caltech, and decided his group should try it. He observed a number of HHJ stars near the lithium boundary (but not as faint as HHJ 3) in mid-October 1994, and included HHJ 430 in the list out of curiosity. I had the same curiosity, and observed HHJ 339 in the initial PPI 15 run in late November 1994. The non-detection of lithium in his faint HHJ targets is consistent with my group's non-detections, and provided further evidence that lithium depletion was complete above the depletion boundary.

Because of my success with PPI 15, and due to the fact that Ben Oppenheimer began to visit Berkeley in the years just after the announcement of Gliese 229B, we eventually collaborated on a paper ([Oppenheimer et al. 1997](#)) which included these odd Pleiades objects. Both of them showed pronounced lithium, which was entirely consistent with their apparent pre-main sequence status (with the implication that they are indeed at about the distance of the Pleiades). Their ages do not appear to be any more than 20–30 Myr (and could be smaller). This conclusion is further supported by their levels of H $\alpha$  emission. Their radial velocities provide further “proof” of cluster membership on the other hand, so the stars present a real conundrum. Taken at face value one might think that star formation had been going on for nearly 100 Myr in the cluster, yet there is no real evidence for intermediate age stars.

Ben and I eventually came up with an interesting dynamical explanation for them. [Oppenheimer et al. \(1997\)](#) posit that the solution is one of dynamical history. Everything is moving in our Galaxy, and not just around the galactic center. We point

out that given the positions and space motions of the cluster and the Taurus-Aurigae star-forming region, it is not that unlikely that they intersected each other a few Myr ago. It would still be very difficult, however, for the Pleiades to actually capture stars from Taurus. Of more interest is the set of young stars which share very similar space motion with the Pleiades (although they are not co-located with it). This set of stars is sometimes referred to as the “Pleiades supercluster”. Other stars with properties similar to HHJ 339 and HHJ 430 are kinematic members of this supercluster.

If one imagines a set of interstellar clouds with similar origin streaming along with similar space motions but somewhat different locations, there is no reason for them all to form stars at the same time. In particular, suppose there was a cloud that was closer to us but formed stars only 20–30 Myr ago and was not dense enough to form a bound cluster. After they were born, the stars in this cloud would begin spreading apart with velocities of a few km/s. Sufficient time passes that the leading edge of this burst of stars could actually be near the Sun. For example, the nearby very young and active star AB Dor is a member of the Pleiades supercluster (Eggen 1995). On the other side, the trailing edge of the burst of stars could be approaching the Pleiades. Such stars could be superposed on the cluster with respect to sky coordinates, would have similar space motions, and would seem to satisfy cluster membership criteria closely enough (if not perfectly). That is our explanation for the brighter lithium HHJ objects.

## 4 Conclusion

The discovery of BDs was the highlight of my astrophysical career. It is rare to find a whole new class of astronomical objects, especially ones that are as much as a few percent as numerous as stars. Our motivations were several, including the joy of the hunt, the possibility that BDs were a significant component of dark matter (which turned out not to be the case), and the interest in observing objects intermediate between stars and planets. My involvement with BDs also led to very enjoyable participation in the debate over “what is a planet” (which examines both the low- and high-mass boundaries for planets). Obviously the discovery involved a lot of friends and collaborators, and I share the experience and credit with them. I was very fortunate in being a faculty member at UC Berkeley, where the Keck telescopes were conceived and where Keck access was possible early on. Astronomers at the Univ. of California and Caltech knew we had a unique opportunity to do important work with this new tool, and many epochal discoveries have been made utilizing it. We owe a debt to the designers and builders of the telescopes, and I especially want to thank Prof. Steven Vogt, who designed and built both of the high-resolution spectrographs that have enabled the bulk of the science that I have done. I also want to thank the organizers of the conference (especially Viki Joergens) who caused this book to be written. It was a pleasure to revisit those exciting days gone by, and to see the tremendous progress that has been made on BDs since then.

## References

- Allard, F., Hauschildt, P., Alexander, D.R., Starrfield, S.: Model atmospheres of very low mass stars and brown dwarfs. *ARA&A* **35**, 137 (1997)
- Barrado y Navascués, D., Stauffer, J.R., Patten, B.M.: The lithium-depletion boundary and the age of the young open cluster IC 2391. *ApJ* **522**, L53 (1999)
- Basri, G.: Lithium near the substellar boundary: a new age diagnostic. *Mem. Soc. Astr. Ital.* **68**, 917 (1998)
- Basri, G.: Observations of brown dwarfs. *ARA&A* **38**, 485 (2000)
- Basri, G., Marcy, G.W., Graham, J.R.: A search for lithium in Pleiades brown dwarf candidates using the Keck HIRES echelle. *ApJ* **428**, 57 (1994)
- Basri, G., Marcy, G.W., Graham, J.R.: Lithium in brown dwarf candidates: the mass and age of the faintest Pleiades stars. *ApJ* **458**, 600 (1996)
- Becklin, E.E., Zuckerman, B.: A low-temperature companion to a white dwarf star. *Nature* **336**, 656 (1988)
- Béjar, V.J.S., Zapatero-Osorio, M.R., Rebolo, R., Caballero, J.A., Barrado, D., Martín, E.L., Mundt, R., Bailer-Jones, C.A.L.: The substellar population of  $\sigma$  Orionis: a deep wide survey. *ApJ* **743**, 64 (2011)
- Bildsten, L., Brown, E.F., Matzner, C.D., Ushomirsky, G.: Lithium depletion in fully convective pre-main-sequence stars. *ApJ* **482**, 442 (1997)
- Blake, C.H., Charbonneau, D., White, R.: The NIRSPEC ultracool dwarf radial velocity survey. *ApJ* **723**, 684 (2010)
- Burke, C.J., Pinsonneault, M.H., Sills, A.: Theoretical examination of the lithium depletion boundary. *ApJ* **604**, 272 (2004)
- D'Antona, F., Mazzitelli, I.: Evolution of very low mass stars and brown dwarfs. I – the minimum main-sequence mass and luminosity. *ApJ* **296**, 502 (1985)
- Delfosse, X., Tinney, C.G., Forveille, T., Epchtein, N., et al.: Field brown dwarfs found by DENIS. *A&A* **327**, L25 (1997)
- Duchêne, G., Kraus, A.: Stellar multiplicity. arXiv1303.3028 (2013)
- Eggen, O.J.: Pre-main-sequence stars in the Pleiades supercluster. *AJ* **110**, 1749 (1995)
- Forrest, W.J., Barnett, J.D., Ninkov, Z., Skrutskie, M., Shure, M.: Discovery of low-mass brown dwarfs in Taurus. *PASP* **101**, 877 (1989)
- Grether, D., Lineweaver, C.H.: How dry is the brown dwarf desert? Quantifying the relative number of planets, brown dwarfs, and stellar companions around nearby sun-like stars. *ApJ* **640**, 1051 (2006)
- Hambly, N.C., Hawkins, M.R.S., Jameson, R.F.: Very low mass proper motion members in the Pleiades. *A&A Suppl.* **100**, 607 (1993)
- Joergens, V.: Binary frequency of very young brown dwarfs at separations smaller than 3 AU. *A&A* **492**, 545 (2008)
- Joergens, V., Müller, A., Reffert, S.: Improved radial velocity orbit of the young binary brown dwarf candidate Cha H $\alpha$  8. *A&A* **521**, 24 (2010)
- Kafatos, M.C., Harrington, R.P., Maran, S.P.: *Astrophysics of Brown Dwarfs*. Cambridge University Press, New York (1986)
- Kirkpatrick, J.D., Beichman, C.A., Skrutskie, M.F.: The coolest isolated M dwarf and other 2MASS discoveries. *ApJ* **476**, 311 (1997)
- Kirkpatrick, J.D., Allard, F., Bida, T., Zuckerman, B., Becklin, E.E., Chabrier, G., Baraffe, I.: An improved optical spectrum and new model FITS of the likely brown dwarf GD 165B. *ApJ* **519**, 834 (1999)
- Kumar, S.S.: The structure of stars of very low mass. *ApJ* **137**, 1121 (1963)
- Latham, D.W., Mazeh, T., Stefanik, R.P., Mayor, M., Burki, G.: The unseen companion of HD114762 – a probable brown dwarf. *Nature* **339**, 38 (1989)
- Liu, M.C., Leggett, S.K.: Kelu-1 is a binary L dwarf: first brown dwarf science from laser guide star adaptive optics. *ApJ* **634**, 616 (2005)

- Luhman, K.L.: The formation and early evolution of low-mass stars and brown dwarfs. *ARA&A* **50**, 65 (2012)
- Magazzù, A., Martín, E.L., Rebolo, R.: A spectroscopic test for substellar objects. *ApJ* **404**, L17 (1993)
- Martín, E.L., Rebolo, R., Magazzù, A.: Constraints to the masses of brown dwarf candidates from the lithium test. *ApJ* **436**, 262 (1994)
- Martín, E.L., Basri, G., Delfosse, X., Forveille, T.: Keck HIRES spectra of the brown dwarf DENIS-P J1228.2-1547. *A&A* **327**, L29 (1997)
- Martín, E.L., Basri, G., Zapatero-Osorio, M.R.: PPL 15: the first brown dwarf spectroscopic binary. *AJ* **118**, 105 (1999a)
- Martín, E.L., Brandner, W., Basri, G.: A search for companions to nearby brown dwarfs: the binary DENIS-P J1228.2-1547. *Science* **238**, 1718 (1999b)
- McCarthy, D.W., Probst, R.C., Low, F.J.: Infrared detection of a close cool companion to Van Biesbroeck 8. *ApJ* **290**, L9 (1985)
- Meynet, G., Mermilliod, J.-C., Maeder, A.: New dating of galactic open clusters. *A&A Suppl.* **98**, 477 (1993)
- Nelson, L.A., Rappaport, S., Chiang, E.: On the Li and Be tests for brown dwarfs. *ApJ* **413**, 364 (1993)
- Oppenheimer, B.R., Kulkarni, S.R., Matthews, K., Nakajima, T.: Infrared spectrum of the cool brown dwarf Gl 229B. *Science* **270**, 1478 (1995)
- Oppenheimer, B.R., Basri, G., Nakajima, T., Kulkarni, S.R.: Lithium in very low-mass stars in the Pleiades. *AJ* **113**, 296 (1997)
- Oppenheimer, B.R., Kulkarni, S.R., Stauffer, J.R.: Brown dwarfs. In: Mannings, V., Boss, A., Russell, S.S. (eds.) *Protostars and Protoplanets IV*, p. 1313. University of Arizona Press, Tucson (2000)
- Rebolo, R., Martín, E.L., Magazzù, A.: Spectroscopy of a brown dwarf candidate in the Alpha Persei open cluster. *ApJ* **389**, L83 (1992)
- Rebolo, R., Zapatero-Osorio, M.R., Martín, E.L.: Discovery of a brown dwarf in the Pleiades star cluster. *Nature* **377**, 129 (1995)
- Rebolo, R., Martín, E.L., Basri, G., Marcy, G.W., Zapatero-Osorio, M.R.: Brown dwarfs in the Pleiades cluster confirmed by the lithium test. *ApJ* **469**, L53 (1996)
- Ruiz, M.T., Leggett, S.K., Allard, F.: Kelu-1: a free-floating brown dwarf in the solar neighborhood. *ApJ* **491**, L107 (1997)
- Stassun, K.G., Mathieu, R.D., Valenti, J.: Discovery of two young brown dwarfs in an eclipsing binary system. *Nature* **440**, 311 (2006)
- Stauffer, J.R., Herter, T., Hamilton, D., Rieke, G.H., Rieke, M.J., Probst, R., Forrest, W.: Spectroscopy of Taurus cloud brown dwarf candidates. *ApJ* **367**, L23 (1991)
- Stauffer, J.R., Hamilton, D., Probst, R.: A CCD-based search for very low mass members of the Pleiades cluster. *AJ* **108**, 155 (1994)
- Stauffer, J.R., Schultz, G., Kirkpatrick, J.D.: Keck spectra of Pleiades brown dwarf candidates and a precise determination of the lithium depletion edge in the Pleiades. *ApJ* **499**, L199 (1998)
- Stauffer, J.R., Barrado y Navascués, D., Bouvier, J., Morrison, H.L., Harding, P., Luhman, K.L., Stanke, T., McCaughrean, M., Terndrup, D.M., Allen, L., Assouad, P.: Keck spectra of brown dwarf candidates and a precise determination of the lithium depletion boundary in the  $\alpha$  Persei open cluster. *ApJ* **527**, 219 (1999)
- Tinney, C.G.: The intermediate-age brown dwarf LP944-20. *MNRAS* **296**, L42 (1998)
- Williams, D.M., Comeron, F., Rieke, G.H., Rieke, M.J.: The low-mass IMF in the rho Ophiuchi cluster. *ApJ* **454**, 144 (1995)
- Zapatero-Osorio, M.R., Bejar, V.J.S., Rebolo, R., Martín, E.L., Basri, G.: An L-type substellar object in Orion: reaching the mass boundary between brown dwarfs and Giant planets. *ApJ* **524**, L115 (1999)
- Zapatero-Osorio, M.R., Martín, E.L., Lane, B.F., Pavlenko, Y., Bouy, H., Baraffe, I., Basri, G.: Lithium depletion in the brown dwarf binary GJ 569Bab. *Astron. Nachr.* **326**, 948 (2005)

# Companions of Stars: From Other Stars to Brown Dwarfs to Planets and the Discovery of the First Methane Brown Dwarf

Ben R. Oppenheimer

**Abstract** The discovery of the first methane brown dwarf provides a framework for describing the important advances in both fundamental physics and astrophysics that are due to the study of companions of stars. I present a few highlights of the history of this subject along with details of the discovery of the brown dwarf Gliese 229B. The nature of companions of stars is discussed with an attempt to avoid biases induced by anthropocentric nomenclature. With the newer types of remote reconnaissance of nearby stars and their systems of companions, an exciting and perhaps even more profound set of contributions to science is within reach in the near future. This includes an exploration of the diversity of planets in the universe and perhaps soon the first solid evidence for biological activity outside our Solar System.

## 1 Why Objects Orbiting Stars Are Important

The most obvious reason for looking for objects orbiting other stars is simply the possibility of finding a new type of object never before seen by human beings. The extreme near vicinities of stars are generally inaccessible to observations because the star's light overwhelms significantly fainter companions or material.

However, the regions of space around stars are now being revealed in unprecedented detail and a whole “universe” of diverse phenomena from different types of brown dwarfs, to planets and disks of material are being studied. At the same time, some fundamental aspects of modern physics and astrophysics are due to the study of objects orbiting other stars. A brief treatment of some of the history of studying companions of stars follows.

---

B.R. Oppenheimer (✉)  
Department of Astrophysics, American Museum of Natural History,  
79th Street at Central Park West, New York, NY 10025 USA  
e-mail: [bro@amnh.org](mailto:bro@amnh.org)

## 1.1 An Early Use of Statistics in Science: The Discovery of Binary Stars

John Michell, an English rector and friend of William Herschel, both of whom were keenly interested in establishing the distance scale to other stars (through parallax and other astrometric measurements), published a truly unique paper in 1767 in which he applied statistics to the distribution of positions of stars on the sky ([Michell 1767](#)). Statistics was not even a formal mathematical field at the time. Indeed, not until the early 1800s would Gauss publish the concept of what became known as a normal or “Gaussian” distribution. Michell’s paper is perhaps one of the earliest applications of statistics to modern science.<sup>1</sup>

Michell simply took the angular distances between nearest neighbors of stars based on the various catalogs available at the time and looked at their distribution, comparing that distribution to what one would expect if they were just randomly positioned in space.

He introduced this idea in the following manner:

... from the apparent situation of the stars in the heavens, there is the highest probability that, either by the original act of the Creator or in consequence of some general law (such perhaps as gravity), they are collected together in great numbers in some parts of Space while in others there are few or none.

The argument I intend to make use of, in order to prove this, is of that kind, which infers either design or some general law, from a general analogy, and the greatness of the odds against things having been in the present situation, if it was not owing to some such cause.

Let us then examine what it is probable would have been the least apparent distance of any two or more stars, any where in the whole heavens, upon the supposition that they had been scattered by mere chance, as it might happen.

Michell concludes that the stars must often be associated in clusters and in pairs through gravitational interaction, and that the probability that this statement is wrong is “0.000076154.”

The importance of this cannot be overstated. First there is the introduction of statistics into astronomy, but more importantly, this was the first concrete evidence that gravity actually operated outside the solar system. Finally, it was the first statement that two stars might orbit each other, and that there exist in all likelihood gravitationally bound clusters of stars. Incidentally, this was only his second publication in the field of astronomy.

William Herschel, slightly later, provided the final confirmation of the existence of binary stars, by being the first to measure astrometric reflex motion due to unseen companions of a number of the brightest stars. This is not an easy task, because it

---

<sup>1</sup>In this same paper, Michell derives the first reasonably accurate distance to Sirius, short by about a factor of four, and discusses why stars twinkle. Later Michell also proposed the concept of black holes based on Newtonian physics. His early calculations are not vastly different from those that use general relativity. Michell was truly a remarkable contributor to modern astrophysics.

requires the detection of aberrant motions of stars, i.e. motions that are not due to parallax or proper motion.<sup>2</sup>

He achieved this in a complex paper ([Herschel 1803](#)) that details data covering a long period of observations:

I shall therefore now proceed to give an account of a series of observations on double stars, comprehending a period of about 25 years, which, if I am not mistaken, will go to prove, that many of them are not merely double in appearance, but must be allowed to be real binary combinations of two stars, intimately held together by the bond of mutual attraction.

Thus, the discovery that stars have gravitationally bound companions resulted in evidence for a fundamental concept in modern physics: that gravity is a universal law. The continued study of binary stars and faint companions of them led to even more interesting advances.

## ***1.2 Discovery of Degenerate Matter: The Companion of Sirius***

In 1844 Friedrich Bessel examined decades of astrometry of the star Sirius. He discovered an anomaly, and after considering various possible explanations, including perturbations in Earth's orbit about the Sun, concluded that there must be an unseen, but massive companion. Its orbit suggested a 50 year period ([Bessel 1844](#)).

Alvan Clark, the great American telescope maker and observer himself, actually saw the companion of Sirius in 1862, as he recalls in his autobiography ([Clark 1889](#)). Clark noted that it was about 8th magnitude or about 4,000 times fainter than Sirius. Using the orbit determined by Bessel, he concluded that the companion had to be about half the mass of Sirius due to its distance being twice that of Sirius from the center of gravity of their orbit. That implied a mass about that of the Sun. This was indeed a strange new type of object, but the physics of what it was would not begin to be revealed for another half century.

Walter Adams, a real pioneer in spectroscopic observations of stars, obtained a spectrum of "Sirius B" in 1915 ([Adams 1915](#)). The spectrum was remarkable in that the temperature of the object would have to be around 25,000 K, while that of Sirius itself was only 10,000 K. Given the fairly well known distance to the system, the measured luminosity,  $L$ , and this new temperature,  $T$ , the Stefan-Boltzmann relation  $L = 4\pi r^2 \sigma T^4$  gives a radius,  $r$ , roughly equal to that of the Earth. With a mass of  $1 M_\odot$ , this peculiar star had a density some 400,000 times that of the

---

<sup>2</sup>Proper motions of stars had been well established much earlier. In 1717 Edmund Halley used ancient catalogs, such as those of Ptolemy, Hipparchos and more recent positions of Aldebaran, Arcturus and Sirius to demonstrate motion ([Halley 1717](#)). Jacques Cassini, in 1740, confirmed the proper motion of Arcturus ([Cassini 1740](#)). By 1770, Tobias Mayer's catalog of 80 proper motions established the direction of motion of the Sun with respect to the stars ([Mayer and Maskelyne 1770](#)).

Earth. At the same time as all of this was going on, the fundamentals of quantum mechanics were emerging. Sirius B, now known to be the first example of a white dwarf, would later be explained through electron degeneracy. Work prompted by the existence of this white dwarf, the first observational constraints on degenerate matter, eventually led to Chandrasekhar's fundamental contributions to physics and stellar structure.<sup>3</sup>

### 1.3 Further Motivation

These are just a few examples of why studying companions of stars can provide major results in physics. Others include the use of eclipsing binaries to measure stellar radii, and of course the first conclusive evidence of gravitational waves, through the detection of orbital period derivatives in binary pulsars.

However, perhaps the most important motivation for studying objects orbiting other stars is simply the fact that we live on a planet that orbits a star. The parallel, that other stars may have planets, is no new idea. Indeed, Epicurus c. 300 BC wrote the following ([Hicks 1925](#)):

Moreover, there is an infinite number of worlds, some like this world, others unlike it.

Some 1,800 years later in 1584, Giordano Bruno ([Greenburg 1950](#)) made the daring assertion that

There are countless suns and countless earths all rotating around their suns in exactly the same way as the seven planets of our system. We see only the suns because they are the largest bodies and are luminous, but their planets remain invisible to us because they are smaller and non-luminous. The countless worlds in the universe are no worse and no less inhabited than our Earth.

This statement is partly why Bruno was burned at the stake due to the dominance of the papacy, which seemed to have little tolerance for conjectures about the universe based on facts. In addition, one can suppose that, even before Epicurus, people imagined that the stars were simply very distant versions of the Sun and that they

<sup>3</sup>A fascinating story surrounds the companion of Sirius and a modern desire among some to believe that societies with ancient roots have known what modern science only recently discovered. In 1950, an anthropologist studying the Dogon tribe in Mali, West Africa, published an account of a ceremony, supposedly performed since “ancient” times, which involves the fact that Sirius, central to their calendar system and mythology, is accompanied by an invisible, very heavy and metallic companion ([Griaule and Dieterlen 1950](#)). How could this ancient ceremony have been established unless an advanced, possibly extraterrestrial, civilization had visited thousands of years ago and told them about it? However, as a number of scientists have pointed out (e.g., [Roxburgh and Williams 1975](#)), the existence of Sirius B was known since the 1860s and its odd nature had been revealed by 1915 in America and Europe. Between 1915 and 1950 the Dogon had been visited by various European missionaries prior to Griaule’s study. Perhaps these visitors and their communications with the Dogon provide a far simpler explanation.

might have their own planets going around them. Note that Aristarchus advanced the idea of a heliocentric model of the solar system around the same time as Epicurus was alive (North 1995).<sup>4</sup>

These historical facts, as well as a fascination with extremely high-resolution imaging and adaptive optics, are some of the motivations that led me to join Shri Kulkarni's group at Caltech for graduate school, in a project that was attempting to find any kind of very faint object orbiting nearby stars, using a relatively new technique. The goal was to find brown dwarfs, objects that had been sought since Kumar's original technical report prepared when he worked at NASA's Goddard Institute for Space Studies in New York (Kumar 1962). However, I also saw an opportunity in developing the technique, since it would eventually lead to imaging and spectra of exoplanets.

## 2 The Discovery of the First Methane Brown Dwarf

Although the main subject of this section did not lead to a major revolution in physics, it is part of the history of an entirely new class of objects predicted by theory. Furthermore, the discovery of this unique object led to the first constraints on models of substellar atmospheres, and eventually, with the many other discoveries of so-called L and T dwarfs, to a bridge between stellar astrophysics and planetary science — a bridge that is still being built as I write this.

In 1994, when I began my graduate research, brown dwarfs were the subject of numerous observational campaigns, primarily deep surveys of young star clusters. Those sorts of searches and their successes are described in detail in Basri's and Rebolo's chapters in this volume. Basri also details some later disproven claims of finding brown dwarf companions of stars. One object, GD 165B, at the time, was quite puzzling. Orbiting a white dwarf, it seemed to be different from the coolest M dwarfs, but it was never accepted as a bona fide brown dwarf (Becklin and Zuckerman 1988). In retrospect, it is the first example of an early L dwarf. In addition, many brown dwarf searches were geared toward determining whether they could be a major component of baryonic dark matter. Since this period, our understanding of brown dwarfs has completely changed. Indeed they are a major part of the population of star-like objects, possibly almost as numerous as stars, but not a major contributor to dark matter. Furthermore, there is a broad diversity in their emergent spectra, a diversity that is not a property of stars. With more than 1,000 known brown dwarfs, the field is rich and extremely active to this day. Indeed, with possible connections to planets, and how the two classes of objects are related, brown dwarf research will remain important for the foreseeable future.

---

<sup>4</sup>The actual book in which Aristarchus describes the first heliocentric model has not survived, but Archimedes in *The Sand Reckoner* leaves no doubt about Aristarchus's idea and the subsequent discussions it caused (see pp. 85–86 in North 1995).

What follows is partly a personal recollection of the events leading to the discovery of Gliese 229B and partly a description of the science.

## 2.1 *The Project at Palomar*

Shortly before my arrival at Caltech, Tadashi Nakajima, a post doctoral fellow working with Kulkarni, had forged a collaboration with a group based at Johns Hopkins University (JHU), led by Sam Durrance, and including David Golimowski. Durrance and Golimowski, with Mark Clampin and Rob Barkhouser, had built a new type of coronagraph designed to image faint objects or disks around nearby stars. This instrument (Fig. 1), called the JHU Adaptive Optics Coronagraph ([Golimowski et al. 1992](#), AOC) had a high-bandwidth (100 Hz) image motion compensator, and the system was designed to have a deformable mirror put in it to permit higher-order wave front correction. The higher-order system was never implemented, due to cost.

In 1989 the JHU team had deployed the AOC at the 40 inch Swope Telescope at Las Campanas Observatory for a one year survey to find circumstellar disks and companions of nearby stars. In December 1990 they moved the instrument to the 2.5 m duPont Telescope, the Carnegie Institute's premier telescope at the time. This effort was a fantastic success, achieving some of the first images of the  $\beta$  Pic disk in the optical that could be used for rigorous photometry within 100 AU of the star ([Golimowski et al. 1993a](#)), images of structure around young stars (e.g., [Clampin et al. 1993](#)), and analysis of close putative companions ([Golimowski et al. 1993b](#)). This body of work comprised a significant part of Golimowski's PhD thesis, completed in 1993 ([Golimowski 1994](#)).

By 1992 the instrument had been moved to the Palomar 60 inch Oscar Meyer Telescope, possible because the optical output of the telescope was quite similar to that of the duPont Telescope. Nakajima, in close collaboration with Golimowski, started a campaign to image the remnant envelopes of star formation as seen in the optical, as reflection nebulae, around a slew of known pre-main-sequence stars ([Nakajima and Golimowski 1995](#)). In parallel, the concept of picking a set of stars with ages under 1 Gyr, but within 25 pc emerged at this point, to form the basis of a survey to find brown dwarfs around them. The idea was simple. Since brown dwarfs fade as they age, the survey should target the younger stars around which brown dwarfs would be brighter compared to their older counterparts (assuming the star and its companion are coeval). Of course, the brown dwarfs had to be there to begin with, and no brown dwarfs were known at the time. This survey began just as I arrived in California ([Nakajima et al. 1994](#)).

The general consensus was that the cooler these things were, the redder and redder they would be. Indeed, a quick calculation, since the peak wavelength of a black body spectrum is in linear proportion to the temperature, suggested that a 1,000 K object should have its peak emission around six times longer wavelength



**Fig. 1** Sam Durrance with the Johns Hopkins University Adaptive Optics Coronagraph in April 1989 at the 40 inch Swope Telescope at Las Campanas, Chile, prior to its move to the Palomar 60 inch telescope for the brown dwarf survey. This instrument, one of the first stellar coronagraphs, was unique at the time. It included a novel system that used the rejected starlight to control a fine guidance system using a quad-cell CCD and a piezo-electric tip/tilt mirror to keep the star centered on the occulting spot. Plans existed to put a deformable mirror in the system, but funds were never raised to implement the full adaptive optics design of the instrument

than that of the Sun (which is roughly 6,000 K and peaks at about 0.6  $\mu\text{m}$ ), or roughly around 3 or 4  $\mu\text{m}$ .<sup>5</sup>

<sup>5</sup>I visited Caltech in the spring of 1994 when I was deciding where to go to graduate school. One of the best parts of that trip was that Shri invited me up to Palomar to spend a night at the Hale Telescope with him, Keith Matthews and Tom Hamilton. I rented a ridiculously small car and went, not knowing that I was going to drive Shri and Tom back to Caltech. Tom is rather tall and courageously squeezed into a half seat in the back of the car, his head tilted against the ceiling for the two hour drive. As we drove down the mountain I had no idea Shri would test me. One of the questions he asked was “what is the peak wavelength of a 1000 K blackbody?” Driving at 70 mph down the freeway, I recall suddenly becoming nervous, but also scrabbling my way through the answer. I got it pretty close, but Shri then started spewing out all kinds of really simple quick

The problem with the survey design, and the constant criticism the project came under, was that the coronagraph worked only in the optical band passes. The  $z$  band ( $\sim 0.85 \mu\text{m}$ ) was as red as it could image, and the CCD's sensitivity at those wavelengths was somewhat diminished. However, I think this is partly why the project was a success. The general wisdom at the time was that to see a brown dwarf, instruments operating at infrared (IR) wavelengths were necessary, and, further, the longer the wavelength used, the better the chances of success were. Numerous previous surveys used the assumption that cool brown dwarfs must be extremely red, and peak in the near-IR. In fact this was not the case. T dwarfs, as we now call them, peak near  $1 \mu\text{m}$  and are actually blue in the IR, due to the complex thermochemistry of their atmospheres (cf. also Cushing's and Baraffe's chapters in this volume). This is especially true because of the abundance of methane, which becomes stable below temperatures of about 1,400 K. Methane is a strong absorber in bands throughout the  $1\text{--}5 \mu\text{m}$  range. Incidentally, at the time, a number of papers suggested that these objects would be orders of magnitude different from black body spectra (e.g., [Burrows et al. 1993](#)), but only one group had predicted the huge effect of methane ([Tsuji et al. 1995](#)). In fact Takashi Tsuji had predicted the importance of methane only shortly after Kumar's first proposal of substellar objects ([Tsuji 1964](#)). Tsuji's work had not been incorporated into any survey designs prior to the discovery of the first methane brown dwarf.

When our survey started, though, we were not thinking of methane. Rather, there was a strong indication from observations of the M dwarfs, that anything cooler than them would not obey black body spectral characteristics, and we had hoped that these brown dwarfs would be bright enough to detect in the optical. Regardless, the key difference between the Palomar AOC survey and others was that there was no color bias at all in the design of the observations and discovery criteria. The only goal was to find any object around a nearby star that demonstrated that it was orbiting the star through detection of common proper motion. This requirement for discovery, simply that the companion followed its presumed primary star through the sky, an extremely strong argument for physical association, had no bias in color. Many other surveys, including surveys of star clusters, invoked color requirements for putative brown dwarf detection and follow-up (e.g., [Rebolo et al. 1995](#); [Basri et al. 1996](#)).

## 2.2 *Observing*

A month and a half after arriving in Pasadena, and in the midst of a heavy course load for my first year, I was up the mountain at Palomar for the first of what would

---

relations of this sort, the kind you can do in your head in seconds. I've never forgotten that, and though he did put me on the spot, I decided on that car ride that I really wanted to work with him. It was a good choice. Shri, though we had our differences at times, could not have been a better thesis advisor.

be well over 230 nights at the observatory over the following four and a half years. Tadashi was, very unfortunately, getting ill, so David Golimowski and I took over for a six night observing run in late October. It is important to note here that, although very few results came out of the first year and a half of AOC observing, our primary goal on this observing trip was to confirm a putative companion to the star Gliese 105, a third or “C” component, which, according to the initial data from a previous observation with the AOC, would have to be one of the lowest-mass stars ever found. With the long nights and hefty setup procedure for the AOC — we had to do almost everything ourselves, which was normal on the 60 inch — exhaustion was the norm. In addition, Dave had to teach me everything, because he could not always be present at all the upcoming observing runs, and I was slated (and wanted) to conduct a majority of the observing for the survey.

The AOC was a rather “hands-on” instrument. Even to change filters, one had to run out of the control room, grab the new filter in its small holder, pull the old one out by unscrewing some fasteners, slide the new one in and run back as fast as possible to start a new exposure and not waste too much time with the camera shutter closed.

On 27 October 1994, Dave and I observed the star we called GL229.<sup>6</sup> The night had excellent atmospheric conditions, especially for the Palomar 60 inch, with  $I$  band measurements indicating roughly 0.5–0.4 arcsec seeing. Coronagraphic efficiency in removing starlight is an extremely strong function of the input image quality — partly why so many new coronagraphs have been built for adaptive optics systems since the 1990s. On this same night, we also observed Gliese 105C and confirmed its companionship (Golimowski et al. 1995a,b). This was a very exciting result from that night, but it would be upstaged quickly by events that were to unfold within 48 h.

On that night, I was in charge of the list of target stars we were observing. I guess because I was tired and excited about Gliese 105C, I forgot to mark the list to indicate that we had already observed Gliese 229. I did note in the notebook (Fig. 2), that there was something “quite red” to the Southeast of the primary star. Note that the field of view of the instrument was about an arcminute, so nearly everything we observed had some kind of other star in the field of view. This was slow work, and in any case, even if we found something interesting, we would have to wait until the following year to allow the star to complete a year’s worth of proper motion before we could see whether a putative companion was actually traveling along with the star. In any case, on this night, neither Dave nor I seemed to care about this little red dot next to Gliese 229.

Two nights later, by virtue of the fact that I had failed to take “GL229” off our list of stars to observe, we pointed the telescope at it again. This time, we knew we had

---

<sup>6</sup>After publication of the discovery of the companion to Gliese 229B, the IAU sent an admonishing letter to Shri that the designation GL was not appropriate because it conflicted with a U. S. Air Force catalog of celestial sources. Officially, we had to call it Gliese 229.

Object	Object Name	UT	Object Number	FILTER	Exposure Time	T/F	Occulting Mass	Notes
E10.20R	GD 5000	02:28	1-02	I	5x60s	—	4.3°	Precise
S31.DP	GD 5000	02:30	1-03	SI	5x60s	—	—	Precise
S32U	GD 5000	03:16	1-03	R	100s	—	—	good seeing
S33U	GL 739	04:15	1-51	I	1000s	50s	—	good seeing
S34U	GL 739	04:37	1-59	R	1000s	50s	—	good seeing
S35U	GL 739	08:52	1-68	SI	100s	—	—	good seeing
E44U	GD 910	05:12	1-70	I	5x60s	—	—	Precise
F53U	GD 810	05:21	1-71	I	5x60s	—	—	Precise
F54U	GD 810	05:21	1-78	I	2x60s	—	—	—
F71U	GL 939	06:27	1-95	I	—	—	—	For focus
S60U	GL 939	05:43	1-99	I	1000s	50s	—	Seeing
S77U	GD 939	06:14	1-93	R	1000s	50s	—	—
S83U	GD 939	06:14	1-94	I	1000s	50s	—	—
S94U	GD 105A	07:20	1-18	I	100s	50s	—	—
S100U	GD 105A	07:15	1-19	R	100s	10s	—	—
S105U	GD 105A	07:23	1-12	I	20s	10s	—	Seeing
S110U	GD 105A	07:23	1-12	R	20s	10s	—	Seeing
S122U	GD 105A	07:44	1-12	I	5x60s	—	—	Just saturated
S123U	GD 105A	07:44	1-12	R	5x60s	—	—	Circles
S124U	GD 105A	08:04	1-12	I	20s	10s	—	—
S125U	GD 105A	08:13	1-12	R	12P	10	—	Focus loss
S126U	D 24	01:29	1-16	I	20s	—	—	Focus loss
S127U	GD 127	01:29	1-27	R	5x60s	—	—	Landsat Standard
S128U	GD 128	04:04	1-18	I	2x60s	—	—	Photometric St. standard
S129U	GL 76	04:04	1-18	R	5x60s	—	—	—
S130U	GL 161	08:26	1-08	I	20s	—	—	Very good
S131U	GL 161	09:45	1-06	R	20s	10ms	—	—
S132U	GD 223	10:00	1-81	I	600s	10ms	9.3°	—
S133U	GL 111	10:00	1-81	R	600s	10ms	9.3°	—
S134U	GD 111	10:07	1-77	I	5x60s	—	—	Good seeing
S135U	GD 111	10:25	1-77	R	5x60s	—	—	Good seeing
S136U	GL 112	10:46	1-88	I	1000s	50s	9.3°	—
S137U	GL 112	11:45	1-90	R	1000s	50s	9.3°	—
S138U	GL 112	12:10	1-22	I	5x60s	—	—	Focus loss
S139U	GL 112	12:34	1-23	R	5x60s	—	—	Focus loss
S140U	GL 229	12:45	1-76	I	500s	30s	4.3°	Focus loss
S141U	GL 229	12:45	1-79	R	1000s	30s	4.3°	Focus loss
S142U	GD 229	12:45	1-98	I	1000s	50s	—	—
S143U	GD 229	12:45	1-98	R	1000s	50s	—	—
S144U	GD 229	12:45	1-98	I	500s	—	—	—
S145U	GD 229	12:45	1-98	R	500s	—	—	—
S146U	GD 229	12:45	1-98	I	500s	—	—	—
S147U	GD 229	12:45	1-98	R	500s	—	—	—
S148U	GD 229	12:45	1-98	I	500s	—	—	—
S149U	GD 229	12:45	1-98	R	500s	—	—	—
S150U	GD 229	12:45	1-98	I	500s	—	—	—
S151U	GD 229	12:45	1-98	R	500s	—	—	—
S152U	GD 229	12:45	1-98	I	500s	—	—	—
S153U	GD 229	12:45	1-98	R	500s	—	—	—

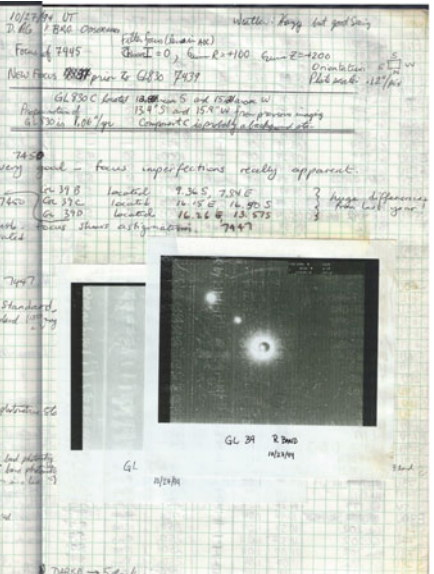


**Fig. 2** Observing log from the first night Gliese 229B was detected, October 27, 1994. The bottom of the log shows that “GL229” was observed as the last star in the night, one with excellent seeing. A short note for the last observation says “one [possible companion] just SE is quite red.” We were too tired to note anything else, and, in fact, had no idea what we had just observed. The images taped into the log book were from an early video printer that allowed us to print images for reminders when reducing the data

something remarkable (Fig. 3). While we were taking darks and flat fields (roughly an hour or two of work after the Sun came up) Dave and I calculated and recalculated the photometry, in rough manner, since we did not have the data in the final format for analysis with a standard software package like IRAF.<sup>7</sup> We realized that night that this object had an extremely red  $R-I$  color of about  $4.3^m$ . I was writing in Tadashi’s notebook, which was generally just reserved for observing notes, so I added a small apology, “Sorry for this mess, Tadashi. —Ben.” But Dave and I were very excited.

I was so excited that, when we started observing the next night, I called Shri, who happened to be in Hawaii, using the relatively new Keck telescope with a beautiful spectrograph, called LRIS. I told him what we had found and said he should get a spectrum of it immediately. Shri, rightly so, did not. I was a graduate student who had only been working with him for a month or so. The Keck telescope was by far the largest in the world and not the kind of observatory that one would flippantly just point at some new object that someone is excited about because of rough

<sup>7</sup>At the time, many instruments produced data in non-standard formats that had to be converted at one’s home institution where better computers were available.

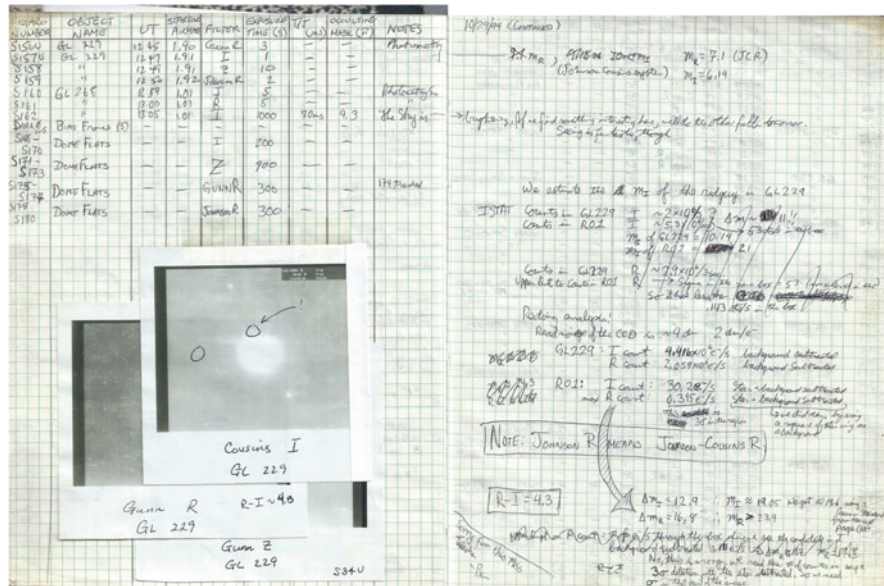


**Fig. 3** Observing log from the second night Gliese 229B was observed, October 29, 1994. Again, “GL229” was observed near the end of the night, but this time around we realized this was a new type of object. Scribbled at right are initial attempts to derive the magnitudes and colors of the companion. None of this work could become public for another year, though, because we had to confirm that this point source, marked in the video printout at left, was in fact orbiting the star

calculations based on very raw data. In retrospect, although I was disappointed Shri did not acquire an optical spectrum of Gliese 229B that night, he made the right call. It turned out to be rather tricky, from an instrument configuration and data-analysis point of view, to obtain that spectrum later (Oppenheimer et al. 1998), and Shri probably would have wasted an hour of Keck time only to obtain data that was not useful. The entire team would have to wait a year to confirm that Gliese 229 and this little red point source shared the same proper motion and indeed were orbiting each other.

I am not a patient person, and this year of waiting to find out more and confirm this new object was a bit of agony. I buried myself in my coursework, more observing and some other projects that I used to distract myself. Everyone on the team was quiet. We discussed nothing of the data, although after running a full analysis on it, the  $r - z$  color was greater than  $4.3^m$ , a color no other star-like object shared. During this time, I recall having to give a short talk on my work for my first year of graduate school, partly as a lead-in to the qualifying exams that, at that time, happened in the very beginning of the second-year. I spoke to the department about the project, what we were doing and hoping to find. It was a terrible talk, but I remember wanting to say something about this mysterious object. I did not. At the end of the talk, someone in the audience said, “Brown dwarfs don’t exist!

We have been looking for them for decades. They aren't there. You should work on something that exists!" I did not respond to this. Of course, he could have been right. We did not know what we had found yet.

### 2.3 “*There’s Methane in that Thing!*”

The eleven months between 29 October 1994 and 14 September 1995 passed, and Shri, Keith Matthews and I were back at Palomar, though on the 200 inch Hale telescope this time, with a wonderful instrument Keith built called D-78 (which simply stands for the 78th cryogenic dewar in a series of pioneering infrared instruments, many of which Keith built). D-78, an infrared camera, had a rudimentary fake coronagraph in it, which consisted of a metal finger that could be placed in the center of the field of view, to prevent saturation from a bright star. Furthermore, it had the capability to take relatively low-resolution spectra of objects within the field of view, using a slit and a grism. We obtained *JHK* images and spectra of Gliese 229 and its companion. Although we knew we had another observing run with the AOC on the 60 inch telescope only a week later, I had hoped that we could confirm that the companion and the star shared proper motion with this data. Generally using two different instruments to conduct precision relative astrometry like this is not a good idea, but we observed a few calibration binary stars with well-known separations and thought we could try. However, something more surprising happened.

When Keith took the first grism spectrum (Fig. 5), it showed up on the display and he said immediately (with some expletives removed), “There’s methane in that thing!” He could see just from looking at the raw data that a large chunk of both the *H* and *K* bands were dark, right where methane is known to absorb light. For reference, we observed Jupiter, which happened to be at a favorable observing angle, and which was the only real comparison we could make at the time. Jupiter showed similar strong spectral features from methane absorption, as it had been known to exhibit for many years. This companion of Gliese 229 was unique. It had to be extremely cool to have methane in it, and there was no doubt at this point that it was either a companion of Gliese 229 or a foreground object that was extremely cool. The astrometry demonstrating common proper motion, though necessary to establish companionship, was not needed to confirm that we had found something new.

I immediately began reducing the data at the telescope and Shri and I started writing the paper. Within a week, we had generated the figure on the left side of Fig. 4, as well as Fig. 5. I also measured the astrometry between A and B using the D-78 data. This work indicated that the two objects were indeed moving across the sky in the same direction and rate, although the astrometry was not as precise as I had hoped. Hedging our bets, by 25 September 1995, we submitted the discovery paper, based on the astrometry and photometry obtained at that point. On 3 October 1995, Shri and I obtained more AOC observations of the system and measured the astrometry (in between changing filters and taking more survey

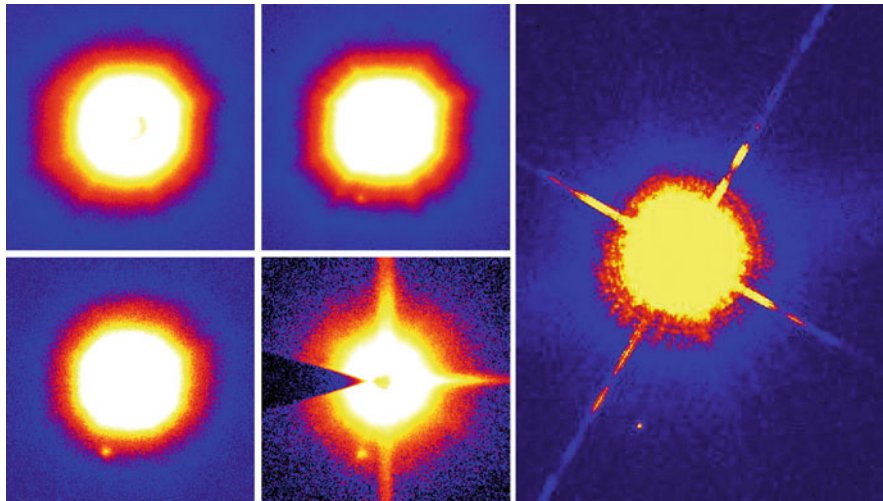


**Fig. 4** Discovery images of Gliese 229B. *Left:* three optical ( $r$ ,  $i$ , *top* and  $z$ , *bottom left*) and one  $K$  band image (*bottom right*) from 1994 and 1995, (adapted from Nakajima et al. 1995). *Right:* Hubble Space Telescope image, demonstrating the enormous effect that image resolution has on revealing faint objects around bright stars. This image is not taken with a coronagraph, while the others were (adapted from Golimowski et al. 1998)

data). The AOC astrometry was dead on. Both the primary star and its companion were co-moving. We sent an addendum to add this information into the paper submitted, and I submitted the paper on the spectrum (Fig. 5) by 12 October 1995, four days after finishing the AOC observing trip. These two papers, which we decided would be better as a pair rather than a single result, present the astrometric confirmation and photometric analysis of Gliese 229B (Nakajima et al. 1995) and its spectrum (Oppenheimer et al. 1995). In the first paper, using the Stefan-Boltzmann relation, that Adams and others used for Sirius B (Sect. 1.2),  $L = 4\pi r^2 \sigma T^4$ , and estimating a radius based on brown dwarf models (roughly a Jupiter radius,  $R_J$ ), we determined that the companion had a temperature of about 1,000 K (which we compared with the models of Tsuji et al. (1995), for additional support), a luminosity of  $4 \times 10^{-6} L_\odot$ , and a probable mass between 20 and 50 Jupiter masses ( $M_J$ ). The spectrum paper (Oppenheimer et al. 1995), which was in print on 1 December 1995, one day after the discovery paper, describes the definitive identification of methane and derivation of the temperature in more detail.<sup>8</sup>

<sup>8</sup>Incidentally, my qualifying exam was scheduled for early November 1995, right in the midst of revising and working to finish the papers and get them accepted for publication. I decided not to study for the test much, since I thought my work on these two papers should take precedence over an exam. I do not regret that decision, and, although Shri and I discussed postponing the exam, we decided I should simply do it. I failed, but I had a really wonderful scientific result. In the end, I retook the exam and did well, some months later.

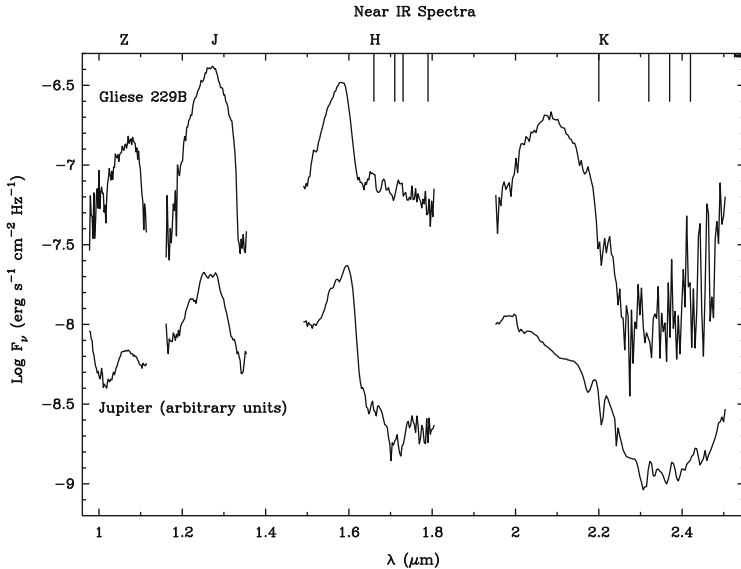


**Fig. 5** First spectrum of Gliese 229B compared with Jupiter (adapted from [Oppenheimer et al. 1995](#)). The locations of absorption band heads due to methane is indicated by the *vertical bars* along the top of the plot in the *H* and *K* bandpasses

Now and then in science, odd and fascinating juxtapositions of events happen. Only weeks earlier in June and September, two warm brown dwarfs were announced by [Basri et al. \(1995\)](#) and [Rebolo et al. \(1995\)](#); see Basri's and Rebolo's chapters in this volume). One week before our result was published, the first definitive detection of a planet-mass object around another star, 51 Pegasi, was also announced ([Mayor and Queloz 1995](#)). In fact, both were initially announced at the Cool Stars IX meeting in Italy in talks given in rapid succession. Our work was presented by I. Neill Reid, a close friend and colleague of Shri's who happened to be going to the meeting.

I recall tremendous excitement at the time. There is nothing like finding something new. Even if it is not an extremely high-profile result, the euphoria of discovery is a very rare feeling, but one that has kept me working in science. Actually discovering something new about the universe is partly our duty as human beings, to understand where we are and what this place is made of. The feeling of having contributed to that process is wonderful, gratifying, and humbling. Humbling because our crude techniques and attempts to measure light from distant sources is our only way, in astronomy, to uncover what remains hidden in the universe. Yet, it is also incredible how much people have deduced or inferred about the universe in these past two or three centuries.

Over the next few years, I finished the survey of nearby stars, unfortunately without another brown dwarf found. But I also continued to study Gliese 229B. As shown in Fig. 6, through data in the optical, near-IR and even out to mid-IR

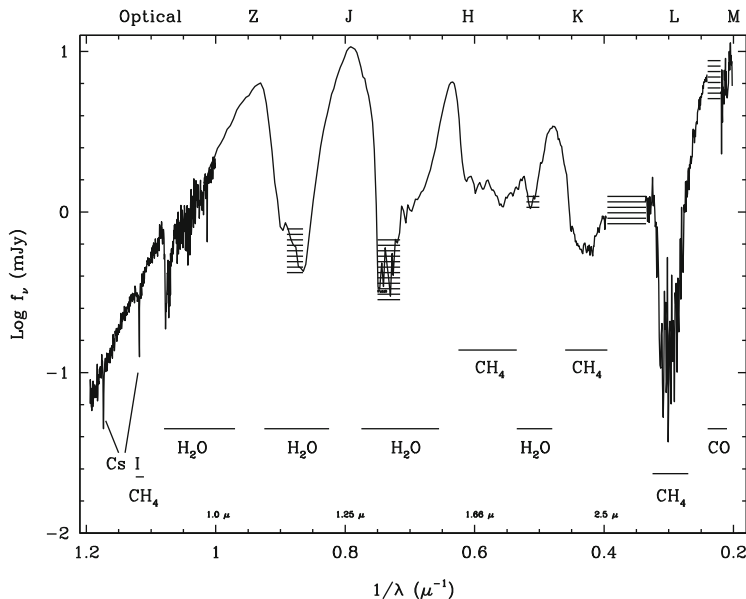


**Fig. 6** The full spectrum of Gliese 229B from optical to thermal IR bands (Oppenheimer et al. 1998). Labeled *horizontal bars* indicate absorption bands due to methane ( $\text{CH}_4$ ), water ( $\text{H}_2\text{O}$ ) and carbon monoxide (CO). Two *atomic lines* are also indicated and are due to neutral cesium (Cs I)

wavelengths of  $13 \mu\text{m}$ , which our group collected, some fascinating aspects of brown dwarf atmospheres emerged. In addition, the theorists went to work immediately. Things such as non-equilibrium chemistry were indicated by the spectrum, perhaps due to huge winds and convection from deeper within the brown dwarf that could cause an apparent imbalance between CO and  $\text{CH}_4$  (see also the chapter by I. Baraffe in this volume). We discovered atomic cesium lines, as well as possible collision-induced absorption due to  $\text{H}_2$  molecules. This all was like a playground in which I learned aspects of thermochemistry and atmospheric science.

Finally, and perhaps most importantly, since astronomers now knew what  $1,000\text{ K}$  objects looked like, they emerged in greater and greater numbers, especially due to the optical Sloan Digital Sky Survey (Abazajian et al. 2003, and references therein) which identified the first isolated methane brown dwarf, four years after Gliese 229B was announced (Strauss et al. 1999).<sup>9</sup> The Sloan discoveries allowed the team working on the infrared 2MASS all sky survey (Skrutskie et al. 2006) to refine their search criteria, and many more methane brown dwarfs were immediately identified by both Sloan and 2MASS. The irony of all this is that the near-IR 2MASS survey, which had a goal of identifying brown dwarfs, could not have found methane dwarfs easily on its own. Their *JHK* colors are so close to many stellar objects,

<sup>9</sup>Dave Golimowski liked to call these “Sloan Clones” at the time.

such as A-type stars, that optical data combined with IR photometry was necessary. However, such data was available.

The field has progressed tremendously and various strange types of brown dwarfs are being discovered even now (e.g. [Faherty et al. 2013](#)). Two new spectral classes, L, which indicates a temperature between M9 and the emergence of methane, and T, which is reserved for objects with methane signatures in their spectra, have been devised ([Kirkpatrick et al. 1999](#); [Martín et al. 1999](#); [Burgasser and Kirkpatrick 2006](#); [Cushing et al. 2008](#)). We have learned that many different processes are involved in determining the emergent spectra of these objects, including age, metallicity, mass, and, perhaps, formation mechanism. Most recently a third new spectral class may be emerging, called Y, meant to be reserved for objects that show ammonia absorption ([Cushing et al. 2011](#); [Kirkpatrick et al. 2012](#), also see Cushing’s chapter in this volume).

Some of this new work hints that the brown dwarfs and planets may not be distinct types of objects. That they may be intrinsically related, or that the two categories have significant overlap in properties. Time will tell, and perhaps some of the unraveling of the mysterious connection between stars, brown dwarfs and planets will come from the new ability of astronomers to conduct what I like to call “remote reconnaissance” of exosolar systems.

### 3 Planets and Remote Reconnaissance of Exosolar Systems

Since 1995, well over 1,000 brown dwarfs, a minority of which are companions of stars, and even more planets and planet candidates have been identified with numerous techniques. As I hope is apparent from the sections above, and the other chapters in this book, the key to understanding these objects in detail is spectroscopy. However, to observe objects that are millions to billions of times fainter than the stars they orbit and only a fraction of an arcsec away from those stars, very precise control of the starlight is necessary, simply to see them, let alone take spectra of them. Fortunately there is considerable effort being expended on this problem, by groups in the US, Europe and Japan. While my own efforts in this direction, Project 1640, are a direct outgrowth of the early coronagraphy used to find Gliese 229B, the technology involved is considerably more advanced. It is already revealing new types of objects orbiting nearby stars. Recently we observed the 1–1.8  $\mu\text{m}$  spectra of all four planets in the HR 8799 system ([Oppenheimer et al. 2013](#)). Although there are other instruments similar to Project 1640, such as the Gemini Planet Imager ([Macintosh et al. 2008](#)), among others, about to begin observations, I use Project 1640 as an example of what we can do now and what we might expect in the near future for the study of companions of stars.

Project 1640, an instrument suite involving four separate optical instruments and corresponding control software, with a complex set of custom data reduction and analysis software, is described in [Oppenheimer et al. \(2012\)](#), [Hinkley et al. \(2011b\)](#), [Hinkley et al. \(2008\)](#) and in detail at the level of circuit diagrams,

cryogenics, control software, interfaces and opto-mechanical design in [Hinkley \(2009\)](#). The latest system performance metrics are given in [Oppenheimer et al. \(2012\)](#), including on-sky contrast measurements. These are described in relation to other projects in high-contrast imaging in [Mawet et al. \(2012\)](#), in particular, their figure 1. In summary, the system is capable of producing images with a speckle floor at roughly  $10^{-5}$  at 1 arcsec separation from a bright star (or  $10^{-7}$  in the lab). This is achieved through the coordinated operation of four optical instruments: a dual deformable mirror, adaptive optics (AO) system with 3629 actively-controlled actuators, called PALM-3000 ([Dekany et al. 2007, 2006](#)); an apodized pupil, Lyot coronagraph (APLC; [Soummer et al. 2009; Sivaramakrishnan and Lloyd 2005; Soummer 2005; Soummer et al. 2003a,b](#)), the design details of which are given in [Hinkley \(2009\)](#); a Mach-Zehnder interferometer that senses and calibrates, through feedback to PALM-3000, residual path-length and amplitude errors in the stellar wave front at the coronagraphic occulting spot for optimal diffractive rejection of the primary star's light (CAL; [Vasisht et al. 2013; Zhai et al. 2012](#)); and an integral field spectrograph that takes 32 simultaneous images with a field of view of  $3.8 \times 3.8$  arcsec spanning the range  $\lambda = 995 - 1,769$  nm with a bandwidth of  $\Delta\lambda = 24.9$  nm per image (IFS; [Hinkley et al. 2011b, 2008; Hinkley 2009; Oppenheimer et al. 2012](#)). Aside from technical advances in high-contrast imaging, numerous results from the project include, among others, the discovery and astrometric and spectroscopic characterization of the Alcor AB system ([Zimmerman et al. 2010](#)), the  $\alpha$  Ophiucus system ([Hinkley et al. 2011a](#)), the  $\zeta$  Virginis companion ([Hinkley et al. 2010](#)), and comprehensive spectral studies of the companion of FU Orionis ([Pueyo et al. 2012](#)) and Z CMa ([Hinkley et al. 2013](#)).

Raw science data generated by Project 1640 are in the form of  $2,040 \times 2,040$  pixel images containing 37,146 closely packed spectra roughly  $30.4 \times 3.2$  pixels in extent. These images are processed into data cubes with dimensions R.A.,  $\delta$  and  $\lambda$ , as described in [Zimmerman et al. \(2011\)](#).

Figure 7 shows how this complex instrument obtains data. The other projects similar to Project 1640 operate in similar ways, although each has some advantages over the other. The point is that such a complex system can and does work. In [Oppenheimer et al. \(2013\)](#), we describe imaging and spectroscopy of the four planets orbiting HR 8799. This system of four planets was discovered and imaged previously ([Marois et al. 2008, 2010a,b](#)). Only limited spectroscopy had been obtained on the two outermost planets ([Bowler et al. 2010; Janson et al. 2010](#)), in addition to a high-resolution  $K$ -band spectrum of the second most distant planet from the star ([Konopacky et al. 2013](#)). Project 1640 achieved spectra and images of all four simultaneously with only a little more than one hour of telescope time. The spectra are shown in Fig. 8. They are all different from each other, and different from any other known objects. In our initial observational attempt to understand what these planets are, we identified some molecular species that could explain the features in the spectra. These are entirely tentative and may not bear the scrutiny of proper theoretical models of these objects. Our preliminary conclusions were the following ([Oppenheimer et al. 2013](#)):

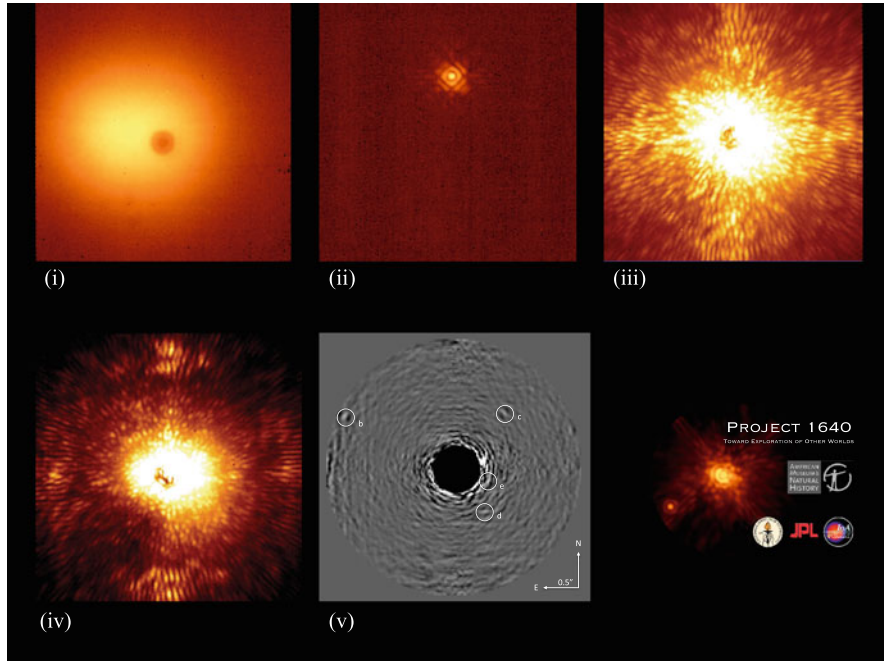


**Fig. 7** Example of how to conduct a remote reconnaissance of another solar system. These panels demonstrate how Project 1640 acquires data that can reveal not only a portrait of another solar system, but also spectra of any point sources in that system simultaneously (shown in Fig. 8). (i) The telescope is pointed at the star. The image shows the star before AO is activated. The black spot in the center is the occulting optic in the coronagraph that blocks out starlight. (ii) The AO system has been turned on, to correct the atmospheric turbulence, and the star image is greatly sharpened, reaching the diffraction limit of the telescope. This is a very short 1.5 sec exposure. (iii) The star is placed under the occulting optic and a long exposure of 5 min is taken. In this image, most of the starlight has been removed, but a remaining pattern of “speckles” fills the field of view. These are due to defects in the optics. (iv) The calibration wave front sensor is turned on and effects the dimming of the speckles. Numerous long exposures are taken over a 1.25 h period. (v) The data are assembled and processed with a novel speckle suppression technique based on advances in computer vision to remove the residual starlight and reveal the exoplanets. Spectra can be extracted once the locations of the planets in the image are determined. See [Oppenheimer et al. \(2012, 2013\)](#)

- b: contains ammonia and/or acetylene as well as CO<sub>2</sub> but little methane.
- c: contains ammonia, perhaps some acetylene but neither CO<sub>2</sub> nor substantial methane.
- d: contains acetylene, methane and CO<sub>2</sub> but ammonia is not definitively detected.
- e: contains methane and acetylene but no ammonia or CO<sub>2</sub>.

What are these objects? They are believed to have effective temperatures around 1,000 K, but they do not share many features in common with Gliese 229B or other

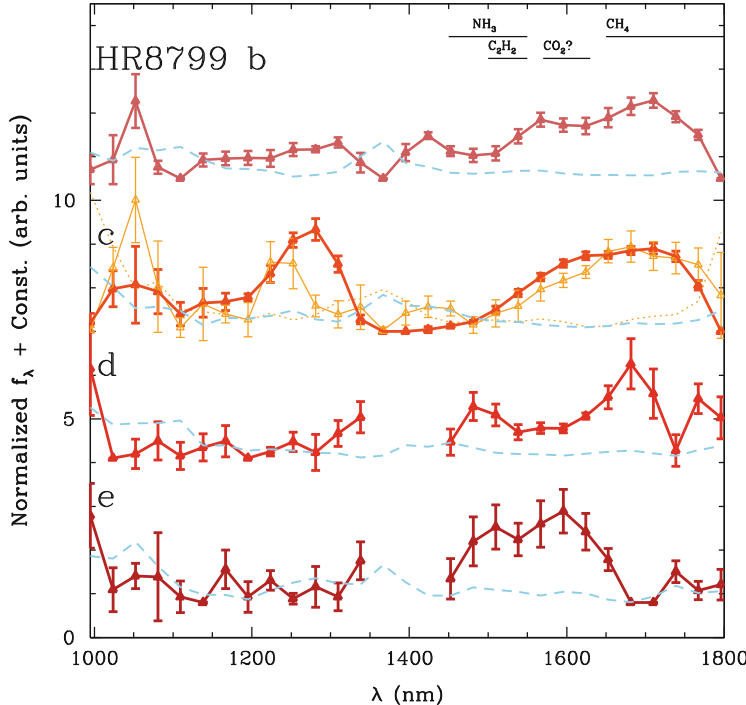


**Fig. 8** Spectra of the four planets orbiting HR 8799 (adopted from Oppenheimer et al. 2013)

T dwarfs, with perhaps the exception of planet e. Similarly even the lowest gravity L dwarf spectra do not seem in agreement with any of these objects.

Within the next few years, new campaigns like that of Project 1640 will obtain spectra of, one might hope, several hundred exoplanets, young gas giants, though who knows what we will actually find? What is clearer than ever is that the population of companions of stars is far more diverse than ever before imagined. What is the full range of planets and brown dwarfs that may be out there? Is it meaningful even to use these terms, or do they distract from understanding the real physics of them?

## 4 All Known Companions of Stars

Here, I seek to examine the questions posed above in more detail by examining gross orbital properties of all known companions of stars to date, without binning them into categories people have made (such as star, brown dwarf or planet). While these properties are not derived from spectroscopy, and they have been measured with many different techniques, my hope, nevertheless, was to find patterns that might

reveal that there are, in fact, real groupings or classes of such companions. My other hope was that perhaps hints of a “fundamental plane” or surface or volume within this complex parameter space might emerge, similar to the fundamental plane for galaxies.

What follows is based on a compilation of orbital properties of some 2,413 companions of stars regardless of the mass of the companion or the primary. Multiple systems are included when available, but systems are only included for which at least  $M_1$  (mass of the primary in solar masses,  $M_\odot$ ),  $M_2$  (mass of the secondary or higher order component in  $M_\odot$ ),  $a$  (physical separation in AU), and  $e$  (eccentricity) are known. Data were collected from published literature and several recent compilations, including [exoplanet.eu](#), [vlmbinaries.org](#), the eclipsing binaries reported in [Gorda and Svechnikov \(1999\)](#), the visual binary orbits in [Söderhjelm \(1999\)](#), the sixth orbit catalog of the Washington visual double star catalog ([Mason et al. 2013](#), WDS), where companions without magnitude measurements are excluded. For the WDS companions, *Hipparchos*-derived distance is required, and masses were estimated using the mass-luminosity relation of [Demory et al. \(2009\)](#) and [Delfosse et al. \(2000\)](#). Finally, 102 of the systems listed in [bdcompanions.org](#) with the necessary parameters were included. Datasets for this analysis were last updated in March 2013.

This is an intrinsically biased set of samples, but I did attempt to include as much data as possible. Of note is the fact that Gliese 229B is not included, partly because the orbital parameters are only weakly constrained at this point, with an estimated period of several hundred years. However, some interesting facts might be hinted at by consolidating all of this data. Usually researchers tend to look at only subgroups of these categories, based on the notion that stars, brown dwarfs and planets are completely unrelated types of objects.

In Fig. 9 the data set is represented showing  $M_2$  in solar masses ( $M_\odot$ ) vs.  $a$ , a parameter space commonly used in the study of exoplanets. One might look at this plot and quickly think there are four or maybe five clumps or groupings of objects: (1) the so-called “hot Jupiters,” planet-mass objects in very tight orbits below about 0.05 AU; (2) a similarly close clump of stellar mass objects, the eclipsing binaries, below about 0.1 AU; (3) a large clump of higher mass planets centered around 2 AU; (4) a huge agglomeration of stellar companions between 10 and 100 AU; and perhaps (5) a clumping of brown dwarf companions emerging below 0.1  $M_\odot$ , from 1 to 10 AU.

There are several key things to note about this plot. For years, visual binaries have been subjected to regular study and updated cataloging. Also for many years, the lower-mass companions of stars, especially K and M dwarfs, have been ignored as uninteresting or unimportant. This results in a dearth of objects in the range from  $\sim 0.7$  to  $0.075 M_\odot$  ( $13 M_J$ ) for  $M_2$ . Of course we know that K and M dwarfs make up about 90 % of the population of stars, and in fact many K- and M-dwarf companions are known with higher-mass primaries. Often these are seen in imaging campaigns and not reported, discarded as uninteresting because a given project may be targeting a different type of companion. Alternatively, for years some of the radial

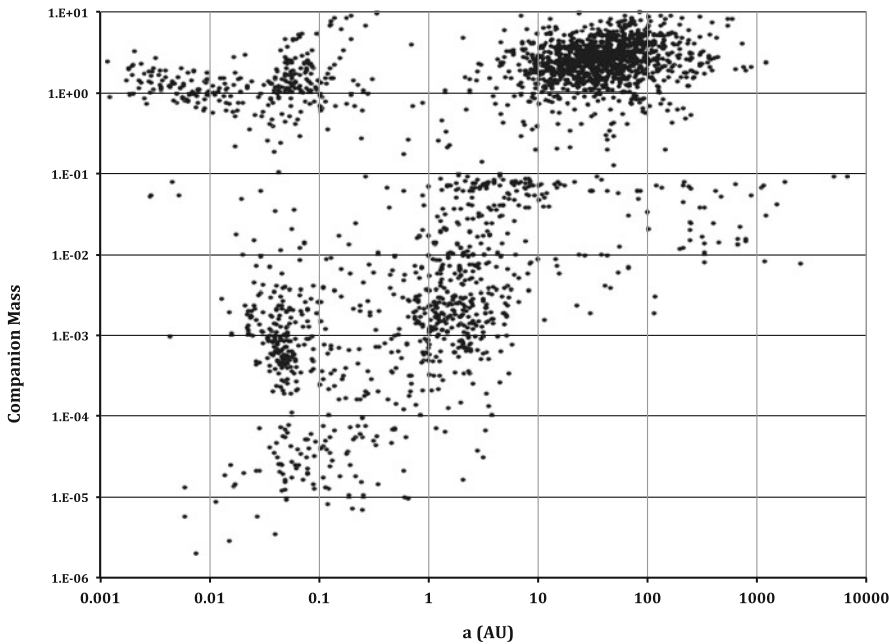


**Fig. 9** Known companions of stars with orbital elements determined as of March 2013, showing companion mass  $M_2$  in solar masses,  $M_\odot$ , on the ordinate and physical separation in AU on the abscissa. Data come from a variety of sources, with an attempt to be as thorough as possible with the literature (see text for data sources.)

velocity searches for planets simply stopped monitoring stars that showed radial velocity gradients that were far too large to be due to a planet.

Another bias is introduced in a similar way by the research on brown dwarfs. Objects believed to be above about  $0.075 M_\odot$  are ignored as uninteresting. This is even stranger, because the general, but somewhat unsubstantiated, consensus for a long time has been that brown dwarfs form the same way stars do and that planet formation is a completely separate process. If brown dwarfs form as stars do, then they should be treated as an extension of the population. It is possible, from a qualitative inspection of Fig. 9, that there is an increasing population of brown dwarfs from the lower masses toward the higher, up to that of the lowest-mass stars, where the gap in the K and M dwarfs exists. If that population from the brown dwarfs through to the large population of massive stellar binaries is a continuous single population, that might lend credence to the notion that brown dwarf companions form the same way that binary stars do. However, it is an equally strong possibility that, as the surveys are increasingly sensitive to these wide brown dwarf companions and planets, the same distribution might also form a continuous grouping with the planets. The suggestion, considering these biases, then, may be that the companions from 100 AU down to just below 1 AU from the highest stellar masses to well below a Jupiter mass constitute a single continuous population.

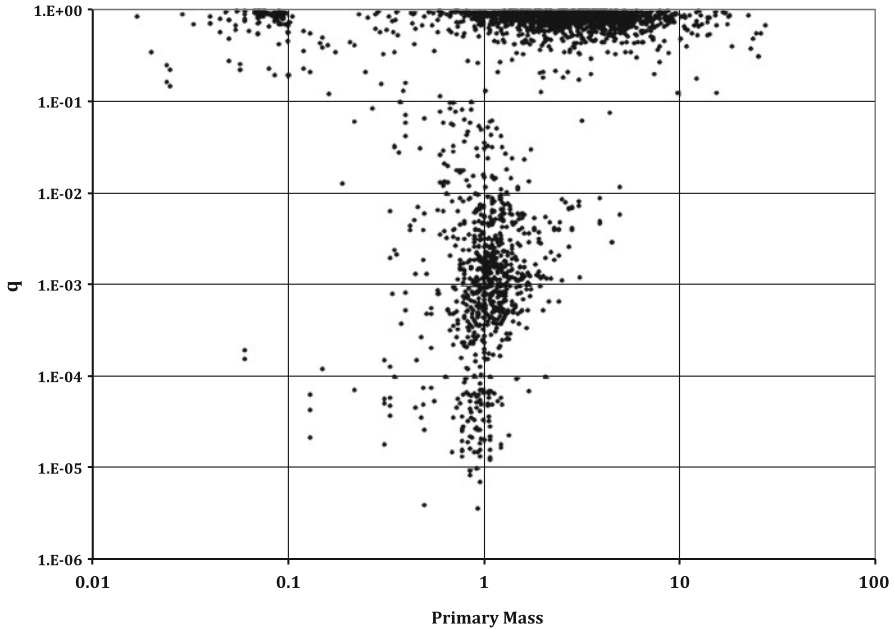


**Fig. 10** Known companions of stars with orbital elements determined as of March 2013, showing the mass ratio,  $q = M_2/M_1$ , versus the primary mass in solar masses,  $M_\odot$ . Significant biases are present (see text)

With regard to the brown dwarf desert — an apparent dearth of brown dwarfs orbiting stars — these plots may shed some light. Shown to be restricted to the range of separations of 0.1–1 AU in Oppenheimer and Hinkley (2009), though still the subject of significant debate, the brown dwarf desert seems apparent in Fig. 9. However, there also may be a similar desert of planets in the same separation ( $a$ ) range, and perhaps even among stellar companions. Is this due to observational bias? Perhaps only time will tell. In a fascinating study, though, Joergens (2006) suggests that this desert might scale with primary mass, and there may be a hint of this in the data (see also Fig. 11). However, from this first plot, it is clear that a full picture will only come from removal of as many observational biases as possible. The easiest biases to remove are those that are introduced by outright choice in surveys (such as ignoring companions that are not the main target of a particular investigation).

The most dramatic depiction of some of the biases in Fig. 9 is shown in Fig. 10, where I have plotted the mass ratio,  $q$ , versus the primary star's mass ( $M_1$ ). Here one can see that “nature favors equal mass binaries” at least for stellar companions. But again, there is a huge lack of companions of stars below  $1 M_\odot$ , due to the bias against studying the most plentiful type of star in the universe, the M- and K-type stars. Note that a sudden clump arises near the top of the plot below  $0.1 M_\odot$ , the product of surveys for binary brown dwarfs. An even starker picture emerges when looking at the very low- $q$  systems, dominated heavily by the search for exoplanets.

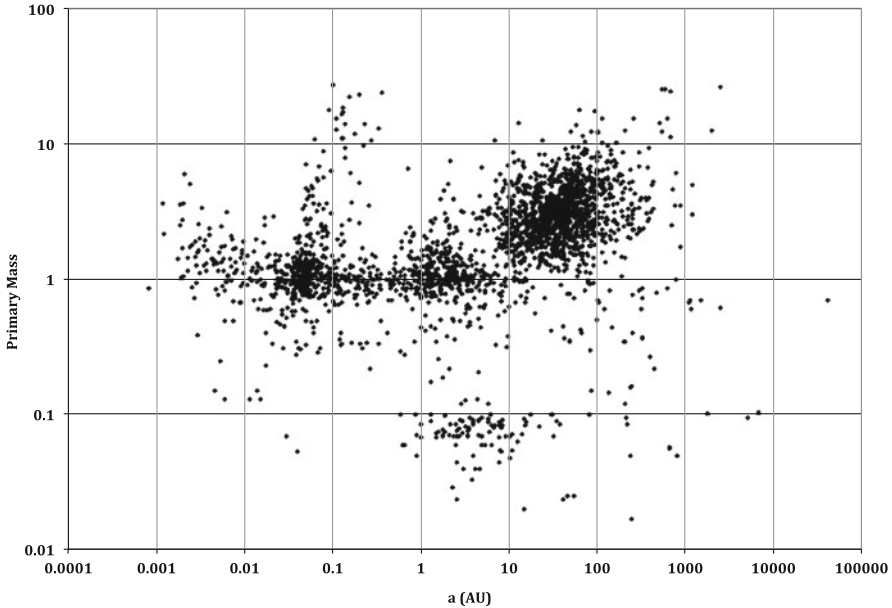


**Fig. 11** Known companions of stars with orbital elements determined as of March 2013, showing the mass of the primary in solar masses ( $M_{\odot}$ ) versus the separation of the companion (regardless of mass). It is unclear that companion separation is a strong function of the type of star a companion orbits. Note that in this plot most of the planetary systems are represented here near  $M_1 = 1M_{\odot}$

Virtually all exoplanets known are around roughly  $1 M_{\odot}$  stars. The new direct imaging campaigns are beginning to find planets around  $2\text{--}5 M_{\odot}$  stars, but little is known of planetary systems around M dwarfs. In addition, there are a few known planet-mass objects orbiting brown dwarfs. There is an interesting, perhaps real, lack of companions of Sun-like stars between  $q = 7 \times 10^{-5}$  and  $1.5 \times 10^{-4}$ , roughly around 20–40 Earth masses, intermediate, for reference, between Neptune and Saturn. Could this be indicative of a different distribution between ice and gas giants, or that perhaps these are two truly different classes of planets? As a side note, there also seems to be an increasing number of planets toward lower mass, especially below ten Earth masses (e.g. Mayor and Queloz 2012). Unfortunately these companions are not all represented here due to orbital constraints insufficient to be included in the compilation.

If we extend this investigation further, the previous paragraph suggests that perhaps there may be differences in the types of companions found as a function of the type of primary star. Thus in Fig. 11 we plot the primary mass vs.  $a$ . Once again the dearth of companions (of all types) within the 0.1–1 AU range is obvious. Even clearer is the observational bias against the low-mass stars. The suggestion that the brown dwarf population is intrinsically related to the higher-mass stellar primaries is strong here, in the sense that it appears that the clump below  $0.1 M_{\odot}$

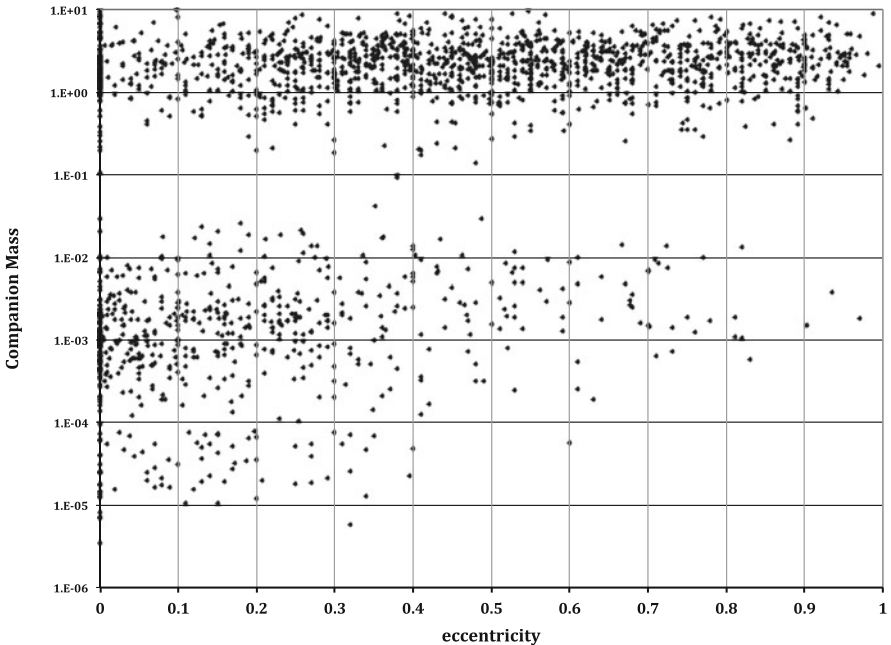


**Fig. 12** Known companions of stars with orbital elements determined as of March 2013, showing companion mass in solar masses ( $M_{\odot}$ ) versus eccentricity of the orbit. The complete lack of objects in the M-dwarf range is likely a heavy observational bias, not a real feature. However, the trend to lower eccentricities in the lowest-mass objects may be real

might be a tail of a distribution that is centered at a much higher mass. It is unclear to me that there is a strong function of orbital separations with primary-star mass.

As one final example of this companion data, Fig. 12 shows the companion mass versus eccentricity of its orbit. This may contain some real information (other than another highlight of bias agains studying M-dwarf companions). Here we may be seeing a hint that as one proceeds toward the lower-mass planets, they tend to favor more circular orbits. It will be interesting to see how this plot develops as more and more examples are found.

To conclude this section, the study of companions of stars, whether they be brown dwarfs, other stars, or planets, must be conducted broadly, without the bindings of human-chosen categories or nomenclature, in order to arrive at a comprehensive understanding. There are some suggestions that these three categories are more intrinsically linked, and that their formation mechanisms may not be entirely distinct, but at least overlapping, or utterly interconnected, modified under certain circumstances due to environment, perhaps. The study of companions of stars has a long way to go still, but we are at an exciting moment.



**Fig. 13** The Adaptive Optics Coronagraph (*left-center*, inside acrylic cylinder), now on permanent exhibition at the Rose Center for Earth and Space in the American Museum of Natural History. The exhibit, meant to highlight coronagraphy and interferometry as the principle techniques for direct detection and study of exoplanets, initially included the original interferometer (atop the two columns) that A. A. Michelson used on the Mt. Wilson 100 inch telescope to directly measure a number of stellar diameters in the 1920s. The interferometer is currently on display at Mt. Wilson

## 5 Into the Future: Will a Companion of a Nearby Star Give Humankind Its First Evidence for Biology Outside the Solar System?

At this point in history, science has shown that not only are the laws of physics the same in all known parts of the universe, but also that chemistry operates universally. What we have no evidence for is that there is any biology other than on Earth. Further, if there is extraterrestrial biological activity, we do not know whether there are any universal aspects to it that are shared with terrestrial biology (such as DNA, or carbon-based biochemistry). Soon, one may imagine, we may find fish under the ice on Europa, or microorganisms or a skeleton on Mars. But what about biological activity outside the solar system, as Michell and Herschel clearly showed for gravitational activity over 200 years ago (Sect. 1.1)?

I am of the opinion that within the next two decades, at most, such evidence will come to light, and, unless SETI actually discovers complex signals that must be from some form of sentience, the evidence for biological activity outside the solar system will be the direct result of studying the companions of stars.

Such evidence will come with the spectroscopic observation of a planet, one that exhibits an atmospheric composition that cannot be explained by thermochemical equilibrium, or even disequilibrium that is due to strong physical processes in the atmosphere. Indeed, we can see the evidence for biological activity on Earth in its spectrum, because the abundances of many molecular species are too large without the global forcing and disequilibrium caused by life forms, whether as simple as early bacteria or as complex as people.

I hope that my arguments for studying companions of stars is convincing. For readers who are interested in details of the state of the art in the field of high-contrast probing of the near vicinities of stars, several recent review articles have been published, including by Oppenheimer and Hinkley (2009), Absil and Mawet (2010), and Traub and Oppenheimer (2011). This is a field driven by technological advances. As such, the AOC used to discover Gliese 229B is on permanent display at my home institution, in a small exhibit which exposes the inner workings of the instrument and explains its use (Fig. 13).

**Acknowledgements** The work described regarding Gliese 229B involved many people other than myself and I am deeply grateful for having been able to work with Tadashi Nakajima, Sam Durrance, Shri Kulkarni, Dave Golimowski, Keith Matthews and Marten van Kerkwijk. It was an honor to conduct such work with them. Project 1640 also involves a great team of collaborators. Further information on them and that project can be found at [www.amnh.org/project1640](http://www.amnh.org/project1640).

## References

- Abazajian, K., Adelman-McCarthy, J.K., Agüeros, M.A., Allam, S.S., Anderson, S.F., Annis, J., Bahcall, N.A., Baldry, I.K., Bastian, S., Berlind, A., Bernardi, M., Blanton, M.R., Blythe, N., Bochanski, J.J., Jr., Boroski, W.N., Brewington, H., Briggs, J.W., Brinkmann, J., Brunner, R.J., Budavári, T., Carey, L.N., Carr, M.A., Castander, F.J., Chiu, K., Collinge, M.J., Connolly, A.J., Covey, K.R., Csabai, I., Dalcanton, J.J., Dodelson, S., Doi, M., Dong, F., Eisenstein, D.J., Evans, M.L., Fan, X., Feldman, P.D., Finkbeiner, D.P., Friedman, S.D., Frieman, J.A., Fukugita, M., Gal, R.R., Gillespie, B., Glazebrook, K., Gonzalez, C.F., Gray, J., Grebel, E.K., Grodnicki, L., Gunn, J.E., Gurbani, V.K., Hall, P.B., Hao, L., Harbeck, D., Harris, F.H., Harris, H.C., Harvanek, M., Hawley, S.L., Heckman, T.M., Helmboldt, J.F., Hendry, J.S., Hennessy, G.S., Hindsley, R.B., Hogg, D.W., Holmgren, D.J., Holtzman, J.A., Homer, L., Hui, L., Ichikawa, S.-i., Ichikawa, T., Inkmann, J.P., Ivezić, Ž., Jester, S., Johnston, D.E., Jordan, B., Jordan, W.P., Jorgensen, A.M., Jurić, M., Kauffmann, G., Kent, S.M., Kleinman, S.J., Knapp, G.R., Kniazev, A.Y., Kron, R.G., Krzesiński, J., Kunszt, P.Z., Kuropatkin, N., Lamb, D.Q., Lampeitl, H., Laubscher, B.E., Lee, B.C., Leger, R.F., Li, N., Lidz, A., Lin, H., Loh, Y.-S., Long, D.C., Loveday, J., Lupton, R.H., Malik, T., Margon, B., McGehee, P.M., McKay, T.A., Meiksin, A., Miknaitis, G.A., Moorthy, B.K., Munn, J.A., Murphy, T., Nakajima, R., Narayanan, V.K., Nash, T., Neilsen, E.H., Jr., Newberg, H.J., Newman, P.R., Nichol, R.C., Nicinski, T., Nieto-Santisteban, M., Nitta, A., Odenkirchen, M., Okamura, S., Ostriker, J.P., Owen, R., Padmanabhan, N., Peoples, J., Pier, J.R., Pindor, B., Pope, A.C., Quinn, T.R., Rafikov, R.R., Raymond, S.N., Richards, G.T., Richmond, M.W., Rix, H.-W., Rockosi, C.M., Schaye, J., Schlegel, D.J., Schneider, D.P., Schroeder, J., Scranton, R., Sekiguchi, M., Seljak, U., Sergey, G., Sesar, B., Sheldon, E., Shimasaku, K., Siegmund, W.A., Silvestri, N.M., Sinisgalli, A.J., Sirkó, E., Smith, J.A., Smolčić, V., Snedden, S.A., Stebbins, A., Steinhardt, C., Stinson, G.,

- Stoughton, C., Strateva, I.V., Strauss, M.A., SubbaRao, M., Szalay, A.S., Szapudi, I., Szkody, P., Tasca, L., Tegmark, M., Thakar, A.R., Tremonti, C., Tucker, D.L., Uomoto, A., Vanden Berk, D.E., Vandenberg, J., Vogeley, M.S., Voges, W., Vogt, N.P., Walkowicz, L.M., Weinberg, D.H., West, A.A., White, S.D.M., Wilhite, B.C., Willman, B., Xu, Y., Yanny, B., Yarger, J., Yasuda, N., Yip, C.-W., Yocom, D.R., York, D.G., Zakamska, N.L., Zehavi, I., Zheng, W., Zibetti, S., Zucker, D.B.: The first data release of the Sloan digital sky survey. *AJ* **126**, 2081 (2003)
- Absil, O., Mawet, D.: Formation and evolution of planetary systems: the impact of high-angular resolution optical techniques. *A&A Rev.* **18**, 317 (2010)
- Adams, W.S.: *PASP* **27**, 236 (1915)
- Basri, G., Marcy, G.W., Graham, J.R.: In: American Astronomical Society Meeting Abstracts #186, Pittsburgh. *Bulletin of the American Astronomical Society*, vol. 27, p. 1214 (1995)
- Basri, G., Marcy, G.W., Graham, J.R.: Lithium in brown dwarf candidates: the mass and age of the faintest Pleiades stars. *ApJ* **458**, 600 (1996)
- Becklin, E.E., Zuckerman, B.: A low-temperature companion to a white dwarf star. *Nature* **336**, 656 (1988)
- Bessel, F.W.: On the variations of the proper motions of Procyon and Sirius. *MNRAS* **6**, 136 (1844)
- Bowler, B.P., Liu, M.C., Dupuy, T.J., Cushing, M.C.: High spatial resolution imaging of thermal emission from Debris Disks. *ApJ* **723**, 850 (2010)
- Burgasser, A.J., Kirkpatrick, J.D.: Stars: chemically peculiar, stars: individual (LEHPM 2-59), stars: individual (APMPM J0559-2903), Stars: Low-Mass, Brown Dwarfs, Stars: Subdwarfs. *ApJ* **645**, 1485 (2006)
- Burrows, A., Hubbard, W.B., Saumon, D., Lunine, J.I.: An expanded set of brown dwarf and very low mass star models. *ApJ* **406**, 158 (1993)
- Cassini, J.: Tables astronomiques du Soleil, de la Lune, des Planetes, des Etoiles fixes et des Satellites de Jupiter et de Saturne; avec l'explication et l'usage de ces memes tables. de l'Imprimerie Royale, Paris (1740)
- Clampin, M., Nota, A., Golimowski, D.A., Leitherer, C., Durrance, S.T.: Coronographic imaging of the bipolar nebula around the luminous blue variable R 127. *APJL* **410**, L35 (1993)
- Clark, A.: Sidereal Messenger **8**, 109–117 (1889)
- Cushing, M.C., Marley, M.S., Saumon, D., Kelly, B.C., Vacca, W.D., Rayner, J.T., Freedman, R.S., Lodders, K., Roellig, T.L.: Atmospheric parameters of field L and T dwarfs. *ApJ* **678**, 1372 (2008)
- Cushing, M.C., Kirkpatrick, J.D., Gelino, C.R., Griffith, R.L., Skrutskie, M.F., Mainzer, A., Marsh, K.A., Beichman, C.A., Burgasser, A.J., Prato, L.A., Simcoe, R.A., Marley, M.S., Saumon, D., Freedman, R.S., Eisenhardt, P.R., Wright, E.L.: The discovery of Y dwarfs using data from the wide-field infrared survey explorer (WISE). *ApJ* **743**, 50 (2011)
- Dekany, R., Bouchez, A., Britton, M., Velur, V., Troy, M., Shelton, J.C., Roberts, J.: In: Ellerbroek, B.L., Calia, D.B. (eds.) *Advances in Adaptive Optics II. Proceedings of the SPIE*, vol. 6272, pp. 627209. SPIE, Bellingham (2006)
- Dekany, R., Bouchez, A., Roberts, J., Troy, M., Kibblewhite, E., Oppenheimer, B., Moore, A., Shelton, C., Smith, R., Trinh, T., Velur, V.: In: Ryan S. (ed.) *Proceedings of the Advanced Maui Optical and Space Surveillance Technologies Conference*, Wailea, 12–15 Sept 2007, p. E64. The Maui Economic Development Board (2007)
- Delfosse, X., Forveille, T., Ségransan, D., Beuzit, J.-L., Udry, S., Perrier, C., Mayor, M.: Accurate masses of very low mass stars. IV. Improved mass-luminosity relations. *A&A* **364**, 217 (2000)
- Demory, B.-O., Ségransan, D., Forveille, T., Queloz, D., Beuzit, J.-L., Delfosse, X., di Folco, E., Kervella, P., Le Bouquin, J.-B., Perrier, C., Benisty, M., Duvert, G., Hofmann, K.-H., Lopez, B., Petrov, R.: Mass-radius relation of low and very low-mass stars revisited with the VLTI. *A&A* **505**, 205 (2009)
- Faherty, J.K., Rice, E.L., Cruz, K.L., Mamajek, E.E., Núñez, A.: 2MASS J035523.37+113343.7: a young, dusty, nearby, isolated brown dwarf resembling a giant exoplanet. *AJ* **145**, 2 (2013)
- Golimowski, D.A.: PhD thesis, Johns Hopkins University, Baltimore (1994)
- Golimowski, D.A., Clampin, M., Durrance, S.T., Barkhouser, R.H.: High-resolution ground-based coronagraphy using image-motion compensation. *Appl. Opt.* **31**, 4405 (1992)

- Golimowski, D.A., Durrance, S.T., Clampin, M.: Coronagraphic imaging of the Beta Pictoris circumstellar disk – evidence of changing disk structure within 100 AU. *APJL* **411**, L41 (1993a)
- Golimowski, D.A., Durrance, S.T., Clampin, M.: Detection of an apparent star 2.1 arcsec from the circumstellar disk candidate Epsilon Sagittari. *AJ* **105**, 1108 (1993b)
- Golimowski, D.A., Fastie, W.G., Schroeder, D.J., Uomoto, A.: Hubble space telescope observations of the very low mass companion to Gliese 105A. *APJL* **452**, L125 (1995a)
- Golimowski, D.A., Nakajima, T., Kulkarni, S.R., Oppenheimer, B.R.: Detection of a very low mass companion to the astrometric binary Gliese 105A. *APJL* **444**, L101 (1995b)
- Golimowski, D.A., Burrows, C.J., Kulkarni, S.R., Oppenheimer, B.R., Brukardt, R.A.: Wide field planetary camera 2 observations of the brown dwarf Gliese 229B: optical colors and orbital motion. *AJ* **115**, 2579 (1998)
- Gorda, S.Y., Svechnikov, M.A.: Empirical L-M, R-M, and M-T<sub>eff</sub> relations for main-sequence stars: components of close binary systems and low-mass stars. *Astron. Rep.* **43**, 521 (1999)
- Greenburg, S.T.: The infinite in Giordano Bruno, with a Translation of His Dialogue, Concerning the Cause, Principle, and One. King's Crown Press, New York (1950)
- Griaule, M., Dieterlen, G.: Un systeme soudanais de Sirius. *J. Soc. Afr.* **20**, 273 (1950)
- Halley, E.: Considerations on the change of the latitudes of some of the Principal Fixt Stars. by Edmund Halley, R. S. Sec. R. Soc. Lond. Philos. Trans. Ser. I **30**, 736 (1717)
- Herschel, W.: Account of the changes that have happened, during the last twenty-five years, in the relative situation of double-stars; with an investigation of the cause to which they are owing. *R. Soc. Lond. Philos. Trans. Ser. I* **93**, 339 (1803)
- Hicks, R.D. (trans.): Diogenes Laertius: Lives of Eminent Philosophers, vol. II. Loeb Classical Library, New York (1925)
- Hinkley, S.: PhD thesis, Columbia University (2009)
- Hinkley, S., Oppenheimer, B.R., Brenner, D., Parry, I.R., Sivaramakrishnan, A., Soummer, R., King, D.: In: Society of Photo-Optical Instrumentation Engineers (SPIE) Conference, Marseille. Society of Photo-Optical Instrumentation Engineers (SPIE) Conference Series, vol. 7015, pp. 701519–701519–10 (2008)
- Hinkley, S., Oppenheimer, B.R., Brenner, D., Zimmerman, N., Roberts, L.C., Parry, I.R., Soummer, R., Sivaramakrishnan, A., Simon, M., Perrin, M.D., King, D.L., Lloyd, J.P., Bouchez, A., Roberts, J.E., Dekany, R., Beichman, C., Hillenbrand, L., Burruss, R., Shao, M., Vasisht, G.: Discovery and characterization of a Faint stellar companion to the A3V star ξ Virginis. *ApJ* **712**, 421 (2010)
- Hinkley, S., Monnier, J.D., Oppenheimer, B.R., Roberts, L.C., Ireland, M., Zimmerman, N., Brenner, D., Parry, I.R., Martinache, F., Lai, O., Soummer, R., Sivaramakrishnan, A., Beichman, C., Hillenbrand, L., Zhao, M., Lloyd, J.P., Bernat, D., Vasisht, G., Crepp, J.R., Pueyo, L., Shao, M., Perrin, M.D., King, D.L., Bouchez, A., Roberts, J.E., Dekany, R., Burruss, R.: Establishing α Oph as a prototype rotator: improved astrometric orbit. *ApJ* **726**, 104 (2011a)
- Hinkley, S., Oppenheimer, B.R., Zimmerman, N., Brenner, D., Parry, I.R., Crepp, J.R., Vasisht, G., Ligon, E., King, D., Soummer, R., Sivaramakrishnan, A., Beichman, C., Shao, M., Roberts, L.C., Bouchez, A., Dekany, R., Pueyo, L., Roberts, J.E., Lockhart, T., Zhai, C., Shelton, C., Burruss, R.: A new high contrast imaging program at Palomar observatory. *PASP* **123**, 74 (2011b)
- Hinkley, S., Hillenbrand, L., Oppenheimer, B.R., Rice, E.L., Pueyo, L., Vasisht, G., Zimmerman, N., Kraus, A.L., Ireland, M.J., Brenner, D., Beichman, C., Dekany, R., Roberts, J.E., Parry, I.R., Roberts, L.C., Jr., Crepp, J.R., Burruss, R., Wallace, J.K., Cady, E., Zhai, C., Shao, M., Lockhart, T., Soummer, R., Sivaramakrishnan, A.: High-resolution infrared imaging and spectroscopy of the Z Canis Majoris system during Quiescence and Outburst. *APJL* **763**, L9 (2013)
- Janson, M., Bergfors, C., Goto, M., Brandner, W., Lafrenière, D.: Spatially resolved spectroscopy of the Exoplanet HR 8799 c. *APJL* **710**, L35 (2010)
- Joergens, V.: Radial velocity survey for planets and brown dwarf companions to very young brown dwarfs and very low-mass stars in Chamaeleon I with UVES at the VLT. *A&A* **446**, 1165 (2006)

- Kirkpatrick, J.D., Reid, I.N., Liebert, J., Cutri, R.M., Nelson, B., Beichman, C.A., Dahn, C.C., Monet, D.G., Gizis, J.E., Skrutskie, M.F.: Dwarfs cooler than “M”: the definition of spectral type “L” using discoveries from the 2 Micron all-sky survey (2MASS). *ApJ* **519**, 802 (1999)
- Kirkpatrick, J.D., Gelino, C.R., Cushing, M.C., Mace, G.N., Griffith, R.L., Skrutskie, M.F., Marsh, K.A., Wright, E.L., Eisenhardt, P.R., McLean, I.S., Mainzer, A.K., Burgasser, A.J., Tinney, C.G., Parker, S., Salter, G.: Further defining spectral type “Y” and exploring the low-mass end of the field brown dwarf mass function. *ApJ* **753**, 156 (2012)
- Konopacky, Q.M., Barman, T.S., Macintosh, B.A., Marois, C.: *Science* **339**, 1398 (2013)
- Kumar, S.S.: Models for stars of very low mass. Technical report, NASA/GISS (1962)
- Macintosh, B.A., Graham, J.R., Palmer, D.W., Doyon, R., Dunn, J., Gavel, D.T., Larkin, J., Oppenheimer, B., Saddlemyer, L., Sivaramakrishnan, A., Wallace, J.K., Bauman, B., Erickson, D.A., Marois, C., Poyneer, L.A., Soummer, R.: In: Presented at the Society of Photo-Optical Instrumentation Engineers (SPIE) Conference, Marseille. Society of Photo-Optical Instrumentation Engineers (SPIE) Conference Series, vol. 7015, pp. 701518–701518–13 (2008)
- Marois, C., Macintosh, B., Barman, T., Zuckerman, B., Song, I., Patience, J., Lafrenière, D., Doyon, R.: Direct imaging of multiple planets orbiting the Star HR 8799. *Science* **322**, 1348 (2008)
- Marois, C., Macintosh, B., Véran, J.: In: Society of Photo-Optical Instrumentation Engineers (SPIE) Conference, San Diego. Society of Photo-Optical Instrumentation Engineers (SPIE) Conference Series, vol. 7736 (2010a)
- Marois, C., Zuckerman, B., Konopacky, Q.M., Macintosh, B., Barman, T.: Images of a fourth planet orbiting HR 8799. *Nature* **468**, 1080 (2010b)
- Martín, E.L., Delfosse, X., Basri, G., Goldman, B., Forveille, T., Zapatero Osorio, M.R.: Spectroscopic classification of Late-M and L field dwarfs. *AJ* **118**, 2466 (1999)
- Mason, B.D., Wycoff, G.L., Hartkopf, W.I., Douglass, G.G., Worley, C.E.: The Washington visual double star catalog (Mason+ 2001–2013). *VizieR Online Data Catalog* **1**, 2026 (2013)
- Mawet, D., Pueyo, L., Lawson, P., Mugnier, L., Traub, W., Boccaletti, A., Trauger, J.T., Gladysz, S., Serabyn, E., Milli, J., Belikov, R., Kasper, M., Baudoz, P., Macintosh, B., Marois, C., Oppenheimer, B., Barrett, H., Beuzit, J.-L., Devaney, N., Girard, J., Guyon, O., Krist, J., Mennesson, B., Mouillet, D., Murakami, N., Poyneer, L., Savransky, D., Vérinaud, C., Wallace, J.K.: In: Society of Photo-Optical Instrumentation Engineers (SPIE) Conference, Amsterdam. Society of Photo-Optical Instrumentation Engineers (SPIE) Conference Series, vol. 8442 (2012)
- Mayer, T., Maskelyne, N.: *Tabulae motuum SOLIS et lunae, novae et correctae; auctore Tobia Mayer: quibus accedit methodus longitudinum promota, eodem autore.* (Gale ECCO, reprint 2010) (1770)
- Mayor, M., Queloz, D.: A Jupiter-Mass companion to a solar-type star. *Nature* **378**, 355 (1995)
- Mayor, M., Queloz, D.: From 51 Peg to Earth-type planets. *New Astron. Rev.* **56**, 19 (2012)
- Michell, J.: Coronagraphic imaging of pre-main-sequence stars: remnant envelopes of star formation seen in reflection. *R. Soc. Lond. Philos. Trans. Ser. I* **57**, 234 (1767)
- Nakajima, T., Golimowski, D.A.: Coronagraphic imaging of pre-main-sequence stars: remnant envelopes of star formation seen in reflection. *AJ* **109**, 1181 (1995)
- Nakajima, T., Durrance, S.T., Golimowski, D.A., Kulkarni, S.R.: A coronagraphic search for brown dwarfs around nearby stars. *ApJ* **428**, 797 (1994)
- Nakajima, T., Oppenheimer, B.R., Kulkarni, S.R., Golimowski, D.A., Matthews, K., Durrance, S.T.: Discovery of a cool brown dwarf. *Nature* **378**, 463 (1995)
- North, J.: *The Norton History of Astronomy and Cosmology*. W. W. Norton, New York (1995)
- Oppenheimer, B.R., Hinkley, S.: *ARA&A* **47**, 253 (2009)
- Oppenheimer, B.R., Kulkarni, S.R., Matthews, K., Nakajima, T.: Infrared spectrum of the cool brown dwarf Gl 229B. *Science* **270**, 1478 (1995)
- Oppenheimer, B.R., Kulkarni, S.R., Matthews, K., van Kerkwijk, M.H.: The spectrum of the brown dwarf Gliese 229B. *ApJ* **502**, 932 (1998)

- Oppenheimer, B.R., Beichman, C., Brenner, D., Burruss, R., Cady, E., Crepp, J.R., Hillenbrand, L., Hinkley, S., Ligon, E.R., Lockhart, T., Parry, I.R., Pueyo, L., Rice, E.L., Roberts, L.C., Shao, M., Sivaramakrishnan, A., Soummer, R., Vasisht, G., Vescelus, F.E., Wallace, J.K., Zhai, C., Zimmerman, N.: In: Society of Photo-Optical Instrumentation Engineers (SPIE) Conference Series, Amsterdam, vol. 8447 (2012)
- Oppenheimer, B.R., Baranec, C., Beichman, C., Brenner, D., Burruss, R., Cady, E., Crepp, J.R., Dekany, R., Fergus, R., Hale, D., Hillenbrand, L., Hinkley, S., Hogg, D.W., King, D., Ligon, E.R., Lockhart, T., Nilsson, R., Parry, I.R., Pueyo, L., Rice, E., Roberts, J.E., Roberts, L.C., Jr., Shao, M., Sivaramakrishnan, A., Soummer, R., Truong, T., Vasisht, G., Veicht, A., Vescelus, F., Wallace, J.K., Zhai, C., Zimmerman, N.: Reconnaissance of the HR 8799 exosolar system. I. Near-infrared spectroscopy. *ApJ* **768**, 24 (2013)
- Pueyo, L., Hillenbrand, L., Vasisht, G., Oppenheimer, B.R., Monnier, J.D., Hinkley, S., Crepp, J., Roberts, L.C., Jr., Brenner, D., Zimmerman, N., Parry, I., Beichman, C., Dekany, R., Shao, M., Burruss, R., Cady, E., Roberts, J., Soummer, R.: Constraining mass ratio and extinction in the FU orionis binary system with infrared integral field spectroscopy. *ApJ* **757**, 57 (2012)
- Rebolo, R., Zapatero Osorio, M.R., Martín, E.L.: Discovery of a brown dwarf in the Pleiades star cluster. *Nature* **377**, 129 (1995)
- Roxburgh, I.W., Williams, I.P.: The Dogon tribe and Sirius. *The Observatory* **95**, 215 1975
- Sivaramakrishnan, A., Lloyd, J.P.: Spiders in Lyot Coronagraphs. *ApJ* **633**, 528 (2005)
- Skrutskie, M.F., Cutri, R.M., Stiening, R., Weinberg, M.D., Schneider, S., Carpenter, J.M., Beichman, C., Capps, R., Chester, T., Elias, J., Huchra, J., Liebert, J., Lonsdale, C., Monet, D.G., Price, S., Seitzer, P., Jarrett, T., Kirkpatrick, J.D., Gizis, J.E., Howard, E., Evans, T., Fowler, J., Fullmer, L., Hurt, R., Light, R., Kopan, E.L., Marsh, K.A., McCallon, H.L., Tam, R., Van Dyk, S., Wheelock, S.: The two micron all sky survey (2MASS). *AJ* **131**, 1163 (2006)
- Söderhjelm, S.: Visual binary orbits and masses POST HIPPARCOS. *A&A* **341**, 121 (1999)
- Soummer, R.: APJL **618**, L161 (2005)
- Soummer, R., Aime, C., Falloon, P.E.: In: Aime, C., Soummer, R. (eds.) *Astronomy with High Contrast Imaging*, Proceedings of the Conference held 13–16 May, 2002 in Nice. EAS Publications Series, pp. 93–105 (2003a)
- Soummer, R., Aime, C., Falloon, P.E.: Stellar coronagraphy with prolate apodized circular apertures. *A&A* **397**, 1161 (2003b)
- Soummer, R., Pueyo, L., Ferrari, A., Aime, C., Sivaramakrishnan, A., Yaitskova, N.: Apodized pupil lyot coronagraphs for arbitrary apertures. II. Theoretical properties and application to extremely large telescopes. *ApJ* **695**, 695 (2009)
- Strauss, M.A., Fan, X., Gunn, J.E., Leggett, S.K., Geballe, T.R., Pier, J.R., Lupton, R.H., Knapp, G.R., Annis, J., Brinkmann, J., Crocker, J.H., Csabai, I., Fukugita, M., Golimowski, D.A., Harris, F.H., Hennessy, G.S., Hindsley, R.B., Ivezić, Ž., Kent, S., Lamb, D.Q., Munn, J.A., Newberg, H.J., Rechenmacher, R., Schneider, D.P., Smith, J.A., Stoughton, C., Tucker, D.L., Waddell, P., York, D.G.: The discovery of a field methane dwarf from Sloan digital sky survey commissioning data. *APJL* **522**, L61 (1999)
- Traub, W.A., Oppenheimer, B.R.: *Direct Imaging of Exoplanets*, pp. 111–156. University of Arizona Press, Tucson (2011)
- Tsuji, T.: Molecular abundance in stellar atmospheres. *Ann. Tokyo Astron. Obs.* **9**(1) 1–110 (1964)
- Tsuji, T., Ohnaka, K., Aoki, W.: In: Tinney, C.G. (eds.) *The Bottom of the Main Sequence – and Beyond*, p. 45. Springer, Berlin/Heidelberg (1995)
- Vasisht, G., Cady, E., Ligon, E.R., Lockhart, M., Shao, M., Wallace, J.K.: A calibration interferometer for speckle control in a coronagraph PASP (2013, submitted)
- Zhai, C., Vasisht, G., Shao, M., Lockhart, T.G., Cady, E., Oppenheimer, B.R., Burruss, R., Roberts, J., Beichman, C., Brenner, D., Crepp, J., Dekany, R., Hinkley, S., Hillenbrand, L., Ligon, E.R., Parry, I., Pueyo, L., Rice, E.L., Roberts, L.C., Jr., Sivaramakrishnan, A., Soummer, R., Vescelus, F.E., Wallace, J.K., Zimmerman, N.: Society of Photo-Optical Instrumentation Engineers (SPIE) Conference Series, Amsterdam, vol. 8447, p. 259 (2012)

- Zimmerman, N., Oppenheimer, B.R., Hinkley, S., Brenner, D., Parry, I.R., Sivaramakrishnan, A., Hillenbrand, L., Beichman, C., Crepp, J.R., Vasisht, G., Roberts, L.C., Burruss, R., King, D.L., Soummer, R., Dekany, R., Shao, M., Bouchez, A., Roberts, J.E., Hunt, S.: Parallactic motion for companion discovery: an M-Dwarf orbiting Alcor. *ApJ* **709**, 733 (2010)
- Zimmerman, N., Brenner, D., Oppenheimer, B.R., Parry, I.R., Hinkley, S., Hunt, S., Roberts, R.: A data-cube extraction pipeline for a coronagraphic integral field spectrograph. *PASP* **123**, 746 (2011)

# Ultracool Objects: L, T, and Y Dwarfs

Michael C. Cushing

**Abstract** The discovery of the first bona fide brown dwarfs in 1995 ushered in a new era in both stellar and planetary astrophysics. The emergent spectra of brown dwarfs are distinct from those of the lowest-mass stars and thus the creation of three new spectral classes, L, T, and Y, were required in order to classify them. In this chapter, I provide a historical review of the creation of these spectral classes and briefly discuss the physical conditions that give rise to the variations in spectral morphology used for classification.

## 1 Introduction

Remarkably the discoveries of the first exoplanet orbiting a normal star (51 Peg b) and the first uncontested field brown dwarf (Gliese 229B) were announced on the same day, October 6, 1995, in Florence, Italy at the *9th Cambridge Workshop on Cool Stars, Stellar Systems, and the Sun*. Brown dwarfs are low-mass objects whose central temperatures are too cool for them to reach an equilibrium configuration where the surface radiative losses are balanced by the energy generated by hydrogen fusion in their cores (Kumar 1963; Hayashi and Nakano 1963). Of course without an internal energy source, brown dwarfs cool over time “like dying embers plucked from a fire” (Burrows et al. 2001). Consequently they obey a mass-luminosity-age relation rather than a mass-luminosity relation like the hotter hydrogen-fusing stars. The study and characterization of the more than two thousand brown dwarfs and exoplanets discovered since 1995 has become a major focus of both the stellar and planetary astrophysics communities. Our understanding of their properties has evolved in parallel because “[w]hatever the mass ( $M$ ) or origin of an extrasolar giant

---

M.C. Cushing (✉)

Department of Physics and Astronomy, University of Toledo, MS 111, 2801 W. Bancroft St.,  
Toledo, OH 43606, USA

e-mail: [michael.cushing@utoledo.edu](mailto:michael.cushing@utoledo.edu)

planet or brown dwarf, the same physics, chemistry, and compositions obtain for both” ([Burrows et al. 2001](#)). That is, when we learn something about brown dwarfs, we learn something about gas giant planets, and vice versa.

The emergent spectra of brown dwarfs are so distinct from those of the cool M stars, that the creation of three new spectral classes, L, T, and most recently Y, was required in order to classify them. In this chapter, I present a historical review of the discovery of the L, T, and Y dwarfs. In particular, I will review the underlying concepts of spectral classification as embodied in the MK System (Sect. 3) and then discuss how the L, T, and Y classification schemes were devised (Sects. 4–6). Finally, I will briefly touch on some of the underlying physics that give rise to the different spectral classes (Sect. 7) and note some outstanding issues that require future attention (Sect. 8). For more detail on these subjects, as well as a discussion of many other aspects of brown dwarf astrophysics, the interested reader is referred to the excellent reviews by J. D. Kirkpatrick and A. J. Burgasser in *Stellar Spectral Classification* ([Gray and Corbally 2009](#)), [Basri \(2000\)](#), and [Kirkpatrick \(2005\)](#). For a more theoretical perspective on brown dwarfs please see [Stevenson \(1991\)](#), [Burrows and Liebert \(1993\)](#), [Allard et al. \(1997\)](#), [Chabrier and Baraffe \(2000\)](#), [Burrows et al. \(2001\)](#), and the chapter by I. Baraffe in this book.

## 2 On the Precipice of the Main Sequence

Over the course of the twentieth century, astronomers slowly extended the M-dwarf spectral sequence to later M subtypes and cooler effective temperatures (e.g., [Adams et al. 1926](#); [Morgan 1938](#); [Kuiper 1942](#); [Joy 1947](#); [Boeshaar 1976](#); [Boeshaar and Tyson 1985](#)).<sup>1</sup> The early classification schemes were devised in the visible region (3,900–7,000 Å) and used the strengths of the titanium oxide (TiO) bands as subtype discriminators. However, M-dwarf spectral energy distributions peak beyond the visible wavelength range so once detectors were invented that were capable of collecting light at  $\lambda > 7,000$  Å, the classification schemes naturally moved to the red optical (6,000–10,000 Å) to take advantage of the increased number of photons (e.g., [Bessell 1991](#); [Kirkpatrick et al. 1991](#)). The most widely used M-dwarf classification system is that of [Kirkpatrick et al. \(1991\)](#) which classifies M dwarfs from M0 to M9 based on the strengths of the TiO and vanadium oxide (VO) bands over the 6,300–9,000 Å wavelength range.

One of the motivations in the search for cooler and cooler dwarf stars was to eventually breach the barrier between the bottom of the hydrogen-burning main sequence and the realm of the brown dwarfs. However, it was not until more sensitive red and near-infrared (1–2.5 μm) detectors were developed and deployed in the late 1980s and early 1990s that brown dwarfs were finally discovered

---

<sup>1</sup>Excellent reviews on the development of the M-dwarf classification systems can be found in [Kirkpatrick et al. \(1991\)](#) and [Gray and Corbally \(2009\)](#).

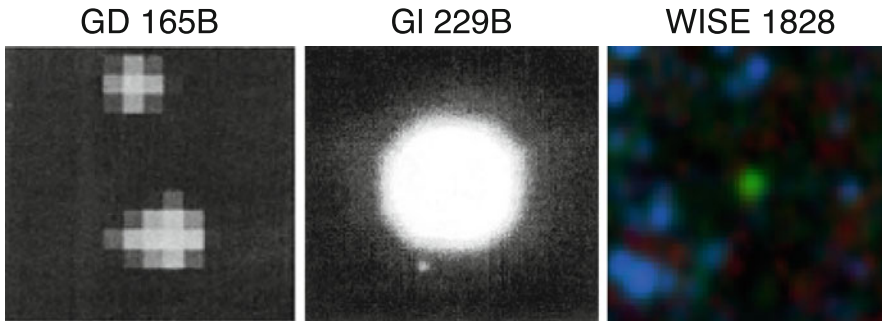


**Fig. 1** Discovery images of the L-, T-, and Y-dwarf archetypes. *Left:* The roughly  $7'' \times 7''$  image of GD 165 A and B was taken in the  $K$  band (Becklin and Zuckerman 1988). GD 165B is the brighter of the two components. *Middle:* The  $25'' \times 25''$  image of Gliese 229 A and B was taken in the  $z$  band (Nakajima et al. 1995). Gliese 229B can be seen as a faint companion at the 7 o'clock position. *Right:* A  $2' \times 2'$  three-color image of WISE J182831.08+265037.7 obtained with *Wide-field Infrared Survey Explorer* (WISE) (Cushing et al. 2011). Blue corresponds to the  $W1$  band ( $3.4\text{ }\mu\text{m}$ ), green to  $W2$  ( $4.6\text{ }\mu\text{m}$ ), and red to  $W3$  ( $12\text{ }\mu\text{m}$ ). All images are oriented so that North is up and East is to the left. The images of GD 165B and Gliese 229B are reprinted by permission from Mcmillan Publishers Ltd: (Nature), copyright 1988, 1995

(see chapters by R. Rebolo, G. Basri, and B. Oppenheimer in this book). Modern evolutionary theory places the edge of the main sequence at roughly  $M \approx 0.075 M_{\odot}$  ( $78.5 M_{\text{Jup}}$ ),  $L_{\text{bol}} \approx 6 \times 10^{-5} L_{\odot}$ , and  $T_{\text{eff}} \approx 1,600\text{--}1,750\text{ K}$  for solar metallicity (Burrows et al. 2001) which means that L dwarfs encompass both very low-mass stars and brown dwarfs while T and Y dwarfs are exclusively brown dwarfs. Collectively, any star or brown dwarf with a spectral type later than M6 is known as an “ultracool” dwarf. Particularly germane in the context of the new spectral classes was the discovery of two ultracool dwarfs, GD 165B and Gliese 229B, because they became the archetypes of the L and T spectral classes.

GD 165B was discovered as part of a near-infrared survey for low-mass star and brown dwarf companions to white dwarfs (see Fig. 1 for the discovery image; Becklin and Zuckerman 1988). Later Kirkpatrick et al. (1993) obtained a spectrum of GD 165B over the  $6,300\text{--}9,000\text{ \AA}$  wavelength range and noted that the spectrum lacked the prominent TiO and VO absorption bands typically found in the spectra of late-type M dwarfs. Thus they were “forced to delay classification until other such objects are discovered.”<sup>2</sup> The left panel of Fig. 2 shows the red spectrum of GD 165B along with the spectrum of BRI 0021–0214, an M9.5 dwarf. The spectrum of GD 165B not only lacks the prominent TiO ( $7,053, 7,589, 8,206, 8,432, 8,859\text{ \AA}$ ) and VO ( $\sim 7,334, \sim 7,851\text{ \AA}$ ) bands present in the spectrum of BRI 0021–0214 but also exhibits the  $8,611\text{ \AA}$  band head of chromium hydride (CrH), the  $8,692\text{ \AA}$  band head of iron hydride (FeH), and the additional alkali lines of Rb ( $7,800, 7,948\text{ \AA}$ )

<sup>2</sup>Tokunaga et al. (1990) obtained a  $K$ -band spectrum of GD 165B and noted that it had deep  $H_2O$  absorption bands which confirmed its cool nature.

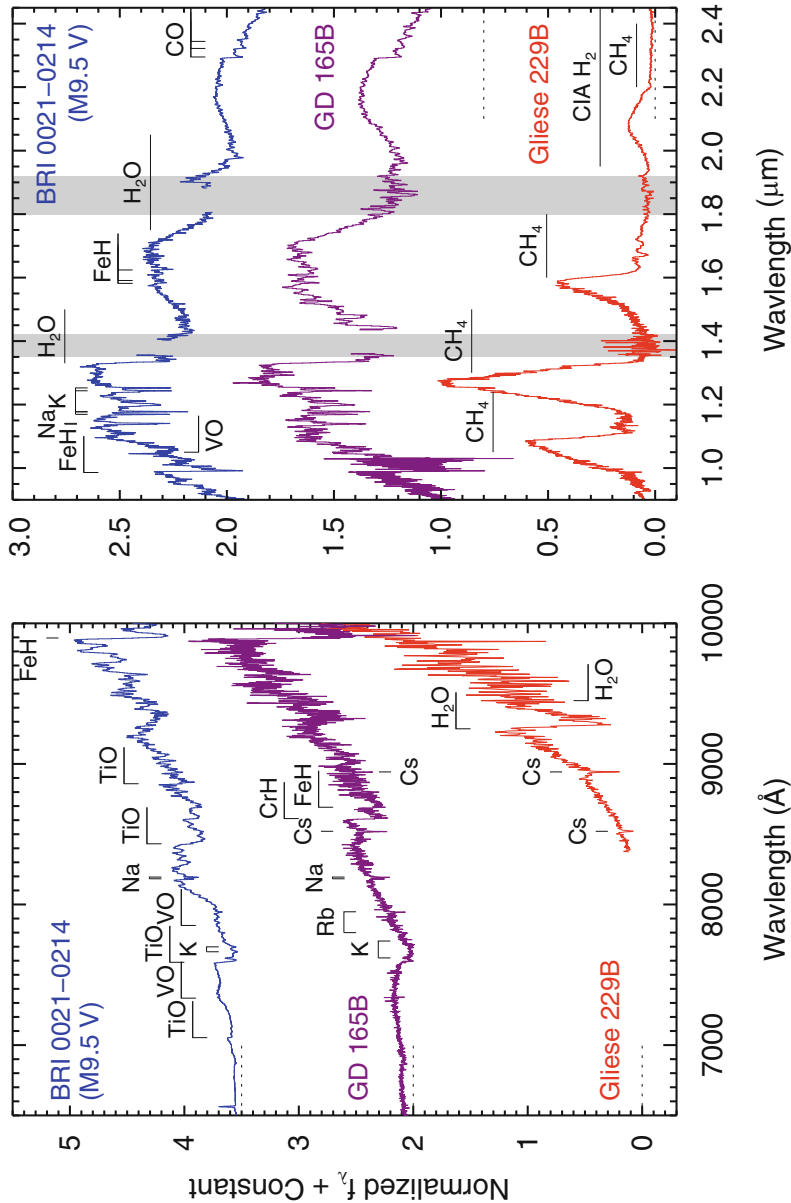


**Fig. 2** *Left:* Red optical spectrum of BRI 0021–0214 (M9.5 V, Reid et al. 1999), GD 165B (Kirkpatrick et al. 1999a), and Gliese 229B (Oppenheimer et al. 1998). Spectra are normalized to unity and offset with constants (dotted lines). *Right:* Near-infrared spectra of BRI 0021–0214 (M9.5 V, Cushing et al. 2005), GD 165B (Kirkpatrick et al. 1999a), and Gliese 229B (Geballe et al. 1996). Wavelengths of high telluric absorption, and thus low signal-to-noise or missing data, are denoted as grey bars. The spectra are normalized to unity at 1.27  $\mu\text{m}$  and offset with constants (dotted lines). Prominent atomic and molecular absorption features are indicated

and Cs (8,521 Å). The K I resonance doublet (7,665, 7,699 Å) also appears heavily broadened such that its profile appears as a single, broad absorption feature. These spectral features would become the hallmark features of the new L spectral class.

Gliese 229B was discovered as a companion to the M1 dwarf Gliese 229A in a search for brown dwarf companions to nearby stars (Nakajima et al. 1995)<sup>3</sup> and one of its discovery images is shown in the middle panel of Fig. 1. Its near-infrared spectrum, along with that of BRI 0021–0214 and GD 165B is shown in the right panel of Fig. 2. The infrared spectra of late-type M dwarfs are characterized by broad absorption bands of water ( $H_2O$ ; centered at 0.95, 1.1, 1.4, 1.8, and 2.3 μm), deep K I (1.169, 1.177, 1.244, 1.253 μm) and Na I (1.138, 1.140 μm) lines in the *J* band, and prominent  $\Delta\nu = +2$  CO overtone band heads beginning at 2.29 μm. Similar spectral features are seen in the infrared spectra of L dwarfs, i.e. GD 165B. In stark contrast, the spectrum of Gliese 229B exhibits deep absorption bands of methane ( $CH_4$ ; centered at 1.15, 1.7, and 2.3 μm) and collision-induced absorption (CIA) of molecular hydrogen ( $H_2$ ; 1.8–2.8 μm)<sup>4</sup> and is qualitatively similar to the spectrum of Jupiter (e.g., Oppenheimer et al. 1995).<sup>5</sup> These spectral features –  $H_2O$ ,  $CH_4$ , and CIA  $H_2$  – would become the hallmark features of the new T spectral class.

Although the brown dwarf status of GD 165B remains uncertain to this day, there was very little doubt that Gliese 229B was a bona fide brown dwarf. Chemical equilibrium calculations indicate that the two dominant carbon-bearing species are CO and  $CH_4$  with CO dominating at higher temperatures and  $CH_4$  dominating at lower temperatures. The two have equal abundances at a temperature of roughly 1,100 K at a pressure of 1 bar (e.g. Lodders 1999). Given the prominent  $CH_4$  absorption bands present in its spectrum, Gliese 229B’s effective temperature must therefore be below ∼1,100 K which, in combination with its low bolometric luminosity of  $\leq 10^{-5} L_\odot$ , was a solid indication of its substellar nature.

Although it was clear that at least one new spectral class was going to be required in order to classify GD 165B- and Gliese 229B-like objects, the choice of letter(s) was not. Martín et al. (1997) were the first to propose ‘L’ as the new spectral class because it would be suggestive of “Low-temperature”. They further suggested that objects confirmed as brown dwarfs via the so-called lithium test (see chapters by R. Rebolo and G. Basri) could be designated ‘ $L_{Li}$ ’ and that objects with spectra similar to that of Gliese 229B could be designated as ‘ $L_{CH_4}$ ’. In contrast, Kirkpatrick (1998) suggested that two new letters were required, one for GD 165B-like objects, and one for Gliese 229B-like objects. Kirkpatrick et al. (1999b) describe in detail

<sup>3</sup>Please see chapter by B. Oppenheimer for a detailed account of the discovery of this benchmark object.

<sup>4</sup>This absorption is due to an induced quadrupole moment of the  $H_2$  molecule that arises from collisions in the gas (Linsky 1969).

<sup>5</sup>It should be noted that the similarities between the spectra of Jupiter and Gliese 229B at near-infrared wavelengths are fortuitous since they are formed by very different processes. The near-infrared spectrum of Gliese 229B arises from the thermal emission of its atmosphere while the near-infrared spectrum of Jupiter arises from sunlight reflecting off of the cloud layers.

**Table 1** The Latin letters and their usage in Astronomy

Letter	Status	Notes
A	In use	Standard spectral class
B	In use	Standard spectral class
C	In use	Standard carbon-star class
D	Ambiguous	Confusion with white dwarf classes, DA, DB, DC, etc.
E	Ambiguous	Confusion with elliptical galaxy morphological types, E0-E7
F	In use	Standard spectral class
G	In use	Standard spectral class
H	Ok for use	
I	Problematic	Transcription problems I0 (10, Io) and I1 (11, II, II)
J	In use	Standard carbon-star class
K	In use	Standard spectral class
L	Ok for use	
M	In use	Standard spectral class
N	In use	Standard carbon-star class
O	In use	Standard spectral class
P	Problematic?	Incorrect association with planets?
Q	Problematic?	Incorrect association with QSOs?
R	In use	Standard carbon-star class
S	In use	Standard spectral class of ZrO-rich stars
T	Ok for use	
U	Problematic?	Incorrect association with ultraviolet sources?
V	Problematic	Confusion with vanadium oxide (VO vs V0)
W	Ambiguous	Confusion with Wolf-Rayet WN and WR classes
X	Problematic	Incorrect association with X-ray sources
Y	Ok for use	
Z	Problematic?	Incorrect implication that we have reached “the end”?

Table 5 from [Kirkpatrick et al. \(1999b\)](#), reproduced by permission of the AAS.

how they settled on ‘L’ for the GD 165B-like spectra and ‘T’ for the Gliese 229B-like spectra. Table 1 is a reproduction of table 5 from [Kirkpatrick et al. \(1999b\)](#) that lists the 26 Latin letters, their usage in astronomical parlance, and a note on the suitability of the letter as a new spectral class. Based on this analysis, [Kirkpatrick et al.](#) suggested the letters ‘H’, ‘L’, ‘T’, and ‘Y’ were possible choices for the new spectral classes. There was already consensus on ‘L’ for at least one class, but [Martín et al. \(1999\)](#) suggested that ‘H’ be used for the Gliese 229B-like objects because ‘T’ could be confused with T Tauri stars and T-associations. However, ‘H’ was never adopted and the Gliese 229B-like brown dwarfs became known as T dwarfs.

The discovery of GD 165B and Gliese 229B in targeted searches of nearby stars hinted that astronomers were on the precipice of discovering a large population of solivagant field L and T dwarfs if only large areas of the sky could be surveyed at red optical and/or near-infrared wavelengths. Fortunately, three such surveys came online in the last decade of the twentieth century: the Two Micron All Sky Survey (2MASS; [Skrutskie et al. 2006](#)) which surveyed the entire sky at  $J$  (1.25  $\mu\text{m}$ ),

$H$  ( $1.65\text{ }\mu\text{m}$ ), and  $K_s$  ( $2.16\text{ }\mu\text{m}$ ), the Deep Near Infrared Southern Sky Survey (DENIS; [Epchtein et al. 1997](#)) which surveyed the southern sky at  $I$  ( $0.85\text{ }\mu\text{m}$ ),  $J$  ( $1.25\text{ }\mu\text{m}$ ), and  $K_s$  ( $2.15\text{ }\mu\text{m}$ ), and the Sloan Digital Sky Survey (SDSS; [York et al. 2000](#)) which surveyed roughly  $10,000\text{ deg}^2$  of the northern hemisphere at  $u'$  ( $3,596\text{ \AA}$ ),  $g'$  ( $4,639\text{ \AA}$ ),  $r'$  ( $6,122\text{ \AA}$ ),  $i'$  ( $7,439\text{ \AA}$ ), and  $z'$  ( $8,896\text{ \AA}$ ). With deep red and infrared observations of large swathes of sky in hand, the stage was set for the first substantive change/addition to the MK System in nearly 50 years.

### 3 Spectral Classification Precepts

Before describing the discovery of the L, T, and Y dwarfs, it is important to review the roots of the modern stellar classification scheme because it is the foundation on which these new spectral classes were appended. The seemingly odd collection of letters that comprise the modern stellar spectral classes first appeared in the *The Draper Catalogue of stellar spectra photographed with the 8-inch Bache telescope as a part of the Henry Draper memorial* ([Pickering 1890](#)). These letters, OBAFGKM, were actually just seven of the thirteen letter types used by Williamina Fleming to classify the initial 10,351 stellar spectra obtained as part of the Harvard Observatory all-sky spectroscopic survey initiated by Edward C. Pickering in 1885. It was Annie Jump Cannon who first placed them into their now familiar order after removing six of the thirteen Fleming types and reordering the remaining letters in her effort to classify the brightest southern-hemisphere stars ([Cannon and Pickering 1901](#)). Ms. Cannon also initiated the practice of subdividing each spectral class using Arabic numerals, e.g. B1. The final component of a modern spectral type, the luminosity class, was added by [Morgan et al. \(1943\)](#) in their seminal work entitled *An Atlas of Stellar Spectra*. It is this classification system that forms the basis of what is now known as the MK System of spectral classification.

Although most astronomers have a vague notion of how the classification of stars proceeds, it is nevertheless prudent to review how this classification scheme was set up and how the spectrum of an unknown source is classified. The process by which the MK System was created is now known as the ‘MK Process’. The salient details of this process were described in detail by one of the originators of the MK system, W.W. [Morgan \(1984\)](#):

1. “By ‘MK Process,’ we label a specific methodology that makes possible the construction and use of systems of classification based on the particular observed characteristics of stellar spectra that have been selected to define the frames of reference. These systems must be autonomous; that is, they are to be defined completely by the appearance of the spectral features in arrays of standard stellar spectra, in a specified interval of wavelength.”
2. “Each of these autonomous systems must also be self-consistent; that is the array of individual standard stars must constitute - and define - an orderly assemblage, from the point of view of the behavior of the spectral lines, bands and patterns, within the spectral intervals of the standard array.”

3. “The autonomy of each array is achieved through its liberation from dependence on the results of stellar-atmospheric computations - or on any other theoretical models.”
4. “Each new system is to be defined by a network of boxes (as in the MK System); and each of the boxes is to be defined by a specific stellar spectrum in a specific wavelength interval.”

Some clarifying comments are in order. First, although it is not stated explicitly, precept #1 should be amended to include “at a specified spectral resolution” since the visibility of weak, yet potentially important spectral features is a function of the spectral resolution. For example, the T spectral class (see Sect. 5) is defined by the appearance of overtone and combination bands of CH<sub>4</sub> in the H and K bands at low spectral resolving power ( $R \equiv \lambda/\Delta\lambda \approx 150$ ). However, weak CH<sub>4</sub> absorption features are clearly detectable at spectral types earlier than T0 in more moderate resolution  $R \approx 2,000$  spectra (e.g., [McLean et al. 2001](#); [Cushing et al. 2005](#)). Yet these brown dwarfs are not classified as T dwarfs because the T-dwarf classification system is defined at low spectral resolution. Precept #2 can be amplified by imagining the spectral sequence in an old-fashioned flip book, where each subtype appears only slightly different than the subtype before or after it. When viewed in rapid succession, the spectral sequence shows a smooth variation in spectral morphology. Precept #3 is particularly germane in the creation of classification schemes for ultracool dwarfs. Although great strides in our understanding of ultracool atmospheres have been made in the last two decades, they remain particularly difficult to model because the opacity due to millions of overlapping molecular lines and a prescription for condensate (i.e. grain) particle growth and sedimentation are required (see Sect. 7). For example, [Cushing et al. \(2008\)](#) used the model atmospheres of Marley and Saumon to fit the 0.6–14.5  $\mu\text{m}$  spectra of a sample of L and T dwarfs and found large variations in the derived effective temperatures depending on what wavelength range was used. Clearly a classification system based on model-derived effective temperatures is undesirable since it would be constantly changing as the model atmospheres improved. What makes a spectral type so useful is that it is forever fixed and independent of models. The calibration of spectral type as a function of physical parameters such as mass, radius, effective temperature, surface gravity, etc. is done after the purely observational classification system has been devised.

Once a grid of spectral standards has been defined, how does one go about classifying the spectrum of an unknown source? W.W. Morgan again provides the answer ([Morgan 1984](#)):

5. ‘The classification of an unknown stellar spectrum makes use of all features (lines, bands, blends, patterns) within the specified wavelength interval. The classification act itself consists of comparisons with the series of standard spectra that define the boxes, with the question: “Is the unknown spectrum (x) ‘like’ or ‘not like’ this particular standard spectrum?”’

Note that the *entire* spectrum over the specified wavelength range is used in the process of classifying an unknown source.

The use of spectral indices, ratios of integrated or average fluxes in two different wavelength intervals, to quantify the variations in the strengths of various absorption lines and bands has become common practice in the brown dwarf community. Indeed spectral indices are central to some of the classification schemes described in the following sections. However useful spectral indices are for capturing how a particular spectral feature changes quantitatively, their use as a primary spectral type indicator violates precept #5 of the MK Process.

## 4 The L Dwarfs

When GD 165B was discovered in 1988, it was a unique object and therefore defied classification. However, once the 2MASS and DENIS surveys began in earnest and discovered tens of objects with similar red optical spectra, it was clear that a new spectral class was indeed required. Two different classification schemes using the 6,000–10,000 Å wavelength range emerged based on discoveries from 2MASS and DENIS (Kirkpatrick et al. 1999b; Martín et al. 1999).

Kirkpatrick et al. (1999b) presented an L-dwarf scheme based primarily on 2MASS discoveries that is rooted in the MK Process and which consists of nine spectral standards ranging from L0 to L8. Table 2 lists the red optical L-dwarf spectral standards and the left panel of Fig. 3 presents the spectral sequence. The standards were chosen to constitute an “orderly assemblage” based on the behavior of the various spectral features. In particular, the L-dwarf sequence is marked by weakening oxide (TiO, VO) bands, enhanced hydride (CrH, FeH) bands, and enhanced alkali lines of Rb I and Cs I. Kirkpatrick et al. also devised spectral indices that measure the strengths of the various absorption features and the slope (redness) of the spectrum. A final spectral type is calculated by the median of types given by four of the ratios.

Martín et al. (1999) presented a second classification scheme for the L dwarfs based primarily on discoveries from DENIS. They defined seven subtypes ranging from L0 to L6 but in contrast to the MK Process, the subtypes were assigned a difference in effective temperature of 100 K based on the effective temperature estimates of Basri et al. (2000). The spectral type of an unknown source is determined by computing a single spectral index, PC3, that measures the spectral slope from 7,540 to 8,270 Å. Although spectral types from both systems appear in the literature, the Kirkpatrick et al. (1999b) system is the most widely used red optical L-dwarf classification system.

The peak of the spectral energy distributions of the L dwarfs is in the near-infrared so a classification scheme at these wavelengths would be optimal. The near-infrared spectra of L dwarfs are qualitatively similar to those of the late-type M dwarfs in that they exhibit deep bands of H<sub>2</sub>O, strong alkali lines of K I and Na I, band heads of FeH, and overtone bands of CO (see Fig. 2). Reid et al. (2001) were

**Table 2** MK-based LTY spectral standards

Subclass	Primary spectral standard	
	Red optical	Near-infrared
L0	2MASS J03454316+2540223	2MASS J03454316+2540233
L1	2MASS J14392836+1929149	2MASS J21304464-0845205
L2	Kelu-1	Kelu-1
L3	2MASS J11463449+2230527	2MASS J15065441+1321060
L4	2MASS J11550087+2307058	2MASS J21580457-1550098
L5	DENIS-P J1228.2-1547	2MASS J08350622+1953050
L6	2MASS J08503593+1057156	2MASS J10101480-0406499
L7	DENIS-P J0205.4-1159	2MASS J01033203+1935361
L8	2MASS J16322911+1904407	2MASS J16322911+1904407
L9	...	DENIS-P J025503.33-470049.0
T0	SDSSp J083717.22000018.3	SDSS J120747.17+024424.8
T1	...	SDSS J083717.21-000018.0
T2	SDSS J125453.90-012247.4	SDSS J125453.90-012247.4
T3	...	2MASS J12095613-1004008
T4	...	2MASS J22541892+2123498
T5	2MASS J15031961+2525196	2MASS J15031961+2525196
T6	SDSS J162414.37+002915.6	SDSS J162414.37+002915.6
T7	...	2MASS J07271824+1710012
T8	2MASS J04151954-0935066	2MASS J04151954-0935066
T9	WISE J174124.25+255319.6	UGPS J072227.51-054031.2
Y0	...	WISE J173835.53+273259.0
Y1	...	WISE J035000.32-565830.2

Spectral standards from [Kirkpatrick et al. \(1999b, 2010, 2012\)](#), [Burgasser et al. \(2003b, 2006b\)](#), and [Cushing et al. \(2011\)](#).

the first to show that the near-infrared spectra of L dwarfs formed a smooth spectral sequence when ordered by their [Kirkpatrick et al. \(1999b\)](#) *red optical* spectral types. Over the years, various spectral indices were devised to measure the depths of the various molecular bands and absorption lines (e.g., [Tokunaga and Kobayashi 1999](#); [Delfosse et al. 1999](#); [Burgasser et al. 2002a](#); [Gorlova et al. 2003](#); [McLean et al. 2003](#); [Allers et al. 2007](#)) but these indices are all tied to red optical subtypes.

The first truly near-infrared L-dwarf classification scheme was proposed by [Geballe et al. \(2002\)](#) and has subtypes ranging from L0 to L9. This system does not consist of a grid of spectral standards but rather is defined by the range of values of certain spectral indices and thus does not conform to the MK Process. For example, an unknown source would be classified as L0 if the value of its H<sub>2</sub>O 1.5 μm index fell between the values of 1.20 and 1.27. A final subtype is assigned by averaging the subtypes derived from the H<sub>2</sub>O 1.5 μm index and other spectral indices. This system is by far the most common near-infrared L-dwarf classification system in the literature.

Interestingly, an MK-based near-infrared scheme was devised only a few years ago and as a result, it is currently used infrequently. This system consists of ten near-infrared spectral standards ranging from L0 to L9 ([Kirkpatrick et al. 2010](#)). Table 2

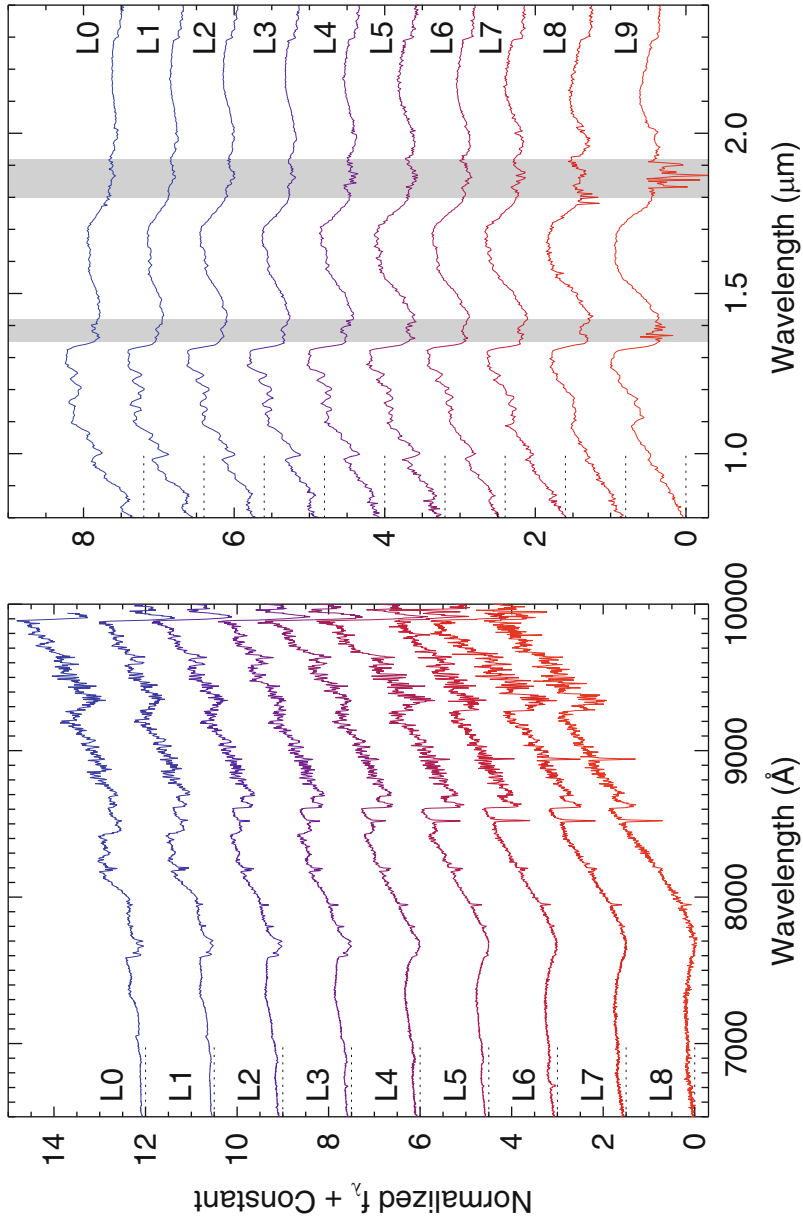


**Fig. 3** *Left:* Red optical spectral sequence (spectral resolution of  $\Delta\lambda = 9 \text{\AA}$ ) of the L dwarf spectral standards given in Table 2. The spectra are from Kirkpatrick et al. (1999b), normalized to unity at  $8,250 \text{\AA}$ , and offset with constants (dotted lines). *Right:* Near infrared spectral sequence ( $R \approx 150$ ) of the L dwarf near-infrared standards given in Table 2. The spectra are from Kirkpatrick et al. (2010), normalized to unity at  $1.27 \mu\text{m}$ , and are offset by constants (dotted lines). Wavelengths of high telluric absorption, and thus low signal-to-noise data, are denoted as grey bars. The identification of prominent atomic and molecular absorption features can be found in Fig. 2.

lists the L-dwarf near-infrared spectral standards and the right panel of Fig. 3 shows the spectral sequence. Classification of an unknown spectrum is accomplished by comparing the entire 0.9–1.4  $\mu\text{m}$  spectrum to the spectral standards and identifying the best match. In this way, this system is fully consistent with the precepts of the MK Process.

## 5 The T Dwarfs

As droves of L dwarfs were being discovered with 2MASS, DENIS, and eventually SDSS, brown dwarfs with near-infrared spectra qualitatively similar to that of Gliese 229B were also being discovered with 2MASS and SDSS. These objects eventually came to populate the T spectral class which is characterized by CH<sub>4</sub> absorption at near-infrared wavelengths. Since the bulk of the T dwarfs identified in the field were discovered using data from 2MASS or SDSS, it is perhaps not surprising that two different spectral classification systems again emerged (Burgasser et al. 2002a; Geballe et al. 2002).

Burgasser et al. (2002a) created a near-infrared MK-based system that was composed of seven spectral standards ranging from T1 to T8. However, like the Kirkpatrick et al. (1999b) L-dwarf system, the Burgasser et al. system broke from the MK Process because the subtype of an unknown T dwarf is determined by averaging the subtypes derived using H<sub>2</sub>O/CH<sub>4</sub> spectral indices and various flux ratios. Geballe et al. (2002) also developed an independent T-dwarf classification scheme that was an extension to their L-dwarf scheme described in Sect. 4 and as such, was not MK-based because it assigned subtypes based on the values of spectral ratios (see Sect. 4 for more details).

Subtypes derived using the two different systems agreed reasonably well, but the existence of two different T-dwarf classification schemes in the literature can lead to confusion. To remedy this situation, the 2MASS and SDSS teams published a unified near-infrared classification scheme for T dwarfs (Burgasser et al. 2006b). This system is MK-based and therefore consists of nine spectral standards spanning from T0 to T8. Table 2 lists the near-infrared T-dwarf spectral standards and the right panel of Fig. 4 shows the T-dwarf spectral sequence.<sup>6</sup> The T spectral sequence is marked by ever increasing H<sub>2</sub>O and CH<sub>4</sub> absorption until the spectrum of the T8/T9 dwarfs consists of narrow emission-like peaks centered at 1.05, 1.27, 1.6, and 2.2  $\mu\text{m}$ . The primary means of assigning a subtype to the spectrum of an unknown T dwarf is via direct comparison to the spectral standards and thus their system is in full accord with the MK Process. However, Burgasser et al. (2006b) also defined several spectral indices that could be used as secondary classifiers. This system is now the only scheme used in the literature for T dwarfs with spectral types between T0 and T8.

---

<sup>6</sup>For completeness, we have included the suggested T9 spectral standard UGPS J072227.51–054031.2 (Cushing et al. 2011) but defer discussion of its inclusion to Sect. 6.

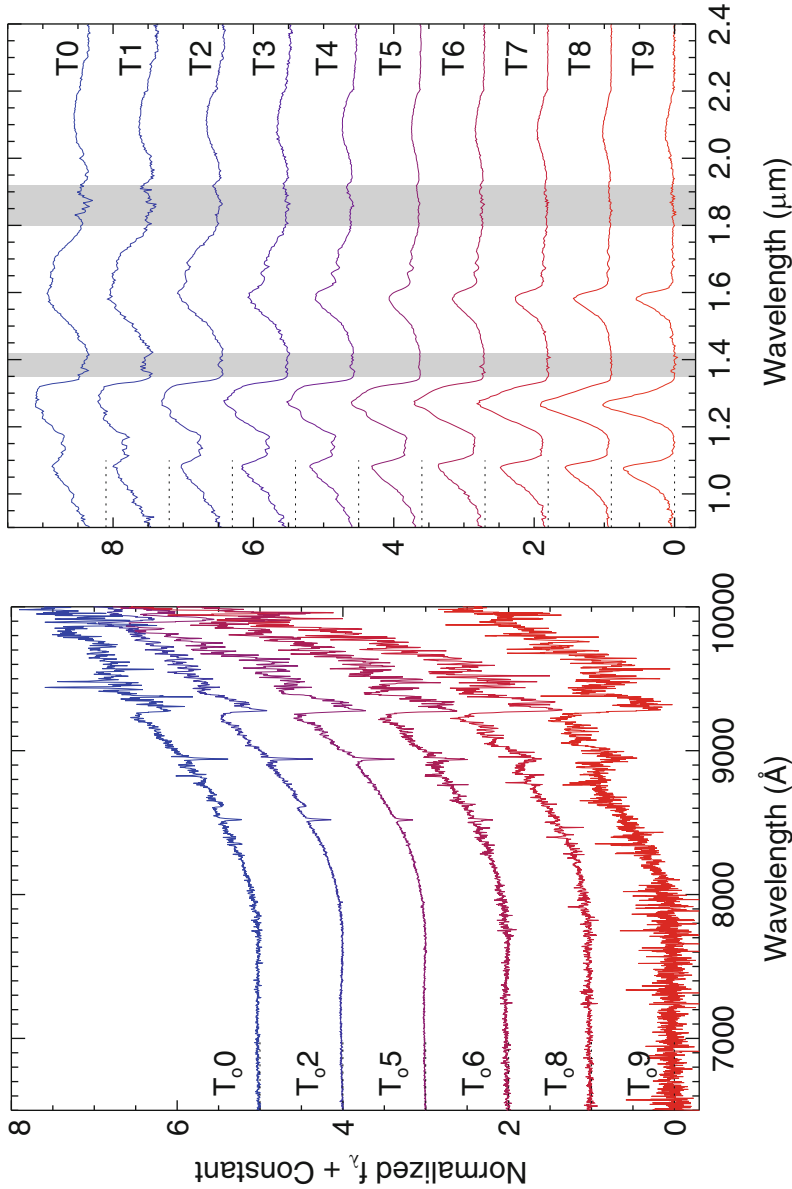


**Fig. 4** *Left:* Red optical spectral sequence ( $\Delta\lambda = 7 \text{ \AA}$ ) of the optical T dwarf spectral standards given in Table 2. The spectra are from Burgasser et al. (2003b) and Kirkpatrick et al. (2010, 2011), normalized to unity at  $9,000 \text{ \AA}$ , and offset by constants (dotted lines). *Right:* Near-infrared spectral sequence ( $R \approx 150$ ) of the T dwarf spectral standards given in Table 2. The spectra are from Burgasser et al. (2006b) and Cushing et al. (2011), normalized to unity at  $1.27 \mu\text{m}$ , and offset with constants (dotted lines). Wavelengths of high telluric absorption, and thus low signal-to-noise data, are denoted as grey bars. Prominent atomic and molecular absorption features can be identified using Fig. 2.

Although the near-infrared is the primary wavelength range over which T dwarfs are now classified, a red optical scheme was also created by [Burgasser et al. \(2003b\)](#). This system is MK-based, and consists of only four spectral standards at  $T_o2$ ,  $T_o5$ ,  $T_o6$ , and  $T_o8$  (where the subscript  $o$  is used to denote an *optical* spectral type). Of course the subtypes of the spectral standards could have easily been defined as T0, T1, T2, and T3, but were instead chosen to correspond to the near-infrared types for ease of use. This system serves to underscore the fact that it is the spectral standards that are the pillars of a classification system and that the labels are arbitrary. [Kirkpatrick et al. \(2012\)](#) recently proposed adding SDSSp J083717.22–000018.3 as the  $T_o0$  standard and WISE J174124.25+255319.6 as the  $T_o9$  standard. Table 2 lists the red optical T-dwarf spectral standards and the left panel of Fig. 4 shows the spectral sequence. This system is not often used given that large telescopes are required to obtain red optical data of T dwarfs.

## 6 The T/Y Boundary and the Y Dwarfs

In just a handful of years the 2MASS, DENIS, and SDSS surveys uncovered hundreds of low-mass stars and brown dwarfs that eventually came to populate the L and T spectral classes. The coolest T dwarfs discovered by these surveys have estimated effective temperatures of order 750 K (e.g., [Burgasser et al. 2006a](#); [Saumon et al. 2007](#)) which left a gap of roughly 600 K between these T8 dwarfs and Jupiter at 124 K ([Hanel et al. 1981](#)) which is a commonly used benchmark for the low-mass end of the brown dwarf regime. Two of the foremost questions were (1) what would brown dwarfs with  $T_{\text{eff}} < 700$  K look like spectroscopically and (2) would a new spectral class be required to classify them?

[Leggett et al. \(2007\)](#) and [Kirkpatrick \(2008\)](#) discuss the various spectral features that might trigger the need for a new spectral class from both an observational and theoretical perspective. Atmospheric models (e.g., [Burrows et al. 2003](#)) as well as the spectra of both Jupiter and Saturn indicate that ammonia ( $\text{NH}_3$ ) absorption bands emerge across the near-infrared as  $T_{\text{eff}}$  falls below 600 K.<sup>7</sup> However, using the  $K$ -band  $\text{NH}_3$  feature from 1.95–2.05  $\mu\text{m}$  is impractical observationally speaking as too little flux emerges from the atmosphere at these wavelengths due to the strong  $\text{H}_2\text{O}$ ,  $\text{CH}_4$ , and CIA  $\text{H}_2$  absorption. Thus, attention focused on the  $\text{NH}_3$  features centered at 1.03, 1.21, 1.31, and 1.52  $\mu\text{m}$ . Other predictions include the weakening and eventual loss of the red optical Na I and K I resonance lines as sodium and potassium condense out of the gas to form  $\text{Na}_2\text{S}$  and  $\text{KCl}$  condensates and an eventual turn towards the red in the  $J - K$  colors.

---

<sup>7</sup>[Saumon et al. \(2006\)](#) have shown the abundance of  $\text{NH}_3$  is reduced by roughly an order of magnitude due to vertical mixing in the atmospheres of brown dwarfs which results in weaker  $\text{NH}_3$  absorption bands. Nevertheless, models that include the impact of this so-called non-equilibrium chemistry still predict the emergence of  $\text{NH}_3$  in the near-infrared, albeit at a slightly lower temperature.

The search for these cool field brown dwarfs continued unabated with the commencement of the UKIRT Infrared Deep Sky Survey (UKIDSS; [Lawrence et al. 2007](#)) and the Canada-France Brown Dwarf Survey (CFBDS; [Delorme et al. 2008b](#)). UKIDSS is a multi-component infrared survey of the northern sky in the  $Z$  ( $0.88\text{ }\mu\text{m}$ ),  $Y$  ( $1.03\text{ }\mu\text{m}$ ),  $J$ ,  $H$ , and  $K$  bands. The most important component from a brown dwarf perspective is the Large Area Survey which covers  $4,028\text{ deg}^2$  to a  $K$ -band depth significantly deeper than 2MASS (18.2 mag versus 14.3 mag).<sup>8</sup> The Canada-France Brown Dwarf Survey will eventually survey  $780\text{ deg}^2$  of the sky in the red optical at  $i'$  and  $z'$ . [Delorme et al. \(2010\)](#) also recently began the Canada-France Brown Dwarfs Survey-InfraRed (CFBDSIR) that will image  $335\text{ deg}^2$  of the CFBDS survey footprint in the  $J$  band.

Ten brown dwarfs with spectral types later than T8 have been identified in UKIDSS and CFBDS ([Warren et al. 2007](#); [Burningham et al. 2008, 2009, 2010, 2011](#); [Delorme et al. 2008a](#); [Lucas et al. 2010](#); [Liu et al. 2011](#)). [Burningham et al. \(2008\)](#) designated ULAS J133553.45+113005.2 as the tentative T9 spectral standard based on the correlation of the  $W_J$  index, which measures the width of the  $J$ -band peak at  $1.27\text{ }\mu\text{m}$  ([Warren et al. 2007](#)), with subtype. [Lucas et al. \(2010\)](#) proposed that UGPS J072227.51–054031.2 (hereafter UGPS 0722–05) be designated the T10 spectral standard. The first hint of  $\text{NH}_3$  absorption at near-infrared wavelengths came from [Delorme et al. \(2008a\)](#) who found evidence for the  $1.52\text{ }\mu\text{m}$   $\text{NH}_3$  band based on their  $\text{NH}_3$ - $H$  spectral index that measures absorption strength on the blue wing of the  $H$ -band peak. However, no evidence of this absorption was found by [Burningham et al. \(2010\)](#) in the spectra of late-type T dwarfs with similar spectral types.

These >T8 dwarfs have effective temperature estimates of  $500$ – $600\text{ K}$  (e.g., [Leggett et al. 2009](#)), which is not significantly cooler than some late-type T dwarfs identified with 2MASS, e.g. 2MASS 09393548–2448279 ([Burgasser et al. 2008](#)). However, the discovery of two brown dwarfs, WD 0806–661B and CFBDSIR J145829+101343B, with estimated effective temperatures of only  $300$ – $400\text{ K}$  left little doubt that cooler brown dwarfs existed. WD 0806–661B was discovered by [Luhman et al. \(2011\)](#) with the *Spitzer Space Telescope* as a wide ( $2,500\text{ AU}$ ) proper motion companion to the white dwarf WD 0806–661 ( $d = 19.2\text{ pc}$ ). It remains undetected in the near-infrared to a limit of 23.9 mag in the  $J$  band ([Luhman et al. 2012](#)), but its brightness in the mid-infrared at  $3.6$  and  $4.5\text{ }\mu\text{m}$  suggests an effective temperature of  $300$ – $345\text{ K}$ . CFBDSIR J145829+101343B was discovered as a tight ( $2.6\text{ AU}$ ) proper motion companion to a  $\sim\text{T9.5}$  brown dwarf CFBDSIR J145829+101343A ([Liu et al. 2011](#)). An effective temperature estimate of  $370 \pm 40\text{ K}$  is slightly higher than that of WD 0806–661B but still qualifies it as one of the coolest brown dwarfs known. Unfortunately, attempts at obtaining spectra of both brown dwarfs have been hampered by their extreme faintness, and in the case of CFBDSIR J145829+101343B, proximity to its primary.

---

<sup>8</sup>The UKIDSS Galactic Plane Survey covered  $1,868\text{ deg}^2$  to a depth of  $K \sim 18.8$  but to date, only a single T dwarf, UGPS J072227.51–054031.2, has been identified using these data ([Lucas et al. 2010](#)).

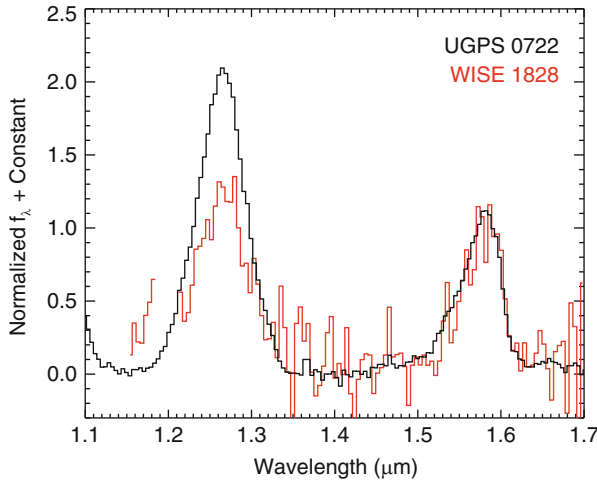


**Fig. 5** *J*- and *H*-band spectra of UGPS 0722–05 and WISE 1828+2650 (Cushing et al. 2011). Spectra are normalized to unity at 1.59  $\mu\text{m}$ . The ratio of the peak fluxes at 1.27 and 1.58  $\mu\text{m}$  in the spectrum of WISE 1828+2650 is near unity which is distinct from the population of known T dwarfs

The discovery of WD 0806–661B and CFBDSIR J145829+101343B confirmed that cooler field brown dwarfs existed but it took the launch of the *Wide-field Infrared Survey Explorer* (WISE, Wright et al. 2010) before a comparatively cool solivagant field object bright enough for follow-up spectroscopy was identified. WISE is an Earth-orbiting NASA mission that surveyed the entire sky at wavelengths of 3.4, 4.6, 12, and 22  $\mu\text{m}$  (hereafter *W1*, *W2*, *W3*, and *W4*). The *W1* and *W2* bands were designed specifically to sample the deep CH<sub>4</sub> absorption band centered at 3.3  $\mu\text{m}$  and the region relatively free of opacity centered at 4.6  $\mu\text{m}$  in the spectra of cold brown dwarfs. Since the peak of the Planck function at these low temperatures is in the mid-infrared, a large amount of flux emerges at 4.6  $\mu\text{m}$ , making the *W1* – *W2* color extremely red.

Just as GD 165B was the prototype L dwarf and Gliese 229B was the prototype T dwarf, WISE J182831.08+265037.7 (hereafter WISE 1828+2650) became the prototype Y dwarf. Its discovery image is shown in Fig. 1. Figure 5 shows the *J*- and *H*-band spectrum of WISE 1828+2650 obtained with the Wide Field Camera 3 (WFC3; Kimble et al. 2008) on-board the *Hubble Space Telescope* (*HST*) and UGPS 0722–05. The peak flux in the *J* band is roughly the same height as the peak flux in the *H* band in units of  $f_\lambda$  making the spectrum of WISE 1828+2650 unique.<sup>9</sup> For this reason, Cushing et al. (2011) identified it as the archetype Y dwarf.

---

<sup>9</sup>The spectrum of WISE 1828+2650 is contaminated by light from a nearby star because WFC3 is a slitless spectrograph. The contamination becomes progressively worse at shorter wavelengths so the ratio between the peak fluxes in the *J* and *H* bands is actually more extreme than near unity.

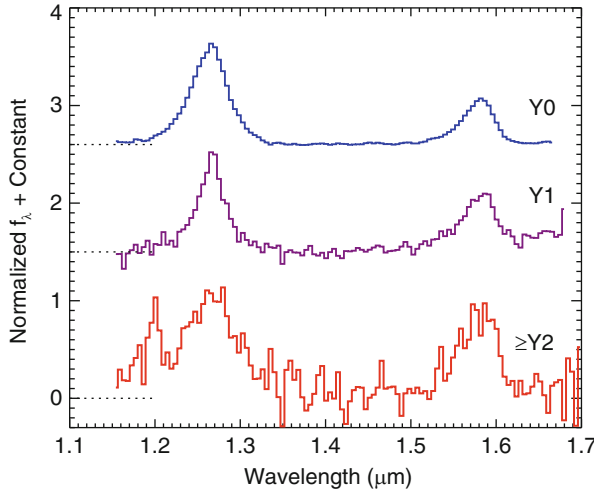


**Fig. 6**  $J$ - and  $H$ -band spectral sequence ( $R \approx 130$ ) of the tentative Y0 and Y1 spectral standards (Cushing et al. 2011; Kirkpatrick et al. 2012), and the  $\geq Y2$  dwarf WISE J1828+2650 (Cushing et al. 2011). Spectra are normalized to unity and offset with constants (dotted lines). Note that the ratio of the peak fluxes at 1.27 and 1.58  $\mu\text{m}$  approaches unity with later subtype

With a prototype Y dwarf in hand, Cushing et al. (2011) attempted to identify the T/Y boundary. The T spectral sequence had already been extended to T10 based on the extrapolation of certain spectral ratios beyond T8 (Burningham et al. 2008; Lucas et al. 2010). In addition to WISE 1828+2650, Cushing et al. (2011) also identified six additional brown dwarfs whose spectra appeared later than UGPS 0722–05 based on the width of the  $J$ -band peak. Using the MK Process (in particular precept #2, cf. Sect. 3), UGPS 0722–05 was selected as the T9 spectral standard based on its near-infrared spectrum. WISE J173835.53+273259.0 (hereafter WISE 1738+2732) was then chosen as the tentative Y0 spectral standard because it exhibited absorption (both visually and by the  $\text{NH}_3$ - $H$  index of Delorme et al. 2008a) on the blue wing of the  $H$ -band peak that was tentatively ascribed to  $\text{NH}_3$ . Bochanski et al. (2011) and Saumon et al. (2012) have identified weak  $\text{NH}_3$  features in higher resolution ( $R \approx 6,000$ ) spectra of UGPS 0722–05 over this wavelength range suggesting the correct carrier of the absorption has indeed been identified. Kirkpatrick et al. (2012) extended the Y sequence by identifying WISE J035000.32–565830.2 as the tentative Y1 spectral standard. They also noted that the peak flux in the  $H$  band relative to the peak flux in the  $J$  band is higher than in WISE 1738+2732 presaging the equal flux heights in WISE 1828+2650 which is currently classified as  $\geq Y2$ .

Table 2 lists the two tentative Y-dwarf spectral standards and Fig. 6 shows the current Y spectral sequence. Y dwarfs are currently classified over the 1.1–1.7  $\mu\text{m}$  wavelength range due to the difficulty of obtaining spectra at other wavelengths (see also Sect. 8). The sequence is marked both by a narrowing of the  $J$ -band peak,

but also a slow drift in the  $J/H$ -peak flux ratio towards unity. There are currently only 14 published Y dwarfs (Cushing et al. 2011; Kirkpatrick et al. 2012; Tinney et al. 2012) but continued mining of the *WISE* survey will no doubt uncover more.

## 7 The Underlying Physics

Effective temperature is the primary parameter that controls almost the entire spectral sequence. In the hotter OBAFGK dwarf stars, it is the variations in atomic line strengths with decreasing temperature (via the Saha Boltzmann equation) that drive variations in the spectral morphology and thus spectral type. However, in the cooler MLTY dwarfs, it is variations in both molecular and condensate (i.e. grain) chemistry with decreasing effective temperature that drive the spectral morphological changes. Indeed the M/L and L/T (and possibly the T/Y) transitions are controlled in part by the formation and subsequent evolution of condensates (see chapter by I. Baraffe).

At atmospheric temperatures of less than 2,400 K, condensates form from the refractory elements (Ti, V, Ca, Al, Fe, Si) which in turn gravitationally settle in the atmosphere to form clouds. With decreasing effective temperature, more and more species condense out until the atmosphere consists of layer upon layer of clouds. The formation of these clouds has two major consequences for the atmosphere. First, the chemistry in the atmospheric layers above the cloud decks is forever altered because the atoms and molecules that make up the condensates are no longer available to participate in chemical reactions. Second, the condensates add opacity to the atmosphere which can, in some cases, dramatically alter the emergent spectrum of the object. Indeed as first suggested by Jones and Tsuji (1997), the weakening of the TiO and VO bands at the M/L transition is a result of the formation of condensates like perovskite ( $\text{CaTiO}_3$ ) and other Ti-bearing species (e.g.,  $\text{Ca}_4\text{Ti}_3\text{O}_{10}$ ,  $\text{Ca}_3\text{Ti}_2\text{O}_7$ ,  $\text{Ti}_2\text{O}_3$ ) as well as solid solution VO and  $\text{VO}_2$  (Lodders 1999; Burrows and Sharp 1999; Allard et al. 2001).<sup>10</sup> Silicate and liquid iron condensates form at slightly cooler temperatures and make the near-infrared colors of cloudy L dwarfs much redder than equivalent-mass objects with clear atmospheres.

Figure 7 shows the effective temperature as a function of spectral type for a sample of L, T, and Y dwarfs. The L-dwarf spectral types are based on the red optical system of Kirkpatrick et al. (1999b) and the T- and Y-dwarf spectral types are based on the near-infrared systems of Burgasser et al. (2006b), Cushing et al. (2011),

---

<sup>10</sup>The reason there are no giant stars classified as ‘L’ in the red optical is because they never get cool enough for the Ti- and VO-bearing condensates to form. Although the luminosity class V were included with L- and T-dwarf spectral types in the early literature, it has since been dropped because there is no chance for confusion. Evans et al. (2003) have, however, classified the peculiar variable V838 Mon as a possible L supergiant given the depths of the near-infrared  $\text{H}_2\text{O}$  bands.

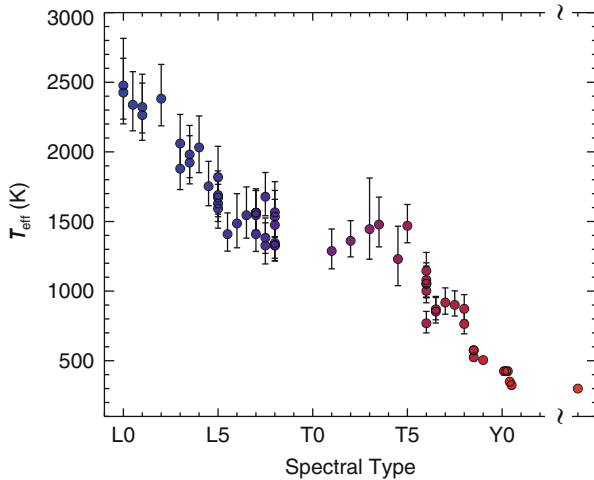


**Fig. 7** Effective temperature as a function of spectral type. L-dwarf spectral types are based on red optical spectra and T- and Y-dwarf spectral types are based on near-infrared spectra. A gap is left between L8 and T0 because there is no L9 subtype in the optical sequence. Temperatures for the L dwarfs and T dwarfs with spectral types earlier than T9 are from [Vrba et al. \(2004\)](#). However, only dwarfs with trigonometric parallax errors less than 30 % of the parallax value are plotted. Temperatures for the T dwarfs with spectral types later than T8 are from [Leggett et al. \(2009, 2012\)](#) while the temperatures for the Y dwarfs are from [Leggett et al. \(2013\)](#). WISE J1828+2650 is currently typed as a  $\geq$ Y2 and so is plotted as a solitary object beyond a spectral type of Y2

and [Kirkpatrick et al. \(2012\)](#). The effective temperatures of stars are often estimated by fitting model atmospheres to observed spectra and the same is certainly true for brown dwarfs (e.g. [Stephens et al. 2009; Testi 2009; Witte et al. 2011](#)). However, a reasonably model-independent estimate of brown dwarf effective temperatures can be obtained by exploiting the fact that the radii of brown dwarfs are nearly independent of both mass and age. Due to their partially electron-degenerate cores (e.g., [Kumar 1963](#)), the mass-radius relation is effectively flat at  $\sim 1 R_{\text{Jup}}$  across two orders of magnitude in mass from 0.1 to  $0.001 M_{\odot}$  (see figure 1 of [Burrows and Liebert 1993](#)). The effective temperatures of the L and T dwarfs shown in Fig. 7 are from the [Vrba et al. \(2004\)](#) and were estimated by measuring their bolometric luminosities and then using the Stefan Boltzmann law ( $L_{\text{bol}} = 4\pi R^2 \sigma T_{\text{eff}}^4$ ) to compute their effective temperatures assuming a fixed radius of  $0.90 \pm 0.15 R_{\text{Jup}}$ . With decreasing effective temperature, it becomes more and more difficult to measure a model independent bolometric luminosity because wavelengths that are easily accessible from the ground contain a smaller and smaller fraction of the total emergent flux. For example, at  $T_{\text{eff}} = 300$  K, only 10 % of the emergent luminosity emerges at  $\lambda < 2.5 \mu\text{m}$  (M. Marley, private communication). Therefore, the effective temperature estimates of the brown dwarfs with spectral types later than T8 in Fig. 7 are based on atmospheric model fits to their near-infrared spectra ([Leggett et al. 2013](#)).

Effective temperature correlates reasonably well with spectral type through the entire LTY sequence, except at the L/T transition where the effective temperature is roughly constant from a spectral type of L8 to T5 (see also [Burgasser et al. 2002a](#); [Golimowski et al. 2004](#); [Testi 2009](#)). This indicates that changes in a parameter (or parameters) other than effective temperature is driving the evolution in the spectral morphology over these spectral types. It is generally accepted that this change is due to rapid loss of the silicate and iron condensate opacity due to some unknown mechanism. Possible candidates include the break up of the condensates clouds ([Ackerman and Marley 2001](#); [Burgasser et al. 2002b](#)) or a sudden downpour of the condensates ([Knapp et al. 2004](#)).

The changes in spectral morphology at the L/T transition also provide a cautionary tale against violating precept #3 of the MK process, i.e. using models to guide the selection of subtypes. Any classification system that attempted to force the subtypes at the L/T transition to have a uniform gradient in effective temperature would create both a dramatic and jarring evolution of the spectral morphology over just a few subtypes.

At spectral types later than roughly T5, effective temperature decreases down to the T/Y boundary. WISE 1828+2650 is plotted as a solitary object beyond a spectral type of Y2 because its exact subtype is currently unknown. Although there is clearly a paucity of objects between the Y0s and WISE 1828+2650 which makes drawing any firm conclusions dangerous, it is nevertheless tempting to suggest that a second temperature plateau may exist at the T/Y boundary. [Morley et al. \(2012\)](#) have shown that the inclusion of additional condensates (Na<sub>2</sub>S, KCl, ZnS, MnS, and Cr) significantly improves the agreement between the model spectra and the observations of late-type T dwarfs and Y dwarfs. This suggests that condensates, in particular Na<sub>2</sub>S, play an important role in shaping the emergent spectra of the late-type T and Y dwarfs. Perhaps the loss of these condensates in a fashion similar to the L/T transition is responsible for the tentative plateau seen in  $T_{\text{eff}}$  at the T/Y transition.

## 8 Outstanding Issues

In just under 20 years, a smooth spectral sequence extending from the edge of the hydrogen-burning main sequence down to brown dwarfs with effective temperatures of roughly 300 K has emerged. However, much work remains before the LTY classification systems become as refined as the MK System for the OBAFGKM stars. Below I discuss just two outstanding issues related to the spectral classification of the L, T, and Y dwarfs.

### Issue #1

As noted in Sect. 7, effective temperature is the primary parameter that controls the spectral morphology of the L, T, and Y dwarfs. Completely absent from that discussion is the impact that variations in surface gravity  $g$  and metallicity

[Fe/H] can have on the emergent spectra and thus spectral type. For the hotter OBAFGKM stars, variations in surface gravity manifest themselves in a variety of ways (e.g. a change in the width of atomic lines) and are encapsulated in the luminosity class (see Sect. 3). Brown dwarfs with spectral “peculiarities” indicative of unusual surface gravities and/or metallicities have been known for some time, e.g. 2MASS J01415823–4633574 a low surface-gravity L dwarf (Kirkpatrick et al. 2006) and 2MASS J05325346+8246465 a metal-poor L dwarf (Burgasser et al. 2003a) but all of the current classification systems are unable to account for these variations because the systems are still one dimensional (e.g., Kirkpatrick 2005).

Cruz et al. (2009) presented the first L-dwarf spectral classification system that uses both temperature and surface gravity sensitive features as criteria for assigning subtypes. The system expands on the Kirkpatrick et al. (1999b) scheme to include three gravity classes labeled  $\alpha$ ,  $\beta$ , and  $\gamma$ . The  $\gamma$  class has a lower surface gravity than the  $\beta$  class which in turn has a lower surface gravity than the  $\alpha$  class. However, this system is currently not MK-based because rather than assign spectral standards for each  $T_{\text{eff}}/g$  bin, it uses surface gravity sensitive spectral indices to assign a gravity class. Nevertheless, this scheme is an important proof-of-concept that shows that it is possible to expand the current LTY classification systems to include the effects of gravity and hopefully in the future, metallicity.

## Issue #2

The tentative Y-dwarf classification scheme proposed by Cushing et al. (2011) and Kirkpatrick et al. (2012) is based in the near-infrared, and in particular focuses on the width of the  $J$ -band peak at  $1.27 \mu\text{m}$  and the blue wing of the  $H$ -band peak at  $1.6 \mu\text{m}$ . There are, of course, other wavelengths that can be used for classification. As noted by Leggett et al. (2007), there is an additional  $\text{NH}_3$  absorption feature centered at  $1.02 \mu\text{m}$  that would manifest itself as a “divot” in the  $Y$ -band peak. This feature would be much easier to identify than the  $H$ -band absorption feature currently used but to date few high S/N  $Y$ -band spectra of the Y dwarfs have been obtained.

The near-infrared is currently the easiest wavelength range over which to obtain a spectrum of a Y dwarf, but as noted above, it contains only a small fraction of the total bolometric luminosity emitted. Given that Y dwarfs emit most of their radiation in the mid infrared ( $3\text{--}20 \mu\text{m}$ ), it seems reasonable to devise a scheme at these wavelengths. Indeed historically as cooler and cooler objects were discovered, the wavelength range used for spectral classification has moved redward from the visible for the hotter stars, to the red optical for the M and L dwarfs, and then to the near-infrared for the T dwarfs. In addition, Cushing et al. (2006) have already shown that T-dwarf spectra over the  $5.5\text{--}14.5 \mu\text{m}$  wavelength range exhibit smooth variations in the strengths of  $\text{H}_2\text{O}$ ,  $\text{CH}_4$ , and  $\text{NH}_3$  absorption bands suggesting that a Y dwarf scheme based at these wavelengths is entirely plausible. However, as of the writing of this chapter, there is no ground- or spaced-based facility capable of obtaining

mid-infrared spectroscopy of the late-type T and Y dwarfs. The NIRSpec and MIRI instruments on board the *James Web Space Telescope* will be capable of obtaining low- to moderate-resolution spectra over the entire 0.6–29  $\mu\text{m}$  wavelength range and will therefore revolutionize the study of the Y dwarfs.

**Acknowledgements** I would like to thank Morag Hastie and J. Davy Kirkpatrick for providing useful comments on early versions of the manuscript and J. Davy Kirkpatrick and Adam Burgasser for ensuring the accuracy of the early history of the L and T dwarfs. The spectra shown in Figs. 2–4 were kindly provided by J. Davy Kirkpatrick, Adam Burgasser, and Sandy Leggett. This paper has benefitted from the SpeX Prism Spectral Libraries, maintained by Adam Burgasser at <http://pono.ucsd.edu/~adam/brownndwarfs/speXprism>, and has made use of the NASA/ IPAC Infrared Science Archive, which is operated by the Jet Propulsion Laboratory, California Institute of Technology, under contract with the National Aeronautics and Space Administration. Finally I also would like to thank Viki Joergens for organizing the thoroughly enjoyable conference *50 Years of Brown Dwarfs: from Theoretical Prediction to Astrophysical Studies* held at Ringberg Castle, Bavaria, Germany in October 2012.

## References

- Ackerman, A.S., Marley, M.S.: Precipitating condensation clouds in substellar atmospheres. *ApJ* **556**, 872–884 (2001)
- Adams, W.S., Joy, A.H., Humason, M.L.: The absolute magnitudes and parallaxes of 410 stars of type M. *ApJ* **64**, 225–242 (1926)
- Allard, F., Hauschildt, P.H., Alexander, D.R., Starrfield, S.: Model atmospheres of very low mass stars and brown dwarfs. *ARA&A* **35**, 137–177 (1997)
- Allard, F., Hauschildt, P.H., Alexander, D.R., Tamanai, A., Schweitzer, A.: The limiting effects of dust in brown dwarf model atmospheres. *ApJ* **556**, 357–372 (2001)
- Allers, K.N., Jaffe, D.T., Luhman, K.L., Liu, M.C., Wilson, J.C., Skrutskie, M.F., Nelson, M., Peterson, D.E., Smith, J.D., Cushing, M.C.: Characterizing young brown dwarfs using low-resolution near-infrared spectra. *ApJ* **657**, 511–520 (2007)
- Basri, G.: Observations of brown dwarfs. *ARA&A* **38**, 485–519 (2000)
- Basri, G., Mohanty, S., Allard, F., Hauschildt, P.H., Delfosse, X., Martín, E.L., Forveille, T., Goldman, B.: An effective temperature scale for late-M and L dwarfs, from resonance absorption lines of Cs I and Rb I. *ApJ* **538**, 363–385 (2000)
- Becklin, E.E., Zuckerman, B.: A low-temperature companion to a white dwarf star. *Nature* **336**, 656–658 (1988)
- Bessell, M.S.: The late-M dwarfs. *AJ* **101**, 662–676 (1991)
- Bochanski, J.J., Burgasser, A.J., Simcoe, R.A., West, A.A.: FIRE spectroscopy of the ultra-cool brown dwarf, UGPS J072227.51-054031.2: kinematics, rotation and atmospheric parameters. *AJ* **142**, 169 (2011)
- Boeshaar, P.C.: The spectral classification of M-dwarf stars. PhD thesis, Ohio State University, Columbus (1976)
- Boeshaar, P.C., Tyson, J.A.: New limits on the surface density of M dwarfs. I – photographic survey and preliminary CCD data. *AJ* **90**, 817–822 (1985)
- Burgasser, A.J., Kirkpatrick, J.D., Brown, M.E., Reid, I.N., Burrows, A., Liebert, J., Matthews, K., Gizis, J.E., Dahn, C.C., Monet, D.G., Cutri, R.M., Skrutskie, M.F.: The spectra of T dwarfs. I. Near-infrared data and spectral classification. *ApJ* **564**, 421–451 (2002a)
- Burgasser, A.J., Marley, M.S., Ackerman, A.S., Saumon, D., Lodders, K., Dahn, C.C., Harris, H.C., Kirkpatrick, J.D.: Evidence of cloud disruption in the L/T dwarf transition. *ApJ* **571**, L151–L154 (2002b)

- Burgasser, A.J., Kirkpatrick, J.D., Burrows, A., Liebert, J., Reid, I.N., Gizis, J.E., McGovern, M.R., Prato, L., McLean, I.S.: The first substellar subdwarf? Discovery of a metal-poor L dwarf with halo kinematics. *ApJ* **592**, 1186–1192 (2003a)
- Burgasser, A.J., Kirkpatrick, J.D., Liebert, J., Burrows, A.: The spectra of T dwarfs. II. Red optical data. *ApJ* **594**, 510–524 (2003b)
- Burgasser, A.J., Burrows, A., Kirkpatrick, J.D.: A method for determining the physical properties of the coldest known brown dwarfs. *ApJ* **639**, 1095–1113 (2006a)
- Burgasser, A.J., Geballe, T.R., Leggett, S.K., Kirkpatrick, J.D., Golimowski, D.A.: A unified near-infrared spectral classification scheme for T dwarfs. *ApJ* **637**, 1067–1093 (2006b)
- Burgasser, A.J., Tinney, C.G., Cushing, M.C., Saumon, D., Marley, M.S., Bennett, C.S., Kirkpatrick, J.D.: 2MASS J09393548-2448279: the coldest and least luminous brown dwarf binary known? *ApJ* **689**, L53–L56 (2008)
- Burningham, B., Pinfield, D.J., Leggett, S.K., Tamura, M., Lucas, P.W., Homeier, D., Day-Jones, A., Jones, H.R.A., Clarke, J.R.A., Ishii, M., Kuzuhara, M., Lodieu, N., Zapatero Osorio, M.R., Venemans, B.P., Mortlock, D.J., Barrado y Navascués, D., Martín, E.L., Magazzù, A.: Exploring the substellar temperature regime down to  $\sim$ 550K. *MNRAS* **391**, 320–333 (2008)
- Burningham, B., Pinfield, D.J., Leggett, S.K., Tinney, C.G., Liu, M.C., Homeier, D., West, A.A., Day-Jones, A., Huelamo, N., Dupuy, T.J., Zhang, Z., Murray, D.N., Lodieu, N., Barrado y Navascués, D., Folkes, S., Galvez-Ortiz, M.C., Jones, H.R.A., Lucas, P.W., Calderon, M.M., Tamura, M.: The discovery of an M4+T8.5 binary system. *MNRAS* **395**, 1237–1248 (2009)
- Burningham, B., Pinfield, D.J., Lucas, P.W., Leggett, S.K., Deacon, N.R., Tamura, M., Tinney, C.G., Lodieu, N., Zhang, Z.H., Huelamo, N., Jones, H.R.A., Murray, D.N., Mortlock, D.J., Patel, M., Barrado y Navascués, D., Zapatero Osorio, M.R., Ishii, M., Kuzuhara, M., Smart, R.L.: 47 new T dwarfs from the UKIDSS large area survey. *MNRAS* **406**, 1885–1906 (2010)
- Burningham, B., Lucas, P.W., Leggett, S.K., Smart, R., Baker, D., Pinfield, D.J., Tinney, C.G., Homeier, D., Allard, F., Zhang, Z.H., Gomes, J., Day-Jones, A.C., Jones, H.R.A., Kovács, G., Lodieu, N., Marocco, F., Murray, D.N., Sipőcz, B.: The discovery of the T8.5 dwarf UGPS J0521+3640. *MNRAS* **414**, L90–L94 (2011)
- Burrows, A., Liebert, J.: The science of brown dwarfs. *Rev. Mod. Phys.* **65**, 301–336 (1993)
- Burrows, A., Sharp, C.M.: Chemical equilibrium abundances in brown dwarf and extrasolar giant planet atmospheres. *ApJ* **512**, 843–863 (1999)
- Burrows, A., Hubbard, W.B., Lunine, J.I., Liebert, J.: The theory of brown dwarfs and extrasolar giant planets. *Rev. Mod. Phys.* **73**, 719–765 (2001)
- Burrows, A., Sudarsky, D., Lunine, J.I.: Beyond the T dwarfs: theoretical spectra, colors, and detectability of the coolest brown dwarfs. *ApJ* **596**, 587–596 (2003)
- Cannon, A.J., Pickering, E.C.: Spectra of bright southern stars photographed with the 13-inch Boyden telescope as part of the Henry Draper Memorial. *Ann. Harv. Coll. Obs.* **28**, 129 (1901)
- Chabrier, G., Baraffe, I.: Theory of low-mass stars and substellar objects. *ARA&A* **38**, 337–377 (2000)
- Cruz, K.L., Kirkpatrick, J.D., Burgasser, A.J.: Young L dwarfs identified in the field: a preliminary low-gravity, optical spectral sequence from L0 to L5. *AJ* **137**, 3345–3357 (2009) [0812.0364](#)
- Cushing, M.C., Rayner, J.T., Vacca, W.D.: An infrared spectroscopic sequence of M, L, and T dwarfs. *ApJ* **623**, 1115–1140 (2005)
- Cushing, M.C., Roellig, T.L., Marley, M.S., Saumon, D., Leggett, S.K., Kirkpatrick, J.D., Wilson, J.C., Sloan, G.C., Mainzer, A.K., Van Cleve, J.E., Houck, J.R.: A spitzer infrared spectrograph spectral sequence of M, L, and T dwarfs. *ApJ* **648**, 614–628 (2006)
- Cushing, M.C., Marley, M.S., Saumon, D., Kelly, B.C., Vacca, W.D., Rayner, J.T., Freedman, R.S., Lodders, K., Roellig, T.L.: Atmospheric parameters of field L and T dwarfs. *ApJ* **678**, 1372–1395 (2008)
- Cushing, M.C., Kirkpatrick, J.D., Gelino, C.R., Griffith, R.L., Skrutskie, M.F., Mainzer, A., Marsh, K.A., Beichman, C.A., Burgasser, A.J., Prato, L.A., Simcoe, R.A., Marley, M.S., Saumon, D., Freedman, R.S., Eisenhardt, P.R., Wright, E.L.: The discovery of Y dwarfs using data from the Wide-field Infrared Survey Explorer (WISE). *ApJ* **743**, 50 (2011)

- Delfosse, X., Tinney, C.G., Forveille, T., Epchtein, N., Borsenberger, J., Fouqué, P., Kimeswenger, S., Tiphène, D.: Searching for very low-mass stars and brown dwarfs with DENIS. *A&AS* **135**, 41–56 (1999)
- Delorme, P., Delfosse, X., Albert, L., Artigau, E., Forveille, T., Reylé, C., Allard, F., Homeier, D., Robin, A.C., Willott, C.J., Liu, M.C., Dupuy, T.J.: CFBDS J005910.90-011401.3: reaching the T-Y brown dwarf transition? *A&A* **482**, 961–971 (2008a)
- Delorme, P., Willott, C.J., Forveille, T., Delfosse, X., Reylé, C., Bertin, E., Albert, L., Artigau, E., Robin, A.C., Allard, F., Doyon, R., Hill, G.J.: Finding ultracool brown dwarfs with MegaCam on CFHT: method and first results. *A&A* **484**, 469–478 (2008b)
- Delorme, P., Albert, L., Forveille, T., Artigau, E., Delfosse, X., Reylé, C., Willott, C.J., Bertin, E., Wilkins, S.M., Allard, F., Arzoumanian, D.: Extending the Canada-France brown dwarfs survey to the near-infrared: first ultracool brown dwarfs from CFBDSIR. *A&A* **518**, A39 (2010)
- Epchtein, N., de Batz, B., Capoani, L., Chevallier, L., Copet, E., Fouqué, P., Lacombe, P., Le Bertre, T., Pau, S., Rouan, D., Ruphy, S., Simon, G., Tiphène, D., Burton, W.B., Bertin, E., Deul, E., Habing, H., Borsenberger, J., Dennefeld, M., Guglielmo, F., Loup, C., Mamon, G., Ng, Y., Omont, A., Provost, L., Renault, J., Tanguy, F., Kimeswenger, S., Kienel, C., Garzon, F., Persi, P., Ferrari-Toniolo, M., Robin, A., Paturel, G., Vauglin, I., Forveille, T., Delfosse, X., Hron, J., Schultheis, M., Appenzeller, I., Wagner, S., Balazs, L., Holl, A., Lépine, J., Boscolo, P., Picazzio, E., Duc, P., Mennessier, M.: The deep near-infrared southern sky survey (DENIS). *The Messenger* **87**, 27–34 (1997)
- Evans, A., Geballe, T.R., Rushton, M.T., Smalley, B., van Loon, J.T., Eyres, S.P.S., Tyne, V.H.: V838 Mon: an L supergiant? *MNRAS* **343**, 1054–1056 (2003)
- Geballe, T.R., Kulkarni, S.R., Woodward, C.E., Sloan, G.C.: The near-infrared spectrum of the brown dwarf Gliese 229B. *ApJ* **467**, L101 (1996)
- Geballe, T.R., Knapp, G.R., Leggett, S.K., Fan, X., Golimowski, D.A., Anderson, S., Brinkmann, J., Csabai, I., Gunn, J.E., Hawley, S.L., Hennessy, G., Henry, T.J., Hill, G.J., Hindsley, R.B., Ivezić, Ž., Lupton, R.H., McDaniel, A., Munn, J.A., Narayanan, V.K., Peng, E., Pier, J.R., Rockosi, C.M., Schneider, D.P., Smith, J.A., Strauss, M.A., Tsvetanov, Z.I., Uomoto, A., York, D.G., Zheng, W.: Toward spectral classification of L and T dwarfs: infrared and optical spectroscopy and analysis. *ApJ* **564**, 466–481 (2002)
- Golimowski, D.A., Leggett, S.K., Marley, M.S., Fan, X., Geballe, T.R., Knapp, G.R., Vrba, F.J., Henden, A.A., Luginbuhl, C.B., Guetter, H.H., Munn, J.A., Canzian, B., Zheng, W., Tsvetanov, Z.I., Chiu, K., Glazebrook, K., Hoversten, E.A., Schneider, D.P., Brinkmann, J.: L' and M' photometry of ultracool dwarfs. *AJ* **127**, 3516–3536 (2004)
- Gorlova, N.I., Meyer, M.R., Rieke, G.H., Liebert, J.: Gravity indicators in the near-infrared spectra of brown dwarfs. *ApJ* **593**, 1074–1092 (2003)
- Gray, R.O., Corbally, C.J.: *Stellar Spectral Classification*. Princeton University Press, Princeton/Woodstock (2009)
- Hanel, R., Conrath, B., Herath, L., Kunde, V., Pirraglia, J.: Albedo, internal heat, and energy balance of Jupiter – preliminary results of the Voyager infrared investigation. *J. Geophys. Res.* **86**, 8705–8712 (1981)
- Hayashi, C., Nakano, T.: Evolution of stars of small masses in the pre-main-sequence stages. *Prog. Theor. Phys.* **30**, 460–474 (1963)
- Jones, H.R.A., Tsuji, T.: Spectral evidence for dust in late-type M dwarfs. *ApJ* **480**, L39 (1997)
- Joy, A.H.: Radial velocities and spectral types of 181 dwarf stars. *ApJ* **105**, 96 (1947)
- Kimble, R.A., MacKenty, J.W., O'Connell, R.W., Townsend, J.A.: Wide Field Camera 3: a powerful new imager for the Hubble Space Telescope. In: Presented at the Society of Photo-Optical Instrumentation Engineers (SPIE) Conference, Marseille. Society of Photo-Optical Instrumentation Engineers (SPIE) Conference Series, vol. 7010 (2008)
- Kirkpatrick, J.D.: Spectroscopic properties of ultra-cool dwarfs and brown dwarf (invited review). In: Rebolo, R., Martín, E.L., Zapatero Osorio, M.R. (eds.) *Brown Dwarfs and Extrasolar Planets*. Astronomical Society of the Pacific Conference Series, vol. 134, p. 405. Astronomical Society of the Pacific, San Francisco (1998)
- Kirkpatrick, J.D.: New spectral types L and T. *ARA&A* **43**, 195–245 (2005)

- Kirkpatrick, J.D.: Outstanding issues in our understanding of L, T, and Y dwarfs. In: van Belle, G. (ed.) 14th Cambridge Workshop on Cool Stars, Stellar Systems, and the Sun, Pasadena. Astronomical Society of the Pacific Conference Series, vol. 384, p. 85 (2008)
- Kirkpatrick, J.D., Henry, T.J., McCarthy, D.W., Jr.: A standard stellar spectral sequence in the red/near-infrared – Classes K5 to M9. *ApJS* **77**, 417–440 (1991)
- Kirkpatrick, J.D., Henry, T.J., Liebert, J.: The unique spectrum of the brown dwarf candidate GD 165B and comparison to the spectra of other low-luminosity objects. *ApJ* **406**, 701–707 (1993)
- Kirkpatrick, J.D., Allard, F., Bida, T., Zuckerman, B., Becklin, E.E., Chabrier, G., Baraffe, I.: An improved optical spectrum and new model FITS of the likely brown dwarf GD 165B. *ApJ* **519**, 834–843 (1999a)
- Kirkpatrick, J.D., Reid, I.N., Liebert, J., Cutri, R.M., Nelson, B., Beichman, C.A., Dahn, C.C., Monet, D.G., Gizis, J.E., Skrutskie, M.F.: Dwarfs cooler than “M”: the definition of spectral type “L” using discoveries from the 2 Micron All-Sky Survey (2MASS). *ApJ* **519**, 802–833 (1999b)
- Kirkpatrick, J.D., Barman, T.S., Burgasser, A.J., McGovern, M.R., McLean, I.S., Tinney, C.G., Lowrance, P.J.: Discovery of a very young field L dwarf, 2MASS J01415823-4633574. *ApJ* **639**, 1120–1128 (2006)
- Kirkpatrick, J.D.,Looper, D.L.,Burgasser, A.J.,Schurr, S.D.,Cutri, R.M.,Cushing, M.C.,Cruz, K.L.,Sweet, A.C.,Knapp, G.R.,Barman, T.S.,Bochanski, J.J.,Roellig, T.L.,McLean, I.S.,McGovern, M.R.,Rice, E.L.: Discoveries from a near-infrared proper motion survey using multi-epoch Two Micron All-Sky survey data. *ApJS* **190**, 100–146 (2010)
- Kirkpatrick, J.D., Cushing, M.C., Gelino, C.R., Griffith, R.L., Skrutskie, M.F., Marsh, K.A., Wright, E.L., Mainzer, A., Eisenhardt, P.R., McLean, I.S., Thompson, M.A., Bauer, J.M., Benford, D.J., Bridge, C.R., Lake, S.E., Petty, S.M., Stanford, S.A., Tsai, C.W., Bailey, V., Beichman, C.A., Bloom, J.S., Bochanski, J.J., Burgasser, A.J., Capak, P.L., Cruz, K.L., Hinz, P.M., Kartaltepe, J.S., Knox, R.P., Manohar, S., Masters, D., Morales-Calderón, M., Prato, L.A., Rodigas, T.J., Salvato, M., Schurr, S.D., Scoville, N.Z., Simcoe, R.A., Stapelfeldt, K.R., Stern, D., Stock, N.D., Vacca, W.D.: The first hundred brown dwarfs discovered by the Wide-field Infrared Survey Explorer (WISE). *ApJS* **197**, 19 (2011)
- Kirkpatrick, J.D., Gelino, C.R., Cushing, M.C., Mace, G.N., Griffith, R.L., Skrutskie, M.F., Marsh, K.A., Wright, E.L., Eisenhardt, P.R., McLean, I.S., Mainzer, A.K., Burgasser, A.J., Tinney, C.G., Parker, S., Salter, G.: Further defining spectral type “Y” and exploring the low-mass end of the field brown dwarf mass function. *ApJ* **753**, 156 (2012)
- Knapp, G.R., Leggett, S.K., Fan, X., Marley, M.S., Geballe, T.R., Golimowski, D.A., Finkbeiner, D., Gunn, J.E., Hennawi, J., Ivezić, Z., Lupton, R.H., Schlegel, D.J., Strauss, M.A., Tsvetanov, Z.I., Chiu, K., Hoversten, E.A., Glazebrook, K., Zheng, W., Hendrickson, M., Williams, C.C., Uomoto, A., Vrba, F.J., Henden, A.A., Luginbuhl, C.B., Guetter, H.H., Munn, J.A., Canzian, B., Schneider, D.P., Brinkmann, J.: Near-infrared photometry and spectroscopy of L and T dwarfs: the effects of temperature, clouds, and gravity. *AJ* **127**, 3553–3578 (2004)
- Kuiper, G.P.: The nearest stars. *ApJ* **95**, 201 (1942)
- Kumar, S.S.: The structure of stars of very low mass. *ApJ* **137**, 1121 (1963)
- Lawrence, A., Warren, S.J., Almaini, O., Edge, A.C., Hambly, N.C., Jameson, R.F., Lucas, P., Casali, M., Adamson, A., Dye, S., Emerson, J.P., Foucaud, S., Hewett, P., Hirst, P., Hodgkin, S.T., Irwin, M.J., Lodieu, N., McMahon, R.G., Simpson, C., Smail, I., Mortlock, D., Folger, M.: The UKIRT Infrared Deep Sky Survey (UKIDSS). *MNRAS* **379**, 1599–1617 (2007)
- Leggett, S.K., Marley, M.S., Freedman, R., Saumon, D., Liu, M.C., Geballe, T.R., Golimowski, D.A., Stephens, D.C.: Physical and spectral characteristics of the T8 and later type dwarfs. *ApJ* **667**, 537–548 (2007)
- Leggett, S.K., Cushing, M.C., Saumon, D., Marley, M.S., Roellig, T.L., Warren, S.J., Burningham, B., Jones, H.R.A., Kirkpatrick, J.D., Lodieu, N., Lucas, P.W., Mainzer, A.K., Martín, E.L., McCaughean, M.J., Pinfield, D.J., Sloan, G.C., Smart, R.L., Tamura, M., Van Cleve, J.: The physical properties of four 600 K T dwarfs. *ApJ* **695**, 1517–1526 (2009)

- Leggett, S.K., Saumon, D., Marley, M.S., Lodders, K., Canty, J., Lucas, P., Smart, R.L., Tinney, C.G., Homeier, D., Allard, F., Burningham, B., Day-Jones, A., Fegley, B., Ishii, M., Jones, H.R.A., Marocco, F., Pinfield, D.J., Tamura, M.: The properties of the 500 K dwarf UGPS J072227.51-054031.2 and a study of the far-red flux of cold brown dwarfs. *ApJ* **748**, 74 (2012)
- Leggett, S.K., Morley, C.V., Marley, M.S., Saumon, D., Fortney, J.J., Visscher, C.: A comparison of near-infrared photometry and spectra for Y dwarfs with a new generation of cool cloudy models. *ApJ* **763**, 130 (2013)
- Linsky, J.L.: On the pressure-induced opacity of molecular hydrogen in late-type stars. *ApJ* **156**, 989 (1969)
- Liu, M.C., Delorme, P., Dupuy, T.J., Bowler, B.P., Albert, L., Artigau, E., Reylé, C., Forveille, T., Delfosse, X.: CFBDSIR J1458+1013B: a very cold ( $>T10$ ) brown dwarf in a binary system. *ApJ* **740**, 108 (2011)
- Lodders, K.: Alkali element chemistry in cool dwarf atmospheres. *ApJ* **519**, 793–801 (1999)
- Lucas, P.W., Tinney, C.G., Burningham, B., Leggett, S.K., Pinfield, D.J., Smart, R., Jones, H.R.A., Marocco, F., Barber, R.J., Yurchenko, S.N., Tennyson, J., Ishii, M., Tamura, M., Day-Jones, A.C., Adamson, A., Allard, F., Homeier, D.: The discovery of a very cool, very nearby brown dwarf in the Galactic plane. *MNRAS* **408**, L56–L60 (2010) [1004.0317](#)
- Luhman, K.L., Burgasser, A.J., Bochanski, J.J.: Discovery of a candidate for the coolest known brown dwarf. *ApJ* **730**, L9 (2011)
- Luhman, K.L., Burgasser, A.J., Labbé, I., Saumon, D., Marley, M.S., Bochanski, J.J., Monson, A.J., Persson, S.E.: Confirmation of one of the coldest known brown dwarfs. *ApJ* **744**, 135 (2012)
- Martín, E.L., Basri, G., Delfosse, X., Forveille, T.: Keck HIRES spectra of the brown dwarf DENIS-P J1228.2-1547. *A&A* **327**, L29–L32 (1997)
- Martín, E.L., Delfosse, X., Basri, G., Goldman, B., Forveille, T., Zapatero Osorio, M.R.: Spectroscopic classification of late-M and L field dwarfs. *AJ* **118**, 2466–2482 (1999)
- McLean, I.S., Prato, L., Kim, S.S., Wilcox, M.K., Kirkpatrick, J.D., Burgasser, A.: Near-infrared spectroscopy of brown dwarfs: methane and the transition between the L and T spectral types. *ApJ* **561**, L115–L118 (2001)
- McLean, I.S., McGovern, M.R., Burgasser, A.J., Kirkpatrick, J.D., Prato, L., Kim, S.S.: The NIRSPEC brown dwarf spectroscopic survey. I. Low-resolution near-infrared spectra. *ApJ* **596**, 561–586 (2003)
- Morgan, W.W.: On the spectral types and luminosities of the M dwarfs. *ApJ* **87**, 589 (1938)
- Morgan, W.W.: The MK system and the MK process. In: Garrison, R.F. (ed.) *The MK Process and Stellar Classification*, p. 18. David Dunlap Observatory, University of Toronto, Toronto (1984)
- Morgan, W.W., Keenan, P.C., Kellman, E.: *An atlas of stellar spectra, with an outline of spectral classification*. The University of Chicago Press, Chicago (1943)
- Morley, C.V., Fortney, J.J., Marley, M.S., Visscher, C., Saumon, D., Leggett, S.K.: Neglected clouds in T and Y dwarf atmospheres. *ApJ* **756**, 172 (2012)
- Nakajima, T., Oppenheimer, B.R., Kulkarni, S.R., Golimowski, D.A., Matthews, K., Durrance, S.T.: Discovery of a cool brown dwarf. *Nature* **378**, 463–465 (1995)
- Oppenheimer, B.R., Kulkarni, S.R., Matthews, K., Nakajima, T.: Infrared spectrum of the cool brown dwarf Gl 229B. *Science* **270**, 1478–1479 (1995)
- Oppenheimer, B.R., Kulkarni, S.R., Matthews, K., van Kerkwijk, M.H.: The spectrum of the brown dwarf Gliese 229B. *ApJ* **502**, 932 (1998)
- Pickering, E.C.: The Draper catalogue of stellar spectra photographed with the 8-inch Baché telescope as a part of the Henry Draper memorial. *Ann. Harv. Coll. Obs.* **27**, 1–388 (1890)
- Reid, I.N., Kirkpatrick, J.D., Gizis, J.E., Liebert, J.: BRI 0021-0214: another surprise at the bottom of the main sequence. *ApJ* **527**, L105–L107 (1999)
- Reid, I.N., Burgasser, A.J., Cruz, K.L., Kirkpatrick, J.D., Gizis, J.E.: Near-infrared spectral classification of late M and L dwarfs. *AJ* **121**, 1710–1721 (2001)
- Saumon, D., Marley, M.S., Cushing, M.C., Leggett, S.K., Roellig, T.L., Lodders, K., Freedman, R.S.: Ammonia as a tracer of chemical equilibrium in the T7.5 dwarf Gliese 570D. *ApJ* **647**, 552–557 (2006)

- Saumon, D., Marley, M.S., Leggett, S.K., Geballe, T.R., Stephens, D., Golimowski, D.A., Cushing, M.C., Fan, X., Rayner, J.T., Lodders, K., Freedman, R.S.: Physical parameters of two very cool T dwarfs. *ApJ* **656**, 1136–1149 (2007)
- Saumon, D., Marley, M.S., Abel, M., Frommhold, L., Freedman, R.S.: New H<sub>2</sub> collision-induced absorption and NH<sub>3</sub> opacity and the spectra of the coolest brown dwarfs. *ApJ* **750**, 74 (2012)
- Skrutskie, M.F., Cutri, R.M., Stiening, R., Weinberg, M.D., Schneider, S., Carpenter, J.M., Beichman, C., Capps, R., Chester, T., Elias, J., Huchra, J., Liebert, J., Lonsdale, C., Monet, D.G., Price, S., Seitzer, P., Jarrett, T., Kirkpatrick, J.D., Gizis, J.E., Howard, E., Evans, T., Fowler, J., Fullmer, L., Hurt, R., Light, R., Kopan, E.L., Marsh, K.A., McCallon, H.L., Tam, R., Van Dyk, S., Wheelock, S.: The Two Micron All Sky Survey (2MASS). *AJ* **131**, 1163–1183 (2006)
- Stephens, D.C., Leggett, S.K., Cushing, M.C., Marley, M.S., Saumon, D., Geballe, T.R., Golimowski, D.A., Fan, X., Noll, K.S.: The 0.8–14.5  $\mu\text{m}$  spectra of mid-L to mid-T dwarfs: diagnostics of effective temperature, grain sedimentation, gas transport, and surface gravity. *ApJ* **702**, 154–170 (2009)
- Stevenson, D.J.: The search for brown dwarfs. *ARA&A* **29**, 163–193 (1991)
- Testi, L.: A low-resolution near-infrared spectral library of M-, L-, and T-dwarfs. *A&A* **503**, 639–650 (2009)
- Tinney, C.G., Faherty, J.K., Kirkpatrick, J.D., Wright, E.L., Gelino, C.R., Cushing, M.C., Griffith, R.L., Salter, G.: WISE J163940.83-684738.6: A Y dwarf identified by methane imaging. *ApJ* **759**, 60 (2012)
- Tokunaga, A.T., Kobayashi, N.: K-band spectra and narrowband photometry of DENIS field brown dwarfs. *AJ* **117**, 1010–1013 (1999)
- Tokunaga, A.T., Brooke, T.Y., Becklin, E.E., Zuckerman, B.: The infrared spectra of possible brown dwarf companions to G29-38 and GD 165A. *Bull. Am. Astron. Soc.* **22**, 1078 (1990)
- Vrba, F.J., Henden, A.A., Luginbuhl, C.B., Guetter, H.H., Munn, J.A., Canzian, B., Burgasser, A.J., Kirkpatrick, J.D., Fan, X., Geballe, T.R., Golimowski, D.A., Knapp, G.R., Leggett, S.K., Schneider, D.P., Brinkmann, J.: Preliminary parallaxes of 40 L and T dwarfs from the US Naval Observatory Infrared Astrometry Program. *AJ* **127**, 2948–2968 (2004)
- Warren, S.J., Mortlock, D.J., Leggett, S.K., Pinfield, D.J., Homeier, D., Dye, S., Jameson, R.F., Lodieu, N., Lucas, P.W., Adamson, A.J., Allard, F., Barrado y Navascués, D., Casali, M., Chiu, K., Hambly, N.C., Hewett, P.C., Hirst, P., Irwin, M.J., Lawrence, A., Liu, M.C., Martín, E.L., Smart, R.L., Valdivielso, L., Venemans, B.P.: A very cool brown dwarf in UKIDSS DR1. *MNRAS* **381**, 1400–1412 (2007)
- Witte, S., Helling, C., Barman, T., Heidrich, N., Hauschildt, P.H.: Dust in brown dwarfs and extra-solar planets. III. Testing synthetic spectra on observations. *A&A* **529**, A44 (2011)
- Wright, E.L., Eisenhardt, P.R.M., Mainzer, A.K., Ressler, M.E., Cutri, R.M., Jarrett, T., Kirkpatrick, J.D., Padgett, D., McMillan, R.S., Skrutskie, M., Stanford, S.A., Cohen, M., Walker, R.G., Mather, J.C., Leisawitz, D., Gautier, T.N., McLean, I., Benford, D., Lonsdale, C.J., Blain, A., Mendez, B., Irace, W.R., Duval, V., Liu, F., Royer, D., Heinrichsen, I., Howard, J., Shannon, M., Kendall, M., Walsh, A.L., Larsen, M., Cardon, J.G., Schick, S., Schwalm, M., Abid, M., Fabinsky, B., Naes, L., Tsai, C.: The Wide-field Infrared Survey Explorer (WISE): mission description and initial on-orbit performance. *AJ* **140**, 1868–1881 (2010)
- York, D.G., Adelman, J., Anderson, J.E., Jr., Anderson, S.F., Annis, J., Bahcall, N.A., Bakken, J.A., Barkhouser, R., Bastian, S., Berman, E., Boroski, W.N., Bracker, S., Briegel, C., Briggs, J.W., Brinkmann, J., Brunner, R., Burles, S., Carey, L., Carr, M.A., Castander, F.J., Chen, B., Colestock, P.L., Connolly, A.J., Crocker, J.H., Csabai, I., Czarapata, P.C., Davis, J.E., Doi, M., Dombeck, T., Eisenstein, D., Ellman, N., Elms, B.R., Evans, M.L., Fan, X., Federwitz, G.R., Fischelli, L., Friedman, S., Frieman, J.A., Fukugita, M., Gillespie, B., Gunn, J.E., Gurbani, V.K., de Haas, E., Haldeman, M., Harris, F.H., Hayes, J., Heckman, T.M., Hennessy, G.S., Hindsley, R.B., Holm, S., Holmgren, D.J., Huang, C., Hull, C., Husby, D., Ichikawa, S., Ichikawa, T., Ivezić, Ž., Kent, S., Kim, R.S.J., Kinney, E., Klaene, M., Kleinman, A.N., Kleinman, S., Knapp, G.R., Korienek, J., Kron, R.G., Kunzst, P.Z., Lamb, D.Q., Lee, B., Leger, R.F., Limmongkol, S., Lindenmeyer, C., Long, D.C., Loomis, C., Loveday, J.,

Lucinio, R., Lupton, R.H., MacKinnon, B., Mannery, E.J., Mantsch, P.M., Margon, B., McGehee, P., McKay, T.A., Meiksin, A., Merelli, A., Monet, D.G., Munn, J.A., Narayanan, V.K., Nash, T., Neilsen, E., Neswold, R., Newberg, H.J., Nichol, R.C., Nicinski, T., Nonino, M., Okada, N., Okamura, S., Ostriker, J.P., Owen, R., Pauls, A.G., Peoples, J., Peterson, R.L., Petravick, D., Pier, J.R., Pope, A., Pordes, R., Prosapio, A., Rechenmacher, R., Quinn, T.R., Richards, G.T., Richmond, M.W., Rivetta, C.H., Rockosi, C.M., Ruthmansdorfer, K., Sandford, D., Schlegel, D.J., Schneider, D.P., Sekiguchi, M., Sergey, G., Shimasaku, K., Siegmund, W.A., Smee, S., Smith, J.A., Snedden, S., Stone, R., Stoughton, C., Strauss, M.A., Stubbs, C., SubbaRao, M., Szalay, A.S., Szapudi, I., Szokoly, G.P., Thakar, A.R., Tremonti, C., Tucker, D.L., Uomoto, A., Vanden Berk, D., Vogeley, M.S., Waddell, P., Wang, S., Watanabe, M., Weinberg, D.H., Yanny, B., Yasuda, N.: The Sloan Digital Sky Survey: technical summary. *AJ* **120**, 1579–1587 (2000)

# Latest News on the Physics of Brown Dwarfs

Isabelle Baraffe

**Abstract** The physics of brown dwarfs has continuously improved since the discovery of these astrophysical bodies. The first important developments were devoted to the description of their mechanical structure, with the derivation of an appropriate equation of state, and the modelling of their atmosphere characterised by strong molecular absorption. New challenges are arising with progress in observational techniques which provide data of unprecedented accuracy. The goal of this chapter is to describe some of the current challenges for the theory of brown dwarfs. Those challenges concern atmospheric dust and cloud, non-equilibrium atmospheric chemistry, the effect of rotation and magnetic fields on internal structure and the very early phases of evolution characterised by accretion processes. The field remains lively as more and more high-quality observational data become available and because of increasing discoveries of exoplanets. Indeed, many physical properties of giant exoplanets can be described by the same theory as brown dwarfs, as described in this chapter.

## 1 Introduction: The First Theoretical Challenges

The history of brown dwarfs is particularly interesting, since their existence was theoretically predicted in 1963 before they were discovered in 1995. Coincidentally at the same time, [Kumar \(1963\)](#) and [Hayashi and Nakano \(1963\)](#) demonstrated that objects less massive than  $\sim 0.08\text{--}0.09 M_{\odot}$  should have their internal structure affected by electron degeneracy as they contract gravitationally after their formation (see also the chapter by T. Nakano in this volume). Those objects should be unable to release enough energy from hydrogen nuclear burning, since their central

---

I. Baraffe (✉)

Physics and Astronomy, University of Exeter, EX4 4QL Exeter, Devon, UK

e-mail: [i.baraffe@exeter.ac.uk](mailto:i.baraffe@exeter.ac.uk)

temperatures begin to decrease after degeneracy proceeds. They should never go through the usual stellar evolution phases, living as “failed” stars. The theoretical calculations of the two pioneer papers in 1963 marked the birth of brown dwarfs 50 years ago. Following these predictions, the motivation was there for more theoretical calculations and evolutionary models for brown dwarfs (Grossman 1970; Straka 1971; Rappaport and Joss 1984), followed by many others. Models based on up-dated microphysics now predict that the mass limit for the onset of electron degeneracy is close to  $0.07 M_{\odot}$  for objects with a solar metal content (i.e. the so-called metallicity) and increases with decreasing metallicity (Chabrier and Baraffe 2000).

With the discovery of the first genuine brown dwarfs about 20 years ago (see the chapters by R. Rebolo, G. Basri and B. Oppenheimer in this volume), the theory and modelling of brown dwarfs have constantly developed and improved. The first major theoretical challenge was the development of an equation of state (EOS hereafter) appropriate for the description of the dense and relatively cool interior of brown dwarfs, accounting for the effects of electron partial degeneracy and interaction between particles, namely, molecules, atoms, ions and electrons (see Chabrier and Baraffe (2000) and references therein). The other major challenge was the development of “cool” atmosphere models characterised by strong molecular absorptions and, for the coolest objects, by condensation processes (see Allard et al. (1997) and references therein).

As brown dwarf observations deliver data with increasing accuracy and level of details, modellers need to increase the sophistication of the theory, requiring new physical ingredients and processes to face the reality of observations. This paper, far from being a comprehensive review of the physics of brown dwarfs, will focus on some recent developments and novelties which I find exciting as they reflect a thriving and innovative field. This choice will hopefully provide guidance and motivate future generation of students and young researcher to work on the theory of brown dwarfs. The paper is organised as follows. I will first discuss current developments in atmosphere and inner structure modelling, respectively. I will then discuss young brown dwarfs and current ideas regarding their very early evolution. I will conclude by providing some of the important topics to develop in the coming years in order to keep the field of brown dwarf active and “young”.

## 2 Recent Advancement in the Modelling

### 2.1 Atmosphere Models

After the discovery of the first brown dwarfs in the 1990s, Teide 1, PPI15 and Gliese 229B (Rebolo et al. 1995; Nakajima et al. 1995; Oppenheimer et al. 1995; Basri et al. 1996) huge advancement in the field was provided by new generations of atmosphere models accounting for improved treatment of molecular opacities. The

atmospheres of objects with effective temperatures cooler than  $T_{\text{eff}} \lesssim 4,000$  K (e.g. low-mass stars, brown dwarfs) are characterised by the formation of molecules ( $\text{H}_2$ ,  $\text{TiO}$ ,  $\text{VO}$ ,  $\text{H}_2\text{O}$ ,  $\text{CO}$ ,  $\text{FeH}$ ,  $\text{CaH}$ , etc.). The strongly wavelength-dependent absorption coefficients resulting from molecular line transitions, along with Rayleigh scattering resulting from light scattering from molecules and characterised by a wavelength dependence  $\propto \nu^4$ , yield a strong departure of the spectra of cool objects from a black-body energy distribution (see e.g. [Allard et al. 1997](#)). Most brown dwarfs are characterised by effective temperatures  $T_{\text{eff}} \lesssim 2,000$  K, except for very young massive brown dwarfs which can be hot enough to exceed this temperature. Below  $T_{\text{eff}} \lesssim 2,000$  K, some molecules condense into liquid and solid phases, forming grains and depleting the atmospheric gas phase of a number of molecules (e.g.  $\text{TiO}$  which will be sequestered in more complex compounds such as perovskite  $\text{CaTiO}_3$ ). Along with the drastic modification of the chemical composition of the atmosphere, atmospheric heating resulting from the large grain opacity (the so-called green house or backwarming effect) strongly impacts the spectral energy distribution of “dusty” brown dwarfs (see more details in the chapter by M. Cushing in this volume). Cool atmosphere models now include more and more complete molecular linelists and better methods to handle many millions of transitions thanks to growing computer facilities (see [Allard et al. 1997](#)). Continuous efforts are devoted to the calculation of more accurate molecular opacities, both in the optical, with main absorbers like  $\text{TiO}$  and  $\text{VO}$ , and in the near-infrared (e.g.  $\text{H}_2\text{O}$ ,  $\text{CO}$ ,  $\text{CH}_4$ ), providing more and more realistic atmosphere models. This progress is made possible with the development of comprehensive molecular linelists, combining ab-initio quantum mechanical treatment and experimental data, which account for the multitude of rotational, vibrational and electronic transitions (see e.g. [Tennyson and Yurchenko 2012](#)). About a decade ago, when brown dwarfs were in their 40s, a breakthrough in the observations of brown dwarfs occurred with the infrared sky surveys DENIS ([Epchtein et al. 1997](#)), SDSS ([York et al. 2000](#)) and 2MASS ([Skrutskie et al. 2006](#)) which provided a wealth of “dusty” L dwarfs and “methane” T dwarfs. Those projects provide key information on the M/L transition, from “clean” to “dusty” atmospheres, and on the L/T transition, characterised by complete or incomplete clearing of dust. Many new questions on dust properties and on its evolution with decreasing effective temperatures were raised and are still open. Similar breakthrough is now occurring with the wide-field survey WISE ([Wright et al. 2010](#)) which pushes the frontiers of cold, isolated object detection further away. The doors of the Y dwarfs realm are now ajar, revealing the promised land of water and ammonia condensation processes. The coldest isolated object discovered at the time of this writing, the Y dwarf WISE 1828+2650 ([Cushing et al. 2011; Beichman et al. 2013](#)), could have an effective temperature as low as  $T_{\text{eff}} \sim 250$  K, bringing brown dwarfs closer and closer to the world of giant planets.<sup>1</sup>

---

<sup>1</sup>Jupiter has an effective temperature  $T_{\text{eff}} \sim 120$  K ([Hubbard et al. 1999](#)).

### 2.1.1 Cloud Models and Chemistry

Interpretation of observations of L, T and Y dwarfs called for new challenges in atmosphere modelling, specifically regarding cloud models and chemistry calculations. Different approaches for dust models with varying complexity exist in the brown dwarf community. They are described in detail in Helling et al. (2008) (see also Marley et al. 2013) and we will briefly summarise below the essential ingredients of each approach.

A simple approach of dust modelling extensively developed and used by Tsuji and collaborators (2002; 2004) assumes that dust forms in a restricted region defined by two temperatures: first by a condensation temperature, below which species condensation is allowed and which will characterise the base of a dust layer, and second by a critical temperature which is a free parameter and defines the top of the dust layer. In these models, the dust particles are assumed to have constant size. A similar approach has been adopted recently in the models of Barman et al. (2011a), but using pressure instead of temperature to define the cloud localisation and thickness. It was used to study the near-infrared spectra of the planetary-mass objects HR8799b (Barman et al. 2011a) and 2MASS1207b (Barman et al. 2011b). Though lacking the complexity of dust physics, those approaches offer the valuable advantage of allowing parameter exploration and of qualitatively understanding the effect of dust (Marley et al. 2013).

More sophisticated approaches to treat dust have been developed, like the models of Ackerman and Marley (2001) which allow for vertical variations of particle number densities and sizes. These models account for the downward transport of particles due to sedimentation through an efficiency parameter  $f_{\text{sed}}$  and for the upward mixing of vapour and condensates via a parameter  $K_{zz}$  characterising the vertical eddy diffusion coefficient. In the models of Allard et al. (2001), yielding the widely used COND and DUSTY models, condensation, coagulation and sedimentation effects are treated within the diffusion approximation following Rossow (1978). These models describe the limiting effects of cloud formation. An additional sophistication to the models of Allard et al. (2001), yielding the so-called BT-Settl models, is provided by an improved description of atmospheric mixing processes (e.g. overshooting and convective mixing) based on 2D radiation hydrodynamics simulations (Freytag et al. 2010). The results of those simulations are used to prescribe a diffusion coefficient characterising the mixing processes. The most detailed cloud model developed to date is based on the work by Helling and Woitke (2006) and Helling et al. (2008). It includes microphysics of grain growth and relaxes the usual assumption of phase equilibrium between gas and cloud particles.

All these different approaches have been extensively compared one to another in Helling et al. (2008), showing the limit and complexity of dust treatment in cool atmospheres. Interestingly enough, these various models have also been systematically compared to the same observations of young isolated field objects in Patience et al. (2012). Figure 1 shows such comparison for the young early L dwarf AB Pic B. This work clearly highlights the important effects of dust treatment

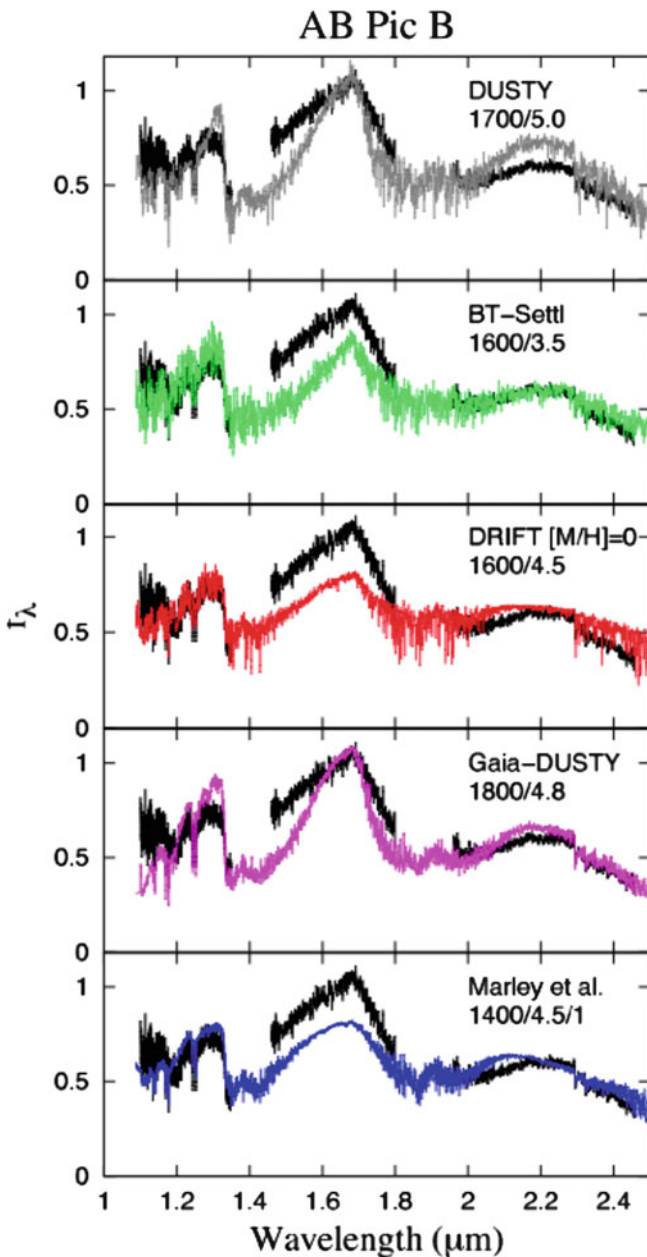


**Fig. 1** Comparison of the observed spectrum of AB Pic B (black line) with various sets of models. The effective temperature and the surface gravity  $\log g$  inferred by such comparison are indicated in each panel for each model used. Note the large differences between the effective temperatures and gravities inferred from different models. Note also that none of the models can correctly reproduce the observed spectrum (figure adopted from [Patience et al. 2012](#))

on synthetic spectra. The figure shows that none of the models can reproduce the observed spectrum. Additionally, the effective temperatures and surface gravities  $g$  (in log) inferred by the comparison between model and observation are indicated in the figure panels for each model used. The predicted effective temperature varies between 1,400 and 1,800 K, and the logarithm of the gravity varies between 3.5 and 5, depending on the model used. This highlights the huge uncertainty of physical properties ( $T_{\text{eff}}$ ,  $\log g$ ) inferred from a comparison between observed and synthetic spectra for dusty objects. It also shows the remaining uncertainties of current models because of their difficulty, no matter how sophisticated the approach is, to reproduce the observed spectra of objects where dust is expected to form. Dust models for brown dwarf (and exoplanet) atmospheres are thus still in their infancy, despite 50 years of theoretical and observational studies in this field. There is still a long way to go to understand and correctly describe the effect of dust in those objects.

Observations of cool brown dwarfs show that, in addition to cloud treatment, non-equilibrium chemistry is also an important process to account for in the models. Departure from equilibrium chemistry in cool atmospheres may be due to various processes, such as irradiation effects in close-in exoplanets, or mixing processes. The latter may take place in brown dwarf atmospheres if the timescale for vertical mixing is shorter than a chemical-reaction timescale. It is expected to occur for the reactions converting carbon monoxide (CO) to methane ( $\text{CH}_4$ ) and nitrogen ( $\text{N}_2$ ) to ammonia ( $\text{NH}_3$ ). The expected observable signatures of this process are overabundance of CO and depletion of  $\text{NH}_3$ . Its existence has long been established in Jovian planets in our solar system (see e.g. [Barshay et al. 1978](#)). For brown dwarfs, predictions of non-equilibrium chemistry was suggested ([Fegley and Lodders 1996](#)) shortly after the discovery of Gliese 229B ([Nakajima et al. 1995; Oppenheimer et al. 1995](#)) and confirmed with the detection of CO in its infrared spectrum ([Noll et al. 1997](#)). Evidences that this process is at work in cool atmosphere accumulated since then. This was again recently illustrated by the study of [Barman et al. \(2011b\)](#) showing that a combination of clouds, given some prescribed thickness, and non-equilibrium chemistry of CO/ $\text{CH}_4$  could both reproduce the photometric and spectroscopic observations of the young planetary-mass objects 2M1207b, as illustrated in Fig. 2. The idea of departure from non-equilibrium chemistry in brown dwarfs is not recent, but it now seems to be a necessary ingredient to include in the models in order to reproduce observed spectra of L and T dwarfs satisfactorily. Similar conclusions were reached in the study of [Burningham et al. \(2011\)](#) in order to reproduce the infrared spectrum of the T8.5 dwarf Ross 458C with an effective temperature of  $T_{\text{eff}} \sim 700$  K.

Finally, improvements are still made on the treatment of gas-phase chemistry, as illustrated in Fig. 3 which compares the effect of different EOS's for the gas phase on synthetic spectra (DRIFT versus DRIFT-ACES [Witte et al. 2009, 2011](#)). The main difference between DRIFT (green curve in Fig. 3) and DRIFT-ACES (red curve in Fig. 3) stems from the treatment of the gas-phase composition in chemical equilibrium. The ACES improvement consists of a coherent fit of gas-phase material data for lower temperatures. Hence, the differences observed in this figure between

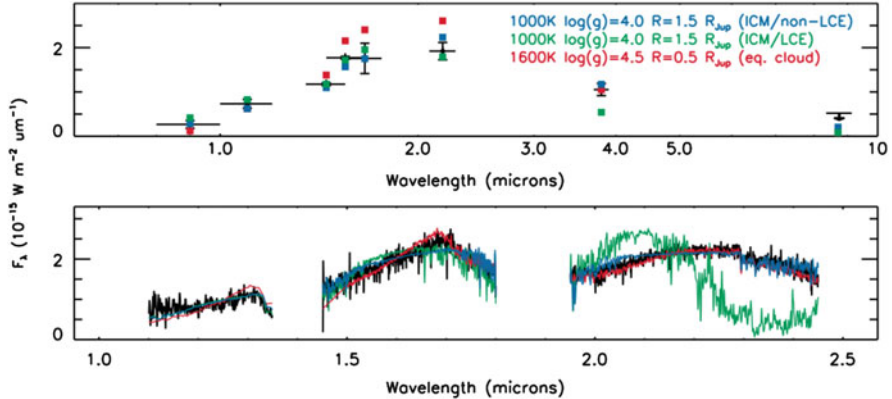


**Fig. 2** Comparison between observations of the planetary-mass object 2M1207b (in *black*) and models assuming equilibrium chemistry (*green*, labelled LCE) and non-equilibrium chemistry (*blue*, labelled non-LCE) (*top*, photometry; *bottom*, spectroscopy). Both models are based on the work of Barman et al. (2011b) including the cloud model described in Barman et al. (2011a) (see also Sect. 2.1.1). These comparisons show the important effect of non-equilibrium chemistry on photometry and spectrum of cool objects (the inferred effective temperature in the present case is  $T_{\text{eff}} \sim 1,000 \text{ K}$ ). For comparison, predictions from a model based on a equilibrium cloud model from Allard et al. (2001) are indicated in *red*. Note the large discrepancy between  $T_{\text{eff}}$  inferred from the latter model ( $T_{\text{eff}} \sim 1,600 \text{ K}$ ) and the models of Barman et al. (2011b). Figure from Barman et al. (2011b) and reproduced by permission of the AAS

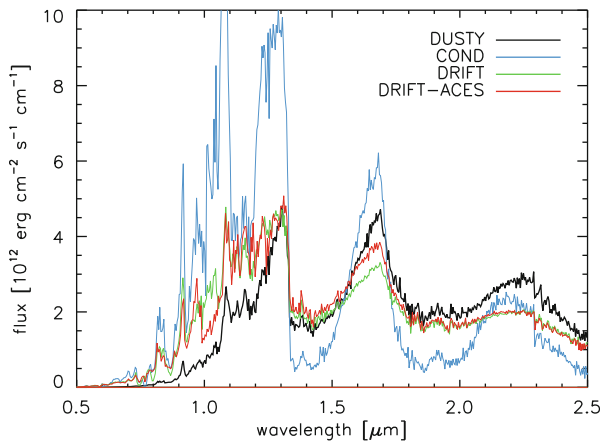


**Fig. 3** Comparison of synthetic spectra based on different treatments of dust (DUSTY, COND, Allard et al. 2001 and DRIFT, Witte et al. 2009) and gas-phase chemistry (DRIFT versus DRIFT-ACES, Witte et al. 2011) (courtesy of C. Helling)

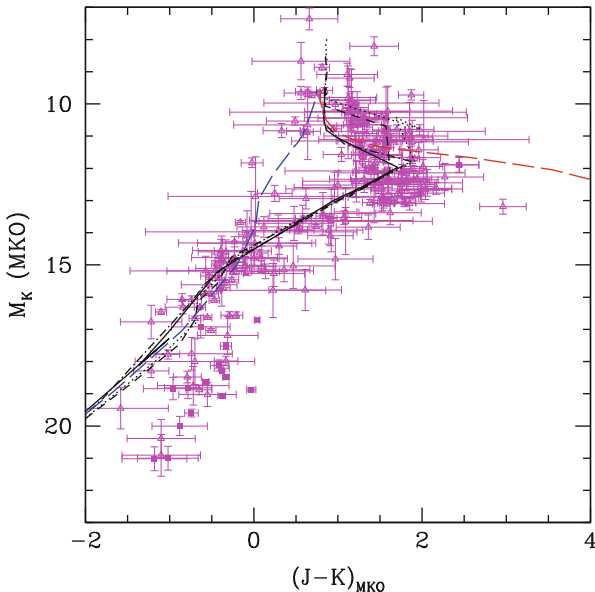


**Fig. 4** Comparison between models and M/L/T dwarfs data in a  $(J-K)$ – $M_K$  diagram. The *black models* are based on the BT-Settl atmospheres (Allard et al. 2012; Baraffe et al. 2013). Isochrones for 0.05, 0.1, 1 and 5 Gyr are displayed. The DUSTY (red) and COND (blue) models at an age of 1 Gyr are also shown for comparison (the data are from Faherty et al. 2012 and Dupuy and Liu 2012)

DRIFT and DRIFT-ACES stem alone from the treatment of the gas-phase chemistry (C. Helling, private communication).

### 2.1.2 The L/T Transition in the Colour-Magnitude Diagram

The description of the L/T transition in a colour-magnitude diagram is a real challenge for theory. This transition is physically characterised by the clearing of dust due to sedimentation of condensed species below the photosphere and the formation of  $\text{CH}_4$ , which is the dominant equilibrium form of carbon below a local temperature of  $\lesssim 1,600 \text{ K}$ , while CO dominates at higher temperatures. The heating of the atmosphere due to the backwarming effect of dust causes infrared colours to become very red, as seen in Fig. 4, whereas the formation of  $\text{CH}_4$ , which strongly absorbs near  $1.6 \mu\text{m}$ , yields the characteristic change to bluer ( $J-H$ ) and ( $J-K$ ) colours (see the chapter by M. Cushing, his Sect. 7). In addition to this well-known change in colours from the red to the blue characteristic of the L/T transition in the near-infrared (see Fig. 4), another major difficulty for models is to describe the scatter of colours for a given magnitude. Several ideas have been suggested to explain this observed property, namely the effect of a single second parameter

like gravity [Burrows et al. \(2006\)](#), or a mixture of effects, namely metallicity, cloud parameters, ages and unresolved binaries ([Saumon and Marley 2008](#)). In the later models, the sedimentation of condensates is characterised by the parameter  $f_{\text{sed}}$  as introduced by [Ackerman and Marley \(2001\)](#), cf. Sect. 2.1.1). Small values of  $f_{\text{sed}}$  indicate that particles grow more slowly, and thus, the condensate load is larger and clouds thicker. Large values of  $f_{\text{sed}}$  correspond to rapid particle growth, with large condensates quickly falling out of the atmosphere and yielding optically and physically thin clouds. A value of  $f_{\text{sed}} \sim 2$  is required to describe the L/T transition (see [Saumon and Marley 2008](#)). In comparison, the BT-Settl models are well reproducing the L/T transition. The latter models have the advantage of having no free parameters to describe the sedimentation/mixing processes, which instead rely on hydrodynamical simulations (see Sect. 2.1.1). But the drawback of using a more physical description of sedimentation in the BT-Settl models is the failure to reproduce the observed scatter of colours. Inspection of Fig. 4 also shows a disagreement between the BT-Settl models and observations for objects fainter than an infrared brightness in the K-band of  $M_K \sim 17$ , with the infrared colour (J-K) remaining almost constant as a function of  $M_K$ , whereas models predict significantly bluer (J-K) colours. This discrepancy is inherent to all current models where the silicate and iron clouds which shape the L-dwarf spectra are predicted to dissipate at the L/T transition. Recently, [Morley et al. \(2012\)](#) suggested the formation of other condensates in the coolest T- and Y-dwarf atmospheres. This solution is attractive since it avoids requiring the reemergence of the silicate clouds, as suggested by [Burgasser et al. \(2010\)](#) to explain the spectrum of the T8 brown dwarf Ross 458C. Those new condensates include sulphide clouds and other species such as Cr and KCl. With a variation of the  $f_{\text{sed}}$  parameter between  $\sim 3$  and 5, models including those new clouds provide a better agreement with observed colours for the coolest T and Y dwarfs ([Morley et al. 2012](#)). The weakness of these models stems from the larger  $f_{\text{sed}}$  parameter than the one required to reproduce the L/T transition. Such a change in sedimentation efficiency now requires a physical explanation in order to provide a satisfactory solution to the discrepancy between models and observations of the coolest dwarfs. This is still an open issue which generates many efforts from modellers to understand this puzzle.

## 2.2 Inner Structure Models

### 2.2.1 Mechanical Structure

Brown dwarf interiors are composed of a mixture of hydrogen (H) and helium (He), with traces of metals (i.e. elements heavier than He). The thermodynamical properties of such mixture are described by an EOS which provides the relationship between state variables like pressure, temperature and volume (or density). The major fraction of the life of a brown dwarf is characterised by the release of its gravitational and internal energy resulting from a hot initial state after its

formation. Only during the very first stage of their evolution, brown dwarfs with masses greater than  $\sim 0.012 M_{\odot}$ , the so-called deuterium-burning minimum mass, can produce nuclear energy due to deuterium fusion in their centre. This nuclear phase is however very short, lasting less than  $\sim 20$  Myr. The main process which transports energy from the deep hot layers to the surface where it is radiated away, producing the observable luminosity, is due to convection. The interior of a brown dwarf is so dense and optically thick that energy transport by radiation is totally negligible. The mechanical structure (which defines the mass-radius relationship) and internal thermal profile of a brown dwarf are thus determined by the EOS of its chemical constituent. Indeed, because interiors of brown dwarfs are essentially fully convective and radiation is negligible, the resulting thermal profile is quasi-adiabatic, with the adiabatic gradient fixed by the EOS (Chabrier and Baraffe 2000). The most widely used EOS to describe the thermodynamic properties of brown dwarf interiors is the semi-analytical Saumon-Chabrier-van Horn EOS (Saumon et al. 1995) for H/He mixtures. Continuous progress is achieved in this field thanks to the growth of computational performances which allow EOS calculations from first principle quantum mechanical calculations. Progress is also achieved thanks to high-pressure experiments which allow to probe EOS in a complex regime where pressure dissociation and ionisation occur, which characterise the interiors of both brown dwarfs and giant planets. The internal structures of these two astrophysical bodies share, indeed, the same pressure-temperature domain and are described by the same H/He EOS (Baraffe et al. 2010; Fortney et al. 2011). Developments of ab-initio EOS and high-pressure experiments are currently very active fields, being motivated by the discovery of numerous exoplanets.

### 2.2.2 Effect of Rotation and Magnetic Fields

Until recently, eclipsing binaries were thought to provide the best validation test of theoretical models for stellar/substellar internal structure and evolution. If the components of a binary system orbit in a plane which is along the line of site of an observer, a so-called eclipsing binary, it is possible to determine with high accuracy the masses and radii of both components. This provides an observed mass-radius relationship which can be compared to model predictions and test fundamental physics like the EOS implemented in the structure models. Eclipsing binaries are thus considered as the best astrophysical laboratories to test the interior physics of stars and brown dwarfs. Many efforts have been and are still devoted to the detection and analysis of eclipsing binary systems. While enough observations now exist to test the low-mass star regime down to the bottom of the main sequence (Ribas 2006), with many more systems expected from the Kepler mission (see e.g. Slawson et al. 2011), brown dwarf eclipsing binaries remain extremely rare, with only a few systems known (Stassun et al. 2006; Irwin et al. 2010).

But the idea strongly entrenched in the community that eclipsing binaries provide the best tests for EOS and interior structure models based on “standard” physics has

recently been called into question. This new challenge yields one of the most recent novelties regarding the physics of low-mass stars and brown dwarfs. It highlights the effect of rotation and/or magnetic fields on the inner structure of fully convective objects, effects which are usually not included in “standard” models. Because eclipsing binaries are fast rotators and very active objects, these systems are indeed the best targets to discover and investigate the effect of rotation and magnetic fields on interior structures. As the importance of the latter processes was first highlighted with the analysis of eclipsing binary systems in the low-mass star regime, I will first discuss these findings before turning to brown dwarfs. This will help discussing, in the second part of this section, the young brown dwarf eclipsing binary system 2M0535-0546 discovered by [Stassun et al. \(2006\)](#). This system shows the puzzling property that the more massive component ( $\sim 0.055 M_{\odot}$ ) has a cooler effective temperature than the less massive component ( $\sim 0.035 M_{\odot}$ ). Such temperature reversal cannot be explained by “standard” models.

The whole story started with increasing evidences for systematic differences between the observed fundamental properties of low-mass stars in eclipsing binaries and those predicted by stellar structure models (see e.g. [Ribas 2006](#) and [Morales et al. 2010](#)).

Particularly, radii and effective temperatures computed from models are 5–10 % lower and 3–5 % higher than observed, respectively. These differences are significant, given the high accuracy of empirical measurements reached nowadays (typically 1–2 %; [Morales et al. 2010](#)). Problems with atmospheric opacities have first been invoked as the source of the discrepancy. Opacities, however, have a modest impact on the stellar radius for these compact stars. Changing the metallicity in the atmosphere by a factor 100 affects the radius by a factor  $\sim 7\%$ , so that the opacity of eclipsing binaries should have to be increased to an unrealistic level to yield the observed 10 % effect on the radius ([Chabrier and Baraffe 1997](#)). Missing opacities thus seem to be unlikely to explain the radius discrepancy. Because eclipsing binaries are fast rotators and magnetically very active, a possible explanation for the radius discrepancy is the inhibition of internal convection, due to rotation and/or magnetic field, yielding a reduction of the internal heat flux and thus a smaller contraction during evolution ([Mullan and MacDonald 2001](#); [Chabrier et al. 2007a](#)). These effects are described in 1D stellar evolution codes by phenomenological approaches, using either the mixing length parameter ([Chabrier et al. 2007a](#)) or a magnetic inhibition parameter ([Mullan and MacDonald 2001](#)) to control the efficiency of convection. In addition to internal convection inhibition, surface spot coverage could contribute to a reduction of the internal heat flux, also yielding a larger radius ([Chabrier et al. 2007a](#)). These scenarios thus provide an appealing explanation for the larger radius in rapidly rotating, very active stars. The value of the equilibrium field inferred in the phenomenological approach of [Chabrier et al. \(2007a\)](#) to hamper convection is consistent with the observationally determined value of magnetic fields of very low-mass stars ([Reiners and Basri et al. 2007](#)) and with the one obtained with 3D resistive magneto-hydrodynamic (MHD) simulations ([Browning 2008](#)). Convection becomes more and more efficient and adiabatic with decreasing mass in this regime, because of increasing mean density

and average interior opacities. The aforementioned decreasing convective efficiency due to magnetic fields is thus expected to be relatively less and less consequential as one moves along the mass sequence from the Sun to the bottom of the main sequence. Such a behaviour is indeed supported by observations (see figure 1 in Chabrier et al. 2007a).

These very same effects of magnetically driven inhibition of convection and spot coverage could also provide a plausible explanation for the temperature reversal observed in the brown dwarf eclipsing binary system 2M0535-0546 (Stassun et al. 2006). Interestingly enough, the primary of this system is a faster rotator than the secondary and displays  $H_{\alpha}$  emission at a level seven times stronger than the emission from the secondary (Reiners et al. 2007). This brings support to the aforementioned scenario, with the primary being more affected by magnetic fields, yielding an increase of its radius and decrease of its effective temperature (Mohanty et al. 2009). To further comfort this idea, Chabrier et al. (2007a) predict a spot coverage of 20–30 % to reproduce the fundamental properties of these binary brown dwarfs (see Fig. 5). Based on high-resolution spectroscopy of the primary, Mohanty et al. (2010) find that  $\sim 70\%$  spot coverage is required for the primary in order to explain the mismatch between the effective temperature inferred from the  $TiO-\epsilon$  band and that from  $KI$  absorption feature. In comparison, Morales et al. (2010) find that a spot coverage of  $\sim 35\%$  provides an overall good agreement between models and observations for several low-mass stars ( $0.2$ – $0.8 M_{\odot}$ ) in eclipsing binary systems. While these numbers look consistent among all analysis, adding support to the effect of spot coverage, very recently, Mohanty and Stassun (2012) casted doubts on this interpretation. They obtained high-resolution spectroscopy for the secondary of the young brown dwarf binary 2M0535-0546 and found the same discrepancy between  $T_{eff}(TiO-\epsilon)$  and  $T_{eff}(KI)$  as reported for the primary. If spots are responsible for the  $T_{eff}$  mismatch found in both the primary and the secondary, they cannot explain the  $T_{eff}$  reversal of the primary. Consequently, if magnetic fields were still responsible for the latter, only convection inhibition in the interior of the primary could be the physical mechanism to solve the problem, but not spot coverage. The issue is far from being settled and this intriguing case deserves more follow-up.

Multi-dimensional hydrodynamical and magneto-hydrodynamical simulations seem to offer a promising avenue to explore those complex processes (Browning 2008; Showman and Kaspi 2013). The effect of rotation on convective flows is illustrated in Fig. 6, showing how rotation organises convection into organised rolls in a fully convective object. The interior rotation profile is constant on cylinders parallel to the rotation axis, reflecting the Taylor-Proudman constraint (Browning 2008, 2013; Showman and Kaspi 2013). The MHD simulations of Browning (2008) show that the magnetic field also strongly impacts the convective flows, reducing the development of differential rotation established in pure hydrodynamical simulations. Magnetic fields can thus play a major role in establishing the interior profile of a fully convective object, yielding some weakening of the convection (Browning 2008). Those results go along the lines of the predictions of Chabrier et al. (2007a). More theoretical and numerical works are clearly required to explore these thrilling issues.

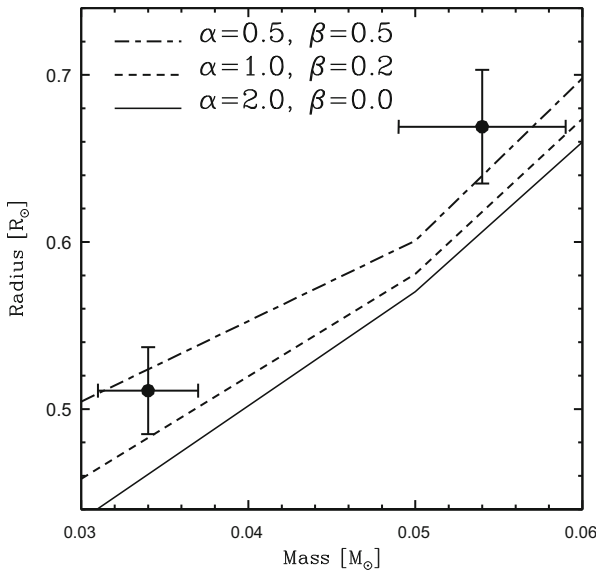


**Fig. 5** Effect of a variation of the mixing length parameter  $\alpha$  and the fractional surface area  $\beta$  covered by cool spots on the mass-radius relationships of young brown dwarfs. The *black data points* are the empirical mass and radius values of the binary brown dwarf 2M0535-0546 (models are from Chabrier et al. 2007a at an age of 1 Myr, corresponding to the inferred age of 2M0535-0546 Stassun et al. 2006)

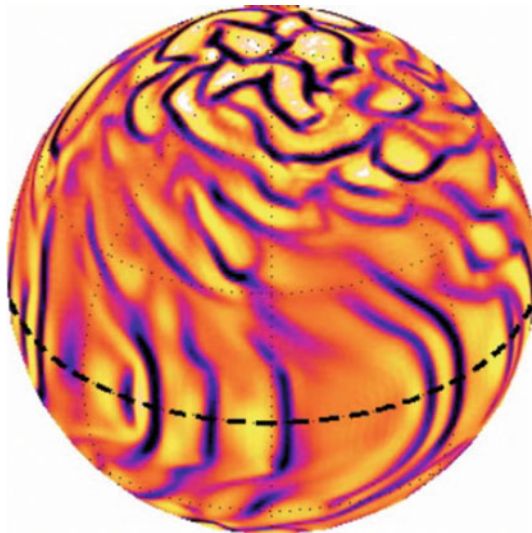


**Fig. 6** Global view of the radial velocity  $v_r$  on spherical surface deep into the interior of a fast rotating, fully convective M dwarf or brown dwarf. Upward flows are *reddish* and downward flows are *blueish* (courtesy of M. Browning 2013)

### 3 The Very Early Evolution of Brown Dwarfs

#### 3.1 Birth and Growth

The broad picture of star and brown dwarf formation starts with a molecular cloud which collapses and fragments, giving birth to prestellar or pre-brown dwarf cores which in turn collapse and produce central protostars or proto-brown dwarfs surrounded by an envelope and an accretion disc. The details are much more complex and are still intensively studied ([McKee and Ostriker 2007](#); [Luhman 2012](#)). Several mechanisms have been proposed for the formation of brown dwarfs (see review by [Luhman \(2012\)](#) and references therein). More and more observational evidences tend to support the idea that brown dwarfs form like stars and arise from the smallest prestellar cores ([Luhman 2012](#)). The recent detection of a pre-brown dwarf core of  $\sim 0.02 - 0.03 M_{\odot}$  ([André et al. 2012](#)) and of proto-brown dwarf candidates of a few Jupiter masses in Taurus ([Palau et al. 2012](#)), if confirmed, would add another credit to the idea that brown dwarf formation is a scaled-down version of low-mass star formation. This is also confirmed by the detection that young brown dwarfs have discs (e.g. [Harvey et al. 2012](#)) and outflows (e.g. [Joergens et al. 2012a,b](#)), like young stars.

A new paradigm based on the idea of episodic accretion is now superseding the standard picture of steady or slowly varying accretion as a function of time onto a protostar or a proto-brown dwarf. The standard picture describes the prestellar core collapse as a quasi-static process, giving rise to a constant accretion rate  $c_s^3/G \sim 10^{-6} M_{\odot}\text{yr}^{-1}$ , with  $c_s$  the speed of sound and  $G$  the gravitational constant ([McKee and Ostriker 2007](#)). An important failure of the standard model is the well-known “luminosity problem” related to the fact that accretion at such rates produces accretion luminosities ( $L_{\text{acc}} \propto \frac{GM_{\star}\dot{M}}{R_{\star}}$ , where  $M_{\star}$  and  $R_{\star}$  are respectively the mass and luminosity of the central accreting object) factors of 10–100 higher than typically observed for protostars embedded within a massive envelope. This classic problem ([Kenyon et al. 1990](#)) was recently aggravated by large surveys of star-forming regions based on the Spitzer Space Telescope which revealed the presence of a large population of low-luminosity embedded sources. The observed protostellar luminosity distributions in all surveyed star-forming regions are found to be strongly inconsistent with the standard model. They are better explained by non-steady accretion processes, with long quiescent phases of accretion interrupted by short episodes of high accretion (see e.g. [Evans et al. \(2009\)](#) and references therein).

Episodic accretion may solve not only the classic luminosity problem of embedded sources (with typical ages  $\ll 1$  Myr) but also another intriguing feature observed in young clusters of a few Myr, namely, the luminosity spread observed in their luminosity-effective temperature diagram (the Hertzsprung–Russell diagram). The origin of this luminosity spread, illustrated in Fig. 7, is highly controversial. Whether it arises from observational uncertainties, physical processes or stems from

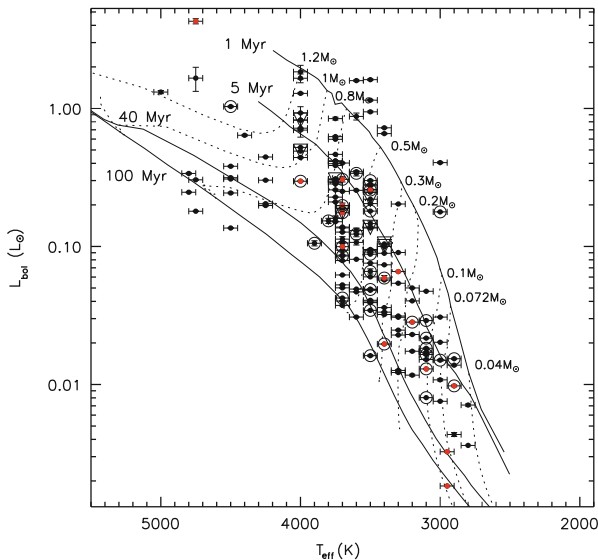


**Fig. 7** Illustration of the observed luminosity spread in the star-forming region  $\lambda$  Orionis ( $\sim 5$  Myr) (courtesy A. Bayo 2011)

a real age spread among young objects belonging to the same cluster are crucial questions for the understanding of star/brown dwarf formation. The interpretation of the luminosity spread as an age spread is used as an argument in favour of slow formation process, taking several Myr to tens of Myr. This view conflicts with our current understanding of star formation characterised by much shorter timescales, typical of shock-dominated turbulence.

### 3.2 Effects of Accretion on the Evolution

To explain the luminosity spread above mentioned, Baraffe et al. (2009) recently suggested the idea that non-steady accretion at very early stages of evolution, during the embedded phases, could still strongly impact the structure of young low-mass stars and brown dwarfs even after a few Myr, i.e. after the main phase of accretion. Accretion effects yield significantly more compact structures, i.e. smaller radii compared to those of non-accreting objects of same mass and age. This contraction stems from the increase in gravitational energy as mass is added, yielding higher central pressures and temperatures compared to the non-accreting case. During high accretion bursts, the accretion timescale  $\tau_{\dot{M}} = M/\dot{M}$  remains smaller than the thermal timescale of the accreting object  $\tau_{KH} = GM^2/(RL)$ . Its structure has thus no time to adjust to the incoming mass and energy, and the radius remains smaller than the non-accreting counterpart of the same mass and age. The more compact

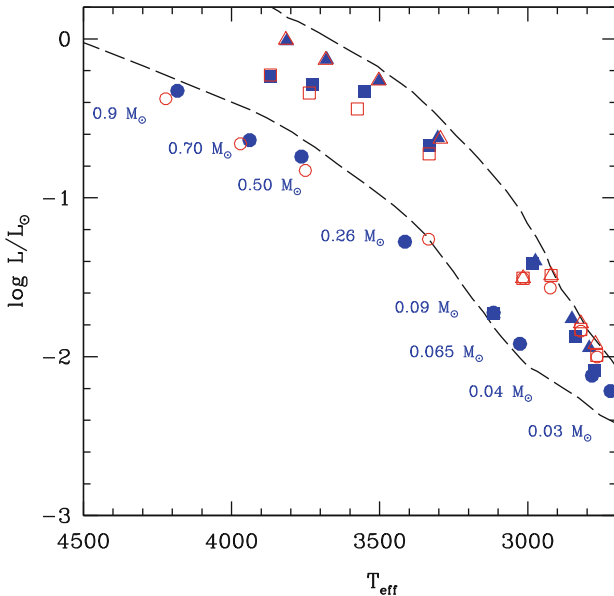


**Fig. 8** Illustration of the luminosity spread predicted by theoretical models including effects of episodic accretion. The *coloured symbols* show the position of objects having the same age (1 Myr) but different accretion histories. They correspond to a coeval population of low-mass objects. The two *long-dashed curves* indicate 1 and 10 Myr isochrones (from Baraffe et al. 2012)

structure of the accreting object results in a fainter luminosity compared to the non-accreting counterpart. The former thus looks “older” than the latter, as illustrated in Fig. 8.

Those effects are not only able to produce a luminosity spread, as shown in Fig. 8, similar to the observed one but can also explain other observational features like unexpected lithium depletion in some young objects Baraffe and Chabrier (2010) or the properties (mass and radius) of FU Ori objects characterised by strong bursts of accretion (Baraffe et al. 2012). This scenario can thus provide an explanation to the luminosity spread which is a better concept than the idea of an age spread, being in better agreement with current observations and with current understanding of star formation. An interesting effect on young brown dwarf evolution, due to the combination of accretion effects and deuterium nuclear burning, was noted by Baraffe et al. (2012). Because the energy released from deuterium fusion can partly overcome the gravitational energy increase due to mass accretion for objects with masses  $\lesssim 0.04 M_{\odot}$ , accretion is predicted to have less effect on the structure of those low-mass brown dwarfs. This must remain true above the deuterium-burning minimum mass, i.e. for  $M \gtrsim 0.01 M_{\odot}$ . Consequently, within this scenario, the luminosity spread in the mass range  $\sim 0.01\text{--}0.04 M_{\odot}$  is predicted to be smaller than for masses below and above. This prediction could be tested by observations to confirm or not the idea of episodic accretion.

The effects of accretion described above are still debated ([Hosokawa et al. 2011](#)) as their description relies on several modelling assumptions. This now requires more robust physical foundations. The origin of the luminosity spread is still an open issue, which should motivate further theoretical and observational studies, given its impact on the global understanding of star and brown dwarf formation. In particular, on the observational front, it is now crucial to study a variety of star-forming environments and the properties of their low-mass stars and brown dwarfs combining alternative age indicators (position in a luminosity-effective temperature diagram, gravity measurement, rotational properties, properties of accretion discs, etc.) to test current ideas about early accretion.

### 3.3 *Brown Dwarf or Planet?*

Another topical debate is how to observationally distinguish a brown dwarf from a planet. This question is relevant if characterising these two families of objects by their formation processes rather than using the IAU definition based on the deuterium-burning minimum mass. The IAU definition is admittedly practical from an observational point of view but is arbitrary with respect to the formation process. Because the two families of objects share a similar mass domain between a few  $M_{\text{Jup}}$  and tens of  $M_{\text{Jup}}$ , defining clear diagnostic enabling to distinguish a genuine brown dwarf from a planet is a key problem in the field. It is however not an easy task ([Chabrier et al. 2007b](#)). For young objects, the luminosity has been suggested as a possible signature of the formation process. The idea was floated with the work of [Marley et al. \(2007\)](#) suggesting that young planets, formed in a protoplanetary disc through the core accretion model, a widely accepted planet formation scenario, should be fainter than predicted by earlier models. This stems from the assumption made in the work of [Marley et al. \(2007\)](#) that all the energy liberated in the accretion shock produced by matter falling onto the forming planet's surface is radiated away and does not contribute to the planet's energy balance (and thus to its luminosity). On the other hand, brown dwarfs forming like stars via gravitational collapse, as described in the previous sections, should be significantly more luminous. Assuming that a fraction of the accretion energy is absorbed by the proto-brown dwarf and contributes to its intrinsic luminosity, brown dwarfs should start from a high initial specific entropy state, the so-called “hot start”.

Within this scenario, the measured luminosity of young planetary-mass objects (provided their age can be estimated) could thus reveal key information on their formation process. Measuring luminosities of such low-mass objects is now a reality with the new generations of adaptive optics systems, such as VLT-SPHERE ([Claudi et al. 2006](#)) or the Gemini Planet Imager (GPI) ([Macintosh 2006](#)), or with the coming successor of the Hubble Space telescope (the JWST, [Gardner et al. 2006](#)) and with the perspective of the European Extremely Large Telescope (E-ELT, [Gilmozzi and Spyromilio 2007](#)). The idea is thus exciting since it might provide an accessible way to disentangle a brown dwarf from a giant planet. Unfortunately, this

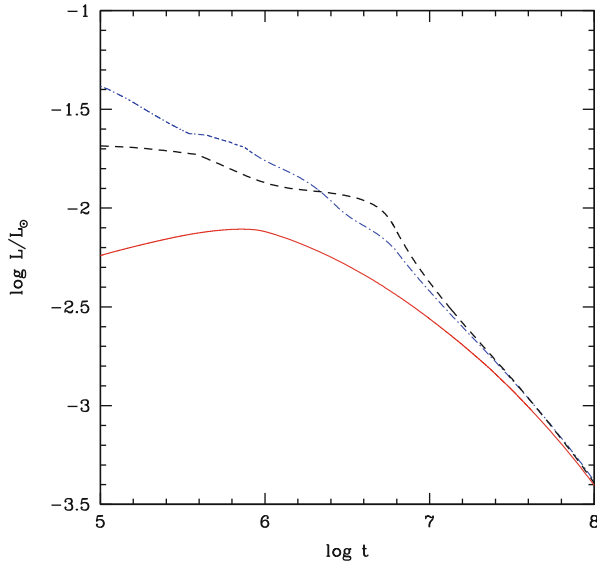


**Fig. 9** Evolution of the luminosity as a function of time of  $0.04 M_{\odot}$  brown dwarfs with different accretion histories. The *red solid line* corresponds to an object formed via “cold” accretion ( $\alpha = 0$ ) and the *blue dash-dotted curve* corresponds to “hot” accretion ( $\alpha = 0.2$ , from the models of Baraffe et al. 2012). The parameter  $\alpha$  corresponds to the fraction of accretion energy absorbed by the accreting object. The *black dashed line* shows the evolution at constant mass

scenario is oversimplified (see e.g. Mordasini et al. 2012). Accretion processes onto forming planets and forming brown dwarfs, despite operating under very different conditions, may share similar properties regarding the fraction of accretion energy radiated away and absorbed by the central object. As illustrated in Fig. 9, different properties of accretion can produce young brown dwarfs with a range of initial luminosities, depending on the accretion rate and the fraction of accretion energy absorbed by the central object. Consequently, the luminosity of young planetary-mass objects certainly tells something about the physics of the accretion process. Whether this diagnostic can reveal anything about the formation process itself (i.e. gravitational collapse versus core accretion) is however debatable and requires more work on the physics of accretion.

## 4 The Future of Brown Dwarf Physics

This brief overview of recent issues in the physics of brown dwarfs shows a lively field with new questions that calls for further developments and new ideas in atmosphere, dust and internal-structure modelling. The treatment of dust and clouds continues being a major issue, requiring increasing level of sophistication in the

modelling. This topic is also becoming of high interest for the understanding of exoplanet atmospheres with an apparent prevalence of dust in those objects, like in the hot Jupiter HD 189733b (Pont et al. 2013). Because of the remarkable level of accuracy of brown dwarf observations, compared to currently available data for exoplanets, one may bet that progress in ultra-cool atmosphere modelling will preferentially come from the brown dwarf community. A new interest is also emerging in the study of variability and “meteorological” processes in brown dwarf atmospheres, problems which are usually restricted to the analysis of planet atmospheres. Processes like cloud disruption can translate into observable signatures that observers are tracking to provide additional constraints on the physical properties of clouds (size, distribution, conditions for destruction, etc.; Buenzli et al. 2012; Radigan et al. 2012). The study of and search for lightning can also provide interesting information on the physical properties of dust in cool atmospheres (Helling et al. 2013). This field develops rapidly due to improved observational techniques to monitor the variability of very faint objects. The exoplanet community can learn a lot from the experience gained on brown dwarfs to understand the atmospheric properties of their favourite objects. In parallel to the continuous development in dust/cloud treatment, major progress has been made and is still coming regarding fundamental physics, with improved line lists for major molecular absorbers. At the time of this writing, a new methane line list is expected from the Exomol project (Tennyson and Yurchenko 2012). It is crucially needed for T and Y dwarfs and exoplanets and may solve the unexplained behaviour of near-infrared colours for the coolest T and Y dwarfs mentioned in Sect. 2.1.2. Further mandatory improvement in the microphysics concerns calculation of molecular line broadening under pressures and temperatures relevant to those cool and dense atmospheres. Current treatment of broadening factors is very rough and mostly relies on models valid at lower pressures and higher temperatures (Homeier 2005). Line broadening, however, plays an important role in shaping the spectra of brown dwarfs. The possibility now to perform accurate comparison between models and observations should motivate more experimental and theoretical studies of line broadening.

Interior structure and evolutionary models for brown dwarfs have considerably improved within the past decade and have now reached their limit based on 1D stellar evolutionary codes and phenomenological approaches. The field is entering a new era based on multi-dimensional magneto-hydrodynamical models. Various tools are available or being developed in the community, which will provide a better description and understanding of complex, but ubiquitous, physical processes like convection, rotation and magnetic fields. Among the available numerical tools, we can quote the anelastic code ASH (Browning 2008), which filters out sound waves and linearises thermodynamical fluctuations around a background reference state. Anelastic solvers are consequently restricted to the study of flows with velocities much smaller than the sound speed, i.e. with very low Mach numbers. They can be applied to most brown dwarf interior processes. Other numerical tools are being developed, based on e.g. time implicit methods (Viallet et al. 2011; Kifonidis and Mueller 2012), which are numerically less limited than anelastic methods and can study low to moderate Mach-number processes on long time scales, relevant

to evolutionary problems. Such tools can study accretion effects on the structure of convective objects in order to better describe the redistribution in the interior of mass and energy accreted onto the surface of an object. These processes are currently studied through phenomenological approaches, assuming instantaneous and uniform redistribution of mass and internal energy brought by the accreted material. Great advancement has also been made and is still expected on the front of formation theories, with three-dimensional MHD simulations including radiation hydrodynamics being now underway to explore the second collapse and the physics of accretion at very early stages of evolution (Masson et al. 2012). All those numerical developments will provide a consistent picture of early and later stages of evolution of brown dwarfs, promising a wealth of exciting and novel results that should further motivate investment in the field of brown dwarf physics.

To conclude, brown dwarfs, as failed stars, are sometimes considered as the “Ugly Duckling” with an image tarnished by the big nuclear-powered stars and the appealing exoplanets. But brown dwarfs are great physical laboratories. Their discovery, as a cosmic confirmation of the effects of matter degeneracy predicted by quantum mechanics, marks a page of modern physics history. Still glowing with youth, they will keep surprising us for a long time.

## References

- Ackerman, A., Marley, M.: Precipitating condensation clouds in substellar atmospheres. *ApJ* **556**, 872 (2001)
- Allard, F., Hauschildt, P.H., Alexander, D.R., Starrfield, S.: Model atmospheres of very low mass stars and brown dwarfs. *ARA&A* **35**, 137 (1997)
- Allard, F., Hauschildt, P.H., Alexander, D., Tamai, A., Schweitzer, A.: The limiting effects of dust in brown dwarf model atmospheres. *ApJ* **556**, 357 (2001)
- Allard, F., Homeier, D., Freytag, B.: Models of very-low-mass stars, brown dwarfs and exoplanets. *RSPTA* **370**, 2765 (2012)
- André, P., et al.: Interferometric identification of a pre-brown dwarf. *Science* **337**, 69 (2012)
- Baraffe, I., Chabrier, G.: Effect of episodic accretion on the structure and the lithium depletion of low-mass stars and planet-hosting stars. *A&A* **521**, 44 (2010)
- Baraffe, I., Chabrier, G., Gallardo, J.: Episodic accretion at early stages of evolution of low-mass stars and brown dwarfs: a solution for the observed luminosity spread in H-R diagrams? *ApJ*, **702**, L27 (2009)
- Baraffe, I., Chabrier, G., Barman, T.: The physical properties of extra-solar planets. *Rep. Prog. Phys.* **73**, 016901 (2010)
- Baraffe, I., Vorobyov, E., Chabrier, G.: Observed luminosity spread in young clusters and FU Ori stars: a unified picture. *ApJ*, **756**, 118 (2012)
- Baraffe, I., et al.: *A&A* (2013, in preparation)
- Barman, T., Macintosh, B., Konopacky, Q., Marois, C.: Clouds and chemistry in the atmosphere of extrasolar planet HR8799b. *ApJ* **733**, 65 (2011a)
- Barman, T., Macintosh, B., Konopacky, Q., Marois, C.: The young planet-mass object 2M1207b: a cool, cloudy, and methane-poor atmosphere. *ApJ* **735**, L39 (2011b)
- Barshay, S.S., Lewis, J.S.: Chemical structure of the deep atmosphere of Jupiter. *Icarus* **33**, 593 (1978)

- Basri, G., Marcy, G., Graham, J.: Lithium in brown dwarf candidates: the mass and age of the Faintest Pleiades stars. *ApJ* **458**, 600 (1996)
- Bayo, A., Barrado, D., Stauffer, J., et al.: Spectroscopy of very low mass stars and brown dwarfs in the Lambda Orionis star forming region. I. Enlarging the census down to the planetary mass domain in Collinder 69. *A&A* **536**, 63 (2011)
- Beichman, C., Gelino, C., Kirkpatrick, J., et al.: The coldest brown dwarf (or Free-floating Planet)?: The Y dwarf WISE 1828+2650. *ApJ*, **764**, 101 (2013, submitted). ([astro-ph/1301.1669](#))
- Browning, M.: Simulations of dynamo action in fully convective stars. *ApJ* **676**, 1262 (2008)
- Browning, M.: (2013, in preparation)
- Buenzli, E., Apai, D., Morley, C., et al.: Vertical atmospheric structure in a variable brown dwarf: pressure-dependent phase shifts in simultaneous Hubble Space Telescope-Spitzer light curves. *ApJ* **760**, L31 (2012)
- Burgasser, A., Simcoe, R., Bochansky, J.J., et al.: Clouds in the coldest brown dwarfs: fire spectroscopy of Ross 458C. *ApJ* **725**, 1405 (2010)
- Burningham, B., Leggett, S., Homeier, D., Saumon, D., et al.: The properties of the T8.5p dwarf Ross 458C. *MNRAS* **414**, 3590 (2011)
- Burrows, B., Sudarsky, D., Hubeny, I.: L and T dwarf models and the L to T transition. *ApJ* **640**, 1063 (2006)
- Chabrier, G., Baraffe, I.: Structure and evolution of low-mass stars. *A&A* **327**, 1039 (1997)
- Chabrier, G., Baraffe, I.: Theory of low-mass stars and substellar objects. *ARA&A* **38**, 337 (2000)
- Chabrier, G., Gallardo, J., Baraffe, I.: Evolution of low-mass star and brown dwarf eclipsing binaries. *A&A* **472**, L17 (2007a)
- Chabrier, G., et al.: Gaseous planets, protostars, and young brown dwarfs: birth and fate. In: Reipurth, B., Jewitt, D., Keil, K. (eds.) *Protostars and Planets V*, p. 623. University of Arizona Press, Tucson (2007b)
- Claudi, R., et al.: The integral field spectrograph of SPHERE: the planet finder for VLT. *Proc. SPIE* **6269**, 62692 (2006)
- Cushing, M., et al.: The discovery of Y dwarfs using data from the wide-field infrared survey explorer (WISE). *ApJ* **743**, 50 (2011)
- Dupuy, T., Liu, M.: The Hawaii infrared parallax program. I. Ultracool binaries and the L/T transition. *ApJS* **201**, 19 (2012)
- Epcstein, N., de Batz, B., Capoani, L., et al.: The deep near-infrared southern sky survey (DENIS). *The Messenger* **87**, 27 (1997)
- Evans, N., et al.: The Spitzer c2d legacy results: star-formation rates and efficiencies; evolution and lifetimes. *ApJS* **181**, 321 (2009)
- Faherty, J., Burgasser, A., Walter, F., et al.: The brown dwarf kinematics project (BDKP). III. Parallaxes for 70 ultracool dwarfs. *ApJ* **752**, 56 (2012)
- Fegley, B., Lodders, K.: Atmospheric chemistry of the brown dwarf Gliese 229B: thermochemical equilibrium predictions. *ApJ* **472**, L37 (1996)
- Fortney, J., Baraffe, I., Millitzer, B.: Giant planet interior structure and thermal evolution. In: Seager, S. (ed.) *Exoplanets*, pp. 397–418. University of Arizona Press, Tucson (2011)
- Freytag, B., Allard, F., Ludwig, H.-G., Homeier, D., Steffen, M.: The role of convection, overshoot, and gravity waves for the transport of dust in M dwarf and brown dwarf atmospheres. *A&A* **513**, 19 (2010)
- Gardner, J., et al.: Science with the James Webb space telescope. *Proc. SPIE* **6265**, 62650 (2006)
- Gilmozzi, R., Spyromilio, J.: The European Extremely Large Telescope (E-ELT). *The Messenger* **127**, 11 (2007)
- Grossman, A.: Evolution of low-mass stars. I. Contraction to the main sequence. *ApJ* **161**, 619 (1970)
- Harvey, P., et al.: A Herschel Survey of cold dust in disks around brown dwarfs and low-mass stars. *ApJ* **755**, 67 (2012)
- Hayashi, C., Nakano, T.: Evolution of stars of small masses in the pre-main-sequence stages. *Prog. Theor. Phys.* **30**, 460 (1963)

- Helling, C., Woitke, P.: Dust in brown dwarfs. V. Growth and evaporation of dirty dust grain. *A&A* **455**, 325 (2006)
- Helling, C., Ackerman, A., Allard, F., et al.: A comparison of chemistry and dust cloud formation in ultracool dwarf model atmospheres. *MNRAS* **391**, 1854 (2008)
- Helling, C., Jardine, M., Stark, C., Diver, D.: Ionization in atmospheres of brown dwarfs and extrasolar planets. III. Breakdown conditions for mineral clouds. *ApJ* (2013, in press). (arXiv:1301.7586)
- Homeier, D.: Molecular line widths for stellar atmospheres. *MmSAI* **7**, 157 (2005)
- Hosokawa, T., Offner, S., Krumholz, M.: On the reliability of stellar ages and age spreads inferred from pre-main-sequence evolutionary models. *ApJ* **738**, 140 (2011)
- Hubbard, W.B., Guillot, T., Marley, M.S., Burrows, A., Lunine, J.I., Saumon, D.S.: Comparative evolution of Jupiter and Saturn. *Planet. Space Sci.* **47**, 1175 (1999)
- Irwin, J., et al.: NLTT 41135: a field M dwarf + brown dwarf eclipsing binary in a triple system, discovered by the MEarth observatory. *ApJ* **718**, 1353 (2010)
- Joergens, V., Pohl, A., Sicilar-Aguilar, A., Henning, Th.: The bipolar outflow and disk of the brown dwarf ISO 217. *A&A* **543**, A151 (2012a)
- Joergens, V., Kopytova, T., Pohl, A.: Discovery of an outflow of the very low-mass star ISO 143. *A&A* **548**, A124 (2012b)
- Kenyon, S.J., Hartmann, L., Strom, K.M., Strom, S.E.: An IRAS survey of the Taurus-Auriga molecular cloud. *AJ* **99**, 869 (1990)
- Kifonidis, K., Mueller, E.: On multigrid solution of the implicit equations of hydrodynamics. Experiments for the compressible Euler equations in general coordinates. *A&A* **544**, 47 (2012)
- Kumar, S.: The structure of stars of very low mass. *ApJ* **137** 1121 (1963)
- Luhman, K.: The formation and early evolution of low-mass stars and brown dwarfs. *ARA&A* **50**, 65 (2012)
- Macintosh, B.: The Gemini Planet Imager. *Proc. SPIE* **6272**, 672430 (2006)
- Marley, M., et al.: On the luminosity of young jupiters. *ApJ* **655**, 541 (2007)
- Marley, M., Ackerman, A., Cuzzi, J., Kitzmann, D.: In: Mackwell, S., Bullock, M., Harder, J. (eds.) *Comparative Climatology of Terrestrial Planets*. University of Arizona Press, Tucson (2013). (astro-ph/1301.5627)
- Masson, J., Teyssier, R., Mulet-Marquis, C., Hennebelle, P., Chabrier, G.: Incorporating Ambipolar and Ohmic diffusion in the AMR MHD code RAMSES. *ApJS* **201**, 24 (2012)
- McKee, C., Ostriker, E.C.: Theory of star formation. *ARA&A* **45**, 565 (2007)
- Mohanty, S., Stassun, K.: High-resolution spectroscopy during eclipse of the young substellar eclipsing binary 2MASS 0535-0546. II. Secondary spectrum: no evidence that spots cause the temperature reversal. *ApJ* **758**, 12 (2012)
- Mohanty, S., Stassun, K., Mathieu, R.D.: Circumstellar environment and effective temperature of the young substellar eclipsing binary 2MASS J05352184-0546085. *ApJ* **697**, 713 (2009)
- Mohanty, S., Stassun, K., Doppmann, G.: High-resolution spectroscopy during eclipse of the young substellar eclipsing binary 2MASS 0535-0546. I. Primary spectrum: cool spots versus opacity uncertainties. *ApJ* **722**, 1138 (2010)
- Morales, J.C., Ribas, I., Jordi, C., et al.: The effect of magnetic activity on low-mass stars in eclipsing binaries. *ApJ* **718**, 502 (2010)
- Mordasini, C., Alibert, Y., Georgy, C., et al.: Characterization of exoplanets from their formation. II. The planetary mass-radius relationship. *A&A* **547**, 112 (2012)
- Morley, C., Fortney, J., Marley, M., et al.: Neglected clouds in T and Y dwarf atmospheres. *ApJ* **756**, 172 (2012)
- Mullan, D.J., MacDonald, J.: Are magnetically active low-mass M dwarfs completely convective? *ApJ* **559**, 353 (2001)
- Nakajima, K., et al.: Discovery of a cool brown dwarf. *Nature*, **378**, 463 (1995)
- Noll, K.S., Geballe, T.R., Marley, M.S.: Detection of abundant carbon monoxide in the brown dwarf Gliese 229B. *ApJ* **489**, L87 (1997)
- Oppenheimer, B., et al.: Infrared spectrum of the cool brown dwarf Gl 229B. *Science* **270**, 1487 (1995)

- Palau, A., de Gregorio-Monsalvo, I., Morata, O., et al.: A search for pre-substellar cores and proto-brown dwarf candidates in Taurus: multiwavelength analysis in the B213-L1495 clouds. *MNRAS* **424**, 2778 (2012)
- Patience, J., King, R.R., De Rosa, R.J., Vigan, A., Witte, S., Rice, E., Helling, Ch., Hauschildt, P.: Spectroscopy across the brown dwarf/planetary mass boundary. I. Near-infrared JHK spectra. *A&A* **540**, 85 (2012)
- Pont, F., Sing, D., Gibson, G., Aigrain, S., Henry, G., Husnoo, N.: The prevalence of dust on the exoplanet HD 189733b from Hubble and Spitzer observations. *MNRAS*, **432**, 2917 (2013, in press)
- Radigan, J., Jayawardhana, R., Lafreniere, D., et al.: Large-amplitude variations of an L/T transition brown dwarf: multi-wavelength observations of Patchy, high-contrast cloud features. *ApJ* **750**, 105 (2012)
- Rappaport, S., Joss, P.: The lower main sequence and the nature of secondary stars in ultracompact binaries. *ApJ* **283**, 232 (1984)
- Rebolo, R., Zapatero Osorio, M., Martín, E.: Discovery of a brown dwarf in the Pleiades star cluster. *Nature* **377**, 129 (1995)
- Reiners, A., Basri, G.: The first direct measurements of surface magnetic fields on very low mass stars. *ApJ* **656**, 1121 (2007)
- Reiners, A., Seifahrt, A., Stassun, K., Melo, C., Mathieu, R.: Detection of strong activity in the eclipsing binary brown dwarf 2MASS J05352184-0546085: a possible explanation for the temperature reversal. *ApJ* **671**, L149 (2007)
- Ribas, I.: Masses and radii of low-mass stars: theory versus observations. *Ap&SS* **304**, 89 (2006)
- Rossow, W.B.: Cloud microphysics – analysis of the clouds of Earth, Venus, Mars, and Jupiter. *Icarus* **36**, 1 (1978)
- Saumon, D., Marley, M.: The evolution of L and T dwarfs in color-magnitude diagrams. *ApJ* **689**, 1327 (2008)
- Saumon, D., Chabrier, G., van Horn, H.: An equation of state for low-mass stars and giant planets. *Astrophys. J. Suppl.* **99**, 713 (1995)
- Slawson, R., et al.: Kepler eclipsing binary stars. II. 2165 eclipsing binaries in the second data release. *AJ* **142**, 160 (2011)
- Showman, A., Kaspi, Y.: Atmospheric dynamics of brown dwarfs and directly imaged giant planets. *ApJ* (2013, submitted). (arXiv:1210.7573)
- Skrutskie, M.F., Cutri, R.M., Stiening, R. et al.: The Two Micron All Sky Survey (2MASS). *AJ* **131**, 1163 (2006)
- Stassun, K., Mathieu, R., Valenti, J.: Discovery of two young brown dwarfs in an eclipsing binary system. *Nature* **440**, 311 (2006)
- Straka, W.: A determination of the lower mass limit for the main sequence. *ApJ* **165**, 109 (1971)
- Tennyson, J., Yurchenko, S.N.: ExoMol: molecular line lists for exoplanet and other atmospheres. *MNRAS* **425**, 21 (2012)
- Tsuji, T.: Dust in the photospheric environment: unified cloudy models of M, L, and T dwarfs. *ApJ* **575**, 264 (2002)
- Tsuji, T., Nakajima, T., Yanagisawa, K.: Dust in the photospheric environment. II. Effect on the near-infrared spectra of L and T dwarfs. *ApJ* **607**, 511 (2004)
- Viallet, M., Baraffe, I., Walder, R.: Towards a new generation of multi-dimensional stellar evolution models: development of an implicit hydrodynamic code. *A&A* **531**, 86 (2011)
- Witte, S., Helling, C., Hauschildt, P.H.: Dust in brown dwarfs and extra-solar planets. II. Cloud formation for cosmologically evolving abundances. *ApJ* **506**, 1367 (2009)
- Witte, S., Helling, C., Barman, T., Heidrich, N., Hauschildt, P.H.: Dust in brown dwarfs and extra-solar planets. III. Testing synthetic spectra on observations. *Journal: Astronomy & Astrophysics* **529**, 44 (2011)
- Wright, E.L., Eisenhardt, P.R.M., Mainzer, A.K., et al.: The wide-field infrared survey explorer (WISE): mission description and initial on-orbit performance. *AJ* **140**, 1868 (2010)
- York, D.G., Adelman, J., Anderson, J.E., Jr., et al.: The Sloan Digital Sky Survey: technical summary. *AJ* **120**, 1579 (2000)

# Index

## A

- Accretion, 156–158
  - episodic, 156
- Adaptive optics, 85–87, 89, 97, 105, 157
- Alcor AB, 97
- Adams, Walter, 83, 93
- Allen telescope array, 23
- Ammonia ( $\text{NH}_3$ ), 96, 98, 143, 146
- Aristarchus, 85
- Astrometry, 37, 83, 92, 93
- Atmosphere, 10, 13, 16, 17, 21, 27, 37, 39, 53, 62, 64, 73, 85, 88, 95, 106, 117, 120, 126, 130, 131, 142–149, 151, 158

## B

- Baryonic dark matter, 85
- Bessel, Friedrich, 83
- Binary
  - brown dwarf (BD), 23, 30, 44, 68–73, 102, 151–153
  - companion, 52, 99–104
  - eclipsing, 84, 100, 150–153
  - pre-main sequence, 27
  - radial velocity, 52, 68–72, 151
  - stars, 82–83, 92
- Biology, 105–106
- Black body spectrum, 86
- Black dwarf, 1, 2, 19, 20
- Bona fide brown dwarfs, 41, 85, 117
- Brown dwarf (individual)
  - Calar 3, 39–41, 44–46, 68
  - G 196-3B, 44
  - GD 165B, 27, 53, 75, 85, 115–118, 121, 128

Gliese 229B, 53, 61, 66, 75, 76

- Kelu-1, 54, 72, 75
- LP 944-20, 23, 54, 73
- PPI 15, 51–77
- Teide 1, 25–46, 61, 63, 66
- WISE 1828+2650, 115, 128–129, 131–132, 143

Brown dwarf desert, 53, 102

Bruno, Giordano, 84

## C

- Calar 3, 39–41, 44–46, 68
- Calar Alto 2.2 m telescope, 39
- Cesium, 95
- Chandrasekhar limit, 6
- Chemistry, 105, 114, 144–148
  - non equilibrium, 95, 126, 146, 147
- Clark, Alvan, 83
- Cloud, 19, 23, 59, 60, 76, 77, 117, 130, 132, 144–149, 154, 158, 159
- Cluster, 26, 29–32, 36–38, 41, 42, 44–46, 54, 55, 57, 59, 62–64, 68, 69, 72, 76, 77, 155
  - age, 31, 57, 66
- Collision-induced absorption, 95, 117
- Colour-magnitude diagram, 46, 55, 58, 59, 148–149
- Common proper motion, 88, 92
- Companions of stars, 81–106
- Convection, 7, 10, 11, 63, 66, 95, 150–152, 159
- Convective overshoot, 63, 64, 66
- Cooling curves, 20, 21
- Cool Stars 9 meeting, Florence, 94
- Coronagraph, 86–89, 92, 93, 96–98, 105

**D**

Deep near-infrared southern sky survey (DENIS), 42, 53, 54, 72, 75, 119, 121, 122, 124, 126, 143

Degeneracy. *See* Electron degeneracy

Deuterium fusion, 150, 156

Diversity, 81, 85

Dust, 76, 143, 144, 146–148, 158, 159

Dynamical mass, 27, 29, 30, 44, 73

**E**

Eccentricity, 100, 104

Electron degeneracy, 2, 5, 6, 8–9, 13–16, 84, 141

Epicurus, 84, 85

Epsilon Indi, 44

Equation of state, 2, 7, 8, 20, 142

Europa, 105

Exoplanets, 23, 56, 85, 98–103, 105, 113, 146, 150, 159, 160

Extra Terrestrials (ET), 23

**F**

Formation, 96, 101, 104, 141, 150, 154–158, 160

Free-floating planetary mass objects, 44

FU Orionis, 97

**G**

G 196-3B, 44

GD 165B, 27, 53, 75, 85, 115–118, 121, 128

Gemini Planet Imager, 96, 157

Gl 569 B, 30

Gliese 105, 89

Gliese 105C, 89

Gliese 229, 46, 89, 91, 92, 117

Gliese 229B, 44, 46, 53, 61, 66, 75, 76, 86, 89–91, 93–96, 98, 100, 106, 113, 116–118, 124, 128, 142, 146

Gravitational waves, 84

Gravity, 82, 83, 99, 120, 132, 133, 145, 146, 149, 157

**H**

Heliocentric model, 85

Herschel, William, 82, 83, 105

HHJ 10, 30

Hipparchos, 83, 100

HR 8799, 96, 97, 99

HR 8799c, 23

Hubble Space Telescope, 21, 72, 93, 128, 157

Hydrogen burning mass limit, 2

Hydrogen burning minimum mass, 5–17

**I**

IAC80 telescope, 31–33, 39

Inner structure, 142, 149–153

Instituto de Astrofísica de Canarias (IAC), 31, 32, 37, 56, 68, 73

Interior models, 2, 21, 58

IRAF, 39, 90

2.5 m Isaac Newton Telescope, 27, 31, 34

**J**

JHU Adaptive Optics Coronagraph, 86

Jupiter, 19, 20, 44, 46, 73, 92–94, 100, 101, 117, 126, 143, 154

**K**

Keck telescope, 37, 39, 42, 43, 46, 73, 77, 90

HIRES, 56, 58, 59, 69, 71

Kelu 1, 42, 54, 72, 75, 122

**L**

L dwarf, 27, 30, 44, 53, 54, 75, 85, 99, 115, 117, 121–124, 128, 130, 131, 133, 143, 144, 149

LHS 2065, 36

Lithium

burning, 16, 29, 57, 63

dating, 62–65

depletion, 16, 27, 30, 56, 57, 62, 64, 68, 72, 73, 76, 156

line at 670.8 nm, 27, 29, 41, 44

observation, 57

test, 29, 41, 46, 51, 54, 56, 57, 59–62, 66–69, 73–76, 117

Low-mass stars, 13–17, 27, 29, 46, 52, 53, 55–57, 73, 103, 115, 126, 143, 150–152, 154, 157

LP 944-20, 23, 54, 73

**M**

Magnetic fields, 55, 66, 151, 152, 159

Mars, 105

2MASS, 42, 53, 75, 95, 118, 121, 122, 124, 126, 127, 133, 135, 143

- Mass function of stellar clusters, 44  
M-dwarf, 37, 56, 62, 72, 75, 85, 100, 103, 104,  
  114, 115, 121, 153  
M6 dwarf, 37, 59, 66  
M9 dwarf, 36, 38  
Methane, 23, 46, 53, 75, 81–106, 117, 143,  
  146, 159  
Methane Brown Dwarf, 81–106  
Michell, John, 82  
MK process, 119, 121, 122, 124, 129, 132  
Molecular opacities, 142, 143
- N**  
Nakajima, Tadashi, 86  
Neptune, 103  
Nordic Optical Telescope (NOT), 32, 33, 35,  
  39
- O**  
 $\rho$  Ophiuchi, 26  
 $\alpha$  Ophiucus, 97
- P**  
Palomar, 52, 59, 86–89, 92  
Palomar Observatory, 32  
Palomar Pleiades objects, 32  
Pan-STARRS, 42  
Planet, 19, 20, 23, 53, 69, 77, 81–106, 114,  
  118, 143, 146, 150, 157–159  
Planetary mass objects, 44, 144, 146, 147,  
  157  
Pleiades  
  age, 30, 58, 62, 63  
  cluster, 29, 30, 32, 38, 41, 45, 46, 57  
  HHJ 3, 58, 59, 68, 76, 77  
  lithium boundary, 58, 64, 69, 76  
  star cluster, 26, 31, 37  
  substellar mass function, 41, 72  
Polytropic index, 6, 7, 9, 11  
PPI 10, 30  
PPI 15, 37, 41, 44, 45, 51–77  
Pre-main sequence stage, 6, 10, 13  
Project 1640, 96–99, 106  
Pulsars, 84
- R**  
Roque de los Muchachos Observatory, 27, 32,  
  35  
Rotation, 150–153, 159
- S**  
Saturn, 19, 103, 126  
Search for Extra Terrestrial Intelligence  
  (SETI), 21, 23, 105  
Sigma Orionis cluster, 44  
Sirius, 82–84  
Sirius B, 83–85, 93  
Sky survey, 52, 95, 118, 119, 127, 143  
Sloan Digital Sky Survey (SDSS), 42, 95, 119,  
  124, 126, 143  
Solar neighbourhood, 44  
Speckle, 52, 97, 98  
Spectra, 29, 36, 37, 39, 41, 44, 55, 59, 61, 62,  
  68, 69, 71, 75, 85, 88, 92, 96–99,  
  106, 114–129, 131–134, 143, 144,  
  146, 147, 149, 159  
Spectral classification, 114, 119–121, 124,  
  132, 133  
Spitzer Space Telescope, 21, 127, 154  
Spot coverage, 151, 152  
Star clusters, 10, 11, 26, 31, 44, 85, 88  
Star-forming region, 26–29, 41, 54, 55, 57,  
  75–77, 154, 155  
Stefan-Boltzmann relation, 83, 93  
Stellar clusters, 26, 44  
Substellar initial mass function, 44
- T**  
Taurus, 26–29, 77, 154  
T dwarfs, 44, 46, 85, 88, 99, 118, 120,  
  124–128, 130–134, 143, 146, 148  
Teide 1, 25–46, 61, 63, 66, 68, 142  
Teide Observatory, 32  
Thermochemical equilibrium, 106  
T Tauri stars, 29, 55, 56, 58, 118
- U**  
UKIDDS, 42  
UX Tau, 28  
UX Tau A, 27  
UX Tau C, 27, 29, 39, 56, 58, 69
- V**  
Vb10, 44  
Very cool stars, 29  
Very Large Array, 23  
Very low-mass stars, 27, 29, 57, 73, 115,  
  151  
 $\zeta$  Virginis, 97

**W**

White dwarf, 6, 8, 19, 20, 84, 85, 115, 118, 127

Wide-field infrared survey explorer (WISE),  
23, 115, 122, 126, 128–132, 143

William Herschel Telescope (WHT), 35, 36,  
39, 40

WISE 1828+2650, 115, 128–129, 131–132,  
143

**Y**

Y Dwarfs, 44, 113–134, 143, 144, 149,  
159

**Z**  
Z CMa, 97